Stability of microbial transglutaminase and its reactions with individual caseins under atmospheric and high pressure

Dissertation

zur Erlangung des akademischen Grades

Doctor rerum naturalium

(Dr. rer. nat.)

TECHNISCHE UNIVERSITÄT DRESDEN

vorgelegt

der Fakultät Mathematik und Naturwissenschaften
der Technischen Universität Dresden

von

Magister der Naturwissenschaften Orquídea de María Pastora Menéndez Aguirre
geboren am 14. Juni 1968 in Mexiko City, Mexiko

Gutachter: Prof. Dr. rer. nat. Dr. Ing. habil. Thomas Henle

Prof. Dipl. Ing. Dr. rer. nat. techn. habil. Harald Rohm

Prof. Dr. Ing. Jörg Hinrichs

Dr. rer. nat. habil. Harshadrai Rawel

Eingereicht am: 3 April 2006
Verteidigt am: 14 September 2006

„Gedruckt mit Unterstützung des Deutschen Akademischen Austauschdienstes“

Acknowledgements

I thank my “Doktorvater” Prof. Dr. rer. nat. Dr. Ing. habil. Thomas Henle for accepting me in his work team, but especially, I am thankful for his guidance, support and his helpful to see a broader perspective. I further acknowledge the supervision of Dr. rer. nat. Uwe Schwarzenbolz in my experimental and writing work. I am deeply indebted to Dr. rer. nat. habil. Harshadrai Rawel for his guidance in the analysis of protein structure. I appreciate Prof. Dipl. Ing. Dr. rer. nat. techn. habil. Harald Rohm for his collaboration in the rheological studies. I would like thank to Prof. Dr. rer. nat. habil. Wolf-Peter Kuhl for his interesting enzyme kinetic course as well as Prof. Dr. rer. habil. Thomas Simat and Prof. Dr. Hans-Joachim Knölker for their participation in my examination.

I would especially thank to Miriam Rugerio Álvarez from “Instituto Tecnológico y de Estudios Superiores de Monterrey, México”, to contribute with her Bachelor thesis in my investigation. Besides, I am thankful to Anja Teichmann for her valuable assistance in protein isolation, DLC Karla Schlosser for her assistance in the amino acid analysis and Annette Jacob for her supervision rheology measurement.

Very special thanks to Dr. Ing. Calvin Onyango for the statistical discussions and his friendship, Dr. rer. nat. Anke Böhm for her supervision in electrophoresis technical and her always sweetness and caring words. To the secretaries Ursula Tomaszewski and especially Uta Paul, I would like to express my thanks for their kindness and helpful in all proceeding. Thank to high pressure team Dr. rer. nat. Uwe Schwarzenbolz, Claudia Partschefeld and Sandy Richter fur their fruiters discussions. I would also like to thank my doctorates colleges Anke Förster, Kai Weigel, Thomas Siegel for their helpful tips in analytical techniques. Thank to Elvira Mavrić, Ana Seidowski, Leticia de Marco, Dr. rer. nat. Heike Raddatz and all my colleges for the good time in the scientific and social events. I will always remember your company.

I thank “Consejo Nacional de Tecnología”, CONACYT, from Mexico, for the four years doctorate scholarship and “Deutschscher Akademischer Austausch Dienst” DAAD, from Germany, for the international exchange program Mexico-Germany. I thank DAAD for the german language scholarship and its always very good assistance during my residence in Germany.

Finally I would like my greatest thankful to my family, who I dedicate for them this Dissertation.

A mi madre Prof. Lic. Juana Aguirre Montalvo

A la memoria póstume de mis abuelos José María y Pastora

A mi hermana Camelia

A la familia Langfermann

A Jörg

Table of contents

1 Introduction 1
2 Theoretical aspects 3
2.1 Transglutaminase 3
2.1.1 Structure of microbial transglutaminase 5
2.2 Microbial transglutaminase in the food industry 7
2.2.1 Food Safety of microbial transglutaminase 7
2.2.2 Digestibility of ε-(γ-glutamyl) lysine isopeptide 8
2.2.3 Application of microbial transglutaminase in food 10
2.3 High hydrostatic pressure in food industry 12
2.3.1 Effect of high hydrostatic pressure on microorganisms 14
2.3.2 Effect of high hydrostatic pressure on enzymes 15
2.3.3 Effect of high pressure treatment on microbial transglutaminase 16
2.3.4 Effect of high pressure on milk and milk products. 17
2.3.5 Effect of simultaneous application of high pressure and microbial transglutaminase on casein 18
2.4 Thermodynamic in biological systems 19
2.4.1 First Law of Thermodynamics 19
2.4.2 Second law of thermodynamics 21
2.4.3 The Free Energy from the combination of the First and Second Laws of Thermodynamics 23
2.4.4 Transition theory in reaction kinetics 25
2.5 Effect of pressure and temperature on biochemical reactions 28
2.5.1 Effect of pressure and temperature on water and buffer solutions 29
2.5.2 Effect of pressure and temperature on protein unfolding 32
2.5.3 Protein stability as a function of pressure, temperature and pH 35
2.5.4 Effect of high hydrostatic pressure and temperature on enzyme 36
2.6 Circular dichroism fundamentals 37
2.6.1 Principle 37
2.6.2 CD spectra of proteins 39
2.6.3 Estimation of the secondary structure of protein in solution 43
3 Materials and methods 45
3.1 Materials 45
3.1.1 Chemicals 45
3.1.2 Expendables 46
3.1.3 Equipment 47
3.2 Transglutaminase unter high pressure 49
3.2.1 Preparation of MTG samples 49
3.2.2 High pressure and thermal treatment 49
3.2.3 Determination of transglutaminase activity 50
3.2.4 Circular dichroism 51
3.2.5 Sodium dodecyl sulfate-polyacrylamide gel electrophoreses 52
3.2.6 Amino acid analysis 55
3.2.7 Qualitative determination of reducing sugar 58
3.2.8 Determination of protein concentration 58
3.3 Affinity of microbial transglutaminase to acid-, α_{s1}- and β-casein under atmospheric and high pressure 59
3.3.1 Isolation and identification of milk proteins 59
3.3.2 Characterisation of isolated casein 62
3.3.3 Kinetic studies 66
3.4 Influence of covalent cross-linking on storage modulus of acid gels obtained by transglutaminase and glucono-δ-lactone 69
3.4.1 Pre-trial experiments 69
3.4.2 Experimental design 70

3.4.3 pH measurement 73
3.4.4 Rheological measurement 73
3.5 Statistical analysis 74
4 Results and discussions 75
4.1 Microbial transglutaminase under high pressure 75
4.1.1 Short thermal inactivation 75
4.1.2 Effect of pressure on inactivation of MTG at constant temperature 76
4.1.3 Effect of high pressure on the conformational structure of MTG 81
4.1.4 Effect of pressure/temperature on the inactivation of MTG 94
4.1.5 Pressure/temperature inactivation kinetic 97
4.1.6 Pressure/temperature contour plot of active and inactivated MTG 103
4.1.7 Hypothetical pressure/temperature MTG plane from the first and the second rate constants 104
4.2 Affinity of microbial transglutaminase to acid casein, α_{s1}- and β-casein under atmospheric and high pressure conditions 107
4.2.1 Isolation and identification of the casein fractions 108
4.2.2 Purity control of isolated caseins by electrophoresis 109
4.2.3 Reaction kinetic studies 112
4.2.4 Kinetic reaction model propose for the reaction of microbial transglutaminase with monomer of acid, $\alpha_{s1,}$- and ß-casein 113
4.2.5 Monitoring of reaction 115
4.2.6 Evaluation of reactions kinetic at atmospheric pressure 120
4.2.7 Evaluation of reactions kinetic at high pressure 125
4.3 Influence of covalent cross-linking on storage modulus of acid gels obtained by transglutaminase and glucono-δ-lactone 131
4.3.1 Preliminary rheological study of casein gelation 131
4.3.2 Central composite rotatable design to study the behaviour of casein gelation with the simultaneous application of glucono-δ-lactone and microbial transglutaminase ... 135
4.3.3 Effect of oligomerisation degree on gel firmness 140
5 Proposes for further studies 143
6 Summary 145
7 References 149
Appendix 161
Publications 171
Declaration 173

Abbreviations

ANOVA	Analysis of variance
APS	Ammonium persulfate
CCRD	Central composite rotatable design
CD	Circular dichroism
CHAPS	3-[(3 cholamidopropyl)dimethylammonium]-1-propanesulfonate
DDT	1,4-Dithiothreitol
deg	Degree
eq.	Equation
Gdl	Glucono-δ-lactone
HAL	Histidinoalanine
LAL	Lysinoalanine
MTG	Microbial transglutaminase
Nα-CBZ-Gln-Gly	Nα-Benzyloxycarbonyl-L-glutamynglycine
PET	Positron emission tomography
rad	Radian
SH	Thiol group
TCEP	tris(2-Carboxyethyl)phosphine, HCl
TG	Transglutaminase
TEMED	N,N,N´,N´-tetramethylethylediamine
TRIS	Tris(hydroxymethyl)-aminomethane
SDS-PAGE	Dodecyl sulphate-polyacrylamide gel electrophores
Z-Gln-Gly	Nα-Benzyloxycarbonyl-L-glutamynglycine

Symbols

A	Physic: Area
A	Spectroscopy: Absorbance
A_L	Spectroscopy: Left absorption
A_R	Spectroscopy: Right absorption
$°C$	Degree Celsius
c	Concentration
d	Degree
E	Enzymology: enzyme
E	Thermodynamic: energy

E_a	Activation energy
E_K	Kinetic energy
E_P	Potential energy
$E_{surrounding}$	Surrounding energy
F	Force
f	Rheology: frequency
$_f$	Final
G	Gibbs energy
G^*	Complex modulus
G'	Storage modulus
G''	Loss modulus
H	Enthalpy
$_i$	Initial
$°K$	Kelvin degree
K	Equilibrium constant
$K_{affinity}$	Affinity constant
K_m	Affinity constant
k	Rate constant
k_{cat}	Catalytic constant
l	Length
^1L_a	Chemistry: electronic excitation state
^1L_b	Chemistry: electronic excitation state
M	Monomeric casein
n	Reaction order
n_r	Residues number
P	Pressure
pH	Negative logarithm of the concentration (mol/L) of the $H_3O^+[H^+]$ ion
Q	Heat
S	Entropy
T	Temperature
t	Time
U	Internal energy
UV	Ultraviolet
V	Volume
ΔV^*	Activation volume

V_{max}	Maximal velocity
W	Work

Greek symbols

α	alpha	
ß	beta	
δ	delta	Rheology: Deformation angle
ε	epsilon	
ϕ	phi	Biochemistry: Torsion angle in backbone protein
γ	gamma	Rheology: deformation
κ	kappa	
λ	lambda	Chemistry: Wavelength
μ		
π	pi	
θ	theta	Circular dichroism: Ellipticity
ω	omega	Rheology: angular frequency
τ	tau	Rheology: shear stress
ψ	psi	Biochemistry: Torsion angle in backbone protein

$\dot{\gamma}$	Rheology: Shear rate
n-π	Chemistry: Electronic excitation state
π-π	Chemistry: Electronic excitation state

Constants

k_B	Boltzmann constant = 1.4 x 10^{-23} J/°K
h	Planck constant = 6.6 X 10^{-34} Js
R	Universal gas constant = 8.3147 J/gmol°K
π	pi ≅ 3.14159

1 Introduction

The application of the commercial microbial transglutaminase from *Streptoverticillium mobaraense* Activa $_{TM}$ MP in milk products is used to improve physical properties like texture in yoghurt and ice cream, increase breaking strength in low and full fat yoghurt as well as to decrease the concentration of stabilizers and solid non fat material (Ajinomoto, 2002). Transglutaminase is an enzyme that catalyses an acyl-transfer reaction introducing a covalent cross-linking between glutamine and lysine amino acid residues. The new covalent cross-links form a network in the protein system, which causes drastic changes in the protein size, conformation and stability of the food products.

Milk proteins are good substrates for transglutaminase, because they contain numerous glutamine and lysine amino acid residues. However, not all of these residues are reactive with transglutaminase. Different authors have suggested some methods to increase the exposition of these reactive residues. The addition of dissociating and reducing agents, as well as, the previous heating and high pressure treatment are some examples. The disadvantage, in the addition of chemical agents, is that they are generally not allowed in food preparations. Furthermore, the thermal treatments cause changes in the nutritional values and in sensory characteristics of food products. For this reason, high pressure could be an alternative treatment with the benefit of keeping reactive groups minimally altered compared to the original quality of the milk proteins. In addition, simultaneous application of microbial transglutaminase and high pressure treatment on milk protein could be used to reduce production cost in milk technology.

Along with the current literature, there is a lack in the information about the conformational changes of microbial transglutaminase in association with inactivation kinetic studies and a pressure/temperature diagram of microbial transglutaminase inactivation is not available. Furthermore, literature provides only little information about the affinity of microbial transglutaminase towards individual milk proteins.

In order to investigate more about this theme, results the thesis: Stability of microbial transglutaminase and its reactions with individual caseins under atmospheric and high pressure, as well as, the study of rheological consequences in acid gels.

The work is in three parts structured. The first part is the analysis of the secondary and tertiary conformation of microbial transglutaminase after treatment at different pressure and

temperature conditions. Additionally, the possible influence of non-enzymatic protein-carbohydrate reactions on microbial transglutaminase activity has to be taken into account. A kinetic study and a pressure/temperature diagram based on the rate constants of microbial transglutaminase inactivation have been performed. The second part is the analysis of microbial transglutaminase affinity towards individual caseins. The kinetics of the reaction of microbial transglutaminase with ß- and α_{s1}-casein isolated from cow's milk is investigated at high and atmospheric pressure treatment. Finally, the third part is the evaluation of rheological properties as gel firmness represented by storage modulus and gelation time of acid-induced casein gels.

2 Theoretical aspects

2.1 Transglutaminase

Transglutaminase (ε-glutaminyl-peptide: amine γ-glutaminyl-transferase, EC 2.3.1.13) (TG) is an enzyme that catalyses the acyl transfer reactions between the γ-carboxamide group of peptide bound glutamine and the ε-amino group of peptide bound lysine to form a ε-(γ-glutamyl)lysine isopeptide bond (figure 2.1-1). Folk (1969) postulated that the reaction mechanism of TG is a ping pong mechanism, in which: 1) A glutamine substrate binds to catalytic cysteine residue of the enzyme in a binary complex as thioester. 2) Ammonia dissociates with the formation of an acyl enzyme intermediate. 3) The acyl enzyme intermediate reacts with a second substrate, either an acyl acceptor, which can be almost any primary amine to form γ-glutamyl-amine product or to water to form glutamic acid product.

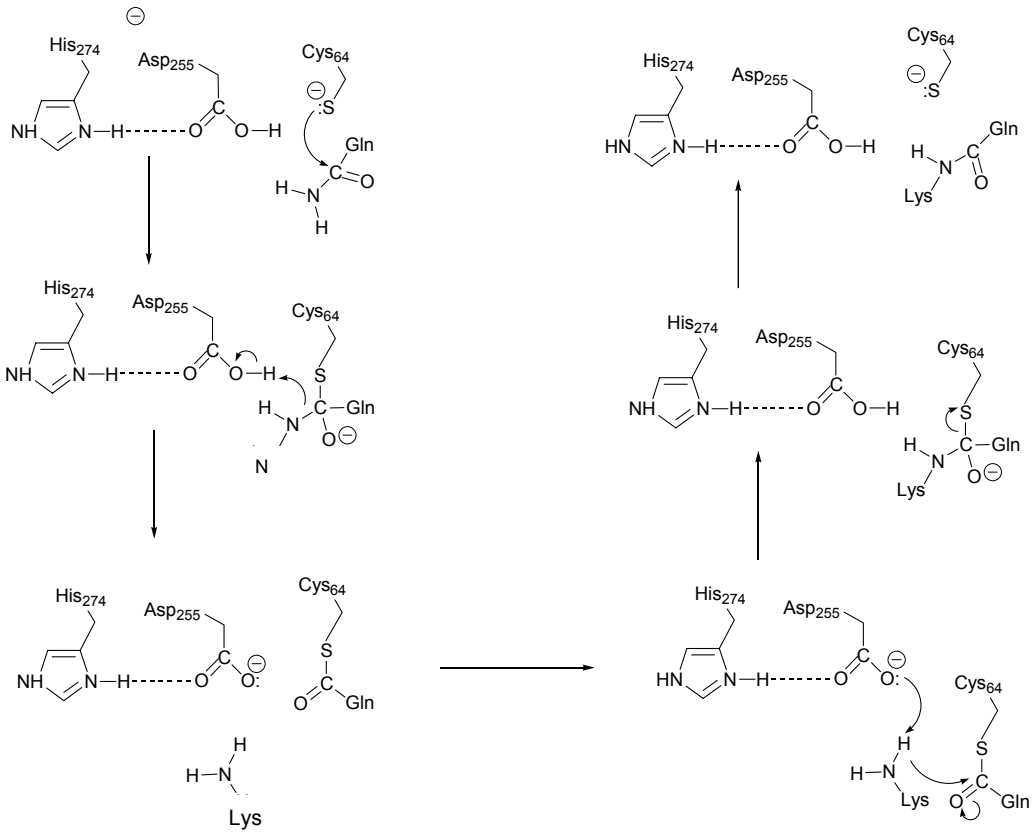

Figure 2.1-1 Hypothetical catalytic mechanism of MTG (Kashiwagi *et al*., 2002) based in the ping pong mechanism of TG postulated by Folk (1969)

However, the acyl-enzyme intermediate can also be hydrolysed in the absence of primary amines but at a slower rate. Transglutaminase exhibits high specificity towards L-glutamine residues as the acyl-donor substrate and lower specificity towards the acyl-acceptor, for this reason the ε-amino group of lysine as well as many primary amines, polyamines and ammonia can act as substrates (Folk, 1969; Griffin *et al*., 2002).

Transglutaminases can be found in plants (Del Duca *et al*., 2000), vertebrate animals (Folk and Cole, 1965), invertebrate animals (Noguchi *et al.*, 2001) and microorganisms (Ando *et al*., 1989). Plant TGs as components of various cell compartments such as chloroplasts, mitochondria, cytoplasm and cell walls are related to growth, differentiation, programmed cell death and stress (Della Mea *et al*., 2004). Animal TGs are Ca^{2+}-dependent enzymes which are widely distributed in body tissues such as liver, lung, intestine, hair follicles, epidermis, prostate, placenta and body fluids such as blood. Since 1960, the isolation, purification and characterisation of TG from mammal body fluids, as human plasma factor $XIII_a$ or thrombin-activated blood coagulation factor XIII (Gorman and Folk, 1980; Traoré and Meunier, 1991) is performed. Transglutaminase from mammal tissue, namely guinea pig liver TG has been widely characterised (Folk and Cole 1966; Folk, 1969; Chung *et al*., 1970, Case and Stein 2003). Human plasma factor $XIII_a$ is localized in the plasma and impedes blood loss by stabilizing fibrin clots during their formation at sites of blood coagulation. Tissue TG has been ascribed to several processes including stabilization of extra cellular matrices, formation of cross-linked cell envelopes, cell matrix assembly, wound healing and cellular adhesive processes (Leblanc *et al*., 2001). Industrial applications of animal TG have been intensively studied (Traoré and Meunier, 1991; Oh *et al*., 1993), but its scarce source and complicated separation and purification procedures made the enzyme very expensive and limits its application in industry.

Since the 1980s, a Ca^{2+}-indepent TG could be obtained from the microorganisms *Streptomyces* sp and *Streptoverticillium* sp with a higher activity than animal TG. In addition, microbial fermentation makes it possible to achieve mass production of transglutaminase at a low cost, which is advantageous for its industrial application in food technology, cosmetics as well as pharmaceutical products and medical treatment (Zhu *et al*., 1995). Motoki *et al.* (1989) and Ando *et al*. (1989) studied the possibility to produce TG from microorganisms. Ando *et al.* (1989) screened about 5000 strains isolated from soil collected from a variety of locations. Among these strains, Streptoverticillium S-8112 was found to have the capability to form the enzyme. Motoki *et al.* (1989) state, that other *Streptoverticillium* strains, such as *S. griseocarneum, S. cinnamoneum* subsp., *S. cinnamoneum* and *S. mobaraense*, also have the ability to produce TG. Ando *et al.* (1992) also found the enzyme in a culture of

Streptomyces sp. The employed medium in the fermentation is composed of glucose and salts, which achieved a TG production with activities of 0.28 to 2.5 U/mL in 72 h depending of the strain used. Téllez-Luis *et al*. (2004), using a medium containing commercial xylose achieved a TG production from *Streptoverticillium ladakanum* with an activity of 0.348 U/mL in 72 h. The temperature of growth was between 25°C and 35°C. MTG is an extracellular enzyme dissolved in the fermentation broth so that it can be recovered through separation of the solid material. The traditional methods, as salting out with ammonium sulphate and sodium chloride, dialysis, ultrafiltration, ion-exchange chromatography, absorption chromatography, gel filtration or isoelectric precipitation can be used to purify the enzyme. According to the method, the total recovery of transglutaminase activity is about 40 to 42%. The obtained enzyme can then be mixed with enzyme stabilizers such as salts, sugars, dextrin (Sakamoto *et al*., 1992; Téllez-Luis, 2004).

2.1.1 Structure of microbial transglutaminase

The primary structure of microbial transglutaminase (MTG) produced by the microorganism *Streptoverticillium* sp. Strain s-8112, which has been identified as a variant of *mobaraense* (Kanaji *et al*. 1993), consists of 331 amino acid residues in a single polypeptide chain with a molecular weight of 37 863 Da (figure 2.1-2). The amino acid sequence of MTG was found to be very different in comparison with animal TG. Although animal TG showed low degrees of homology in their amino acid sequences, a similarity in certain regions, especially around the predicted active site of the cysteine residue is observed (figure 2.1-3). The enzyme MTG contains a single cysteine residue, Cys64, with a free thiol group, which is essential for its catalytic activity, indicating that the MTG is a member of the thiol protease family.

```
  1 DSDDRVTPPA EPLDRMPDPY RPSYGRAETV VNNYIRKWQQ VYSHRDGRKQ
 51 QMTEEQREWL SYGCVGVTWV NSGQYPTNRL AFASFDEDRF KNELKNGRPR
101 SGETRAEFEG RVAKESFDEE KGFQRAREVA SVMNRALENA HDESAYLDNI
151 KKELANGNDA LRNEDARSPF YSALRNTPSF KERNGGNHDP SRMKAVIYSK
201 HFWSGQDRSS SADKRKYGDP DAFRPAPGTG LVDMSRDRNI PRSPTSPGEG
251 FVNFDYGWFG AQTEADADKT VWTHGNHYHA PNGSLGAMB VYESKFRNWSE
301 GYSDFDRGAY VLTFLPKSWN TAPDKVKQGW P
```

Fig 2.1-2 Complete amino acid sequence of MTG from Streptoverticillium sp s-8112. The cysteine residue in the active site is marked (Cys64).

Microbial TG			
Streptoverticillium sp. s-8112	59	WLSYGCVGVTWVNSGQYPTNR	79
Animal TG from			
human factor XIIIa	309	VRYGQCWVFAGVFNTFLRCLG	329
guinea pig liver	271	VKYGQCWVFAAVACTVLRCLG	291
Protease			
Papain	153	GSCGSCWAFSAVVTIEGIIKI	273

Fig 2.1-3 Comparison of amino acid sequences in active sites of microbial and animal transglutaminase with a protease.

Kashiwagi *et al*. (2002) reported that the overall crystal structure of MTG from *Streptoverticillium mobaraense* form a single compact domain with overall dimensions of 65 x 59 x 41 Å. The enzyme adopts a disk-like shape and has a deep cleft at the edge of the disk. The cysteine residue, Cys64, is located at the bottom of the cleft, which is designated as the active site cleft. The MTG structure belongs to the α + ß folding class. The secondary structures are arranged so that ß-sheet is surrounded by α-helices, which are clustered into three regions. The central ß-sheet domain is formed by seven anti-parallel ß-strand leaving a cleavage between strands $ß_5$ and $ß_6$, who are linked together with only one hydrogen bond. The first cluster of α-helices (α_1, α_2 and α_3), is on the left side, where the cysteine residue, Cys64 is located on the loop between α_1 and α_2 helices. The second α-helices cluster (α_4, α_5 and α_{10}) is on the right side and the third group of α-helices (α_6, α_7, α_8 and α_9) is located on the bottom of the front view of the molecule. The active site cleft has a depth of 16 Å. The side walls of the active site cleft are composed of several loops and are separated by a distance of about 13 Å. The loops of the left side wall of the cleft are tightly associated with many polar and hydrophobic interactions, which provide a stable structure. The loop of the right wall has a flexible characteristic. The Cys64 is specifically located at the bottom active of the site cleft, formed by $ß_5$, $ß_6$ strands, the α_{11} and the loop between α_2 and α_3. The cysteine residue is surrounded by Phe254, Asp255, Asn276 and His277, but has contact only with Phe254 through van der Waals interactions and is sufficiently exposed to the solvent with a surface area of 17 to 21 Å. Kashiwagi *et al*. (2002) proposed the three residues Cys65–His274–Asp255 as the catalytic triad for the MTG.

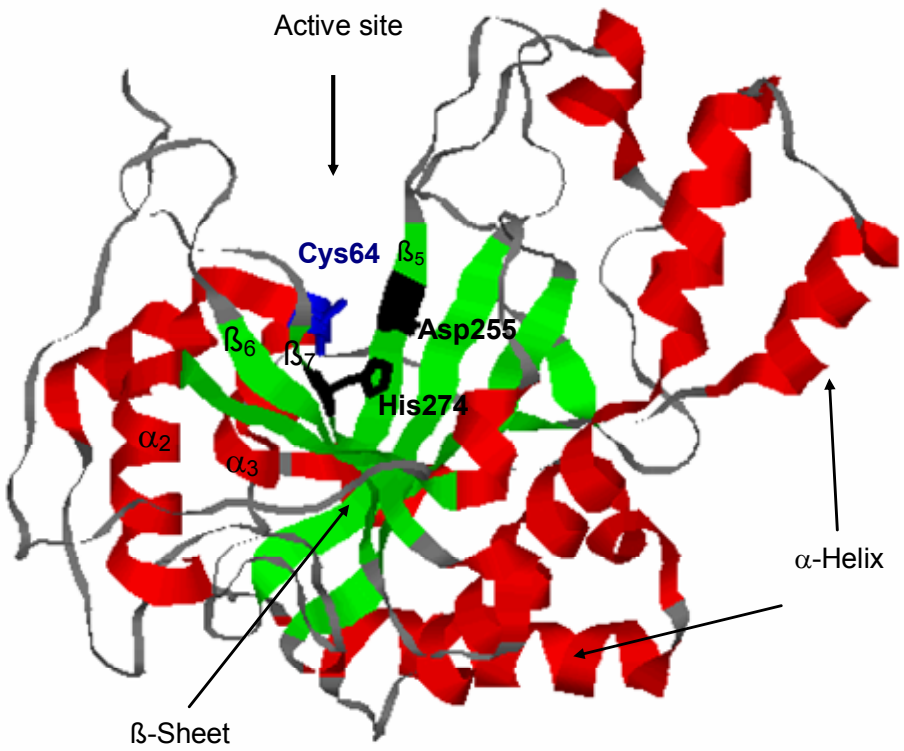

Figure 2.1-4 Microbial transglutaminase structure (Kashiwagi *et al*., 2002)

2.2 Microbial transglutaminase in the food industry

Since a microbial transglutaminase has been industrialised, its capacity to form ε-(γ-glutamyl) lysine isopeptide cross-links has been applied as a means of improving functional properties of food proteins. The use of the enzyme in the food industry, as well as the digestibility of its resulting ε-(γ-glutamyl) lysine isopeptide product has been also investigated for different instances (Raczynski *et al*., 1975; Fink *et al*., 1980).

2.2.1 Food Safety of microbial transglutaminase

The Novel Food Regulation (EC) No. 258/97 and the Food Safety for Additive (89/107 EEC) of the European Commission, as well as, the U.S. Food and Drug Administration in the division of the Center for Food Safety and Applied Nutrition, Office of Food Additive Safety (2002) published the GRAS Notice No. GRN 000095 to designate microbial transglutaminase from *Streptoverticillium mobaraense* produced by Ajinomoto as a substance generally recognized as safe.

2.2.2 Digestibility of ε-(γ-glutamyl) lysine isopeptide

Studies of metabolic fate of ε-(γ-glutamyl) lysine isopeptide showed that the digestive enzymes of ordinary mammalian do not cleave this isopeptide after the ingestion (Seguro *et. al*., 1996) and for this reason, since the 1970s, its digestibility in animal has been investigated (Raczynski *et al*., 1975; Fink *et al*., 1980). Several studies stated that the cleavage of the isopeptide with the concomitant Lys liberation is explained by the activity of the enzymes γ-glutamyltranspeptidase (γ-GT) and γ-glutamylcyclotransferase (γ-GCT). Both enzymes are principally present in the kidney, liver, pancreas, and intestine (Szewczuk *et al*., 1974; Tate *et al*., 1985). The enzyme γ-glutamylcyclotransferase cleaved the ε-(γ-glutamyl) lysine isopeptide bond resulting the liberation of free L-Lys residue and 5-oxoproline, which is future metabolised by 5-oxoprolinase to Glutamic acid due 5-oxoprolinase (5-OP). The enzyme γ-glutamyltranspeptidase induces the liberation of free L-Lys and the formation of a new isopeptide (figure 2.2-1).

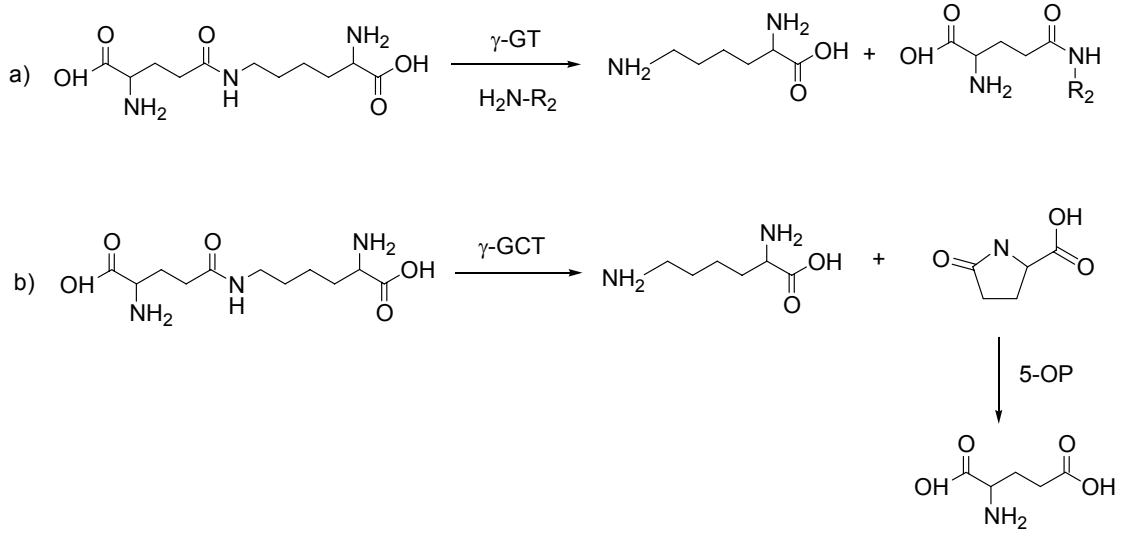

Figure 2.2.-1 Cleavage of ε-(γ-glutamyl) lysine isopeptide by a) γ-glutamyltranspeptidase (γ-GT) and b) γ-glutamylcyclotransferase (γ-GCT).

In vitro digestibility studies using ^{3}H-labelled ε-(γ-glutamyl) lysine by Raczynski *et al.* (1975) reported that there is no cleavage of isopeptide bond in the digestive tract and the isopeptide passed across the intestinal wall unchanged and is metabolised by other organs. In our work group, Hultsch *et al*. (2005) performed *in vitro* and *in vivo* studies using ^{18}F-labelled ε-(γ-glutamyl) lysine in order to investigate the biodistribution, catabolism and elimination of this isopeptide in male Wistar rats. The labelling results showed that the coupling reaction of ε-(γ-glutamyl) lysine isopeptide with [^{18}F]SFB resulted in two different labelling products due to

the presence of two primary amino groups in the isopeptide: **^{18}F**-labelled-Gln-Lys (isopeptide of a substituted α-NH_2-Gln) and Gln-Lys-labelled-**F^{18}** (isopeptide of an unsubstituted α-NH_2-Gln). The *in vitro* results demonstrated that the both labelling products showed a different behaviour: The isopeptide of a substituted α-NH_2-Gln remained almost unchanged in the different exanimate tissue homogenates, whereas the isopeptide of an unsubstituted α-NH_2-Gln is generally transformed. The faster degradation was observed in the kidney homogenate, a rapid degradation was also observed in liver homogenates and after in pancreas homogenate and the slowest degradation were observed in intestine homogenates. The degradation of this isopeptide was related with the enzymatic activities of γ-glutamyltranspeptidase and γ-glutamylcyclotransferase. The biodistribution studies showed that the isopeptide of a substituted α-NH_2-Gln exhibited a higher accumulation in the kidney compared to the isopeptide of an unsubstituted α-NH_2-Gln, which after 5 min a 36% of total radioactivity was detected in the urine. Positron Emission Tomography (PET) results showed that the radioactivity of Gln-Lys-labelled-**F^{18}** isopeptide is delivered via the renal pelvis to the ureter after 2 min and after 20 min only a few radioactivity could be observed in the kidneys. In contrast, accumulation of the radioactivity of **^{18}F**-labelled-Gln-Lys isopeptide in the cortex of the kidney was observed (figure 2.2-2).

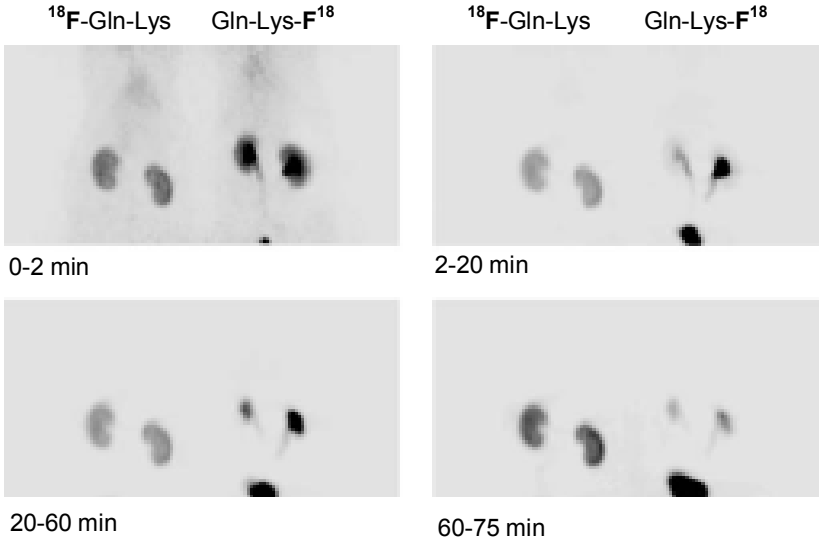

Figure 2.2-2 Representative coronal images of small animal PET studies showing ^{18}F-radioactivity distribution of abdominal region after application of 15 MBq of Gln-Lys-labelled-**F^{18}** isopeptide and **^{18}F**-labelled-Gln-Lys isopeptide, at different time intervals (Hultsch *et al*., 2005, modified).

However, the *in vivo* metabolism results demonstrated that the both labelling isopeptides were transformed in the livening organism. For the isopeptide of an unsubstituted α-NH_2-Gln, metabolites could be found in urine as well as in blood and in kidney, whereas for the isopeptide of a substituted α-NH_2 Gln, metabolites were found only in the urine. The authors

showed a cleavage of the unsubstituted α-amino group of the Gln of the isopeptide and suggested that conventional peptide bonds of a peptide containing an isopeptide bond are cleaved by peptidases soon after absorption, so that the isopeptide is liberated and there is no longer a substitution of the α-amino group, then a subsequently cleaved can be occurred. Thereby, the authors also suggested that it appears that the use of MTG in food products and its isopeptide do not pose a risk to health of the consumers (Hultsch *et al*., 2005).

2.2.3 Application of microbial transglutaminase in food

Since the approbation of the different international instances to used microbial transglutaminase (MTG) produced by the microorganism *Streptoverticillium mobaraense* in the food industry, the commercial MTG produced by Ajinomoto has been applied in a variety of food proteins in order to improve the characteristic of several commercial food products. The formation of additional covalent cross-links causes changes in the size, conformation, viscosity, gelation and stability of different protein foods like soy, gluten, muscle, myosin, globulin, casein or whey, so that, the appearance and texture of a great variety of food systems can be modified using MTG during food processing. For example, studies by Hazová *et al.* (2002) revealed that the addition of MTG on wheat flour causes a positive effect on the texture and distribution of pores resulting in higher loaves of bread and pastry using enzyme concentrations of 3.5 to 4.5 mg/kg flour. Preservation of the nutritional value, sensory and microbiological quality, persisted even during the storage of frozen croissants for 90 days. Ramirez *et al.* (2000) demonstrated that the surimi gels from silver carp elaborated using MTG have better mechanical properties. A shear stress of 146 kPa and shear strain of 1.59 kPa were achieved by employing a MTG concentration of 8.8 g/kg of surimi at 39.6°C for 1h. Uresti *et al.* (2005) evaluated the mechanical properties of a restructured fish product from arrowtooth flounder (*Athersthes stomias*), an under-utilised fish specie in the Alaska Golf, obtained by the application of high pressure and MTG. Texture profile analysis demonstrated that the addition of MTG in fish protein previously treated at 600 MPa for 5 min, increases the strength of the gel product.

In milk products, MTG has been used to increase firmness in yoghurt. In our work group, Lauber *et al*. (2000) found that formation of isopeptide cross-links from skim milk incubated with MTG had direct relation with the yoghurt consistence (figure 2.2-3).

The rheological results indicated that the breaking strength of gels increased from 550 to 920 cN and was accompanied with a casein oligomerisation from 10.0 to 25.8% with a concomitant intermolecular ε-(γ-glutamyl) lysine isopeptide increase. These results are in

agreement with Farnsworth *et al*. (2002), who reported that the used MTG concentrations between 2 and 4 U/g protein increases the yoghurt viscosity from $4.43x10^3$ to $2.72x10^5$ and $1.12x10^6$ MPa·s, respectively.

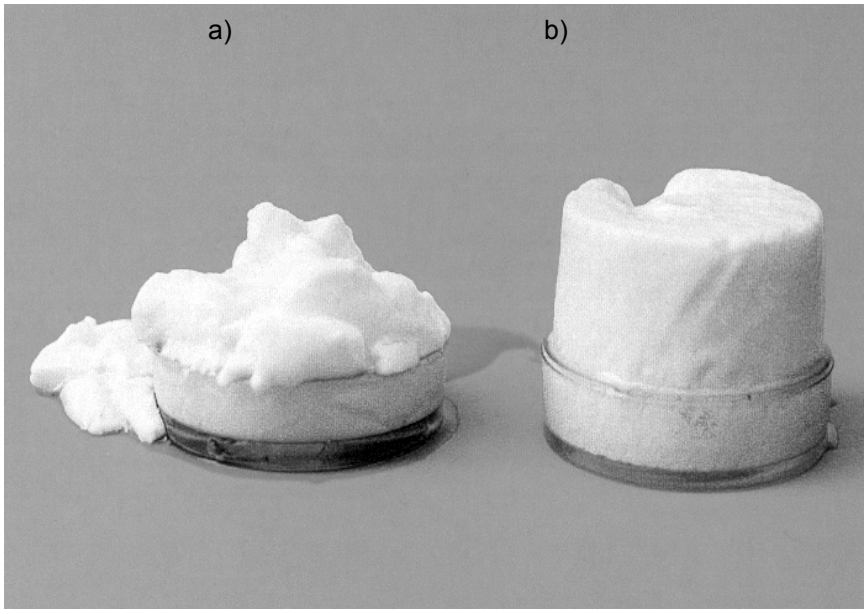

Figure 2.2-3Yoghurt from skim milk incubated at 40°C for 2 h following a treatment at 80°C for 5 min. a) Without MTG. b) With 100 U MTG/L (Adopted from Lauber *et al*., 2002).

Further studies of Lauber *et al.* (2002) showed the effect of different treatments on the firmness of gels from milk. Application of heat at 80°C for 2 min, high pressure at 400 MPa and 23°C for 1h, addition of 3 U MTG/g protein at 23°C for 1h and the simultaneous application of MTG and high pressure were analysed. The results demonstrated that after the addition of MTG and incubation at 400 MPa and 23°C for 1 h results in the highest firmness of gel (figure 2.2-4). In order to know the formation of covalent isopeptide cross-links due to MTG under different pressure treatment, oligomerisation grade from sodium casein was analysed using gel permeation chromatography. The results showed an increased casein oligomerisation from samples treated with the simultaneous application of MTG and high pressure in a range from 200 to 400 MPa at 40°C (Lauber *et. al*., 2001). Recent studies in our laboratory using skim milk (Partschefeld and Döhler, 2005) revealed a very similar degree of oligomerisation: 34% from samples treated with MTG at 0.1 MPa at 50°C and 37% from samples treated with MTG at 400 MPa at 50°C. The results also show, that the formation of dimer was favoured by the enzymatic reaction at 400 MPa, whereas the formation of trimers was favoured in milk previously treated at 400 MPa followed by the enzymatic reaction at 0.1 MPa.

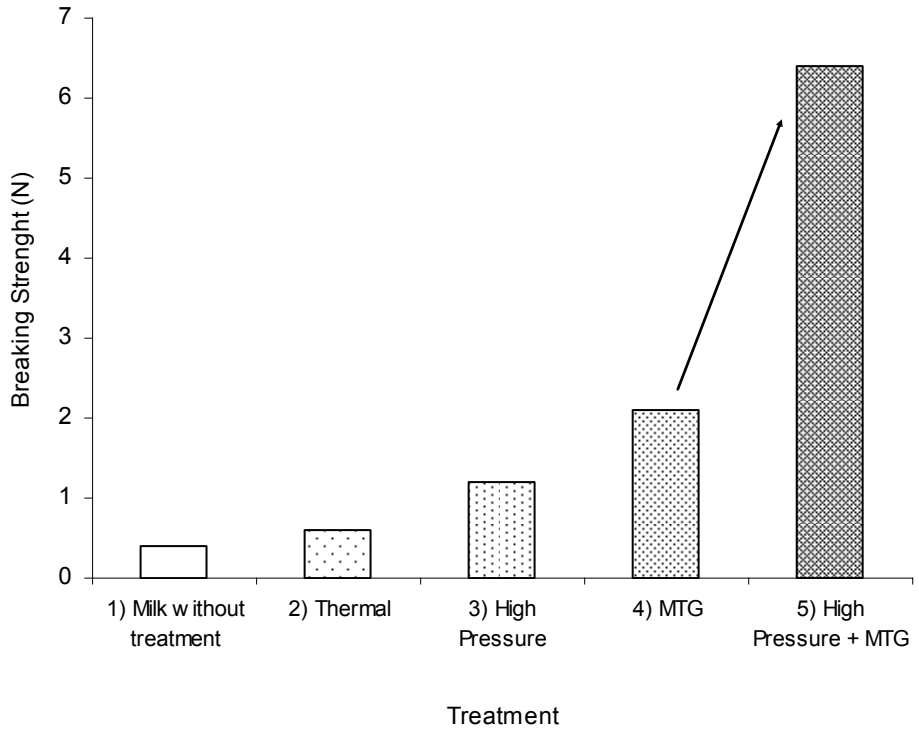

Figure 2.2-4 Breaking Strength from milk after different treatments. 1) Milk without treatment. 2) Milk at 0.1 MPa and 80°C for 2 min. 3) Milk at 400 MPa, 23°C, 1h. 4) Milk at 0,1 MPa and 23°C, 1h + 3 U MTG /g protein. 5) Milk at 400 MPa and 23°C, 1h + 3 U MTG /g protein (Adopted from Lauber, 2002, modified).

These results stated that MTG can be also used with simultaneous application of high pressure treatment. But, what is high pressure processing? Why does use this technology in food system? How does this technology benefit consumers? In order to explain the effect of high pressure on MTG and milk proteins, an overview of high hydrostatic pressure in food industry is described in the next section.

2.3 High hydrostatic pressure in food industry

Salting, drying, curing, heat treatment, refrigeration or freezing are conventional methods of preserving food. Nevertheless, with the necessity to enhance retention of flavours and nutrient value as well as to improve functional properties and sensory quality of food products, the last few years have seen the development of a new technology: high pressure sterilization. High hydrostatic pressure processing is a food processing method where food is subjected to elevated pressure (until 1 000 MPa) with or without the addition of heat. In this technology, vegetative microorganisms are destroyed at above 600 MPa without the accompanying chemical changes caused by heat. There are not undesirable textural changes due to reduced crystal size and multiple ice-phases formed by freezing process and there are no alterations in flavours provided by the curing and salting treatments

(Barciszewski *et al*., 1999). High pressure has the beneficial effect to disrupt non-covalent bonds in macromolecules, such as protein and polysaccharides and has little effect on vitamins, and other molecules responsible for flavour and colour (Datta and Deeth, 1999). However, high pressure is not the optimal process for all variety of food products. The physical, chemical and sensorial changes are different for each food system. For example, minced pork meat undergoes a degradation of the red colour after high pressure treatment at 600 MPa and 4°C for 10 min (Krzikalla *et al*., 2005). The colour change is also dependent for the addition of ascorbic acid (figure 2.3-1).

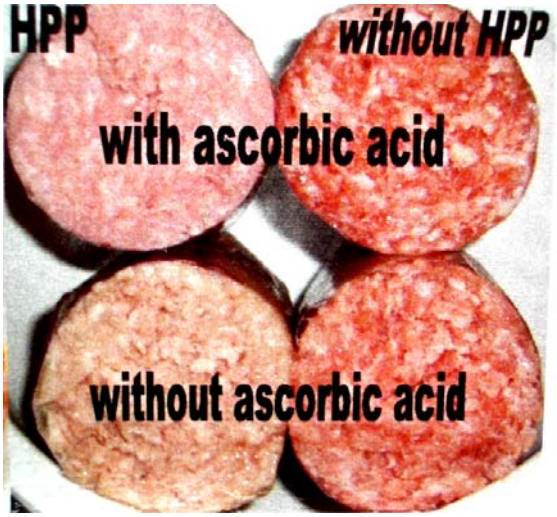

Figure 2.3-1 Treated and untreated minced pork with and without acid ascorbic (Adopted from Krzikalla *et al*., 2005)

In 1992, apple, strawberry and pineapple jams appeared on the japanese Market as the first commercial food products processed by high pressure technology. The commercialisation of orange and grapefruit juices using this technology was not successful due to the small market available for these products. However, since 1995, processing of rice cake, hypo-allergic rice and single portion cooked rice have been increased their production volume in the market. At the beginning of the year 2000, a high pressure research group works in collaboration with about 60 Japanese food companies to develop food in commercial scale (Suzuki, 2003). On the European and American markets, the commercialisation of pressurised products like orange juice (UltiFruit®, Pernod Richard Company, France), acidified avocado purèe guacamole (Avomex Company in the US, Texas/México), sliced ham, both cured-cooked and raw-cooked (España Company, Spain) in small scale has started (Tewari *et al*., 1999).

In a typical high pressure process, the product is packed in a flexible container, usually a plastic bottle, and is loaded into a high pressure vessel filled with a pressure-transmitting hydraulic fluid, which is normally water because of its compatibility with food materials. A mixture of water and ethyleneglycol can also be used. The hydraulic fluid is pressurised in the chamber with a pump, and this pressure is transmitted through the package into the food from all sides. High pressure process on food is carried out between 300 and 1000 MPa from 2 to 30 min at temperature ranges from 20 to 50°C. Because the pressure is transmitted uniformly in all directions simultaneously, the food product retains its shape, even at extreme pressures. As high heat is not required, the sensory characteristics of the food are retained (Earnshaw, 1996).

High hydrostatic pressure processing can affect a wide range of biological structures in food materials. This alteration can be used in the food industry as an antimicrobial effect and for modification of functional properties of food products (Kalchayanand *et al*., 1998; Datta and Deeth, 1999; Ghoshal *et al.*, 1999; Indrawati, *et al*., 2000; Touch *et al*., 2003).

2.3.1 Effect of high hydrostatic pressure on microorganisms

Microbial inactivation due to high hydrostatic pressure is based principally on the destruction or inactivation of microbial cells through a combination of physiological, biochemical and physical effects on microorganism. The efficiency of cell damage of microorganisms increases with the combined action of pressure, temperature, time of application and the characteristics of suspending media. The function and characteristics of the cell membranes of microorganism are destroyed because the macromolecules like polysaccharides and proteins are irreversibly modified leading to increased permeability of the membrane (Datta and Deeth, 1999). In addition, according to the mass transfer theory, the degree of mass transfer depends on pressure and resistance of the membrane. The pressurized cells show increased permeability. Then, more solvent can enter into the cell and compounds like organelles can permeate through the cell membrane (Shouqin *et al*., 2005). Bacteria, yeasts and molds are sensitive to pressurisation below 700 MPa in a temperature range between 45 and 50°C. However, to inactivate bacteria spores, for example from Clostridium botulinum, it is necessary to apply pressures of 500 to 700 MPa at a temperature range from 90 to 110 °C (Kalchayanand *et al.*, 1998). Because spore-forming bacteria and spores are destroyed only under certain high pressure conditions, the European Commission and the Food and Drug Administration FDA, have introduced regulatory laws leading to the introduction of new pressurized products. European food safety authorities, in order to ensure the highest level of protection of human health had published: “2001/424/EC: Commission Decision of 23 May

2001 authorising the placing on the market of pasteurised fruit-based preparations produced using high-pressure pasteurisation under Regulation (EC) No 258/97 of the European Parliament and of the Council (notified under document number C(2001) 1462) Official Journal L 151, 07/06/2001 P. 0042 – 0043".

2.3.2 Effect of high hydrostatic pressure on enzymes

Inactivation or activation of enzymes can be used in industry depending on the needed product properties. For example, stability of pectin methylesterase (PME) and α-amylase during juice clarifying are required to obtain high concentrations of carotene and flavours (Chen *et al*., 1987). However, inactivation of PME and polygalacturonase (PG) are necessary to retain viscosity in the tomato processing industry (Kalamaki *et al.* 2003), as well as to avoid cloud loss during juice and nectar storage (Corredig *et al*., 2001). The decrease in viscosity in tomato products is a direct consequence of the degradation of pectin substances by the endogens enzymes PME and PG (Hernández and Cano, 1998). Because PG induces the breakdown of the pectin molecules, it is the main cause for texture and viscosity loss, whereas PME leads to a cloud reduction in juices. Thus, an optimal treatment in tomato puree products should include a complete PG inactivation. However, PG is a very heat resistant enzyme, which needs high temperature with long time treatment for its inactivation (30 min at 90°C). At this condition, PME activity is destroyed, but change in colour, flavour, taste and nutritional quality are obtained. Crelier *et al*. (2001) proposed the use of high pressure and thermal treatment to achieve a complete inactivation of PME and PG in tomato pulp. The study showed that PME is a heat labile enzyme at atmospheric pressure and it is stabilised against thermal denaturation in a pressure range from 500 to 600 MPa, whereas PG, which is very resistant to thermal denaturation at atmospheric pressure, is easily inactivated by a combination of moderate pressure and temperature (400 MPa and 45°C).

In the last years high pressure treatment has also been applied to induce structural changes in globular protein substrates to increase enzyme-substrate binding. Traditionally, the application of reducing agents or urea was used to induce protein unfolding (Patel *et al.*, 2004) to expose potential substrate amino acid residues to the surface area (Touch *et al.*, 2003). Unfolding of some proteins using high pressure treatment has been successfully utilised (Nanoka *et al.*, 1997). However, there are proteins, which present a reversible behaviour under this treatment. For example, Møller *et al*. (1998) reported that after depressurisation from a treatment at a temperature range from 5 to 20°C and 150MPa for 30 min, renaturation of ß-lactoglobulin in TRIS buffer at pH 7.1 is observed. This is not in agreement with the study by Ikeuchi *et al*. (2001), who stated that at pH 7.0 and 20°C the

reaction is irreversible. However, at pH 2.0 and 20°C, pressure induces reversible denaturation of ß-lactoglobulin.

2.3.3 Effect of high pressure treatment on microbial transglutaminase

Kinetics studies of MTG under high pressure have also been undertaken by other authors. Lee and Park (2002) performed a Michaelis-Menten kinetic study in a reaction system of MTG with the synthetic specific substrate carbobenzoxy (CBZ)-L-glutamylglycine. The experiments were performed at 25°C in a pressure range from 0.1 to 500 MPa for 10 min. From the equation of straight line at 0.1 MPa a maximal velocity of 928 units and a K_m value of 24.5 mM are given. The results of the samples were treated at 0.1, 400 and 500 MPa demonstrated that the maximal velocity changes with pressure, while the affinity constants for all treatments are very similar, indicating that affinity constants were pressure independent and only the maximal velocities were affected (figure 2.3-2).

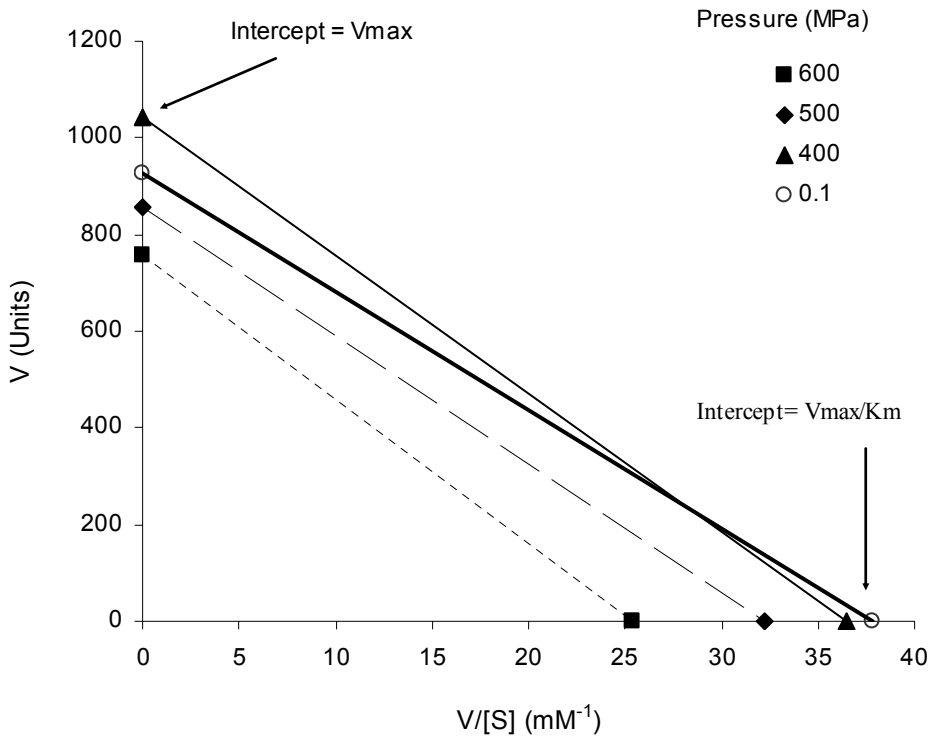

Figure 2.3-2 Hans-Augustinsson-Hofstee plot (V against $V/[S]$) of pressurized MTG at 400 to 600 MPa for 10 min (Adopted from Lee and Park, 2002, modified)

In addition, the enzyme maintains 60% of the initial activity even after pressurization at 600 MPa for 60 min. Lauber (2001) reported a loss of 50% enzyme activity at 40°C and 500 MPa after 15 min. The inactivation kinetic study performed in a temperature range from 20 to 60°C and a pressure from 0.1 to 600 MPa within a time range from 0 to 2 h, showed higher values

of pressure dependent rate constants with increasing temperature. Moreover, activation volumes of –7.1±0.4, -17.4±4.0 and –2.3±0.8 cm3/mol at 20, 40, 60°C respectively were reported by Lauber *et. al*. (2001). These results indicated that, in comparison with other endogens milk enzyme, MTG shows stability to high pressure. For example, alkaline phosphatase has activation volume of -65 cm^3/mol at 40°C (Rademacher, 1999).

2.3.4 Effect of high pressure on milk and milk products.

The first application of high pressure treatment on milk was used for preservation due to inactivation of microorganisms, but more recent studies have demonstrated that the changes on the protein functionality can be useful in the production of high quality milk products, such as cheese and yoghurt (Law *et al*., 1998; Lauber *et al.*, 2000; Keenan, *et al*., 2001; Farnsworth et al., 2002; Abbasi and Dickinson 2002)

High pressure treatment of skim milk leads to substantial changes in the whey protein fraction and disperses casein micelles into smaller structural units (Ikeuchi *et al*., 2000; Harte *et al*., 2003). Studies on goat's milk (Law *et al*., 1998) demonstrated that pressure treatment at 500 MPa and 20°C caused disruption of micelles into smaller particles with a higher solubility in the serum.

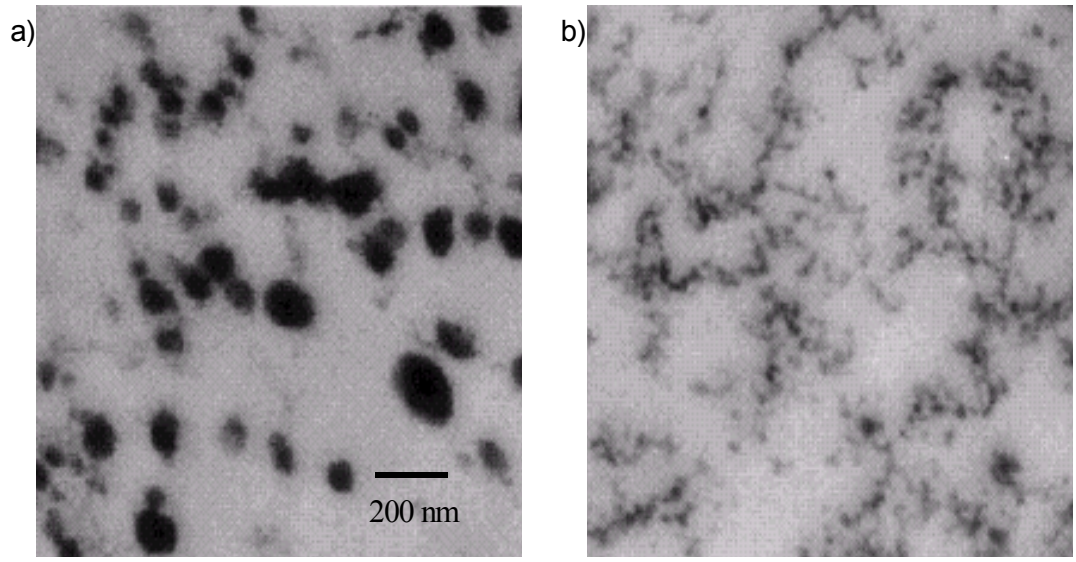

Figure 2.3-3 Transmission electron micrographs of spry dried milk powder before a) Native sample. b) Sample treated at 20°C and 400 MPa for 40 min (Adopted from Keenan *et al*., 2001).

In the figure 2.3-3 is showed that treatment at 45°C and pressures from 300 to 400 MPa results in casein aggregates, larger than the micelles in the original milk, whereas at 45°C and 500 MPa, disruption of the micelles with the formation of smaller and less easily to

sediment fragments are occurred. In investigations using spray dried milk powder (Keenan *et al*., 2001), it was observed that the application of pressures above 200 MPa led to an irreversible disintegration of casein micelles. The average diameter (measured by light scattering) of the particles produced after pressure treatment of skim milk becomes progressively smaller with increasing pressure up to 500 MPa. The protein network analysed by transmission electron microscopy shows a decrease of the average diameter of the native spherical micellar particles between 100 to 300 nm sizes after pressure treatment at 400 MPa.

2.3.5 Effect of simultaneous application of high pressure and microbial transglutaminase on casein

Because high pressure treatment causes micelle disintegration (Harte *et al*., 2003), it could be possible that higher numbers of potential glutamine residues could be exposed to the solvent able to react with MTG. This theory was investigated by Lauber *et al*. (2001), who found that in a sodium caseinate system isolate from skim milk, the addition of MTG under high pressure is capable to form covalent cross-linked proteins. Casein treatment at 400 MP without MTG showed no formation of new oligomers and the samples treated simultaneously at high pressure and enzyme (400 MPa with 1.5 U MTG/g protein) revealed an increase in the oligomerisation degree from 21 to 52%. Further experiments performed in a mixed system of ß-lactoglobulin and ß-casein under 400 MPa demonstrated that a part of the oligomerisation is consisting of heterodimers from ß-casein cross-linked with ß-lactoglobulin (Lauber *et al*., 2002).

Recent studies in our laboratory have investigated the MTG-reactive glutamine residues of ß-casein and ß-lactoglobulin under atmospheric and high pressure. Richter (2004), using ß-casein and triglycine as labelling reagent in the presence of MTG (4 U/g protein) at 0.1 MPa and 40°C for 1 h, suggested that potential MTG-reactive glutamine residues of ß-casein could be located at Gln (72 or 79 or 89), Gln (117 or 123 or 141 or 146 or 160 or 167), Gln182, and Gln (188 or 194 or 195). With an increasing MTG concentration to 20 U/g protein, seven reactive glutamines, Gln (72 or 79 or 89), Gln (117 or 123 or 141 or 146 or160 or 167), Gln182, and Gln (188 or 194 or 195) Gln54, Gln56, Gln184 were observed. Furthermore, Partschefeld (2005) found that there are no new MTG-reactive glutamines after ß-casein treatment at 400 MPa and 40°C for 1 h. However, ß-lactoglobulin labelled under the same conditions and incubated at 0.1 MPa and 40°C for 1 h shows no-reactive glutamines, but after treatment at 400 MPa at 40°C for 1h, Gln5, Gln13 Gln35 and Gln59 were exposed as new MTG-reactive glutamines (Richter, 2004).

Biochemical reactions involved in biological processes under high pressure lead to chemical and physical changes. In order to understand the inactivation and reaction kinetics of transglutaminase it is essential to give a broad overview of the thermodynamic principles (Klotz, 1986; Smith *et al*., 1997; Atkins, 2000; Hinrichs, 2000).

2.4 Thermodynamic in biological systems

In biological systems, many reactions are regarded as the conversion of substance A into B. These systems, representing a chemical transformation of A to B, are usually catalysed by an enzyme. Alternatively, A and B can be the same substance, and e.g. represent the structural change of a protein from the native state A to the unfolded state B. The state of the biological system is determined by the concentrations and the state functions temperature and pressure of A and B.

2.4.1 First Law of Thermodynamics

The First Law of Thermodynamics is the law of the conservation of energy. The energy of the universe is constant and the energy can be transferred from a system to its surroundings, or vice versa, but it cannot be created or destroyed. Instead, energy is converted from one form to another, for example work to heat, from heat to light or from chemical to heat.

The mathematical balance for the First Law of Thermodynamic is expressed by equation 2.4-1, as all the energy into a system ΔE_{System} is equal to the surrounding energy of the system $\Delta E_{Surrounding}$:

$$\sum E_{System} + \sum E_{Surrounding} = 0 \qquad \text{(eq. 2.4-1)}$$

Where, $E_{System} = \Delta U + \Delta E_K + \Delta E_P$ and $E_{Surrounding} \equiv \pm Q \pm W$

If, in a closed system, the kinetic energy change (ΔE_K) and the potential energy change (ΔE_P) are zero, then the work (W) done on a system and the energy transferred as heat (Q) to a system or vice versa, lead to a change in the internal energy given as:

$$\Delta U \equiv \pm Q \pm W \qquad \text{(eq. 2.4-2)}$$

In a biochemical system, when no material is exchanged with the surroundings, the system is closed and would proceed until an equilibrium state. The conversion of A into B is counterbalanced by an equal and opposite conversion of B to A, so, at the equilibrium, the net flux of A to B is zero (figure 2.4-1).

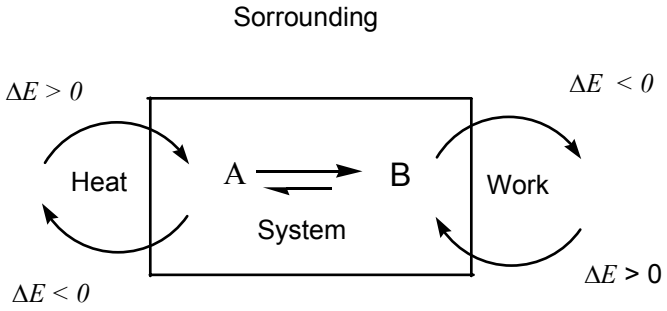

Figure 2.4-1 Energy balance in a closed system

As common convention $Q>0$ is employed, when heat is absorbed by the system and $W>0$, represents the work done by the system. Thus, the mathematical statement of the First Law of thermodynamic is expressed by the equation 2.4-3

$$\Delta U = Q_{rev} + W \qquad \text{(eq. 2.4-3)}$$

For infinitesimal changes in the internal energy:

$$dU = dQ_{rev} + dW \qquad \text{(eq. 2.4-4)}$$

The system and work

When the system $A \longrightarrow B$ involves a change in volume, the system has to do work on the surroundings corresponding to the net change in volume.

Mechanical work is defined by product of force, F, acting through a distance, dl : $dW = -Fdl$. The force, F, necessary to move a system can be determined by considering pressure, P, which is the application of force, F, to a surface, and the concentration of that force in a given area, A, is given by $P = \frac{F}{A}$ and the distance, dl, is the relation of the volume variation in a given area, which is $dl = \frac{dV}{A}$. Replacing, $dW = -P \cdot A \cdot \frac{dV}{A}$. Thus, the mathematical equation for work as a function of pressure and volume is given as:

$$\Delta U = Q_{rev} + W \qquad \text{(eq. 2.4-5)}$$

Then internal energy of the system is

$$dU = dQ_{rev} - PdV \qquad \text{(eq. 2.4-6)}$$

Enthalpy

The amount of heat given off or absorbed during a reaction is not equal to the change in the internal energy of the system, because some of the heat is converted into work, then dU is less than dQ and for this reason it was necessary to introduce the thermodynamic property, a functional state variable, Enthalpy H, which is the sum of the internal energy of the system plus the product of the pressure of the system times the volume of the system.

$$H \equiv U + PV \qquad \text{(eq. 2.4-7)}$$

At constant pressure, P, a volume change, dV, requires an amount of work equal to $P\Delta V$. When the volume change increases, dV, and hence PdV, is positive, so the work is done by the system. When the volume change decreases, dV, and hence PdV, is negative, so that work is done on the system. Consequently, the total work done by a system, Wt, is the sum of the work due to the net volume change, PdV, and the remaining, useful work, W: $Wt = W \pm PdV$. Then:

$$dU = dQ - W \pm PdV \qquad \text{(eq. 2.4-8)}$$

The function of $dU \pm PdV$ is know as the change in enthalpy dH

$$dH = dQ - dW \qquad \text{(eq. 2.4-9)}$$

At constant pressure with no additional work, the heat given off or absorbed during a chemical reaction is equal to the change in the enthalpy of the system.

$$dH = dQ \qquad \text{(eq. 2.4-10)}$$

2.4.2 Second law of thermodynamics

With the second law of thermodynamics, it is possible to identify whether one state is accessible from another by a spontaneous change and it can be expressed as the state function, Entropy, S.

Entropy

Entropy has a variety of thermodynamic and physical interpretations as a heat engine, a state function and a measure of disorder of a system.

Thermodynamic definition of entropy

During a reversible *(rev)* process in which an amount of heat dQ is applied at constant temperature, T, the thermodynamic definition of entropy is expressed by the mathematical equation

$$dS = \frac{dQ_{rev}}{T} \qquad \text{(eq. 2.4-11)}$$

The change of entropy, dS, in a system is defined as the heat absorbed from the surrounding, dQ, divided by the temperature, T, when the process is a thermodynamically reversible process. That means that during a chemical reaction, the temperature of the substance changes as heat is applied or extracted.

Entropy as a state function

A reversible reaction is considered if a system changes from an initial equilibrium state, i, to a final equilibrium state, f, and returning back to state, i, with net entropy change of zero. The mathematical interpretation is given as: $\Delta S_f = \Delta S_i$, the process is reversible:

$$dS = 0 = \int_i^f \frac{dQ}{T} \qquad \text{(eq. 2.4-12)}$$

An irreversible reaction is considered if the entropy of the final equilibrium state, *f*, is higher. The mathematical interpretation is given as $\Delta S_f > \Delta S_i$, the process is irreversible :

$$dS > \int_i^f \frac{dQ}{T} \qquad \text{(eq. 2.4-13)}$$

According to spontaneity criteria

The entropy change of the system plus the entropy change of the surroundings must increase: $\left(\frac{Q}{T}\right)_{System} + \left(\frac{Q'}{T}\right)_{sorrounding} > 0$, can be expressed as equation 2.4-14

$$\Delta S_{System} + \Delta S_{Sorrounding} > 0 \qquad \text{(eq. 2.4-14)}$$

Then, the process is spontaneous when:

$$\sum\left(\frac{Q}{T}\right) = \sum \Delta S > 0 \qquad \text{(eq. 2.4-15)}$$

and the process is at equilibrium when:

$$\sum\left(\frac{Q}{T}\right) = \sum \Delta S = 0 \qquad \text{(eq. 2.4-16)}$$

2.4.3 The Free Energy from the combination of the First and Second Laws of Thermodynamics

The combination of the First and Second Laws of thermodynamics as postulated by Gibbs and Helmholtz can evaluate the transformations of the reaction components without the changes in the surroundings. The state function is called free energy, ΔG.

The Helmholtz energy, A, is expressed by the equation:

$$A \equiv U - TS \qquad \text{(eq. 2.4-17)}$$

Where a change in a system at constant temperature and volume is spontaneous if:

$$dA_{T,V} \leq 0 \qquad \text{(eq. 2.4-18)}$$

Gibbs energy or free energy, G, expressed by equation:

$$G \equiv H - TS \qquad \text{(eq. 2.4-19)}$$

Where a change in a system at constant temperature and pressure is spontaneous if:

$$dG_{T,P} \leq 0 \qquad \text{(eq. 2.4-20)}$$

That means that a chemical reaction will proceed spontaneously if and only if the change in free energy is negative.

Influence of pressure and temperature on the system

When the pressure and temperature are not constant in the system, the change in Gibbs energy undergoes a thermodynamic change

$$G \equiv H - TS \equiv U + PV - TS \qquad \text{(eq. 2.4-21)}$$

For infinitesimal changes: $dG = dU + PdV + VdP - TdS - SdT$, where $dU = TdS - PdV$

After substitution and elimination of terms, the following equation is achieved:

$$dG = VdP - SdT \qquad \text{(eq. 2.4-22)}$$

The equation states that a change in Gibbs energy G is proportional to changes in pressure, P, and temperature, T. At constant temperature or pressure the mathematical expressions are achieved:

$$\left(\frac{\partial G}{\partial P}\right)_T = V \qquad \text{(eq. 2.4-23)}$$

$$\left(\frac{\partial G}{\partial T}\right)_P = -S \qquad \text{(eq. 2.4-24)}$$

Temperature dependence of free enthalpy at constant pressure

It is known that the equilibrium of a system depends on the Gibbs energy G and to know how this energy varies with temperature, it is expressed as the G variation in terms of the Entropy S.

At constant pressure $\left(\frac{\partial G}{\partial T}\right)_P = -S$ and from the combination of the both laws according to enthalpy energy $S \equiv -\frac{G-H}{T}$ results:

$$\left(\frac{\partial G}{\partial T}\right)_P = \frac{G-H}{T} \qquad \text{(eq. 2.4-25)}$$

The equilibrium constant of a chemical reaction is related to G/T rather than to G itself. The Gibbs-Helmholtz equations show how G/T changes with temperature. Solving different partial derivates the Gibbs-Helmholtz equation is applied to changes of the physical state and the chemical reaction at constant pressure, it can be written as:

$$\left(\frac{\partial(\Delta G/T)}{\partial T}\right)_P = -\frac{\Delta H}{T^2} \qquad \text{(eq. 2.4-26)}$$

Pressure dependence of Free Enthalpy at constant temperature

The pressure dependence of Gibbs free energy in a closed system is given by the combined first and second laws and the definition of Gibbs free energy $dG = VdP - SdT$ as discussed from the equation 2.4-22.

At constant temperature $dT=0$ and after the integration of the remaining terms $G_{P_f} - G_{P_i} = V\int_{P_i}^{P_f} dP$ (P_i = initial pressure, P_f = final pressure)

For not very compressible solids and liquids the volume can be regarded as constant:

$$G_{P_f} = G_{P_i} \qquad \text{(eq. 2.4-27)}$$

For slightly compressible solids and liquids the isothermal compressibility can be defined as:

$$\kappa = \frac{1}{V}\left(\frac{\partial V}{\partial P}\right)_T \qquad \text{(eq. 2.4-28)}$$

So, with κ regarded at constant temperature T, an expression for volume V, as a function of pressure P can be found.

2.4.4 Transition theory in reaction kinetics

The central concept of the transition-state theory is that reactants or native protein structures are in equilibrium with a transition state species, which then proceeds to create products or unfolded proteins (Klotz, 1986). In general, unimolecular reaction can be represented by:

$$A \overset{K^*}{\longleftrightarrow} A^* \longrightarrow B \qquad \text{(eq. 2.4-29)}$$

Where $K^* = \frac{[A^*]}{[A]}$ defines the equilibrium constant for the formation of the transition state species.

Temperature and pressure dependence of the system can be analysed using the Gibbs free energy or free activation enthalpy, ΔG^*.

$$\ln K^* = -\frac{\Delta G^*}{RT} \qquad \text{(eq. 2.4-30)}$$

Temperature dependence of the rate constant

According the First and Second Laws of Thermodynamics: $\Delta G^* = \Delta H^* - \Delta S^* T$ (from equation 2.4-19) is valid. Where ΔH^*, ΔS^*, are the enthalpy and entropy difference between the transition state of a reactant or protein and the ground state of the reactant or native protein, respectively.

Inserting $\Delta G^* = \Delta H^* - T\Delta S^*$ in equation 2.4-29 results in $\ln K^* = -\frac{\Delta H^* - T\Delta S^*}{RT}$

In addition, considering that rate constant $\frac{k_{P,T}}{k_{P,0}}$ is proportional to the quasi equilibrium constant K^* of the active complex formation, are obtains:

$$\ln \frac{k_{P,T}}{k_{P,0}} \propto \left(\frac{-\Delta H^* - T\Delta S^*}{RT}\right) \propto \left(\frac{\Delta S^*}{R}\right) \cdot \left(\frac{-\Delta H^*}{RT}\right) \qquad \text{(eq. 2.4.31)}$$

Then, the Eyring equation is obtained:

$$\ln \frac{k_{P,T}}{k_{P,0}} = \left(\frac{-\Delta H^*}{RT}\right) \text{ and } \ln \frac{k_{P,T}}{k_{P,0}} = \frac{k_B T}{h}\left(\frac{-\Delta S^*}{R}\right)$$

Where the Eyring equation shows that ΔH^*, ΔS^* are analogue amounts and can be related with the Arrhenius equation, $\ln \frac{k_{P,T}}{k_{P,0}} = -\frac{Ea}{RT}$.

Then:

$$\ln \frac{k_{P,T}}{k_{P,0}} = \left(\frac{-\Delta H^*}{RT} \right) = \left(\frac{-E_a}{RT} \right) \qquad \text{(eq. 2.4-32)}$$

Pressure dependence of the rate constant

As the volume change for the reaction ΔV is the parameter that emerges from an analysis of the pressure dependence of the equilibrium, the parameter derived from the pressure dependence of the rate constants is the activation volume for the reaction ΔV^*.

At constant temperature the Gibbs free energy is equivalent to pressure times the volume change: $\Delta G^* = P \cdot \Delta V^*$. In association with $\ln K \approx \ln \frac{k_{P,T}}{k_{0,T}}$, equation 2.4.31 turns into:

$$\ln \frac{k_{P,T}}{k_{0,T}} \cong -\left(\frac{\Delta G^*}{RT} \right) = -\left(\frac{\Delta V^*}{RT} \right) P \qquad \text{(eq. 2.4.33)}$$

The pressure dependence of the rate constants is expressed in terms of the activation volume, ΔV^* and indicates the variations in volume on the way to the transition state and is also dependent of the quasi equilibrium constant, K^*, or rate constant, $k_{P,T}$.

Reaction and activation volumes interpretation

The volume change in a biochemical reaction is the difference between the final volume state V_B (volume of product or unfolded protein) and initial volume states V_A (volume of reactant or native protein), which is given by:

$$\Delta V = V_B - V_A \qquad \text{(eq. 24.34)}$$

Analogous expressions between volume change and the activation volume can be derived from the equilibrium constant *(K)* and the rate constant *(k)* of a general unimolecular reaction (equation 2.4-35 and 2.4.36), which are visualised in figure 2.4-2:

$$\Delta V = \left(\frac{\partial \Delta G}{\partial P} \right)_T = -RT \left(\frac{\partial \ln K}{\partial P} \right)_T \qquad \text{(eq. 2.4.35)}$$

$$\Delta V^* \cong \left(\frac{\partial \Delta G^*}{\partial P}\right)_T = -RT\left(\frac{\partial \ln k}{\partial P}\right)_T \qquad \text{(eq. 2.4-36)}$$

Pressure effects on chemical and biochemical reactions are governed by Le Chatelier´s principle, which states that at equilibrium a system tends to minimize the effect of any external factor by which it is perturbed (Tauscher, 1995). Consequently, the application of pressure to a system in equilibrium favours a reduction in volume to minimize the effect of pressure. Thus reactions which results in a decrease of volume, $\Delta V<0$, are enhanced by pressure, while reaction resulting in a positive reaction volume, $\Delta V>0$, are slowed down by pressure (Jaenicke, 1983).

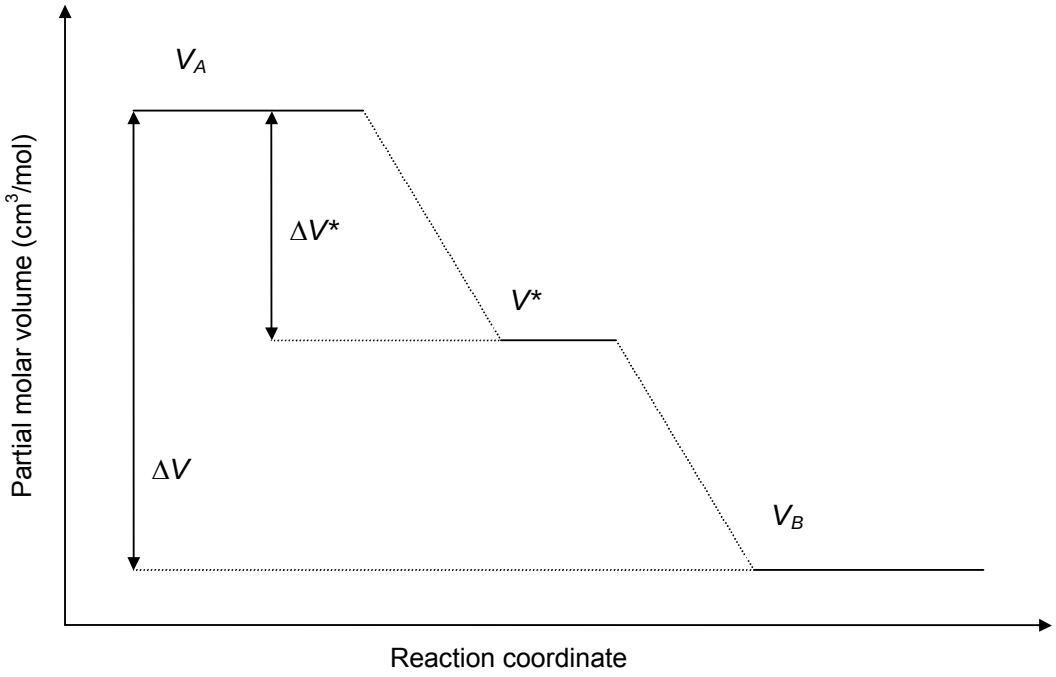

Figure 2.4-2 Example of a volume profile of a general unimolar reaction $A \longleftrightarrow A^* \longrightarrow B$ at high pressure (Tauscher, 1995).

The reaction volume ΔV in biochemical system can be interpreted by combination of the pressure response of a dissolved substance and the interaction of this substance with the solvent. The several intrinsic contributions occur as a consequence of changes in free volume due to the packing density and the formation or breaking of covalent bonds of molecules (Tauscher, 1995). The solvation contributions occur as any change in volume associate with changes in polarity, electrostatic and dipole interaction of molecules with the solvent during the reaction. Mozhaev *et al*. (1996) and Jaenicke (1983) reported that bond formation, charge separation and concentration of equal charges, hydration of polar and

hydrophobic groups and protein denaturation results in a volume contraction, whereas bond scission, protonation and ion par formation, protein association results in volume expansion (table 2.4-1).

Table 2.4-1 Volume changes, ΔV, associate with relevant biochemical reactions at 25°C (Jaenicke, 1983)

Bond type	Reaction	ΔV (cm^3/mol)
Protonation/ion pair formation	Protein-COO^- + H^+ ⟶ Protein-COOH	+10.0
	Protein-NH_3^+ + OH^- ⟶ Protein-NH_2 + H_2O	+20.0
Hydrogen bond	Poly-lysine	-1.0
Hydrophobic hydration	C_6H_6 ⟶ $(C_6H_6)_{water}$	-6.2
Hydration of polar groups	n-Propanol ⟶ $(\text{n-Propanol})_{water}$	-4.5
Protein association	Microtubule formation	+90.0
Protein denaturation	Myoglobin (pH 5, 20°C)	-98.0

2.5 Effect of pressure and temperature on biochemical reactions

The water contained in biological system interacts with proteins, amino acids, carbohydrates and sugars, salt as well as other components of the matrix. Because pressure induces ionisation of water and solutes, the charge state of molecules is influenced. In particular, proteins can be affected, leading to reversible or irreversible unfolding, because the weakest non-covalent interactions between amino acid residues, that support the protein tertiary structure, are first destabilized and then replaced by protein-water interactions (Mozhaev *et al*., 1996).

The increase or decrease of the dissociation volume of the solvent (ΔV_a) and the inactivation volume (ΔV^*) or change in total volume (ΔV) of a protein caused by high pressure, is a consequence of bond breaking, formation of new bonds or changed salvation of amino acids group, which reflect the different changes of the intermolecular forces on molecules (Barciszewski *et al*., 1999). For this reason, the knowledge of the ionisation volume of water and buffer, as well as the activation volume and volume change of proteins over a range of pressures and temperatures give a thermodynamic description of a biochemical reaction.

2.5.1 Effect of pressure and temperature on water and buffer solutions

Application of high hydrostatic pressure forces ice and liquid water to adopt structures that are more compact. Water is nearly incompressible only to 4 vol% at 100 MPa and 22°C and to 15 vol% at 600 MPa and 22°C (Tauscher, 1995). At low temperature, the solid water (ice) is the stable phase, at moderate temperatures and high pressure, the liquid water, is the stable phase and at high temperature and low pressure, vapour water (gas), is the stable phase. Phase transition of water depends on pressure, for example, at –10°C and 0.1 MPa (atmospheric pressure) water is solid. However, at –10°C in a pressure range from about 150 to 450, water is liquid, as is illustrated in the phase diagram of water (figure 2.5-1). The water exposed to pressure does not freeze at 0°C because the transition of the liquid to the ice is accompanied by an increase in volume, which counteracts pressure (Smith *et al*., 1997).

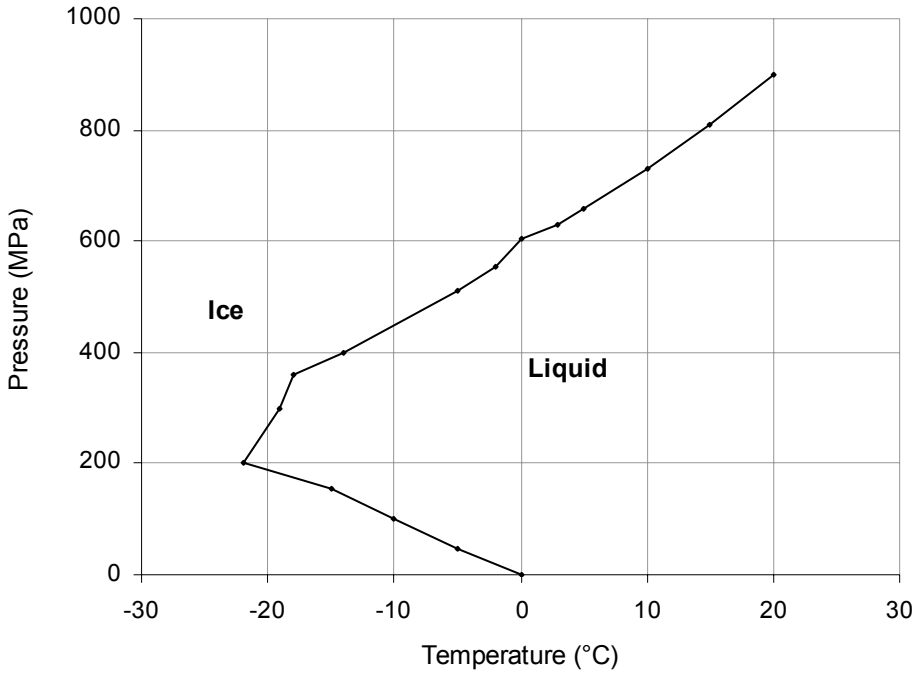

Figure 2.5-1 Phase diagram of water (Adopted from Smith *et al.*, 1997, modified)

Self-ionisation of water is promoted by pressure; the ionisation volume of water is –22.2 cm^3/mol at 25°C. Volume contraction is brought about by strong electrostriction around the formed ions (Tauscher, 1994). From the ionisation reaction of water, equilibrium constant is obtained, which is called ionisation constant or dissociation constant symbolised by K_w.

$$2H_2O \underset{}{\overset{K_w}{\rightleftharpoons}} H_3O^+ + OH^- \qquad \text{(eq. 2.5.1)}$$

Absolutely pure water is neutral, although even traces of impurities could shift the pH value. The constant K_w is sensitive to pressure and temperature and increases with rise of these

parameters. For this reason, the pH of non-absolute pure water can be modified with a change of these variables.

The pH of weak acids can be altered by temperature and pressure processing. The ionisation constant of weak acids increases with increasing applied pressure, leading to change of pH and volume of aqueous buffer solutions under high pressure (Zipp and Kauzmann, 1973; Neuman *et al*., 1973; Stippl *et al*., 2005).

The pressure dependence of the dissociation constant K_a gives the apparent volume change for the ionisation volume, ΔV_a, of an acid (Zipp and Kauzmann, 1973).

$$HA \rightleftharpoons A^- + H^+ \qquad \text{(eq. 2.5.2)}$$

Where $\left(\frac{\partial \ln K_a}{\partial P}\right)_T = -\frac{\Delta V_a}{RT}$

Hence, the changes of ln Ka and ΔV_a values are pressure dependent. When the buffer concentration is high (above 0.05 M), pressure-induced changes in pH do not significantly alter the concentration ratio term and can be attributed directly to changes in pK_a, then, $\frac{\partial(pH)}{\partial P} \approx \frac{\partial(pK_a)}{\partial P}$

Neuman *et al.* (1973) reported the pH changes of TRIS, acetic acid, cacodylic acid and phosphate buffer solutions as pressure dependences of the ionisation constants at constant temperature (figure 2.5-2). Increases in ΔpK_a values for acetic acid, cacodylic acid, and phosphate are obtained with increasing pressure. However, the ΔpK_a of TRIS had a non-significant decrease. In terms of the ionisation equilibrium, acetic acid, cacodylic acid, and phosphate, increase the number of formal charges under high pressure treatment, whereas acid dissociation of TRIS·HCl occurs without a change in the number of charged species:

$$TRISH^+ + H_2O \longrightarrow TRIS + H_3O^+ \qquad \text{(eq. 2.5.3)}$$

Dissociation with charge formation leads to a substantial volume concentration due to solvation effects and processes characterized by volume decreases. Reactions with little

volume change are less pressure dependent (Zipp and Kauzmann, 1973; Neuman *et al*., 1973, Tauscher, 1995).

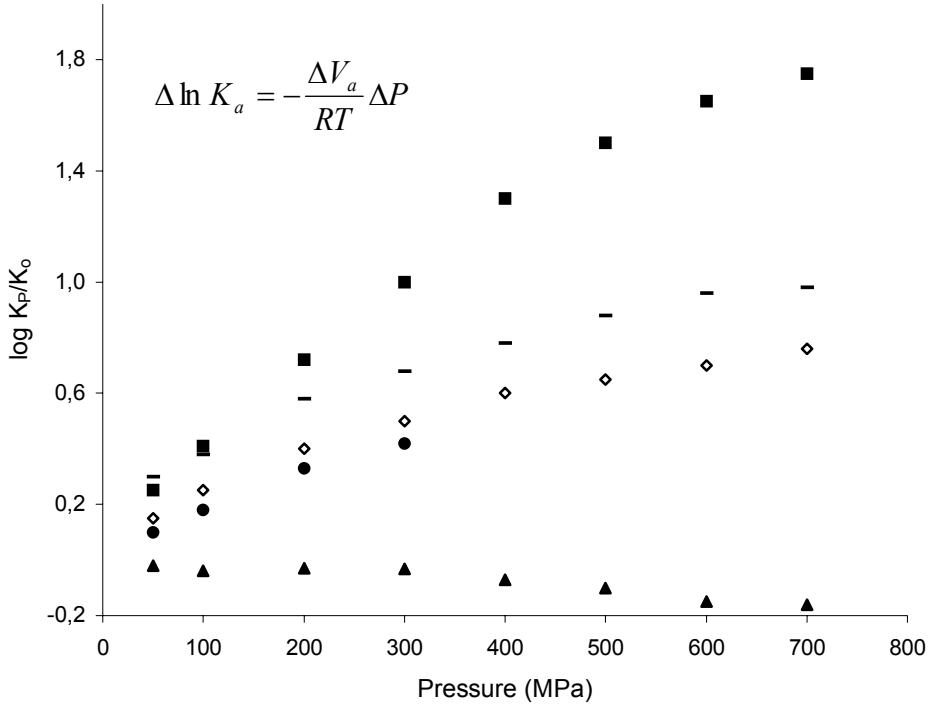

Figure 2.5-2 Pressure dependence of ΔlnK_a of calculated values of log K_P/K_0. (■) phosphate. (-) indicator *p*-nitrophenol, (◇) cacodycil acid, (●) acetic acid (▲) TRIS (Adopted from Neuman *et al*.,1973, modified).

Along with the ionisation of water and buffer, the solvation of proteins is influenced with corresponding effects on the protein structure and volume. (Rasper and Kauzmann, 1961; Kauzmann *et al*., 1961). The protonation and ionisation behaviour of water and some buffers under high pressure are listed in table 2.5-1.

Table 2.5-1 Dissociation volume of different buffers

Reaction	ΔV_a (cm^3/mol)	Reference
$H^+ + OH^- \longrightarrow H_2O$	+21.3 +22.2	Jaenicke (1983) Tauscher (1995)
$TRISH^+ + H_2O \longrightarrow TRIS + H_3O^+$	+1	Neuman *et al*. (1973)
$Imidazole + H^+ \longrightarrow Imidazole\text{-}H^+$	-1.1	Jaenicke (1983)
$H_2PO_4^{2-} + H^+ \longrightarrow H_2PO_4^-$	-25.3 -25.9	Neuman *et al.* (1973) Tauscher (1995)
$CO_2 + 2H_2O \longrightarrow HCO_3^- + H_3O^+$	-29.2	Tauscher (1995)

2.5.2 Effect of pressure and temperature on protein unfolding

The native conformation of protein molecules (N) in aqueous solution is only stable within restricted conditions (Kauzmann *et al.*, 1961) of temperature, pressure and solvent composition (ion strength and pH). When one of these conditions is modified, the non-covalent intramolecular interactions such as hydrophobic, van der Waals, electrostatic, ionic and hydrogen bonding, which stabilise the native state, are affected and a reversible or irreversible unfolding or denaturation (U) is initiated (Schulz and Schirmer; 1979; Urzica, 2004).

Protein unfolding or denaturation at high pressure is characterized by a negative molar volume change, $-\Delta V$ (figure 2.5-3). The negative volume change upon unfolding is originated from closer interactions between the polypeptide chains and water including hydration of the polypeptide backbone and amino acid side chains with the concomitant elimination of packing defects (Frye, 1998).

Native protein (N) $\xrightarrow{\quad -\Delta V \quad}$ Denatured protein (U)

Figure 2.5-3 Representation of a non-reversible protein unfolding reaction.

High temperature induces irreversible protein denaturation, because original disulfide bonds are destroyed, whereas these covalent bonds are pressure insensitive (Mozhaev *et al*., 1996). However, the effect of pressure and temperature is a complex phenomenon. Hawley (1971), for example, reported that high pressure induces protein denaturation, whereas moderate pressure may stabilize the native form.

The effect of pressure, P, and temperature T, on protein stability can be analysed using kinetic and thermodynamic parameters to perform a phase diagram *(P, T)*. A phase diagram of a protein represents the transition phase between the native and unfolded state over a range of pressures and temperatures. Calculation of Gibbs free energy by the relation $\Delta G = -RT \ln K$ (from equation 2.4-30) is used to obtain the kinetic data for the transition phase at constant ΔG. The equilibrium between these native and unfolded states occurs when there is no difference between the Gibbs free energy of both states ($\Delta G=0$). Since $d\Delta G = \Delta V dP - \Delta S dT = 0$ (from equation 2.4-22) along such a line, the Clausius-Clapeyron relation is obtained:

$$\frac{dP}{dT}_{\Delta G=0} = \frac{\Delta S}{\Delta V} \qquad \text{(eq. 2.5.4)}$$

The stability of chymotrypsinogen, in a pressure range from 0.1 to 400 MPa and temperature range from 0 to 50°C at a constant pH 2.07 (Hawley, 1971), is cited to represent an example of a phase diagram (figure 2.5-4). Remembering that, at atmospheric pressure the transition occurs with $\Delta S>0$, whereas at constant temperature the transition occurs with $\Delta V<0$. Then, since the slope from the relation $\frac{dP}{dT}_{\Delta G=0}$ is positive, the volume change, ΔV, is shifted towards positive values with increasing pressure. At about 160 MPa, the transition temperature is pressure independent$\left(\frac{dP}{dT}_{\Delta G=0} = 0\right)$, thereby indicating that $\Delta V=0$ at this point. At about 25°C the transition pressure becomes temperature independent$\left(\frac{dP}{dT}_{\Delta G=0} = 0\right)$, indicating that $\Delta S=0$.

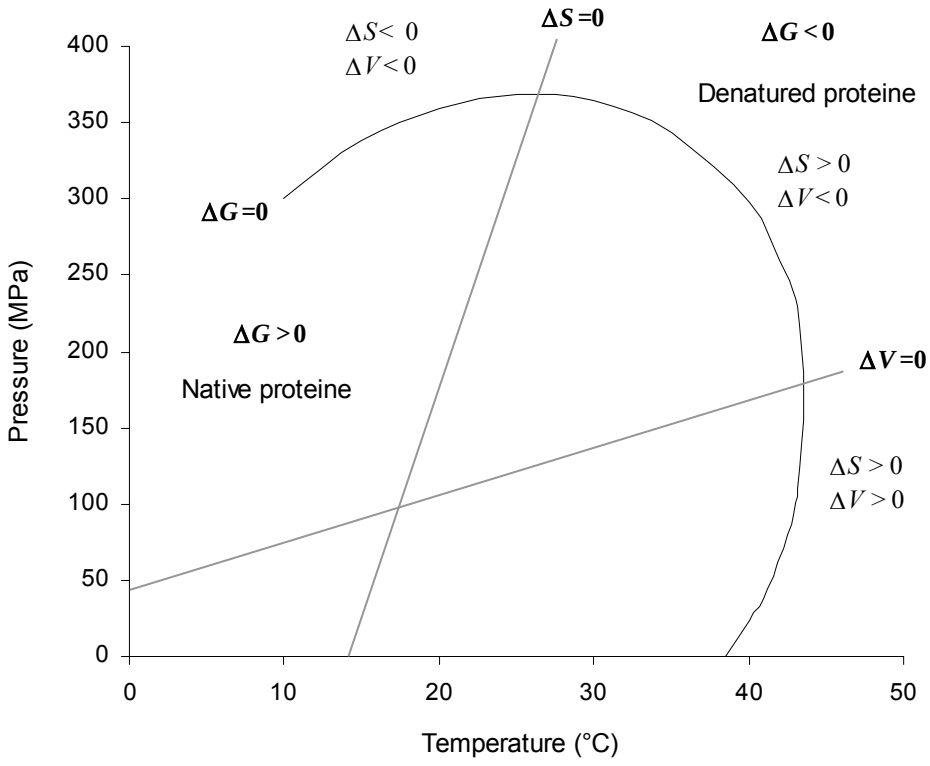

Figure 2.5-4 Phase diagram of pressure temperature transition map of a protein (Adopted from Hawley, 1971, modified)

Pressures below 150 MPa cause a reversible or irreversible change of quaternary structures of proteins by favouring the dissociation of oligomers. The increase of conformational fluctuations leads to increased water and solvent exchange with the protein interior. Pressures of about 200 MPa cause significant changes of tertiary structure. Application of 700 MPa could cause a loss of secondary structure and protein aggregation leads to a non-reversible denaturation process. However, pressures between 400 and 800 MPa cause reversible unfolding of small proteins. Although high pressure induces protein denaturation, covalent bonds are unaffected up to 1000 MPa (Datta and Deeth, 1999). In addition pressure denatured proteins retain elements of their secondary structure, while the heat denatured proteins have nearly complete random coil configuration (Urzica, 2004).

Table 2.5-2 Numbers of hydrogen bonds in bovine pancreatic trypsin inhibitor at high pressure

Bond	crystal	Low pressure (0.1 MPa)	High pressure (1000 MPa)
whole protein	33.31	35.4±2.0	38.0±2.8
total O···HN	23.21	25.5±2.0	27.02±2.1
O···side chain	3.3	6.0±1.1	8.5±1.4
N···side chain	4.4	4.5±0.8	4.6±0.8
side chain – side chain	2.3	3.4±1.2	3.8±0.9
$C^*_{(side\ chain)}$ ··· water		9	28

H, O, N represents hydrogen, oxygen, nitrogen backbone atom. C* represent the excluded backbone carbons.

Jaenicke (1983), based on reaction volumes from some representative biochemical reactions (table 2.5-2), suggested that ion pairs and hydrophobic interactions are the most important targets of high pressure effects and hydrogen bonds are less important, whereas Kitchen *et al*. (1992), based on solvation study of amino acid residues from bovine pancreatic trypsin inhibitor, suggested that hydration of the protein molecules as well as hydrogen bond formation has influence on protein unfolding. The number of backbone to backbone hydrogen bonds increases from 25 at low pressure (0.1 MPa) to 27 at high pressure (1000 MPa). However, the total number of excluded backbone carbons increase from 9 at low pressure (0.1 MPa) to 28 to high pressure (1000 MPa) as is shown in table 2.5-2. Solvation numbers of carbon, oxygen and nitrogen atoms in the molecule increase with increasing pressure, but the most notable change was the increase of the solvation shell around the hydrophobic groups.

2.5.3 Protein stability as a function of pressure, temperature and pH

As described previously, unfolding or denaturation of proteins is a function of pH, temperature, T, and pressure, P. For this reason, it is important to describe the simultaneous effect of these variables on protein denaturation in a phase diagram.

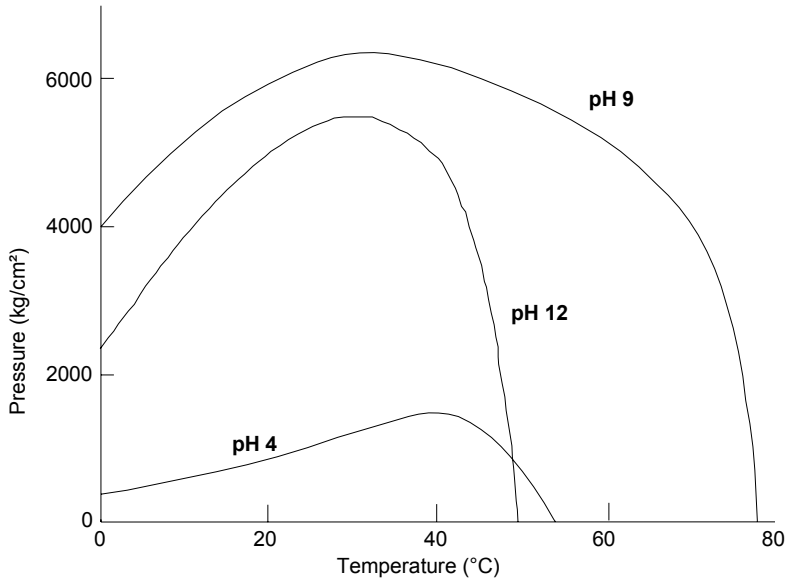

Figure 2.5-5 Phase diagram of pressure temperature transition map of metmyoglobin. Contour of different constant pH in the pressure-temperature plane at which $\Delta G=0$ for the denaturation of protein (Adopted from Zipp and Kauzmann, 1973, modified).

Zipp and Kauzmann (1973) investigated the denaturation of metmyoglobin at pressures from 0 to 600 MPa, temperatures from 0 to 80°C and a pH range from 4 to 12. The constant pH contours represent a phase diagram *(P, T,* pH*)* on which $\Delta G=0$ for the denaturation reaction (figure 2.5-5). Each curve represents that at any pH range there is a range in pressure in which the protein undergoes the transition change: Native $\rightarrow$ Denatured. The plot shows that the pH maximum stability depends in a complex manner on temperature and pressure. For example, metmyoglobin at pH 9 and 25 °C is stable until about 620 MPa, whereas at pH 9 and 60°C it is stable until about 500 MPa. At pH 12 and 25°C, however, the protein is stable until about 530 MPa, and at pH 12 at 0.1 MPa (atmospheric pressure) and temperatures above 50°C the protein occurs in the denatured state. The metmyoglobin in figure 2.5-5 presents a maximal stability toward pressure and temperature at pH 9, whereas at pH 4 it shows a very low stability range. Volume changes for denaturation of metmyoglobin, calculated at 20°C on the equilibrium, were -60, -100 and -155 mL/mol at pH 10, ~6 and ~4 respectively, because the negative reaction volume indicates pressure-induced protein

denaturation, it was demonstrated that protein stability depends on pressure as well as on temperature and pH.

2.5.4 Effect of high hydrostatic pressure and temperature on enzyme

Enzymes are proteins or protein complexes, which catalyse biochemical reactions. The effect of high pressure on enzymes and their inactivation mechanisms is similar to protein denaturation processes (Urzica, 2004). However, depending on the enzyme structure, substrate or enzyme-substrate binding, high pressure can increase or decrease the rate of enzyme-catalysed reactions (Datta and Deeth, 1999).

Table 2.5-3 Reaction volumes of enzyme inactivation under high pressure

Enzyme	Temperature (°C)	Pressure (MPa)	pH	ΔV (cm^3/mol)	Reference
Lysozyme from egg	23	0,1-1100	7.6	-19.7	Li *et al*. 1976
	69	0,1-500	3.9	-10.5	Samarasinghe *et al*.,1992
PME from banana	60	700-900	7.0	-55.8	Ly-Nguyen *et al.*, 2003
PME from carrot	10	600-700	7.0	-54.7	Ly-Nguyen *et al*., 2002b
PME from orange	10	400-900	7.0	-24.6	Van den Broeck *et al*.,1999
PME from strawberry	10	850-1000	7,0	-10.8	Ly-Nguyen *et al*., 2002a
Lypoxygenase from green bean	10	200-700	6.1	-27.5	Indrawati *et a*l., 2000
	20			-29.8	
	40			-19.8	

PME Pectin methylesterase

Oligomeric enzymes can be inactivated at low pressure (<200 MPa) by oligomer dissociation and unfolding of hydrophobic groups (Silva *et al.*, 1986, Paladini and Weber, 1993, Gorovits *et al*., 1994). For example, investigations of Zhou *et al*. (2000) reported that the activity of cytoplasmatic creatine kinase depends on its dimeric state. However, this criterion can not be always generalized, as demonstrated by Tanaka *et al*. (2001), who found that the pressure increase in a range from 0.1 to 400 MPa perturbs the local structure of sweet potato ß-amylase without dissociation of its tetrameric structure. Monomeric enzymes can be more

stable and it is necessary to apply higher pressure for their inactivation (Jaenicke, 1983). Enzyme inactivation by high hydrostatic pressure has been investigated by several research groups and generally reported as inactivation volumes, ΔV^*, (table 2.5-3).

After the literature review is stated that the changes on the activation volumes of proteins and enzymes induced by pressure are the result of changes on their conformational structure. The structural changes of proteins in aqueous solutions can be calculated using different methods, for example, Circular Dichroism Spectroscopy, Fourier Transform Infrared Spectroscopy and Nuclear Magnetic Resonance Spectroscopy. In this work, circular dichroism is presented.

2.6 Circular dichroism fundamentals

Circular dichroism (CD) is the difference between the absorption of the left (A_L) and right (A_R) handed circularly-polarised light in chiral molecules and is measured as a function of wavelength.

2.6.1 Principle

Linear and circular polarised light

Light in the form of a plane wave in space is said to be linearly polarised. Light is a transverse electromagnetic wave, but natural light is generally un-polarised, all planes of propagation being equally probable. If light is composed of two plane waves of equal amplitude, differing in phase by 90°, then the light is said to be circularly polarized (figure 2.6-1). If two plane waves of differing amplitude are related in phase by 90°, or if the relative phase is other than 90°, then the light is said to be elliptically polarized.

When circularly polarised light passes through a solution containing an optically active substance, the left and right circularly polarised components of the plane polarised light are absorbed by different amounts as A_L and A_R, respectively. When the remaining components of the light are recombined, they appear as elliptically polarized light (figure 2.6-2).

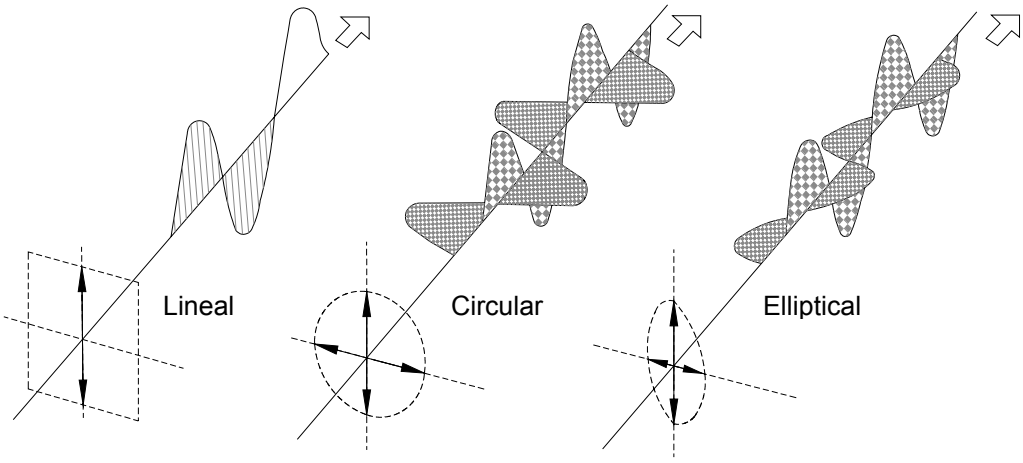

Figure 2.6-1 Linear and circular polarised light.

The difference in the left and right handed absorbance is in the range of 0.0001 absorbance units, corresponding to an ellipticity, of a few 1/100th of a degree. The ellipticity term is defined by θ.

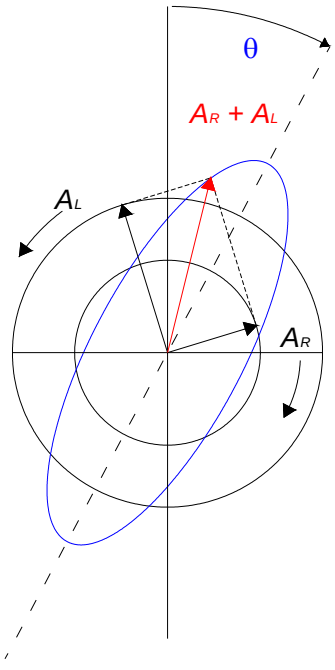

Figure 2.6-2 Schematic representation of linear polarised light as a superposition of opposite circular polarized light of equal amplitude and phase. A_L and A_R represent the absorption of left and right circular polarised light of the active substance. The sum of the vectors results an ellipse θ.

The raw data plotted on the chart recorder represent the ellipticity of the sample in radians: $\theta_r = \frac{2.303}{4}(A_L - A_R)[rad]$, which can be converted into degrees $\theta_d = \frac{2.303}{4}(A_L - A_R) \cdot \frac{180}{\pi}[rad]$.

Mean molar ellipticity per residue is used to compare ellipticity values of proteins and peptides:

$$\theta_{mr} = \theta_d \cdot \frac{M}{c \cdot l \cdot n_r} \qquad \text{(eq. 2.6-1)}$$

Where l, is path length, c concentration, M molecular weight an nr number of residues. The units of CD spectroscopy are reported in decimol: $\theta_{mrd} = \frac{\theta_{mr}}{10}\left[\frac{\deg \cdot cm^2}{dmol \cdot residue}\right]$

2.6.2 CD spectra of proteins

Biological macromolecules such as proteins are composed of chiral molecules, which are optically active elements, and because they can adopt different types of three-dimensional structures, each type of molecule produces distinct CD spectra.

CD in the far ultraviolet

CD spectra in the far ultra violet region (190-250 nm) are widely used for the characterisation of secondary elements of the protein structure. At these wavelengths, the chromophore is the peptide bond, and the signal arises when it is located in a regular, folded environment.

Amide chromophore

The amide chromophore along with the direction and magnitude of the $n-\pi^*$ and $\pi-\pi^*$ transition moments of the amide group is shown in the figure 2.6-3. The $n-\pi^*$ transition involves non-bonding electrons of oxygen atom of the carbonyl and $\pi-\pi^*$ transition involves the π electrons of the carbonyl and intensity and energy of these transitions depends on Ψ and Φ angles that means, of the secondary structure (Moffitt, 1956).

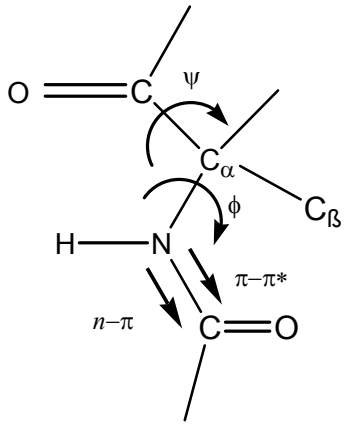

Figure 2.6-3 The amide bond of the polypeptide backbone shown with the moments of the $n-\pi^*$ and the $\pi-\pi^*$ transition (Adopted from Moffitt, 1956).

Structure stability of the peptide bond, can be explained by the electronic resonance character of the O=C-N structure. Pauling and Corey (1951), reported, as shown in figure 2.6-4, that in the structure I the C-N bond contains only axial symmetric σ–electrons allowing free rotation, whereas structure II has σ and π- electrons in the C-N bond giving rise to a large dipole moment and inhibiting rotation.

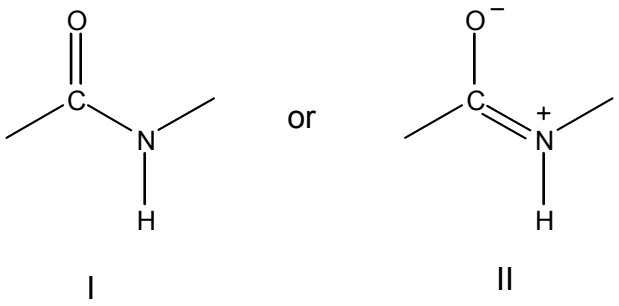

Figure 2.6-4 Electronic resonance character of peptide bond due to the π like molecular orbital that extends over O-C-N. I represent σ–electrons. II represent σ and π- electrons (Adopted from Pauling and Corey, 1951)

A polypeptide chain in solution folds up according to the polarity of the side chains it contains and the rotation of the peptide backbone bond angels is largely determined by Van der Waals radii of the side chain. The torsion angles define the tilt between two neighbouring amide planes, the plane of the peptide bond with the Cα at the center of the rotation. The two bonds in which rotation is allowed: R—Cα—NH, known as the Φ bond and the CO—Cα—R known as Ψ bond (Nosoh and Sekiguchi, 1991). Thus, backbone conformation of a peptide can be calculated through the interplay of rotation around the bonds defined by the torsion angles Φ and Ψ (figure 2.6.3).

The amide chromophore in a polymer

Since amide chromophores interact in the folded protein, it is the three dimensional arrangement of these chromophores that affects the electronical structure and therefore, the spectrum of the whole protein.

The monomer units of two chromophores in an ordered array are described by their wave functions ψ_1 and ψ_2. The oscillation of excitation energy between $\psi^*\psi_2$ and $\psi_1\psi^*$ and the all over excited state of the dimer is given by: $\psi = \frac{1}{\sqrt{2}}(\psi_1\psi_2^* \pm \psi_1^*\psi_2)$.

Excitation splitting is the result of the interaction of the monomers of a chromophore in an ordered structure and the calculation of the CD spectrum can be performed by the interactions of the $n-\pi^*$ and $\pi-\pi^*$ transition moments (Greenfield and Fasman, 1969).

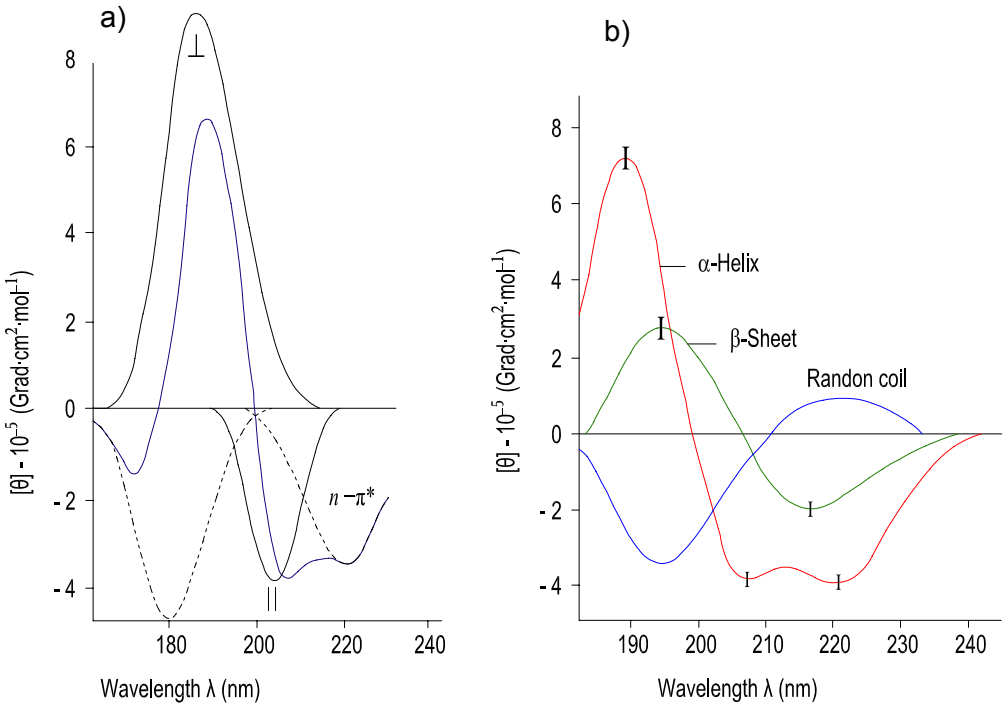

Figure 2.6-5 a) CD spectra of poly-L-alanine in the $n-\pi^*$ transition $\pi-\pi^*$ parallel (II) and perpendicular (⊥) transition (Adopted from Quadrifoglio and Urry 1968). b) CD spectra of poly-L-alanine showed the cotton effect of α-helix, ß-sheet and random coli structure (Adopted from Greenfield and Fasman 1969)

For example, poly-L-lysine can adopt three different conformations merely by varying the pH and temperature. Random coil at pH 7.0, α-helix at pH 10.8 and ß-form at pH 11.1 after heating to 52°C and recooling (Rosenheck and Doty, 1961; Sarkar and Doty, 1966). Figure

2.6-5 shows that the CD spectra of the random coil are made up of the two bands of the amide chromophore, a positive at 212 nm in the $\pi - \pi^*$ transition and a negative at 195 nm in the transition $n - \pi^*$. The ß-sheet spectra display a negative band at 218 nm in the transition $\pi - \pi^*$ and a positive at 196 nm in the transition $n - \pi^*$. The α-helix spectra are the most complex, because the exciton coupling of the $\pi - \pi^*$ transitions leads to a positive $\pi - \pi^*$ transition ($\perp$) at 191 nm and negative $\pi - \pi^*$ transition (II) at 208 nm. In addition, the negative $n - \pi^*$ transition shifts to 222 nm (Sarkar and Doty, 1966, Greenfield and Fasman, 1969).

CD in the near ultraviolet

The near ultraviolet wavelengths (250 to 350 nm) are used to determine differences between the folded and unfolded state of a protein and in the different participation of each of the chromophores in the transition. The aromatic residues in a protein absorb at these wavelengths. If these aromatic residues are held rigidly in an asymmetric environment, they exhibit CD bands. The band of CD depends upon both the specific environment and the freedom of rotation around Cα, Cβ and Cγ bonds. For this reason, the optical activity is a function of the folded structure of the protein. The aromatic chromophores in the near UV region have only $\pi - \pi^*$ transition. This transition is in the plane ^1L_a and $1L_b$. Each of these transitions is in the plane of the π bonding system, where ^1L_a and ^1L_b are perpendicular to each other (Mulkerrin; 1996).

The phenylalanine chromophore

The phenylalanine side chain contains benzene, therefore has a high degree of symmetry and chromophore, which is weakly absorbing. The spectrum of phenylalanine has four vibronic bands at 245, 256, 262 and 267.

The tyrosine chromophore

Tyrosine has a hydroxyl substituent on the benzene ring and is more asymmetric than phenylalanine. Therefore, there is a significant increase in the intensity of the ^1L_b band. The tyrosine band is at about 276 nm with a shoulder at 283 nm.

Tryptophan chromophore

The tryptophan chromophore also has two transitions, ^1L_a and ^1L_b. The ^1L_a transition dipole results in negative charge density that is confined to the more hydrophobic region of the indole ring. Tryptophan bands are characterised by the bands at about 290 and 298 nm.

2.6.3 Estimation of the secondary structure of protein in solution

The methods of CD analysis assume that the spectra of a protein can be represented by a linear combination of the spectra of its secondary structural elements (Greenfield and Fasman, 1969; Chen et al., 1974). The mean residue ellipticity, θ, at any wavelength, λ, of protein in aqueous solution is expressed as:

$$\theta_\lambda = f_H \theta_H^n + f_\beta \theta_\beta + f_t \theta_t + f_R \theta_R + noise \qquad \text{(eq. 2.6-2)}$$

With the two constraints: $1 \geq f_j \geq 0$ and $\Sigma f_j = 1$

Where θ_λ is the CD of the protein as a function of wavelength, f is the fraction of each secondary structure and θ_H, θ_β and θ_R are the ellipticities of each α-helix, ß-form, ß-turn and unordered form, n refers to the average number of peptide units per helical segment in a protein molecule. The noise term includes the contribution of aromatic chromophores.

Estimation of the secondary structure is made principally using algorithms, which calculate a set of orthogonal basis spectra, all of which represent some part of each of the secondary structural elements. The basis spectra are derived from the CD spectra of proteins from which the secondary structural content has been determined by crystallography. It is the solution of each of the secondary structural elements in the protein (Mulkerrin, 1996). The principal algorithms to calculate secondary structure are: Standard for linear regression, which is used for evaluating the effects of mutations, ligands and solvents on protein conformation, used by Greenfield and Fasman (1969) in the study of polypeptides with known conformation.

Ridge regression, CONTIN, developed by Provencher and Gloeckner (1981), fits the CD of unknown proteins by a linear combination of the spectra of a large date base of proteins with known conformations. In this method, the contribution of each reference spectrum is kept small unless it contributes to a good agreement between the theoretical best-fit curve and the raw data (Provencher and Gloeckner 1981).

In variable selection, VARSLC, an initial large database of proteins with known spectra and secondary structures is selected. Some of the protein spectra are then eliminated systematically to create new date bases with a smaller number of standards. SVD is performed using all of the reduced data sets and the ones fulfilling selection criteria for a good fit are averaged (Manavalan and Johnson, 1987).

Self consistent methods, SELCON, program performed by Sreerama and Woody, is a modification of VARSLC that is faster to use. With suitable references, this program can be used to estimate the contribution of the P2 conformation in proteins and the length of helical and beta segments (Sreerama and Woody, 1993a; Sreerama and Woody, 2000).

CDSSTR developed by Johnson (1999) is also a modification of VARSLC which use all possible combinations of a fixed number of proteins in the reference set.

Presuming the reports by several authors (Greenfield and Fasman, 1969; Manavalan and Johnson, 1987; Provencher and Gloeckner 1981; Sreerama and Woody, 1994, Johnson, 1999), the table 2.6-1 shows advantage and drawback of some of the most popular algorithms used to estimate secondary structure of proteins. The authors recommend SELCON program to determine conformation of globular protein in solution and CONTIN with a suitable set of reference to calculate polypeptide conformation.

Table 2.6-1 Advantage and drawback of some algorithm to calculate secondary structure of proteins from CD spectra

Method	**Advantage**	**Drawback**
CONTIN	Relatively good estimate of ß-turns	References are different for every fit
VARSLC	Superior fit	Very slow
SELCON	Good estimates of ß-sheet and turns in proteins	Poor fits of spectra of polypeptides with high ß-sheet content
CDSSTR	The most accurate analysis results	Very slow

A comparative study of CONTIN, SELCON and CDSSTR realised by Sreerama and Woody (2000), indicate that while CDSSTR performed the best with a smaller reference and a larger wavelength range, the performance of individual secondary structures were mixed. For this reason, the authors recommend that all three methods can be used in conjunction for a reliable analysis.

3 Materials and methods

3.1 Materials

3.1.1 Chemicals

Acetic acid 100% p.a.	AppliChem, Darmstadt, Germany
Acrylamide 2X, analytical grade	Serva, Heidelberg, Germany
Ammonium persulfate, analytical grade	Laborchemie Apolda, Germany
Nα-Benzyloxycarbonyl-L-glutamylglycine	Sigma-Aldrich, Steinheim, Germany
α_{s1}-Casein for biochemistry	Merck, Darmstadt, Germany
ß- Casein (isolated according Aschaffenburg, 1963)	Institut für Lebensmittelchemie TU-Dresden, Germany
ß-Lactoglobulin (isolated according Konrad and Lieske, 1997)	Hochschule Anhalt (FH), Köthen, Germany
Coomasie ® Brillant Blue G 250	Serva, Heidelberg, Germany
Cytochrom c for biochemistry	Merck, Darmstadt, Germany
Ethanol abs, HPLC grade	CHN, Fridolfing, Germany
1,4-Dithiothreitol, electrophoresis grade	ICN Biomedicals, Ohio, USA
Folin & Ciocalteu´s phenol reagent 2.0 Normal	Sigma-Aldrich, Steinheim, Germany
Gel filtration LMW calibration kit	Amersham Biosciences, England
Glucono-δ-lactone 99.5%	Calbiochem ®, Darmstadt, Germany
Glutathione, reduced form, 98%	Sigma,-Aldrich, Steinheim, Germany
Glycerine 86 – 88% for analysis	Riedel-de Haën, Seelze, Germany
Hydrochloric acid 37%, analysed reagent	J.T. Baker, Deventer, Holland
Imidazole pure	Serva, Heidelberg, Germany
Iodoacetamide, research grade	Serva, Heidelberg, Germany
Iron III chloride 99% for analysis	Filsum, Filsum, Germany
L-Glutamic acid γ-monohydroxamate	Sigma-Aldrich, Steinheim, Germany
Lactose/D-Galactose Enzymatic BioAnalysis	R-Biopharm AG, Darmstadt, Germany
N-N´-Methylene bisacrylamide 2X, analytical grade	Serva, Heidelberg, Germany
Orange G (C.I. 16230)	Merck, Darmstadt, Germany
Protein Test Mixture 6 for SDS-PAGE	Serva, Heidelberg, Germany
2-Propanol gradient grade for liquid chromatography	Merck, Darmstadt, Germany
Sodium acetate anhydrous, GR for analysis	Merck, Darmstand, Germany
Sodium chloride, GR for analysis	Merck, Darmstadt, Germany
Sodium hydroxide, pellets extra pure	Merck, Darmstadt, Germany

Sodium laurylsulfate·Na-salt 2xcryst. analytical grade	Serva, Heidelberg, Germany
Sodium phosphate dibasic dihydrate, puriss. p.a.	Sigma-Aldrich, Steinheim, Germany
Sodium phosphate dibasic dihydrate, GR for analysis	Merck, Darmstadt, Germany
Sodium phosphate monobasic monohydrate, puriss. p.a.	Sigma-Aldrich, Steinheim, Germany
N, N, N´, N´-Tetramethylethylenediamine, for synthesis	Merck, Darmstand, Germany
TCEP Hydrochloride 101.1%	Calbiochem ®, Darmstadt, Germany
Transglutaminase from *Streptoverticillium mobaraense* Transglutaminase Activa $_{TM}$ MP, Sample	Ajinomoto, Hamburg, Germany
Transglutaminase from guinea pig liver (Factor $XIII_a$)	Sigma-Aldrich, Steinheim, Germany
Tris(hydroxymethyl)-aminomethane, GR for analysis buffer substances	Merck, Darmstadt, Germany
Trichloroacetic acid, crystal form, >99%	J.T. Backer, Deventer, Holland
Urea, pearl form, >99%	Fluka, Steinheim, Germany

3.1.2 Expendables

Centrifugal filters	Ultrafree ® - CL Microcentrifuge Filters Millipore NMWL 10,000DA, regenerated cellulose membrane Sigma-Aldrich, Steinheim, Germany
Concentrator	Vivaspin 15R 10,000 MWCO, modified regenerated cellulose membrane Viva Science, Hanover, Germany
Dialysis membrane	Type 27 12 – 16 kD pore size 24 A Biomol Feinchemikalien, Hamburg, Germany
Filters	Spartan 14/0.45 RC Regenerated cellulose membrane Schleicher & Schell, Dassel, Germany Anotop 25 Plus Inorganic membrane Whatman, Dassel, Germany
Reaction tube for high pressure treatment	Cryo-Röhrchen 2 and 5 mL Carl Roth + Co.KG, Karlsruhe, Germany

3.1.3 Equipment

Balance	BP 121 S, BP 3100 S Sartorius, Göttingen, Germany
Centrifuge	5804, Eppendorf AG, Köln, Germany 6000 I, Heraeus, Hanau, Germany
Chromatography system	Biological LP System with a Model 2128 Fraction collector and a Model 1325 Chard Recorder Bio Rad Laboratories, München, Germany HPLC pump K-1001 with an UV detector K-2500, electrically driven 6-Port-Multi-Channel Valve, Interface Box Knauer, Berlin, Germany
Data analysis:	Software CDPro using CONTIN method using a 48-protein reference set (Sreerama, Woody 2000)
Electrophoresis system	SE 600 Hoeffer Unit, Amersham Biosciences Europe, Hamburg, Germany with a Powder Supply Model 1000/500, Bio Rad Laboratories, München, Germany
Lyophilisation device	Beta 1-8 K, Martin CHRIST, Osterode, Germany
Magnetic stirrers	Ikamag ® RH, IKA-Werke, Staufen, Germany Motor KMGE electronic, IKA-Werke, Staufen, Germany
Nitrogen determination system	Digestion Unit K-435 with a Scrubber B-414, and a Digestion Unit K-435 Büchi Labortechnik, Flawil, Switzerland
pH-Meter	pH 526, WTW, Weinheim, Germany
Rheology equipment	Physica UM oscillation rheometer with a Couette (CC27/Pr-150Q- DIN 53019) cylinder Physica Messtechnik GmbH, Stuttgart, Germany
Spectrophotometer	UV/ Visible Spectrophotometer Ultrospec 100 Pharmacia Biotech, Freiburg, Germany
Spectropolarimeter	Jasco J 710 spectropolarimeter Jasco Labor- und Datentechnik GmbH, Gross-Umstadt, Germany
Water bath	RM6 LAUDA Burgwedel, Germany
Ultrasonic wave	Sonorex RK52H, Bandelin electronic, Berlin, Germany

High hydrostatic pressure equipment	High Pressure laboratory Unit Dieckers GmbH & Co.KG, Willich-Neersen, Germany

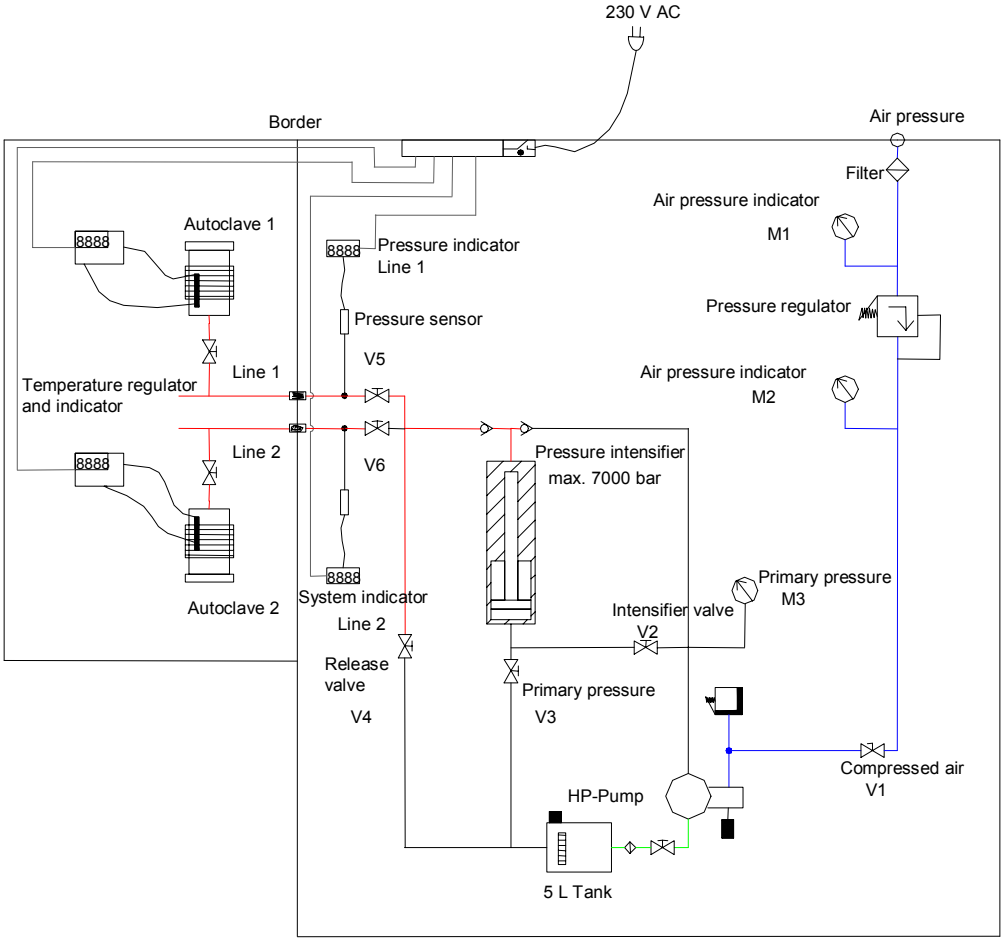

Figure 3.2-1 High hydrostatic pressure laboratory unit. (—) 0.16 MPa air pressure (—) 100 MPa high pressure supply. (—) 700 MPa high pressure supply (—) return.

Conditions of high hydrostatic pressure laboratory unit

High pressure range (MPa):	0.1 to 600
Temperature range (°C):	23 to 80
Volume sample (mL):	1.5 to 5
High pressure system:	Water: ethylene-glycol mixture (1:1)
$\Delta P/\Delta t$ (MPa/min):	300
Decompression time (s):	30
Maximal pressure loss (%)	4

3.2 Transglutaminase unter high pressure

Laboratory high hydrostatic pressure equipment was used to analyse inactivation kinetics of microbial (MTG) and animal transglutaminase at 0.1 to 600 MPa. Conformational change of MTG structure under high pressure was analysed using circular dichroism spectroscopy (CD) and formation of products was analysed using SDS-PAGE electrophoresis and amino acid analysis.

3.2.1 Preparation of MTG samples

a) MTG sample for enzyme kinetic

Microbial transglutaminase (0.4655 g) from *Streptoverticillium mobaraense,* Activa $_{TM}$ MP, was dissolved in 90 mL 0.2 mol/L TRIS-acetate buffer and the pH adjusted to 6.0 using 0.2 mol/L TRIS solution. The volume was then made up to 100 mL using the same buffer to obtain an activity of 40 U/100mL.

Animal transglutaminase (0.98 mg) from guinea pig liver was dissolved in 4 mL 0.2 mol/L TRIS-acetate buffer pH 6.0 and the pH adjusted to 6.0 using 0.2 mol/L TRIS solution. The volume was then made up to 5 mL using the same buffer to obtain an activity of 0.56 U/mL.

Enzyme stock solutions were cooled to 6°C, placed into polypropylene tubes (2 mL) without trapping air bubbles and stored at 6°C until required for high pressure and thermal treatment (section 3.2.2).

b) MTG sample for circular dichroism spectroscopy, sodium dodecyl sulfate-polyacrylamide gel electrophoreses and amino acid analysis

Microbial transglutaminase (0.4655 g) from *Streptoverticillium mobaraense*, Activa $_{TM}$ MP, was dissolved in 9 mL 0.2 mol/L TRIS-acetate buffer and the pH adjusted to 6.0 using 0.2 mol/L TRIS solution. The volume was then made up to 10 mL using the same buffer.

Enzyme stock solutions were cooled to 6°C, placed into polypropylene tubes (5 mL) without trapping air bubbles and stored at 6 °C until when required for high pressure and thermal treatment (section 3.2.2).

3.2.2 High pressure and thermal treatment

High-pressure levels were generated using a hydrostatic pump and water: ethylene-glycol mixture (1:1). The pressure was built up at the rate of 300 MPa/min and the decompression

time was less than 30 sec. Polypropylene tubes containing guinea pig liver TG and MTG samples (section 3.2.1a and 3.2.1b) were placed into the preheated pressure vessels of the hydrostatic pressure machine. The samples were treated at 0.1 (atmospheric pressure), 200, 400, 600 MPa for 10 to 60 min at 10, 30, 40 and 50°C. The same procedure was used to perform the thermal treatment. The samples were incubated at 0.1 MPa for 2, 4, 6, 8 and 10 min at 60, 70 and 80°C. Enzyme activity was measured immediately after treatment by hydroxamate method (section 3.2.3).

Separation of soluble and irreversible protein precipitation

After high pressure and thermal treatment, the samples were centrifuged in cone-shaped glass tubes at 1 157 *x g* for 15 min to separate irreversibly precipitated protein. Enzyme activity and structure of soluble protein was analysed using hydroxamate method (section 3.2.3) and circular dichroism (section 3.2.4). Precipitated protein was analysed using SDS-PAGE electrophoresis (section 3.2.5) and amino acid analysis (section 3.2.6).

3.2.3 Determination of transglutaminase activity

Material

Enzyme solution

Animal transglutaminase and MTG solutions before and after high pressure and thermal treatment (3.2.1 and 3.2.2) were used.

Substrate solution for microbial transglutaminase from Streptoverticillium mobaraense.

0.1 mol/L hydroxylamine, 10 mmol/L glutathione, 30 mmol/L Nα-CBZ-Gln-Lys

69.5 mg hydroxylamine hydrochloride was dissolved in 5 mL 0.2 mol/L TRIS-acetate buffer pH 6.0 and pH was adjusted to 6.0 using 0.2 mol/L TRIS solution. Then, 101.1 mg Nα-CBZ-Gln-Lys and 30.73 mg glutathione was added. The pH was adjusted to 6.0 using 0.2 mol/L TRIS solution and the volume made up to 10 mL with 0.2 mol/L TRIS-acetate buffer pH 6.0.

Substrate solution for transglutaminase from guinea pig liver (Factor $XIII_a$).

0.1 mol/L hydroxylamine, 10 mmol/L glutathione, 30 mmol/L Nα-CBZ-Gln-Lys, 5 mmol/L $CaCl_2$:

The preparation was carried out as described above incorporating additionally 5.6 mg $CaCl_2$

Ferric chloride-trichloroacetic acid reagent

5% (w/v) ferric chloride solution (5.0 g ferric chloride hexahydrate in 100 mL 0.1 mol/L HCl)

12% (w/v) trichloroacetic acid (12.0 g trichloroacetic acid in 100 mL distilled water)

12% (v/v) HCl (32.43 mL HCl in 100 mL distilled water)
Equal volumes were mixed using a magnetic stirrer until a clear and transparent yellow solution was obtained.

Calibration curve
A stock solution was prepared by dissolving 8.1 mg L-Glutamic acid gamma–monohydroxamate in 20 mL TRIS-acetate buffer pH 6.0. The solution was diluted to obtain concentrations of 0.0, 0.5, 1.0, 1.5, 2.0, 2.5 mmol/L. The different dilutions were treated under the same conditions of the sample to obtain a calibration curve.

Method
Enzyme sample solution (0.5 mL) was added to 1 mL substrate solution that was previously incubated at 37°C for 10 min. Immediately, after enzyme sample solution addition, the sample was vortex mixed and further incubated at 37°C for 10 min. Ferric chloride-trichloroacetic acid reagent (1.5 mL) was added and vigorously mixed to stop the reaction. To separate any insoluble material, the sample was centrifuged at 1500 *x g* for 10 min. The supernatant was measured after 20 min at 525 nm using an Ultrospec 1000 spectrophotometer (Pharmacia Biotech, Freiburg, Germany). An enzyme unit is defined as the amount of enzyme which catalyses the formation of 0.5 μmole of hydroxamate per min from Nα-CBZ-Gln-Lys and hydroxylamine at pH 6.0 at 37 °C (Folk and Cole, 1969).

3.2.4 Circular dichroism

Material
Soluble protein samples obtained from high pressure and thermal treatment (section 3.2.2) were again centrifuged at 1928 x g in a Vivaspin 15R concentrator assembly having a membrane with a 10,000 MWCO (HY, Viva Science, Hannover, Germany) in order to eliminate lactose and maltodextrins. Seven washings were made with 10 mL 0.1 mol/L phosphate buffer pH 7.0 until free reducing sugars were no longer detectable (Fehling method section 3.2.7). The samples were concentrated until protein concentration of ~0.2 mg/mL (Lowry method section 3.2.8).

Method
Far-UV circular dichroism (CD) of the samples was recorded in the range of 178–260 nm at a enzyme concentration of 0.2 mg/mL phosphate buffer 0.1M, using a Jasco J 710 spectropolarimeter (Gross-Umstadt GmbH, Germany). A quartz cylindrical cell having 1 mm path length was used for the measurements. The following parameters were used: step

resolution, 1 nm; speed, 20 nm per min, band width, 1 nm, response, 4 s and sensitivity, 200 mdeg. Mean ellipticity using a mean residue molecular weight of 38 and 331 amino acid residues for MTG was calculated from amino acid sequence of the subunits (SWISS-PROT database, http://us.expasy.org/, USA). The CD spectra were analysed by a curve-fitting software CDPro using CONTIN method (Sreerama and Woody, 2000) to obtain the secondary structural contents of the proteins. The estimation was performed using a 48-protein reference set (Sreerama and Woody, 2000).

3.2.5 Sodium dodecyl sulfate-polyacrylamide gel electrophoreses

Irreversible precipitated protein samples obtained from high pressure and thermal treatment (section 3.2.2) were dissolved in 1 mL 0. 4 M TRIS-HCl buffer pH 8.0 containing 2% SDS. The samples were analyzed using a SDS-PAGE with a gradient of 5, 8 and 12 % acrylamide gels following the procedure of Lane (1978) with modifications in sample preparation and running conditions as described below.

Material

Stock solution for sample preparation

Buffer for liquid sample pH 8.0

4.84 g TRIS, 0.03 g EDTA, 2.0 g SDS, 13.8 mL glycerol 87 % and 0.01 g orange G in 100 mL double-distilled water.

Buffer for solid sample pH 8.0

4.84 g TRIS, 0.03 g EDTA, 2.0 g SDS, 13.8 mL glycerol 87 % and 0.01 g orange G in 50 mL double-distilled water.

Iodoacetamide solution 20 % (w/v)

20 mg iodoacetamide in 100 μL double-distilled water

1,4-Dithiothreitol (DTT) stock solution

150 mg DTT in 200 mL double-distilled water

Stock solutions for gel preparation

30% Acrylamide stock (30% T)

29.1 g acrylamide 2x and 0.9 g N,N´-methylene bisacrylamide in 100 mL double-distilled water.

Gel buffer pH 8.5

36.6 g TRIS, 0.3 g SDS were dissolved in 50 mL double-distilled water and pH adjusted to 8.9 using 6 mol/L HCl. The volume was made up to 100 mL with double-distilled water.

Ammonium persulfate (APS) solution:
430 mg APS in 1 mL double-distilled water.

Stock solution for electrophoresis buffers:
Anode buffer; 0.2 mol/L TRIS-HCl pH 8.9:
96.4 g TRIS was dissolved in 2 L double-distilled water and pH adjusted to 8.9 using 2 mol/L HCl. The volume was made up to 4 L with double-distilled water.
Cathode buffer; 0.1 mol/L TRIS- tricine pH 8.2
12.1 g TRIS, 17.9 g tricine were dissolved in 750 mL double-distilled water then 1 g SDS was added and dissolved. The pH was adjusted to 8.2 using 6 mol/L HCl and the volume made up to 1 L with double-distilled water.

Stock solution for coomassie staining
Fixing solution; trichloroacetic acid 12% (w/v)
20.0 g trichloroacetic acid in 1 L double-distilled water
Staining solution
45 mg coomassie G-250 in 1 L destaining solution
Destaining solution
Water: methanol: acetic acid (65:25:10)

Protein standard solution
2 mg protein test mixture 6 for SDS-PAGE (Serva, Heidelberg, Germany) in 1 mL sample buffer.

Gel cassette assembly and casting
Each vertical gel cassette consisted of two cleaned and degreased glass plates (18 x 16 cm), two 1.50 mm thickness spacers and two clamps. The plates were aligned and placed into a casting stand with a rubber gasket bottom to seal.

A discontinuous concentration gel cassette was performed by mixing three different concentrations of a 30% acrylamide stock solution. High percentage of acrylamide at the bottom of the gel (resolving gel) and low percentage at the top (stacking gel) were applied as is showed in table 3.2-1.

Table 3.2-1 Discontinuous concentration acrylamide gel for SDS-PAGE

	Gel composition (% Acrylamide)		
	12%	8%	5%
30% Acrylamide stock (mL)	10.04	2.64	1.64
Gel buffer (mL)	8.30	3.30	2.50
Glycerol 87 % (mL)	2.50	0.80	-
⬇			
Degassed in a ultrasonic bath for 30 min			
⬇			
Cooled to 20 °C			
⬇			
Made up to (mL)	25.00	10.00	10.00
⬇			
TEMED (µL)	12.50	5.00	5.00
APS solution (µL)	25.00	10.00	20.00

Method

Sample preparation and loading

Native sample of MTG (section 3.2.1) was concentrated from 6 to 2 mL by centrifugation at 1928 *x g* using a Vivaspin 15R concentrator. Liquid sample buffer pH 8.0 (1 mL) was added to the concentrated sample and vigorously mixed using a vortex mixer until obtain a homogeneous liquid.

Buffer for solid sample pH 8.0 (1 mL) was added to irreversible precipitate samples (section 3.2.2) and vigorously vortex mixed to obtain a homogeneous liquid. DTT solution (10 µL) was added to 500 µL homogeneous samples. The solution was boiled for 5 min and cooled to 20 °C. Iodoacetamide solution (51 µL) was added to sample and allowed to stand for 30 min then centrifuged at 2 000 *x g* for 2 min. Samples were loaded on the vertical gel.

The gel cassette was disassembled from the casting stand and washed with distilled water. The comb was removed and each well was washed with double-distilled water to remove unpolymerised acrylamide. The cleaned gel cassette was placed in the upper buffer chamber with a glass plate to the opposite side and each well was filled with cathode buffer. Aliquots of 12 and15 µL of protein standard solution and MTG samples were loaded slowly into the

wells. The unit was assembled with a cooling water system after aggregation of anode buffer into the lower chamber and cathode buffer into the upper chamber.

Coomassie staining

After electrophoresis the gel was carefully submerged into the fixing solution for 30 min, then washed three times with distilled water and submerged into the coomassie staining solution for approximately 45 min or until the defined bands appeared. To remove excessive coloration, the gel was washed for a few minutes with a destaining solution and finally packed in polyethylene folio.

Running conditions

Electrophoresis unit:	Vertical SE 600 Hoeffer, Biosciences Europa , Germany
Number of gels:	1
Glass plate dimensions	18 x 16 cm
Gel thickness:	1.50 mm
Cooling system:	RM6 LAUDA CFR-free Burgwedel, Germany
Running temperature:	10 °C
Powder Supply:	Model 1000/500, Bio Rad, Germany

Table 3.2-2 Running parameters for SDS-PAGE electrophoresis

	Time (h)	Voltage (V)	Current (mA)
Starting:	0.30	400	35
Final:	8.00	800	65

3.2.6 Amino acid analysis

Material

Sample preparation

Irreversible precipitated protein samples from high pressure an thermal treatment (section 3.2.2) were dialysed at 6°C using a dialysis membrane type 27 (Biomol Feinchemikalien, Hamburg, Germany). After removal of sugars, the samples were freeze-dried and stored at –18°C.

Acid hydrolysis of samples

Freeze-dried precipitated protein (10 to 11 mg) were hydrolysed in 10 mL 6 mol/L HCl following the procedure of Henle *et al*. (1991).

Elution buffer system

Buffer number	Buffer	Molar (mol/L)	pH
1	Deionised water with 0.1 % Tetrahydrofuran		-
2	Sodium citrate	0.2	3.18
3	Sodium citrate	0.2	4.20
4	Deionised water with 0.1 % Tetrahydrofuran		-
5	Sodium citrate	1.2	6.45
6	Na OH	0.4	-

Method

Amino acid analysis was performed with an Alpha Plus Amino Acid Analyser (LKB Biochrom, Freiburg, Germany) using an ion exchange chromatograph with a sodium system. The chemicals, standards, analysis and the conditions of running were performed using procedures described in Henle *et al.* (1991, 1997). The elution profiles were detected by an ultraviolet detector (K-2501 Knauer, GmbH, Berlin) at 280 nm for furosine and a fluorescence detector (RF-535 Shimadzu Corporation, Japan) at excitation/emission of 335/385 nm for pentosidine. Subsequently, amino acids were detectable via derivatisation with ninhydrin. Peak integrations were evaluated using chromatography software (EuroChrom 2000, Knauer GmbH, Berlin).

Sample preparation and loading

Dried sample from acid hydrolysis was dissolved in 0.2 mol/L sodium citrate buffer pH 2.2 and passed through a 0.20 μm membrane filter before subjecting it to the amino acid analyser.

Operating conditions

Amino acid analyser equipment:	4151 Alpha Plus LKB Biochrom, Freiburg, Germany
Column:	Analytic ion exchange chromatography 125 mm × 4.6 mm PEEK
Media of column:	Harz 5 μm f. Na-System Laborbedarf und Analysentechnik K. Grüning, Olching, Germany
Temperature system:	55-90 °C
Sample concentration:	1 mg protein per 1 mL
Injection volume	50 μL
Flow rate :	16 mL/h

Table 3.2-3 Running parameters program for furosine detection

Number	Time	Temperature (°C)	Buffer	Nin
1	6:00	55	2	ON
2	19:00	90	3	ON
3	5:00	70	5	ON
4	16:00	90	5	ON
5	12:00	90	5	ON
6	9:00	90	5	ON
7	8:00	90	6	ON
8	8:00	90	2(20%)	ON
9	1000	55	2	ON
10	0:00	55	2	ON
11	1:00	55	2	ON
Detection	Ultraviolet λ = 280 nm			

Table 3.2-4 Running parameters program for pentosidine detection

Number	Time	Temperature (°C)	Buffer	Nin
1	5:00	55	2	OFF
2	0:05	55	3	OFF
3	0:025	55	2	OFF
4	0:05	55	3	OFF
5	0:25	55	2	OFF
6	0:05	55	3	OFF
7	0:25	55	2	OFF
8	0:05	55	2(20%)	OFF
9	0:25	55	2	OFF
10	0:10	55	3	OFF
11	0:20	55	2	OFF
12	0:10	55	3	OFF
13	0:20	55	2	OFF
14	19:00	55	3	OFF
15	5:00	65	4	OFF
16	21:00	90	4	OFF
17	5:00	90	4	OFF
18	15:00	90	5	OFF
19	8:00	90	6	OFF

20	8:00	90	2	OFF
21	8:00	90	2(20%)	OFF
22	12:00	55	2	OFF
23	0:00	55	2	OFF
24	1:00	55	2	OFF
Detection :	Fluorescence $\lambda_{Ex}/\lambda_{Em}$ = 335/385			

3.2.7 Qualitative determination of reducing sugar

Fehling

Material

Fehling solution A (6.9 g $CuSO_4 \cdot 5H_20$ made up to 100 mL with distilled water)

Fehling solution B (34.6 $KNaC_4H_4O_6 \cdot H_2O$ and 10 g NaOH made up to 100 mL with distilled water)

Methylene blue indicator, 1% aqueous solution

3.2.8 Determination of protein concentration

Kjeldahl

Method

MTG (0.5 g) and a Kjeldahl tablet catalyst were dissolved in 10 mL H_2SO_4 in a Kjeldahl flask. Then, they were digested about 6 h and distilled in the units of a Büchi Kjeldahl equipment. The ammonia was trapped in acid boric 2% solution and titrated with HCl 0.5 N.

Lowry

Material

Lowry solution A (0.1% $CuSO_4 \cdot 5H_20$, 0.2% Na tartrate in 400 mL distilled water)

Lowry B (10% Na_2CO_3) in 400 mL

Lowry C (Mixed solution A + B and made up to 1 L)

5% SDS

0.8 mol/L NaOH

2N Folin-Ciocalteu´s phenol

2 mg BSA in 40 mL 1% SDS

Solution D (1 volume of Lowry C + 2 volumes of 5% SDS + 1 volume 0.8 mol/L NaOH)

Solution E (1 volume of 2N Folin-Ciocalteu´s phenol + 5 volumes of distilled water)

Method

Protein sample (< 100 μg protein) was dissolved in 1 mL solution D and reposing for 10 min. Then, solution E (0.2 mL) was added and vortex. The sample was measured after 30 min at 750 nm using an Ultrospec 1000 spectrophotometer (Pharmacia Biotech, Freiburg, Germany). Calibration curve was performed under the same conditions of the sample in a protein concentration range from 20 to 100 μg protein.

3.3 Affinity of microbial transglutaminase to acid-, α_{s1}- and β-casein under atmospheric and high pressure

The studies on the reaction kinetics of microbial transglutaminase using acid-, α- and β-casein as substrate at 0.1 and 400 MPa at 40°C were carried out in the laboratory high hydrostatic pressure equipment to investigate the affinity of the enzyme with the different individual caseins. Isolation and characterisation of milk protein was performed using isoelectric precipitation, ion exchange chromatography, native and sodium dodecyl sulfate-polyacrylamide gel electrophoresis.

3.3.1 Isolation and identification of milk proteins

Isolation of acid casein by isoelectric precipitation

Acid casein was obtained by isoelectric precipitation at 20°C. Raw cow milk (500 mL) from Saxony, Germany, was diluted with distilled water (1:1), and then defatted three times by centrifugation at 300 *x g* for 15 min and 4°C. The obtained skim-milk was magnetically stirred while adjusting the pH to 4.6 using 1 mol/L HCl. The precipitated casein was filtered through a cotton mesh and then dispersed in 500 mL water and re-dissolved using 1 mol/L NaOH until pH 7.0 was attained. This procedure was repeated once to improve the purity of the casein. The casein was washed twice with acetone and once with ethanol, then re-dissolved distilled water (300 mL) and the pH adjusted to 7.0 using 1 mol/L NaOH. Acid casein solution was freeze-dried and stored at –18°C.

a) Fractionation of acid casein by differential solubility

Acid casein was fractioned by differential solubility in urea solution (Aschaffenburg, 1963). Freeze-dried Acid casein (~30 g) was dissolved in 3.3 mol/L urea solution (1 L) and magnetically stirred while adjusting the pH to 7.5 using 1 mol/L NaOH. The precipitated (γ-, α- and κ-casein) was separated by centrifugation at 300 x g for 15 min and 4°C. The supernatant, which remain ß-casein, was adjusted to pH 4.9 using 1 mol/L HCl, then the

volume was made up to 2 L with distilled water and warmed at 30°C until obtain a second precipitate (ß-casein). The procedure was repeated once to improve purity of the ß-casein.
The precipitated ß-casein solution was dialysed against water at 6°C during 3 days using a dialysis membrane type 27. After desalting, the isolated fractions were freeze-dried and stored at –18°C.

b) Isolation of α_{s1}- and ß-casein by ion exchange chromatography

Isolation of α_{s1}- and ß-casein was carried out by ion exchange chromatography following the procedure of Schwarzenbolz (2000). The procedure was performed at 20 °C using a Biological LP system with a Source 30 Q ion exchange media (Pharmacia-LKB, Freiburg, Germany) at a flow rate of 10 mL/min using the elution buffer 0.02 mol/L imidazole (pH 7.0) containing 3.3 mol/L urea and 0.05% thioglycerine with a concentration gradient of 0.5 mol/L NaCl. Extinction of column eluate was measured at 280 nm and collected in 10 mL volumes using a fraction collector.

Material

Elution buffer A

2.72 g imidazole, 396.4 g urea and 1.0 mL thioglycerine were dissolved in 1 L distilled water and the pH adjusted to 7.0 using 6 mol/L HCl. The volume was made up to 2 L with distilled water.

Elution buffer B

1.362 g imidazole, 198.20 g urea, 29.25 g NaCl and 0.5 mL thioglycerine were dissolved in 500 mL distilled water and pH adjusted to pH 7.0 using 6 mol/L HCl. The volume was made up to 1 L using distilled water.

Elution buffers A and B were filtered using a 0.45 μm regenerated cellulose filter (Schleicher & Schell, Dassel, Germany) and degassed in an ultrasonic bath for 45 min.

Packing and stabilisation of ion exchange column

Source 30 Q ion exchange media (Pharmacia-LKB, Freiburg, Germany) was dissolved in 20% ethanol and packed in a 16 mm/10 cm Pharmacia column to form a bed volume of 20 mL. Stabilization of the column was performed by passing of 1 volume of water and 5 volumes elution buffer A at a flow rate of 5 to 10 mL/min.

Method

Sample preparation and loading

5 g lyophilised acid casein; 50 mg TCEP and 18 g urea were dissolved in 50 mL elution buffer A. The pH was adjusted to 7.0 using 6 mol/L HCl. The volume was then made up to

100 mL with elution buffer A. The solution was passed through a 0.45 μm membrane filter before subjecting 6 mL portions to a chromatography column.

Operating conditions

Chromatography equipment:	Biological LP System with a Model 2128 Fraction collector and a Model 1325 Chart Recorder, Bio Rad Laboratories, München, Germany
Column:	16 mm i.d. x 10 cm height Amersham-Pharmacia, Freibug, Germany
Column media:	Source 30 Q ion exchange, Pharmacia-LKB, Freiburg, Germany
Column volume:	20 mL
Temperature system:	20 °C
Sample concentration:	50 mg/ mL elution buffer A
Injection volume:	6 mL
Elution buffer A:	0.02 mol/L imidazol pH 7.0 Containing: 3.3 mol/L urea and 0.05 % (v/v) thioglycerine
Elution buffer B:	0.02 mol/L imidazol pH 7.0 Containing: 3.3 M urea , 0.05 % (v/v) thioglycerine, 0.5 mol/L NaCl
Flow rate:	10 mL/min
Detection:	Ultraviolet λ = 280 nm

Concentration gradient of NaCl:

Elution buffer A [mL]	Elution buffer B [%]
0	15
100	15
300	25
800	50
850	50
1050	100
1200	100
1210	15
1300	15

The different fractions were collected and dialysed against water at 6°C during 3 days using a dialysis membrane type 27 (Biomol Feinchemikalien, Hamburg, Germany). After desalting, the isolated fractions were freeze-dried and stored at –18°C. Purity and characteristics of the isolated casein was analysed by polyacrylamide gel electrophoresis (section 3.2.5).

3.3.2 Characterisation of isolated casein

Isolated caseins were characterised by a polyacrylamide with urea and a sodium dodecyl sulfate-polyacrylamide gel electrophoresis following the procedure of Jovin *et al*. (1970), cited by Westermeier (1997) and Lane (1978) and modified by Böhm (2002).

a) Polyacrylamide gel electrophoresis using urea

The purity of casein from isoelectric precipitation as well as α- and ß-casein obtained from ion exchange chromatography was analysed using 12% polyacrylamide gel containing 5 mol/L urea in a standard vertical Hoeffer SE 600 electrophoresis unit (Amersham Biosciences, Hamburg, Germany).

Materials

Stock solution for sample preparation

Sample buffer:

15.0 g urea and 0.01 g bromophenol blue were dissolved in 6.25 mL gel buffer and made up to 25 mL with double-distilled water.

Stock solutions for gel preparation

30% Acrylamide stock (30% T)

29.1 g acrylamide 2x and 0.9 g N,N´-Methylene bisacrylamide dissolved in 100 mL double-distilled water.

Gel buffer pH 8.9:

36.6 g TRIS and 0.46 mL N,N,N´,N´-Tetramethylethylenediamine were dissolved in 48.0 mL 1 mol/L HCl. The pH was adjusted to 8.9 using 2 mol/L HCl and made up to 100 mL with double-distilled water.

Ammonium persulfate solution:

430 mg APS in 1 mL double-distilled water.

Stock solution for electrophoresis unit

Electrophoresis buffer pH 8.3

15.0 g TRIS and 72.0 g glycine (87%) were dissolved in 2 L double-distilled water and the pH adjusted to 8.4 using 4 mol/L HCl. The volume was made up to 5 L with double- distilled water.

Stock solution for coomassie staining

Fixing solution; trichloroacetic acid 12% (w/v)

20.0 g trichloroacetic acid in 1 L double-distilled water

Staining solution

45 mg coomassie G-250 in 1L destaining solution

Destaining solution

Water: methanol: acetic acid (65:25:10)

Protein standard solution

2 mg protein test mixture 6 for SDS-PAGE (Serva, Heidelberg, Germany) in 1 mL sample buffer.

Gel cassette assembly and casting

Each vertical gel cassette consisted of two cleaned and degreased glass plates (18 x 16 cm), two 1.50 mm thickness spacers and two clamps. The plates were aligned and placed into a casting stand with a rubber gasket bottom to seal.

15.0 g urea was dissolved in 6.25 mL gel buffer and 25.0 mL 30% acrylamide stock and made up to 50 mL with double-distilled water. The gel solution was degassed in a ultrasonic bath for 30 min then cooled to 20 °C. Ammonium persulfate solution (18 μL) was added to gel solution and immediately applied into the cassette then a 1.50 mm thickness comb was inserted without trapping air bubbles. Polymerisation of gels was carried out at 20°C for 3 h. To prevent drying of gels, a plastic bag was placed above the gel cassettes. The gel was stored at 6°C for maximal 3 days.

Method

Sample preparation and loading

Freeze-dried sodium caseinate, α- and ß-casein (3 mg) were dissolved in 1 mL sample buffer then centrifuged at 2000 *x g* for 2 min. Soluble protein of samples was loaded on the vertical gel.

Gel cassettes were disassembled from the casting stand and washed with distilled water. The comb was removed and each well was washed with double distilled water to remove unpolymerised acrylamide. Cleaned gel cassettes were placed into the upper buffer chamber with a glass plate to the opposite side and each well was filled with electrophoresis buffer (pH 8.3). Aliquots of 4, 3 and 4 μL of whole-, α- and ß-casein respectively were loaded slowly into the wells. The same electrophoresis buffer was added into the upper and lower chamber and the unit was assembled with a cooling water system.

Operating conditions

Electrophoresis unit:	Vertical SE 600 Hoeffer, Biosciences Europe, Germany
Number of gels:	1
Glass plate dimensions:	18 x 16 cm
Gel thickness:	1.50 mm
Cooling system:	RM6 LAUDA CFC, Burgwedel, Germany
Running temperature:	10°C
Power supply:	Model 1000/500, Bio Rad Laboratories, München, Germany

Table 3.3-1 Running parameters for native electrophoresis

	Time (h)	Voltage (V)	Current (mA)
Starting:	0.25	400	25
Final:	3.00	800	50

Coomassie staining

After running the gel was carefully submerged into the fixing solution for 30 min, then washed three times with distilled water and submerged into the coomassie staining solution for approximately 45 min or until the defined bands appeared. To remove excessive coloration, the gel was washed for a few minutes with a destaining solution and finally packed in polyethylene folio.

b) Sodium dodecyl sulphate-polyacrylamide gel electrophoresis

Acid casein from isoelectric precipitation as well as α- and ß-casein obtained from ion exchange chromatography were characterised using a 12, 8 and 5% gradient polyacrylamide gel containing 5 mol/L urea using a Hoeffer SE 600 standard vertical electrophoresis unit (Amersham Biosciences, Hamburg, Germany).

Material

Stock solution for sample and gel preparation, electrophoresis unit, coomassie staining and Protein standard solution were prepared as described in section 3.2.5.

Gel cassette assembled and casting

Gel cassette assembled and casting was performed following procedure described in section 3.2.5 with the following modifications:

Table 3.3-2 Discontinuous concentration acrylamide gel for SDS-PAGE

	Gel composition (% Acrylamide)		
	12%	8%	5%
Urea (g)	7.50	3.00	3.00
30% Acrylamide stock (mL)	10.04	2.64	1.64
Gel buffer (mL)	8.30	3.30	2.50
Glycerol 87% (mL)	2.50	0.80	0.00
⬇			
Degassed in a ultrasonic bath for 30 min			
⬇			
Cooled to 20°C			
⬇			
Made up to (mL)	25.00	10.00	10.00
⬇			
TEMED (µL)	12.50	5.00	5.00
APS solution (µL)	25.00	10.00	20.00

Method

Sample preparation and loading

Freeze-dried sodium caseinate, α- and ß-casein (3 mg) were dissolved in 1 mL sample buffer. DTT solution (10 µL) was added to 500 µL casein samples then boiled for 5 min and cooled to 20°C. Iodoacetamide solution (51 µL) was added to samples and after 30 min centrifuged for 2 000 *x g* for 2 min. Soluble protein of samples was loaded on the vertical gel.

Gel cassette was disassembled from the casting stand and washed with distilled water. The comb was removed and each well was washed with double-distilled water to clear unpolymerised acrylamide. The cleaned gel cassette was placed into the upper buffer chamber with a glass plate to the opposite side and each well was filled with cathode buffer.

Aliquots of protein standard solution (13 µL) and 5 µL of each whole, α- and ß-casein samples were loaded slowly into the wells. The unit was assembled with a cooling water system after aggregation of anode buffer into the lower chamber and cathode buffer into the upper chamber. After running, the gel was stained with coomassie following procedure described in section 3.2.5.

Operating conditions

Electrophoresis unit:	Vertical SE 600 Hoeffer, Biosciences Europe , Germany
Number of gels:	1
Glass plate dimensions	18 x 16 cm
Gel thickness:	1.50 mm
Cooling system:	RM6 LAUDA CFR-free Burgwedel, Germany
Running temperature:	10 °C
Power Supply:	Model 1000/500, Bio Rad, Germany

Table 3.3-3 Running parameters for SDS-PAGE electrophoresis

	Time (h)	Voltage (V)	Current (mA)
Starting:	0.30	400	35
Final:	6.50	800	65

3.3.3 Kinetic studies

Reaction kinetics of MTG with acid casein, α_{s1}- and ß-casein at 0.1 and 400 MPa at 40°C was analysed by monitoring casein oligomerisation using gel permeation chromatography (section 3.3.3b).

a) Incubation experiments

Stock solution of microbial transglutaminase (0.166 U /mL)

Powder of MTG (0.0179 g) was dissolved in 8 mL 0.2 mol/L TRIS-acetate buffer pH 6.0 and pH was adjusted to pH 6.0 using 0.2 mol/L TRIS solution. The volume was made up to 10 mL with the same buffer.

Stock solution of casein

Freeze-dried acid casein (250 mg), β-casein (250 mg) or α_{s1}-casein (50 mg), respectively, were separately dissolved in 15 mL 0.2 mol/L TRIS-acetate buffer pH 6.0 then magnetically stirred at 25 °C. The pH was adjusted to 6 and the volume made up to 20 mL with the same buffer.

Reaction

Stock solution of microbial transglutaminase (0.30 mL) at 6 °C was added to 4.7 mL casein solution at different concentrations (table 3.3-4 and 3.3-5) at 6 °C and immediately vortex mixed. Enzyme-substrate solution was applied into a 2 mL polypropylene tube without trapping air bubbles and placed into preheated pressure vessels of the hydrostatic pressure machine. The samples were treated at 0.1 and 400 MPa at 40 °C for 0, 5, 10, 15 and 20 min at as described in tables 3.3-4 and 3.3-5. The pressure was built up at the rate of 300 MPa/min and the decompression time was less than 30 s.

Table 3.3-4 Preparation of acid-casein and ß-casein as substrate for MTG kinetics

Final casein concentration (mg/mL)	0.125	0.50	0.75	1.50	2.0	3.00
Stock solution of casein (mL) at 6 °C	0.05	0.20	0.30	0.60	0.80	1.20
0.2 mol/L TRIS-acetate buffer pH 6.0 (mL) at 6 °C	4.65	4.45	4.40	4.10	3.90	3.50
⬇						
Vortex mixed						
⬇						
Stock solution of MTG (mL) at 6 °C	0.30	0.30	0.30	0.30	0.30	0.30
⬇						
Vortex mixed						
⬇						
Applied in 2mL polypropylene tube without air bubbles air						
⬇						
Reaction conditions:						
Temperature (°C):	40					
High pressure (MPa):	0.1 and 400					
Time of reaction (min):	5, 10, 15, 20					

Table 3.3-5 Preparation of α_{s1}-casein as substrate for MTG kinetics

Final casein concentration (mg/mL)	0.125	0.50	0.75	1.00	1.75	2.00
Stock solution of casein (mL) at 6 °C	0.25	1.00	1.50	2.00	3.50	4.00
0.2 mol/L TRIS-acetate buffer pH 6.0 (mL) at 6 °C	4.45	3.70	3.20	2.70	1.20	0.70
⬇ Vortex mixed ⬇						
Stock solution of MTG (mL) at 6 °C	0.30	0.30	0.30	0.30	0.30	0.30
⬇ Vortex mixed ⬇						
Reaction conditions						
Temperature of reaction (°C):	40					
High pressure (MPa):	0.1 and 400					
Time of reaction (min):	5, 10, 15, 20					

After reaction time, the sample was placed in a water bath at 80°C for 5 min and then immediately cooled to 20°C before gel permeation chromatography analysis (section 3.3.3b).

b) Gel permeation chromatography

Decrease of monomeric casein was measured by gel permeation chromatography following the procedure of Schwarzenbolz (2000).

Material

Elution buffer

360.36 g urea, 5.84 g NaCl, 14.20 g Na_2HPO_4, 1.00 g CHAPS were dissolved in 500 mL distilled water. After complete dissolution pH was adjusted to 6.8 using concentrated HCl. The volume was made up to 1 L. The buffer was filtered using a 0.45 μm regenerate cellulose filter and degassed in an ultrasonic bath for 30 min.

Sample buffer

1.0 g 1,4-Dithiothreitol (DTT)/100mL elution buffer.

Method

Sample preparation and loading

After high pressure and thermal treatment, 0.54 g urea, 8 mg DTT and 1 mg CHAPS were dissolved in 1.5 mL MTG-casein sample and incubated at 4°C for 20 h, then filtered through a 0.45 μm membrane filter before subjecting 500 μL portions to a gel permeation chromatography column.

Chromatographic analysis was performed at 25 °C with a Knauer WellChrom HPLC system with a high performance gel filtration column (Superdex 200 HR 10/30) at a flow rate of 0.5 mL/min using the elution buffer. Detection was made in the ultraviolet region (280 nm) and the chromatograms analysed by a curve-fitting software EuroChrom 2000.

Operating conditions

Chromatography equipment:	HPLC pump K-1001 with an UV detector K-2500, electrically driven 6-Port-Multi-Channel Valve, Interface Box, Knauer WellChrom, Berlin, Germany
Column:	Superdex 200 HR 10/30, Pharmacia-LKB Freiburg, Germany
Temperature system:	25 °C
Sample concentration:	0.25 to 3 mg protein per 1 mL sample buffer
Injection volume :	500 μL
Sample buffer:	mol sodium phosphate pH 6.80 Containing: 6 M urea , 0.1 M NaCl, 0.1% CHAPS,1% DTT
Elution buffer:	mol/L sodium phosphate pH 6.80 Containing: 6 mol/L urea , 0.1 mol/L NaCl, 0.1% (CHAPS)
Flow rate :	0.5 mL/min
Detection:	Ultraviolet λ = 280 nm
Data analysis	EuroChrom 200 program, Knauer WellChrom, Berlin, Germany

3.4 Influence of covalent cross-linking on storage modulus of acid gels obtained by transglutaminase and glucono-δ-lactone

3.4.1 Pre-trial experiments

Whole casein (5% w/v) was added to 0.014 M phosphate buffer (pH 6.8). The casein solutions were heated from 20 to 40 °C within 2 min and inoculated with two different concentrations of MTG (0 and 6 U/g casein) at four levels of glucono-δ-lactone (0.164, 0.124,

0.334 and 1 g/g casein). Immediately, rheological measurements were performed as described in section 3.4.4.

Pre-trial experiments were set up using a matrix in a completely randomised design with two replicates. Date were analysed by Duncan's multiple range test using Olivares program (1990). Significant differences were defined at $p < 0.05$.

3.4.2 Experimental design

The preliminary results were then used to design the central composite rotatable design (CCRD) with two factors and two levels like represented in figure 3.4-1.

The design may be subdivided into three parts.
1.- The four points (-1, -1), (1, -1), (-1, 1) and (1,1) constitute a 2^2 factorial.
2.- The four points (-1.414, 0), (1.414, 0), (0, -1.414), (0, 1.414) are the extra points included to form a central composite design with α = 1.414. The figure formed by these points is called a star.
3.- Five points are added at the center to give roughly equal precision for dependent variable within a circle of radius 1.

An experimental plan was performed to analyse the rheological properties of acid gels. The independent variables were enzyme and glucono-δ-lactone (Gdl) concentrations while storage modulus (G'), loss factor (tan δ) as well as gelation time were the measured responses. The levels used for each variable were varied according to a CCRD. Experiments were randomized in order to minimise the effects of unexplained variability in the observed responses due to extraneous factors. Matrix computation was elaborated with coded variable to facilitate the regression analysis and optimum point determination. Response functions for the gels were assumed to be approximated by second-degree polynomial equations:

$$y = b_0 + b_1 x_1 + b_2 x_2 + b_{11} x_1^2 + b_{22} x_2^2 + b_{12} x_1 x_2 \qquad (34.\text{-}1)$$

where b_0 was the value of the fitted response at the center point of the design, b_1, b_2 the linear terms; b_{11}, b_{12} the quadratic terms and b_{12} the cross-product regression terms. Regression analysis, optimisation and mapping of the fitted response surfaces were achieved using Design- Expert software program (Design-Expert version 6, Stat-Ease Inc., USA).

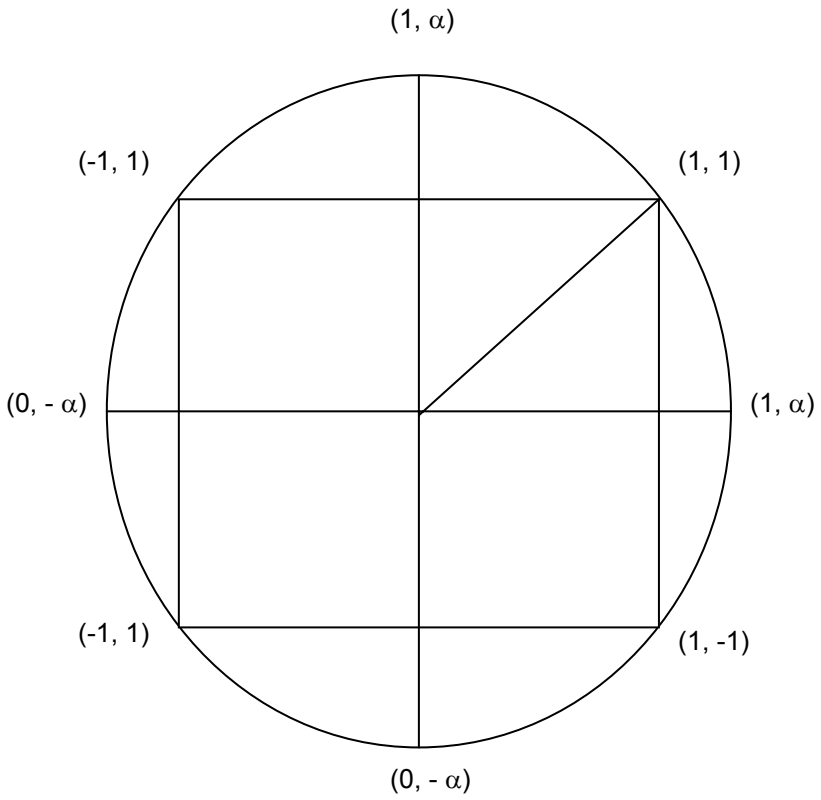

Figure 3.4-1 Central composite rotatable design with two variables.

Table 3.4-1 Arrangement and response central composite rotatable design (CCRD)

Experiment No.	Independent variables			
	Uncoded		Coded	
	U MTG/g casein x_1	g Gdl/g Casein x_2	x_1	x_2
1	5.82	0.334	1	1
2	5.82	0.214	1	-1
3	0.98	0.334	-1	1
4	0.98	0.214	-1	-1
5	3.41	0.358	0	1.414
6	3.41	0.189	0	-1.414
7	6.83	0.274	-1.414	0
8	0.00	0.274	1.414	.0
9	3.41	0.274	0	0
10	3.41	0.274	0	0
11	3.41	0.274	0	0
12	3.41	0.274	0	0
13	4.41	0.274	0	0

3.4.3 pH measurement

Samples were prepared as described in section 3.4.1 and the process acidification was followed with a WTW pH electrode (526 WTW, Weinheim, Germany).

3.4.4 Rheological measurement

Material

Casein samples solution (3.4.1 and 3.4.2)

Method

Sample preparation and loading

Portions of 22 mL sample solution were transferred into the concentric cylinder system at 40°C and covered with silicone oil to prevent evaporation. Dynamic rheological properties were measured using an oscillation rheometer as described by Schorsch *et al.* (2000a).

Running conditions

Rheometer	Physica UM oscillation rheometer Physica Messtechnik, Stuttgart, Germany
Concentric cylinder system	CC27/Pr -150 Q-DIN 53019
Temperature system (°C)	40
Frequency (Hz)	1
Amplitude deformation (%)	10

Following the rheological measurement, the gels were quickly heated to 80°C and maintained at this temperature for 2 min in order to inactivate the enzyme. Subsequently, the gels were lyophilised and stored at 4 °C until chromatographical analysis (section 3.4.5).

3.4.5 Gel permeation chromatography

After rheological measurement, the degree of oligomerisation of the acid gels was analysed by gel permeation chromatography following procedure of Schwarzenbolz (2000).

Material

Elution buffer and sample buffer were prepared as described in section 3.3.3b.

Method

Sample preparation and loading

Lyophilised gel samples (4 mg) from acid gels were dissolved in 2 mL sample buffer containing 1% DTT. After incubation at 4°C for 20 h the samples were filtered through a 0.45 μm membrane filter before subjecting 150 μL portions in to a gel permeation chromatographic column for analysis. Chromatography analysis was performed as described in operating conditions of the section 3.3.3b.

3.5 Statistical analysis

Analysis of Varianza (ANOVA), Tuckey and Duncan multiple range tests in a 95% confidence interval were calculated to compare the significant difference among the means of the results using Olivares Program (Olivares, 1990).

The mathematic adjustment of the hyperbolical curves in chapter 4.2 were performed using Sigma Plot Software (Systat GmbH, Germany) and DynaFit Software (Bioking, Ltd, USA).

The kinetic pressure/temperature diagram in chapter 4.1 and the mathematic model, Central Composite Rotatable Design (CCRD) in chapter 4.3 were performed using Design-Expert software Program (Design-Expert version 6, Stat-Ease Inc., USA).

4 Results and discussions

4.1 Microbial transglutaminase under high pressure

Application of high pressure treatment to a protein solution provides a way to perturb the its structure and interactions with the solvent without broking primary structure (Kitchen *et al*., 1992). Thereby, high pressure can be used to explain a more detail description of kinetic, thermodynamic and structural changes of protein unfolding (Mozhaev *et al*., 1996). If a simultaneous application of pressure/temperature on protein unfolding or enzyme inactivation is studied, the volume change and thermal energy are used separately to interpret the effect of both variables on the denaturation process (Samarasinghe *et al.,* 1992).

The influence of high pressure between a microbial and a tissue animal transglutaminase was compared. The effect of high pressure and thermal treatment on MTG inactivation was investigated based on the structural changes of MTG and its relation with the loss of enzyme activity. Secondary and tertiary structures, as well as products from protein-protein and protein-reducing sugar were analysed to know the different causes that leads enzyme inactivation. Finally, to interpret the simultaneous effect of pressure and temperature treatment, a kinetic study of MTG inactivation was also performed at different pressure and temperature within a long time until the enzyme achieves a 50% residual activity to performed pressure/temperature inactivation diagram.

4.1.1 Short thermal inactivation

Thermal inactivation of MTG at 0.1 MPa at 60, 70 and 80°C for 0, 2, 4, 6, 8 and 10 min was analysed to investigate temperature conditions to achieve a total and irreversible enzyme inactivation (figure 4.1-1). Residual enzyme activities after treatment at 60°C for 5 and 10 min were 11 and 7%, respectively. Complete inactivation was achieved at 80°C for 2 min. Enzyme activity did not recover after incubation at 37°C for 180 min. This demonstrated that temperatures above 80°C induce irreversible enzyme inactivation, which could be caused by a complete irreversible protein unfolding leading to an exposure of hydrophobic groups, scrambled structures, formation of non-native disulfide bridges and enzyme aggregation. In addition, high temperature processing could cause hydrolysis of peptide bonds and chemical reactions between proteins and carbohydrates, which are discussed in chapter 4.1.3.2.

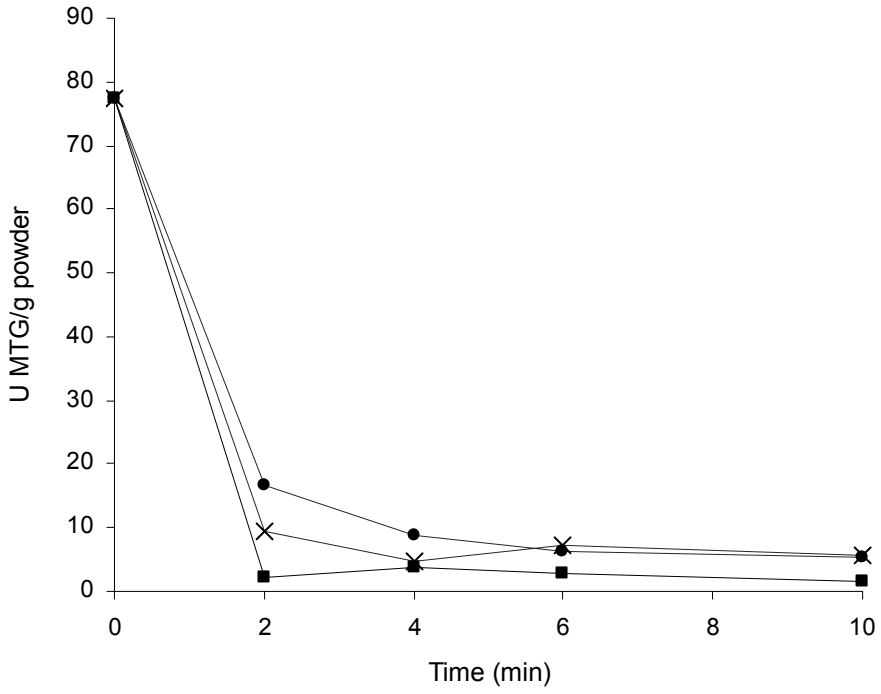

Figure 4.1-1 Thermal inactivation of MTG at 0.1 MPa at high temperature from 2 to 10 min. (-●-) 60°C, (-x-) 70°C, (-■-) 80°C.

4.1.2 Effect of pressure on inactivation of MTG at constant temperature

High pressure inactivation of MTG and guinea pig liver TG at 0.1, 200, 400 and 600 MPa and 40°C for 0 to 60 min within a range time from 0 to 60 min studied considering thermodynamic data analysis. Kinetic parameters were calculated from experimental data using the following terms: reaction order *(n)*, rate constants *(k)* and activation volumes (ΔV^*). In general, an *n*th-order rate equation can be written as

$$dA/dt = -kA^n \qquad \text{(eq. 4.1-1)}$$

Where A is the response property, k the rate constant, t the treatment time and n the reaction order. For a first order reaction, the integration of equation 4.1-1 for a decay process at constant pressure and temperature is given by:

$$\ln[A_p / A_{(0,t)}] = -k(t - t_0) \qquad \text{(eq. 4.1-2)}$$

Applied on enzymes, A_0 in equation 4.1-2 is referred to as the activity at t=0 and A represents the activity at different time points of physical treatment (temperature or pressure).

High hydrostatic pressure inactivation data of MTG and guinea pig liver TG at 40°C in a pressure range between 0.1 to 600 MPa within a time range of 0 to 60 min were analysed with the linearisation of equation 4.1-2 using logarithmic data transformation. The response value [lnA/A_0] as a function of inactivation time at constant temperature revealed, that the rate of MTG and guinea pig liver TG inactivation followed a first-order kinetic model (figure 4.1-2).

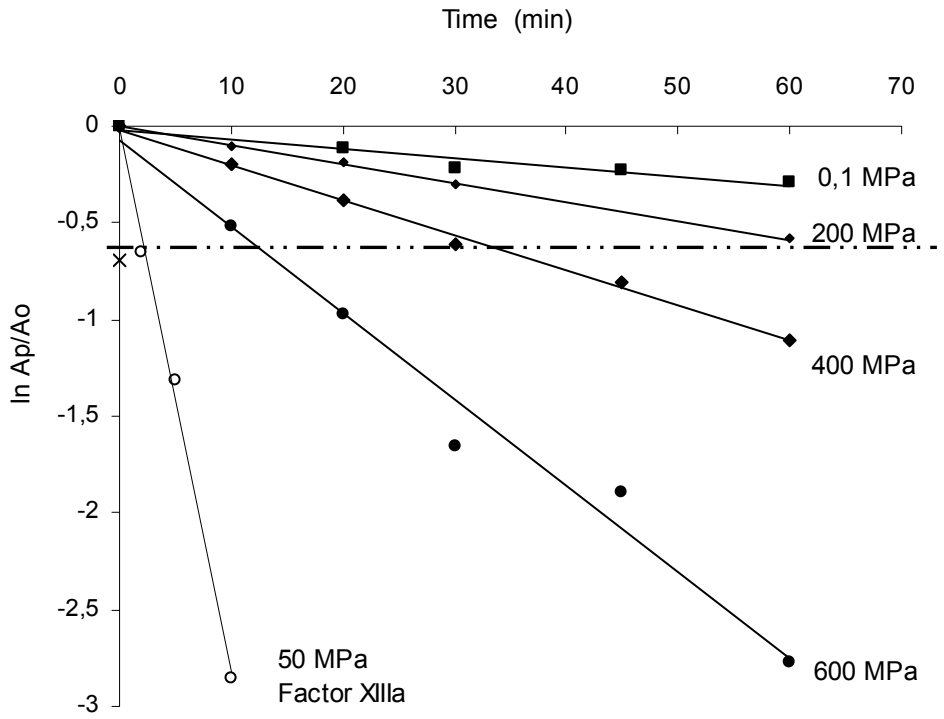

Figure 4.1-2 Inactivation of MTG and guinea pig liver TG (Factor $XIII_a$) by high-pressure treatment at 0.1, 200, 400 and 600 MPa and 40°C. The dotted line shows 50% enzyme inactivation.

Inactivation rate constants were derived from the slope of the regression lines. The estimated rate constants value *(k)* of MTG and guinea pig liver TG (Factor $XIII_a$) are summarised in table 4-1-1. The rate constant values *(k)* of MTG in a range from 0.1 to 600 MPa at 40°C in a time range from 0 to 60 min showed that inactivation velocity of MTG increased with higher pressure. The rate constant value *(k)* of guinea pig liver TG reached a value 26.6±4.5 $x10^{-3}$ min^{-1} at 50 MPa, whereas MTG had a lower value (18.3±2.5 $x10^{-3}$ min^{-1}) at treatment at 400 MPa, which indicated that guinea pig liver TG had a very high inactivation velocity and demonstrated that this enzyme is not stable under high pressure treatment, as is hypothetically suggested in the end of this section.

Table 4.1-1 Estimated inactivation rate constants for the isobaric inactivation of MTG and factor $XIII_a$

Enzyme	Pressure (MPa)	Inactivation rate constante ($1x10^{-3}$ min^{-1})	Regression coefficients
MTG	0.1	4.7±0.89	0.92
	200	9.7±2.19	0.99
	400	18.3±2.15	0.99
	600	47.7±6.7	0.97
Factor $XIII_a$	50	26.6±4.5	0.92

The pressure dependence of the rate constant *(k)* at a certain temperature was described as an activation volume ΔV^* as given in the Eyring relation:

$$\ln[k / k_{(0,t)}] = -\frac{\Delta V^*}{RT}(P - P_0)$$

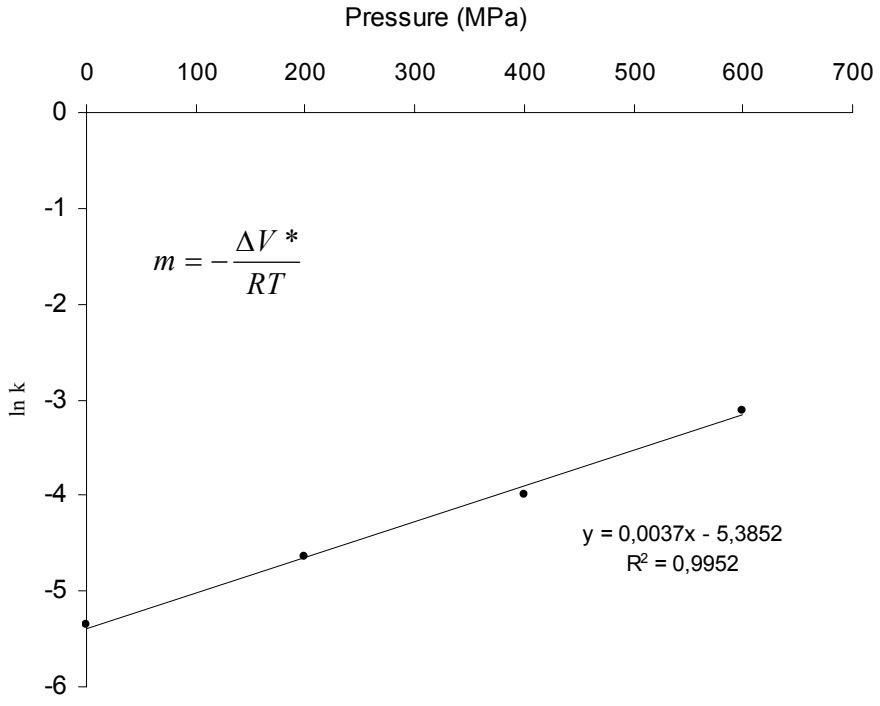

Figure 4.1-3 Inactivation of MTG by high-pressure treatment at 0.1, 200, 400 and 600 MPa and 40°C

From chapter 2.4.4 (equation 2.4-33) and represented in figure 4.1-3. Where k_o is the rate constant at pressure P_0, P is the value of applied pressure, ΔV^* is the activation volume at a

certain temperature, T is the absolute temperature, and R is the universal gas constant. Plotting the rate constant of MTG inactivation at 40°C as a function of pressure, an inactivation volume of –10.2±0.5 cm^3/mol is obtained. This value corresponds closely to at reported by Lauber *et al*. (2001), who found a inactivation volume of -17.4±0.4 cm^3/mol.

Considering Braun-Le Chatelier´s principle, $\Delta V^* < 0$ favours the denaturation of proteins and accelerates of the enzyme inactivation under pressure (Jaenicke, 1983). Therefore, the inactivation volume of MTG (-10.2±0.5 cm^3/mol) demonstrates that this enzyme has a higher pressure stability than phosphatase (-58 cm^3/mol), γ-glutamyltransferase GGT (-65cm^3/mol) or α-amylase (-45 cm^3/mol) at 40°C (Rademacher, 1999).

Effect of high pressure on the structure of the animal transglutaminase from pig liver tissue (Factor $XIII_a$)

Pig liver tissue TG (Factor $XIII_a$) in a 0.2 mol/L TRIS-acetate buffer pH 6 achieved a 50% inactivation in only 3 min. The fast inactivation of this enzyme can be explained by two important considerations: its non-protection by additives and its conformational structure.

1) Non-protection by additives

An important consideration to discuss the low stability of pig liver TG under high pressure in comparison to MTG is its purity. Pig liver TG (Factor $XIII_a$) was purchased from Sigma (Steinheim, Germany) as a pure enzyme, whereas MTG Activa $_{TM}$ MP (Ajinomoto, Germany) is a commercial power containing 90% lactose and 9% maltodextrin. Enzymes for industrial use are generally protected by additives to maintain its conformation, prevent structural changes and unfolding aggregation (Aberer *et al.,* 2002). As, the pig liver TG is not protected by additive, a very fast inactivation was achieved. The pressure induced hydrophobic groups to the surface upon unfolding, and then, strong hydrophobic attraction among denatured enzymes induced unfolding aggregation and loss of enzyme activity.

On the contrary, the secondary structure of MTG (discussed in chapter 4.1.3) with its concomitant high enzyme activity could be better conserved by lactose and maltodextrine. These additives could reduce protein denaturation due to decreasing water activity. The polyhydric molecule lactose; modifies the water environment surrounding MTG, competing for and replacing the free water. This causes a modification on the hydration shell of the protein and avoids hydrophobic aggregation. The modification confers protection to MTG,

maintaining its conformational structure and its enzyme activity. Stabilisation of protein under high pressure using sugar or salts is in agreement with Iametti *et al*. (1998), which stated that ovoalbumin treated under high pressure were more stable when the samples contained 10% sucrose or 10% NaCl.

2) Enzyme structure: A hypothetical theory

The crystal structure of pig liver TG has not yet been reported, it is not possible to describe exactly, why the enzyme is not stable under high pressure. However, other authors have compared this enzyme with other tissue TG. For example Chica *et al.* (2003), reported that the percentage of identity of the catalytic domains of read seam tissue TG with the pig liver tissue TG is higher than 55% and the percentage of homology is around 70%. Furthermore, all of the active site residues (Trp236, Cys272, His300, Trp329, His332 and Tyr515) are conserved in all sequenced of tissue transglutaminases, including the human TG, which the catalytic domain has 58% identity and 70% homology with the fish TG. For this reason, the authors take the read seam tissue TG structure as a model to propose a role of conserved active site Tyr and Trp residues. Then, based on pig liver tissue TG stability study of Venere *et al.* (2000) and taking as model the structure of read seam tissue TG, it can be suggested that the animal TG represent a shallow, narrow cleft running diagonally in its surface passing over the active site, which could be easily destroyed under high pressure (figure 4.1-4).

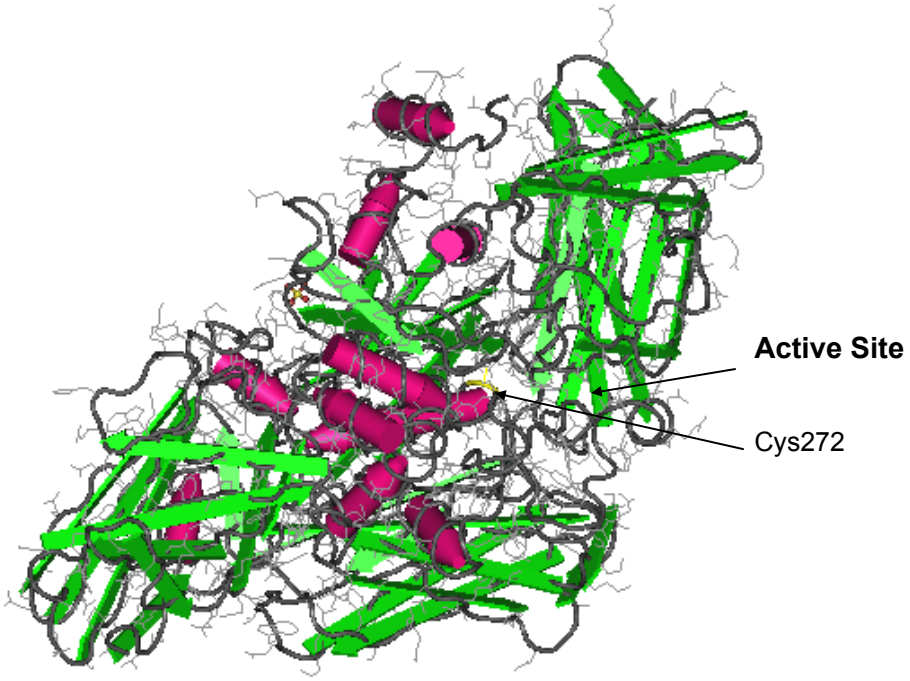

Figure 4.1-4 Animal transglutaminase from read seam tissue *(*Noguchi *et al*., 2001).

4.1.3 Effect of high pressure on the conformational structure of MTG

The folded state of a protein or an enzyme is determined by an ensemble of well defined substructures, which held together by non-covalent interactions between molecular groups within the protein and between these groups and the solvent (Ludescher, 1996). These non-covalent bonds involve van der Waals interactions between nearby atoms, electrostatic interactions between charged groups and permanent dipoles, hydrogen bonding, polar donor and acceptor groups and hydrophobic interactions between non-polar side chains and the hydrophilic solvent. Folded and unfolded state can be represented by two state reactions in which the native protein, N, is altered into unfolded or denatured state, U: N → U.

The unfolded state of a protein can be achieved by the application of a high concentration of denaturing agents, changes of pH or high temperature treatment (Dubey and Jagannadham, 2003; Sun *et al*., 1998). High pressure treatment induces weakening of non-covalent bonds, hydration of amino acid residues with changes in the solvent accessibility of hydrophobic groups and subsequently changes in the protein structure (Kitchen, 1992; Mozhaev, 1996; Barciszewski 1999). These changes cause protein unfolding with a concomitant loss of its stability in solution or enzyme activity (Sun *et al*., 1998; Dubey and Jagannadham, 2003).

Conformational changes of native MTG structures in relation to protein concentration, enzyme activity, as well as secondary reactions were analysed after high temperature and pressure treatment. MTG samples with low protein concentration (11.7 μg/mL by Lowry method) and high protein concentration (117 μg/mL by Lowry method) were evaluated at high pressure treatment (40°C and 0.1, 200, 400 and 600 MPa for 30 to 60 min) and high temperature treatment (80°C at 0.1 MPa for 2 min). At high temperature treatment as well as pressure treatment above 600 MPa, protein precipitation was observed in samples with high protein concentration. Samples containing 117 μg protein/mL undergo a irreversible precipitation of MTG after treatment at 600 MPa and 40°C for 30 to 60 min and at 0.1 MPa at 80°C for 2 min. Soluble protein of the native samples decreased from 117 to 91 and 66 μg/mL after incubation at 600 MPa and 40°C for 30 and 60 min, respectively. After treatment at 0.1 MPa and 80°C for 2 min, only 36 μg/mL protein remained in solution. This protein precipitation phenomenon is in agreement with other authors. Zipp and Kauzmann (1973) found that metmyoglobin precipitation was observed under specific conditions of pressures and temperatures in a pH range from 5 to 9. For example, although protein denaturation was achieved at 20°C, 450 MPa and pH 6, protein precipitation was not detected until increasing temperature above 75°C. However protein precipitation was not observed in samples treated

at any combination of pressure and temperature in a range from 0.1 to 600 MPa and 0 to 80°C if the pH was below 5 and above 9. The authors proposed that pressure tends to solubilise the denatured protein, but it is more possible that protein solubility is a function of the charged side chains of a protein. The total charge on a protein in solution depends principally of the solution pH and the pK_a of the side chain titratable groups. When the side chain is basic, a doubly positive species exist at low pH and when the side chain is acid, a double negative species exits at high pH. The charged carboxylic and amino groups interact strongly with water, therefore, protein remains in solution (Ludescher, 1996). Based on these amino acids chemical properties, it could be proposed that, in a puffer TRIS-acetate 0.2 mol/L at pH 6, the aspartic and glutamic acid, as well as Lys, His and Arg residues of MTG surface molecules are not strongly charged. In addition, proximity of molecules was enhanced by increasing protein concentration. For this reason, precipitation and aggregation in samples with high protein concentration was obtained. That is also in agreement with Iametti *et al*., (1998), who reported that the formation of insoluble aggregates is favoured by high protein concentration. They found that solubility ovoalbumin samples with a concentration of 0.5 and 2 mg/mL remained around 100% solubility after treatment at 450 MPa at pH 6.0, but the solubility of sample with a concentration of 5 mg/mL was reduced to around 50%.

Precipitation of the protein proved that the stability of native enzyme was a function of high pressure and thermal treatment, as well as protein concentration, revealing that the rupture of non-covalent bonds that are responsible for its intrinsic stability. Irreversible precipitation of MTG at 40°C and 600 MPa could be caused by protein unfolding followed by protein-protein association via hydrophobic group interactions, hydrogen bonding and finally disulfide bonds formation from the thiol groups of Cys64, which are favoured at high protein concentration. To explain this theory, changes in the MTG structure of soluble protein and analysis of precipitated protein is following discuss.

a) Soluble protein

Changes in the tertiary structure

The CD spectrum of a protein in the near ultraviolet wavelength region (250-320 nm) corresponds to the orientation of aromatic amino acids and is used to determine the tertiary structure of protein. The signals, magnitudes and wavelengths of aromatic CD bands cannot be quantitatively calculated. However, these spectra represent a highly sensitive criterion for the native state of a protein and can be generally used to explain the folded conformation. Tertiary structure changes of native MTG after high pressure treatment at 40°C and 0.1, 200, 400 and 600 MPa for 30 to 60 min and high temperature treatment at 80°C at 0.1 MPa for 2

min were analysed in the near ultraviolet wavelength range from 250 to 320 nm (Mulkerrin 1996). CD spectra in aromatic regions (figure 4.1-5) are characterised by the band around 252, 256, 262 and 268 nm for phenylalanine, (continues grey circles); around 275 and 283 nm for tyrosine (continues black circles) and around 290 and 298 nm for tryptophan (dashed circles).

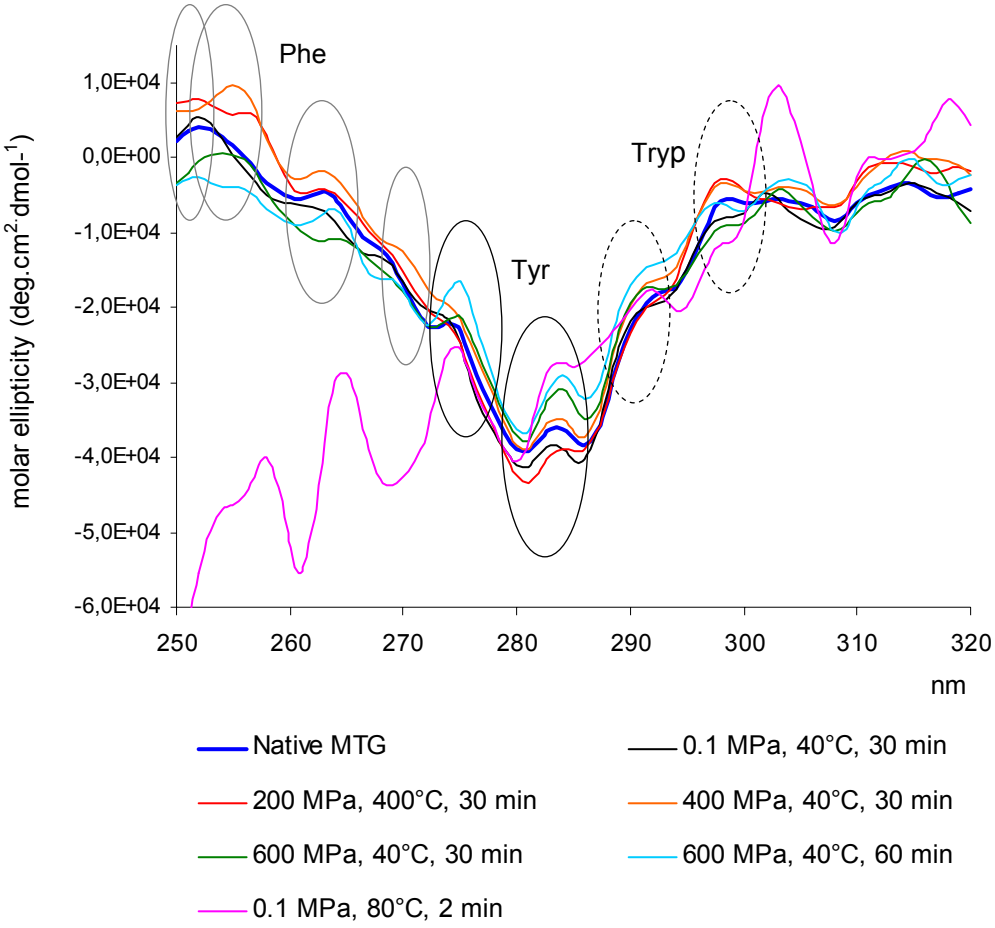

Figure 4.1-5 Near CD spectra of MTG after thermal and high pressure treatments

Spectra of the native MTG sample showed different profiles in comparison to the treated samples. Intensity of phenylalanine bands increased only in samples treated at 200 and 400 MPa at 40 °C for 30 min, but the profile of this band was completely absent in the samples treated at 40°C at 600 MPa and 0.1 MPa and 80°C for 2 min. The intensity of tyrosine bands at about 283 nm increased proportionally with increasing pressure treatment above 400 MPa at 40 °C for 30 min and the highest peak was achieved in sample treated at 0.1 MPa and 80 °C for 2 min. Depending on the individual treatment, the intensity of the tryptophan bands (290 and 298 nm) either increased or decreased, but did not show a certain tendency. The tertiary structure of the native enzyme was mainly altered at 600 MPa and 40 °C for 60 min

and a short thermal treatment at 0.1 MPa and 80°C for 2 min was sufficient to achieve a complete unfolded state.

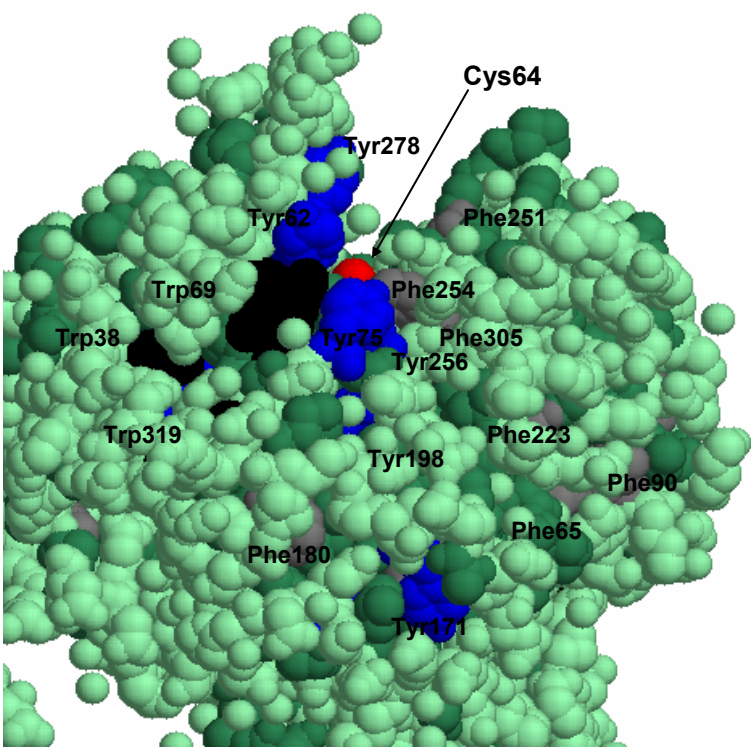

Figure 4.1-6 Microbial transglutaminase from Streptoverticillium mobaraense displayed as space fill to represent the different hydrophobic groups: Phe (grey), Trp (black), Tyr (blue), hydrophobic region (dark green). The Cys64 (red) is located at the bottom of the active site (Kashiwagi *et al*., 2002).

Profile bands of phenylalanine (252, 256, 262, 268) and tryptophan (290, 298) were not very distinct (figure 4.1-5), probably because these amino acid residues are located within the hydrophobic MTG region (figure 4.1-6) or because phenylalanine carries a symmetric chromophore, which is weakly absorbing (Mulkerrin, 1996). However, the small contribution of phenylalanine (Beychok, 1965) showed that these hydrophobic regions were not destroyed after the high pressure treatment but were destroyed after thermal treatment. The band at 283 nm for tyrosine increased distinctly at 0.1 MPa at 80°C and proportionally with increasing pressure above 400 MPa, which suggests that this amino acid residue is more exposed to the TRIS-acetate buffer in comparison to phenylalanine and tryptophan residues. The former phenomenon can be explained by the fact that high pressure and high thermal treatment changes the polar hydroxyl group of tyrosine from the undissociated state at neutral pH and standard condition to the dissociated state favouring its hydrophilicity (Nosoh and Sekiguchi 1991). High pressure treatment could induce distinct solvation around hydrophobic groups on the active site of MTG. Then, based on the figure 4.1-6 (Kashiwagi *et al*., 2002), it is proposed that Phe251, 254; Trp69 and especially Tyr278, 62, 75 were exposed on the surface of molecule. These results agree with Kitchen *et al*. (1992), who

demonstrated that 0_{η} of the tyrosine35 residue of bovine pancreatic trypsin inhibitor increases its percent solvent accessibility from 4.6 after treatment about 10 MPa and to 9.5 after treatment about 1000 MPa. Thus, the intensity variation of these amino acids were associated with the mobility of their aromatic side chains and their exposure to the TRIS-acetate buffer, leading to loss of the MTG tertiary structure with subsequently instability in solution.

Changes in secondary structure

Spectra in the far ultraviolet wavelength range (190 to 260 nm), which correspond to the amide region, were used to characterise the conformational structure of the enzyme (figure 4.1-7). Native MTG showed typical α-helix spectra indicated by a negative $\eta - \pi^*$ transition band at 222 nm and a $\pi - \pi^*$ transition, namely a positive perpendicular $\pi - \pi^*$ transition band at 191 and a negative parallel $\pi - \pi^*$ transition band at 208 (Sarkar and Doty, 1966; Mulkerrin, 1996., Venere *et al*., 2000).

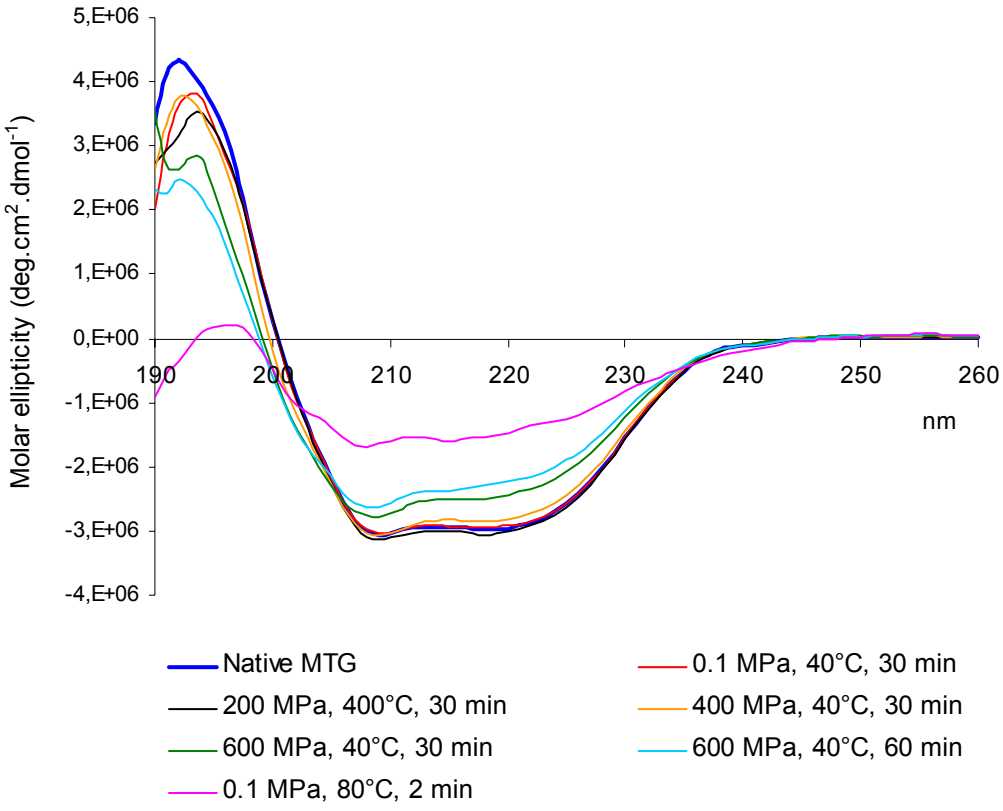

Figure 4.1-7 Far-UV CD spectra of MTG after thermal and high pressure treatments

The negative shifted CD signal at 222 nm primarily corresponds to the backbone peptide bond $\eta - \pi^*$ transition and reflects alterations in the secondary structure, especially in the α-helix content of the enzyme (Gratzer *et al*., 1961; Mulkerrin, 1996). As already cited in chapter 2.6.2, the stability of the peptide backbone is explained by mesomeric effect of the peptide bond, to the π molecular orbital extends over 0=C-N, where double bond character changes between the O-C and C-N bond (Nosoh and Sekiguchi 1991). For this reason, the decreased cotton-effect at 222 nm of MTG reflects alterations in the secondary structure and could suggest that treatment above 600 MPa at 40°C for 30 min caused drastic changes to the α-helices of the MTG conformation. A short thermal treatment at 80°C for 2 min was sufficient to achieve maximum loss of the original structure (figure 4.1-8).

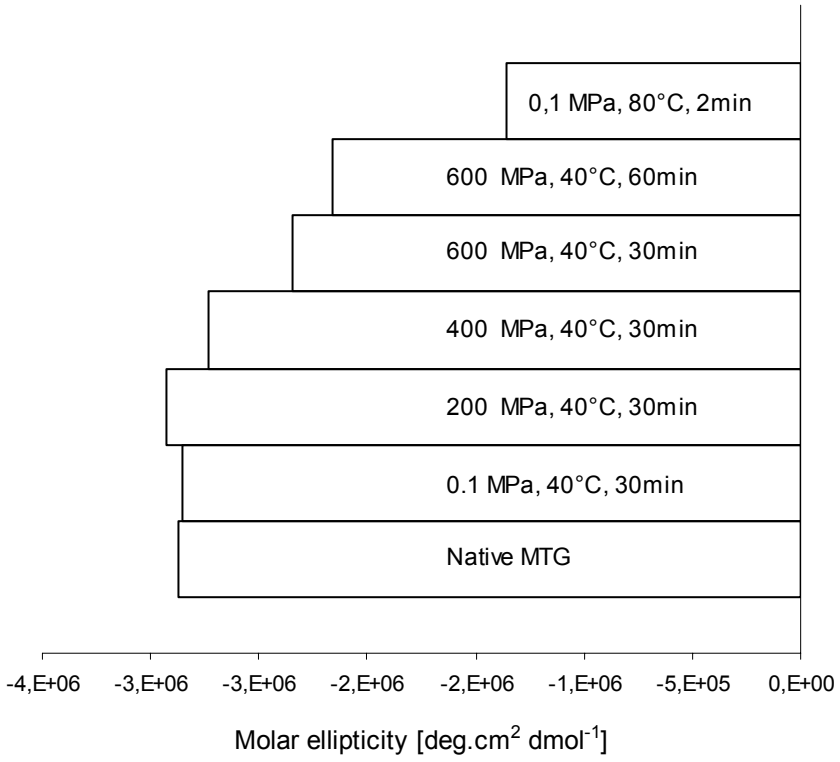

Figure 4.1-8 CD signals at 222 nm of MTG after thermal and high pressure treatment.

Because amide chromophores and the long-range order is responsible for the characteristic spectra of each of the secondary structure elements of a molecule, the CD spectra from the far-UV region can be used to predict the secondary structure of proteins (Greenfield and Fasman, 1969). In this work, the CONTIN mathematic algorithm with a set of 48 protein basis spectra, each representing a secondary structure element (Provencher and Gloeckner, 1981; Sreerama and Woody, 2000), was used to calculate the secondary structure for soluble MTG.

The results showed that native MTG consisted of 24.5% α-helix, 23.8% β-strand, 21.1% β-turn and 30.7% unordered structure (table 4.1-2). A loss of α-helix and an increased percentage of unordered structure occurred after high pressure and thermal treatment. After treatment at 400 and 600 MPa at 40 °C for 30 min, the content of α-helix decreased to 32.3 and 19.7% respectively. Massive destruction of α-helix to a residual amount of 6.5% was observed after thermal treatment at 80°C for 2 min. After treatment at 200 MPa and 40°C for 30 min, the content of α-helix was closely to native MTG.

Table 4.1-2. Secondary structure of MTG under high pressure and thermal treatment.

Treatment with MTG	H* %	S* %	Turn* %	Unrd* %	Rest Activity %
1. Native	24.5	23.8	21.1	30.7	100
2. 40 °C, 0.1 MPa, 30 min	23.5	23.6	21.0	31.9	85
3. 40 °C, 200 MPa ,30 min	24.2	22.9	21.0	31.9	94
4. 40 °C,400 MPa, 30 min	23.3	23.9	21.2	31.5	83
5. 40 °C, 600 MPa ,30 min	19.7	25.9	20.9	33.5	55
6. 40 °C, 600 MPa, 60 min	17.2	27.5	20.6	34.8	38
7. 80 °C, 0.1 MPa, 2 min	6.50	28.2	18.4	46.9	0

* H = α-Helix; S = β-strand; Turn = β-Turn; Unrd = unordered

Conformational modification of the secondary structure was also accompanied by a corresponding loss of the enzymatic activity (table 4.1-1). Elevated enzyme activity was recorded with higher contents of α-helix structure elements. Tauscher (1995) reported that β-sheet structures are nearly incompressible and more stable against pressure than α-helix structures. Nosoh and Sekiguchi (1991) reported that hydrophilic residues are found predominantly in α-helices, which concur with the tertiary structure of MTG proposed by Kashiwagi *et al.* (2002). The enzyme is arranged in a way that the active site located between β-strand domains, is surrounded by α-helices (figure 4.1-9).

Pressure induced degradation of this conformation would primarily take place at these α-helical areas on the molecule's surface, leading to an alteration of the tertiary structure with subsequent consequences on substrate binding. Therefore, it can be suggested that enzyme

activity at elevated pressures is closely related to the depth active site cleft, the relative stability of α-helix and the outstanding stability of the central β-strand structure.

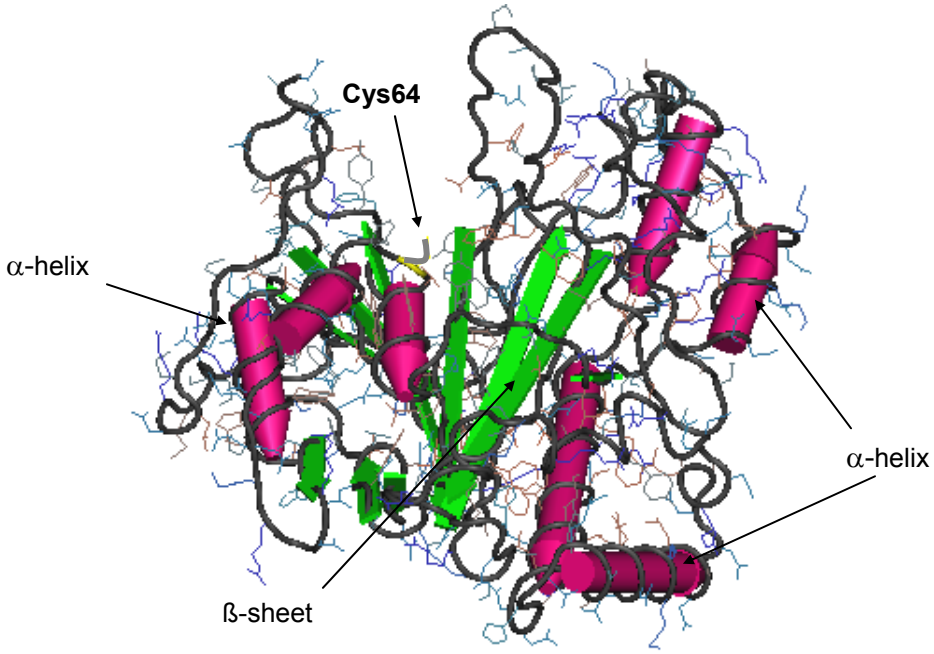

Figure 4.1-9 Microbial transglutaminase from *Streptoverticillium mobaraense (*Kashiwagi *et al.,* 2002).

The behaviour of the changes on the tertiary and secondary structure of MTG under high pressure are in agreement with the structure change of ovoalbumin under high pressure and 25°C within a range time from 0 to 10 min (Iametti *et al*., 1998). The near-UV CD spectra of ovoalbumin treated at 450 MPa is very similar to the native protein. Protein treatment at 600 and 800 MPa lead to a partial loss and complete destroyed spectra, respectively. The same behaviour is observed for the far-UV spectra and the negative CD signal at 222 nm, correspondent to the backbone peptide, decreased as function of pressure too. However, the author did not report contain of α-helix, ß-sheet structure and only stated that at the harshest treatment conditions (800 MPa for 10 min), the soluble ovoalbumin did not conversion of secondary structure to an unfolding random coli.

The comparison of both results indicated that MTG is more stabile than ovoalbumin under high pressure. This can be attributed to the high concentration of lactose and maltodextrin, which protect the MTG (discussed in chapter 4.1.2 in the section of hypothetic theory of the effect of high pressure on the structure of the animal transglutaminase from pig liver tissue, Factor $XIII_a$). In addition, the biochemical and physicochemical characteristics of theirs amino acids sequence as well as secondary structures of the protein play also very important roles. For example, the four free thiol groups of cysteine residues of ovoalbumin formed disulfide

groups under high pressure (Iametti *et al*., 1998) with a consequently loss of protein stability. This result is also in agreement with this work, where pressure induces disulfide bond formation, as is discussed in the next chapter.

b) Irreversible precipitated protein

Irreversible precipitated protein that could be observed only in samples with a high protein concentration after treatment at 600 MPa and 40 °C for 60 min and 0.1 MPa at 80 °C for 2 min was analysed by SDS-PAGE electrophoresis (figure 4.1-10). One band with a molecular weight of approximately 40 kDa from reduced native MTG was obtained (lane 3). A peculiar double band was identified from non-reduced native MTG (lane 2). Because the MTG sample was concentred from 117 to 234 μg protein/mL, a higher proximity among molecules in solution was achieved. This could induce a reduction of distance between a pairs of atom (Nosoh and Sekiguchi, 1991). Based on this theory, it is speculated, that the band below the typical reduced MTG band could be a hydrogen bond between the Oη of Tyr62 or Tyr75 with Cys64. Nevertheless, in this work it was not made experiments to verify this hypothesis. In non-reduced samples after thermal treatment, a representative band of MTG protein (Lane 4) and the formation of dimers and other compounds with molecular weights between 29 and 90 kDa were detected. Dimers and high molecular weight compounds significantly declined after sample reduction, but were not completely depolymerised (lane 4 and 5). The lower molecular weight compounds between 29 and 40 kDa in the lane 4 and 5, could be indicate the formation of new products with low molecular. Non-reduced samples treated at high pressure also showed the formation of dimers and high molecular weight compounds (lane 7), and the intensity of these bands after reduction (band 8) was stronger in comparison to the reduced heat-treated samples (band 5).

Disulphide bonds

The partial decrease in intensity of dimer bands demonstrated that most of the irreversibly denatured protein after treatment at 0.1 MPa and 80°C for 2 min and 600 MPa at 40°C for 60 min was induced by disulphide linkages between MTG molecules. Kashiwagi *et al.* (2002) reported that Cys64 of MTG is a catalytic residue that it is situated at the bottom of the active cleft site (figure 4.1-6 and 4.1-9). Hydropathy analysis of the sequence of the MTG by Kanaji *et al.* (1993) showed that this Cys64 is located in a hydrophobic region situated in a hydrophilic area. High pressure and thermal treatment of native MTG force the amino acid residues packed in the interior of the molecule to disperse in the solvent upon unfolding. Among these amino acid residues, the Cys64 of MTG is exposed more to the TRIS-acetate

buffer with the consequence of the formation of disulfide bonds to neighbouring protein molecules with subsequently protein aggregation.

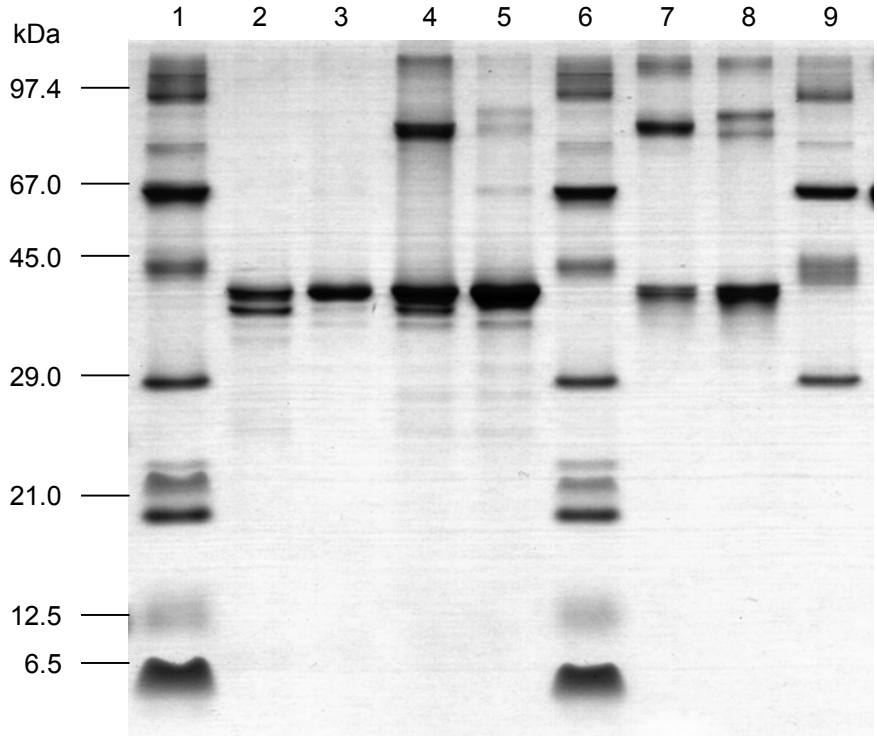

Figure 4.1-10 SDS-PAGE of MTG after different treatment at high pressure and high thermal treatment. 1) Molecular mass standard. 2) Non-reduced native MTG. 3) Reduced MTG. 4) Non-reduced MTG; 0.1 MPa, 80 °C, 2 min. 5) Reduced MTG; 0.1 MPa, 80 °C, 2 min. 6) Molecular mass standard . 7) Non reduced MTG; 600 MPa, 40 °C, 60 min. 8) Reduced MTG; 600 MPa, 40 °C, 60 min. 9) Molecular mass standard.

Formation of disulphide bonds could cause the inactivation of MTG under high pressure and after thermal treatment. However, commercial MTG powder is a mixture of lactose (90%), maltodextrine (9%) and protein (1%). For this reason, the incomplete reduction of low molecular weight compounds in lanes 4 and 5, as well as high molecular weight compounds in lanes 5 and 8, suggested the formation of other compounds with low and high molecular weight. This new compounds could resulted from a variety of reactions such as protein polymerisation via isopeptides and Maillard reaction between amino acids residues and lactose. Furthermore, formation of lysinoalanine and compounds of the early and advanced stages of the Maillard reaction have been found in protein samples treated under high hydrostatic pressure (Springer, 2004; Moreno *et al.*, 2003; Schwarzenbolz, 2002).

In order to investigate the covalent cross-linkages identified in SDS-PAGE electrophoresis, lysinoalanine (LAL), histidinoalanine (HAL), furosine and pentosidine in precipitated protein

samples were analysed. LAL and HAL were not found in native and treated samples (detection limit 2 μg/g protein); however, products of the Maillard reaction were detected. Furosine and pentosidine were measured as indicators of the early and advanced stage of the Maillard reaction, respectively.

Maillard products

The Maillard reaction or non-enzymatic glycosylation reactions start from the condensation between the carbonyl group of a reducing sugar and a free amino group of protein. A variety of intermediates is formed by different pathways, which in the end yield flavour components and brown melanoidins of higher molecular weight. These reactions depend on different factors such as oxygen and water content, as well as temperature and pH of the system. The Maillard reaction can be divided into three stages: the early, advanced and final Maillard reactions (Hodge J, 1953 cited by Moreno J, 2003).

High pressure might influence the Maillard reaction with consequences on flavour, color and nutritional value of foods. Investigations of Tamaoka *et al*. (1991) indicated that the early stages of Maillard reaction are little affected by pressure, whereas Isaacs and Coulson (1996) stated that the initial condensation processes is accelerated with pressure, while the subsequent reaction steps are slowed down. However, Schwarzenbolz *et al.* (2002) reported an enhanced formation of pentosidine and suppression of pyrraline with increasing pressure.

The initial stage of the Maillard reaction in commercial MTG powder could involve the condensation of a lactose molecule to an ε-NH_2 amino group of a lysine residue to form a glycated protein. After addition of the amine to the carbonyl group, one molecule of water is eliminated to form a Schiff base and subsequent cyclization leads to a N-substituted glycosylamine. This first glycation product is than transformed to a more stable ketoamine, lactulosyllysine, via the Amadori rearrangement. The reaction is catalysed by weak acids (Berg, 1993). The lactulosyllysine content in MTG samples treated at 0.1 MPa at 80°C for 2 min and 600 MPa at 40°C for 60 min, was analysed by the furosine method (Brandt and Erbersdobler, 1972 as cited by Krause, 2005; Henle *et al*. (1991) by ion exchange chromatography after acid hydrolysis using 6 N HCl for 24 h (figure 4.1-11).

The furosine content in MTG samples increased from 13.6 μg/g protein to 261.0 and 238.5 μg/g protein in samples treated at 600 MPa and 40°C for 60 min and 0.1 MPa and 80°C for 2 min, respectively (figure 4.1-11). However, the furosine concentration was not significantly different ($P>0.05$) between the two treatments. This result did not agree with Hill *et al*. (1996),

who stated, that the early stages of the Maillard reaction are suppressed when pressure was applied to a xylose-lysine system at 50°C in a sodium bicarbonate buffer at pH 8 and a glucose-lysine system at 60°C in a phosphate buffer at pH 7 respectively. The difference of the results may be explained by pressure shifting the equilibrium of $H_2PO_4^- \rightleftarrows HPO_4^{2-} + H^+$ and $CH_3COOH \rightleftarrows CH_3COO^- + H^+$ to the right-hand side. Ionisation of the phosphate and carboxylic acid groups cause a decrease in pH and the subsequent reduction in the rate of Maillard reaction (Neuman *et al*, 1973., Tauscher *et al.*, 1995, Hill *et al*.1996) This explain, because at low pH, the protonated lysines are in equilibrium and for this reason are less reactive to reducing sugars. Moreover, because the ionisation of sugar in alkaline medium (pH>7) is higher, transformation of sugar from cyclic to reducible form decrease with decreasing pH (Berg, 1993).

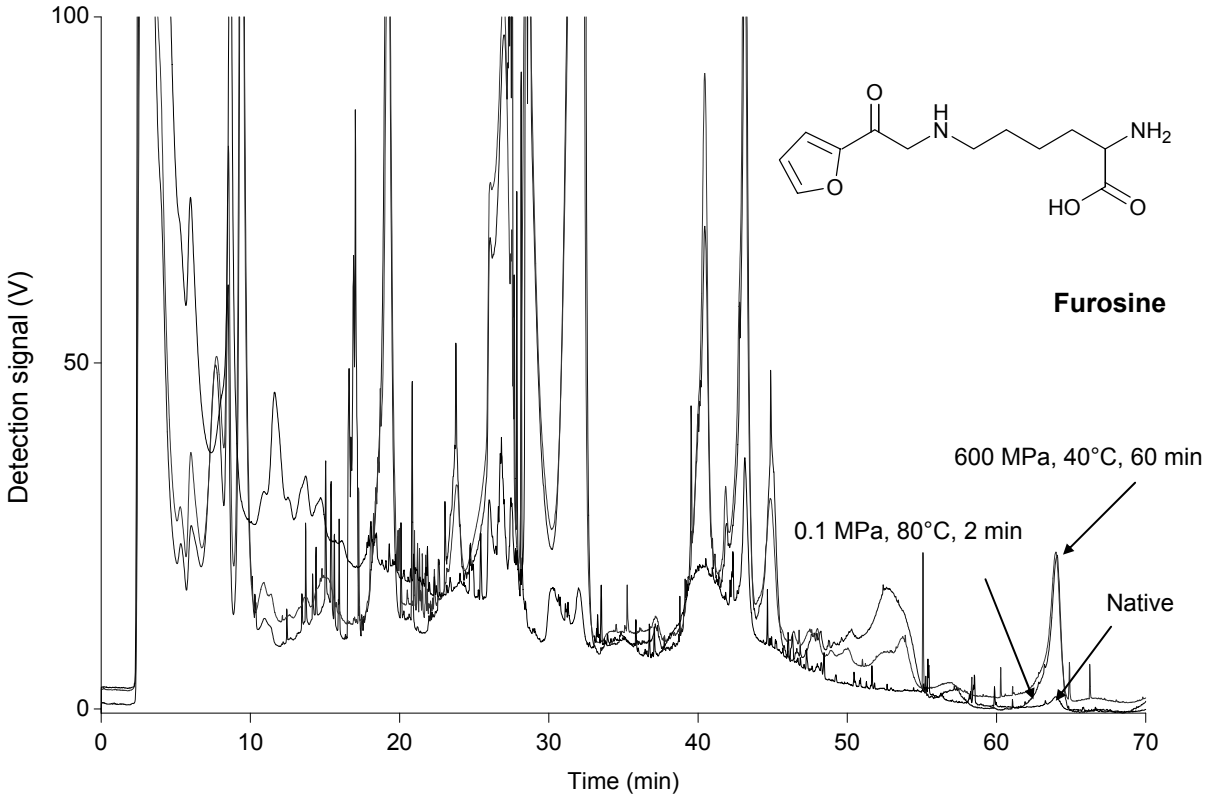

Figure 4.1-11 Ion exchange chromatography of furosine formation from native MTG and MTG treated at 400 MPa at 40°C for 60 min and 0.1MPa at 80°C for 2 min.

The furosine contents of 50 to 70 μg/g protein for bovine milk and 200 to 250 μg/g protein for human milk have been reported (Schlimme and Buchheim, 1995). Therefore, it can be stated that the furosine concentration found in MTG samples after the high pressure and high thermal treatment are in the range of dairy food products.

The cause of advanced Maillard reactions can be accessed by indicator molecules, such as pentosidine. This cross-link amino acid, in which one arginine and one lysine residue are linked together by a pentose (Sell and Monnier, 1989), is formed by reaction of proteins with carbohydrates as aldoses, ketoses, dicarbonyl sugars as well as Amadori compounds. The formation of pentosidine in MTG samples was analysed by amino acid analysis (Henle *et al*., 1997). Pentosidine was not detected in the native sample (detection limit 0.02 μ/g protein), whereas 13.7 and 6.7 μg/g protein were formed in the samples treated at 600 MPa and 40°C for 60 min and 0.1 MPa and 80°C for 2 min, respectively (figure 4.1-12). This agrees well with the results of Schwarzenbolz *et al*. (2002).

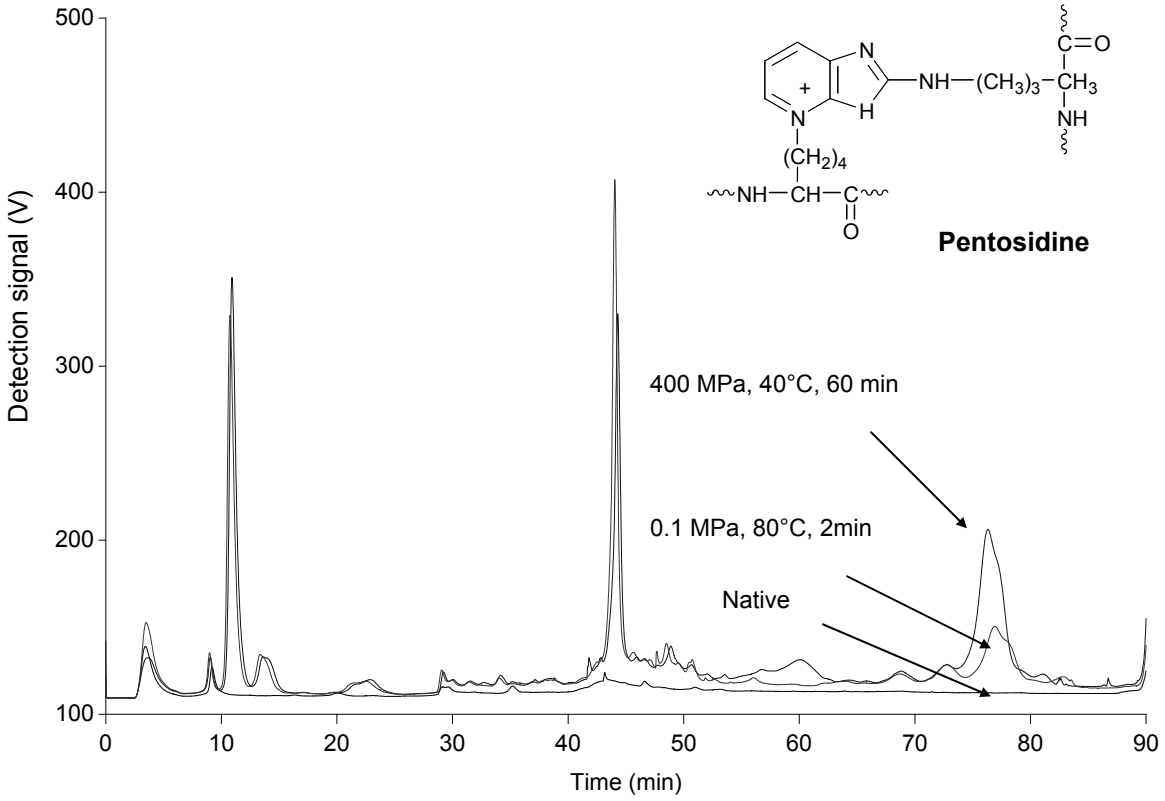

Figure 4.1-12 Ion exchange chromatography of Pentosidine formation from native MTG and MTG treated at 400 MPa at 40°C for 60 min and 0.1MPa at 80°C for 2 min.

Schwarzenbolz (2002) reported a pentosidine content in a system of ß-casein-ribose in a pressure stabile buffer, increasing from not detectable to 4.8 mg pentosidine/100 g protein (48 μg/g protein), after treatment at 600 MPa at 60°C for 2 h. In addition, pentosidine content of the sample treatment at this high pressure condition was about 6 times higher than the sample treatment at atmospheric pressure. These results suggest that, the analysed parameter pentosidine could be more affected by high pressure than high temperature treatment. That could be in agreement with Grandhee and Monnier (1991), who investigated the effect of temperature on pentosidine formation. They reported that in an equimolar

system of D-ribose:arginine:lysine at pH 7.4, pentosidine productions were about 0.1% at 37°C, 1.1% at 80°C and 2.8 % at 65°C after 60 min. Then, although at 80°C induced formation of pentosidine, this temperature was not the optimal. However, formation of pentosidine is also dependent on sugar type, ratio of sugar:arginine:lysine, as well as, the pH of the system. Moreover, the Maillard reactions are a very complex system that needs more experiments designs to explain its mechanisms under high pressure.

However, it could be suggest that the pentosidine contents found in MTG samples after treatment are higher than in other food products as sterilized milk (0.1 to 2.6 μg/g protein), evaporated milk (0.3 to 0.6 μg/g protein) and milk powder (not detected to 0.4 μg/g protein). Among commercially available products, only roasted coffee contains higher pentosidine levels (10.8 to 39.3 μg/g protein) as is reported by Henle *et al.* (1997).

MTG had a high stability in a pressure range from 0.1 to 600 MPa and a constant temperature at 40°C within a time range from 0 to 60 min, because the secondary structure and the active site remain relative stabile up 400 MPa. Increasing pressure loads to the loss of its conformational structure and protein polymerisation with a concomitant MTG inactivation. Then, after to know some reactions of MTG inactivation process, in the next section is discussed the MTG stability under simultaneous application of pressure and temperatures.

4.1.4 Effect of pressure/temperature on the inactivation of MTG

Inactivation of a pure and single-chain protein may be regarded as a two-component system: active and inactive protein. The reaction can be a reversible or irreversible and the stability behaviour of the enzyme can be exhibited by the elliptical shape of the stability phase diagram over a pressure/temperature plane (Tauscher, 1995; Crelier *et al*., 2001). To obtain further knowledge about the simultaneous effect of high pressure and temperature on MTG stability, inactivation kinetics data from the experiments performed at 10, 30, 40, 50°C at 0.1, 200, 400 and 600 MPa within a time range from 0 to 140 h were analysed.

Reaction model

At all temperatures within a long time, the inactivation velocity of MTG followed a kinetic behaviour with two parts: a first and very fast step and a second very slow step, as shown for the inactivation kinetic of MTG at 40°C in a pressure range from 0.1 to 600 MPa (figure 4.1-13)

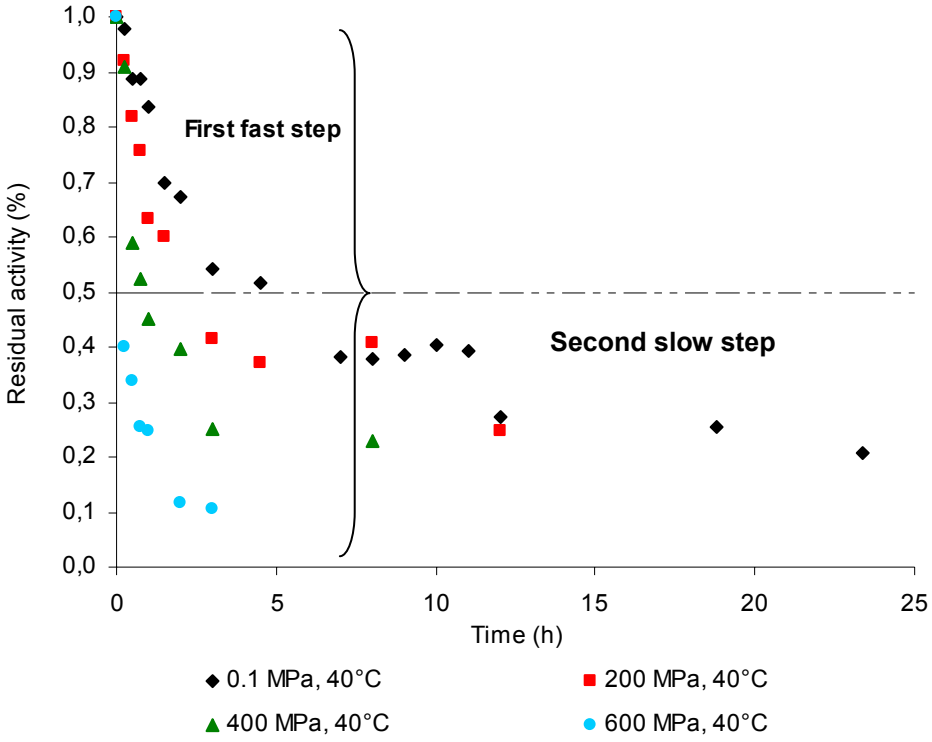

Figure 4.1-13 Residual activity of MTG after high-pressure treatment at 40°C in a pressure range from 0.1 to 600 MPa within a time from 0 to 24 h.

A single kinetic phase, with a single rate constant, implies that all the molecules are following the same pathway, with the same rate constant. A kinetic with two-phase behaviour could indicate that the MTG inactivation was caused by more than one factor. The inactivation of the enzyme could be proceed in a first reversible reaction, followed by a second to achieve the inactivate state. Then, the enzyme inactivation of the Transglutaminase Activa $_{TM}$ MP under high pressure is occurred due to complex reactions (figure 4.1-14), which involved reversible/irreversible protein unfolding, aggregation and formation of other products. Each for these products is favoured by protein concentration, temperature and pressure conditions.

Reactivation of MTG after treatments at atmospheric pressure (0.1 MPa) and 10, 40, 60, 70, 80°C, as well as treatments at 200, 400 and 600 MPa and 40°C, were not observed. However, the results from chapter 4.1.4 demonstrated that pressure and temperature induces inactivation of commercial MTG due to three principal factors: 1) Structural changes of enzyme conformation, 2) formation of disulfide via Cys64, and 3) formation of Maillard products from reactions between protein and lactose. The factor 1 can lead to reversible reaction, whereas, the factors 2 and 3 should lead to irreversible enzyme inactivation (4.1-14).

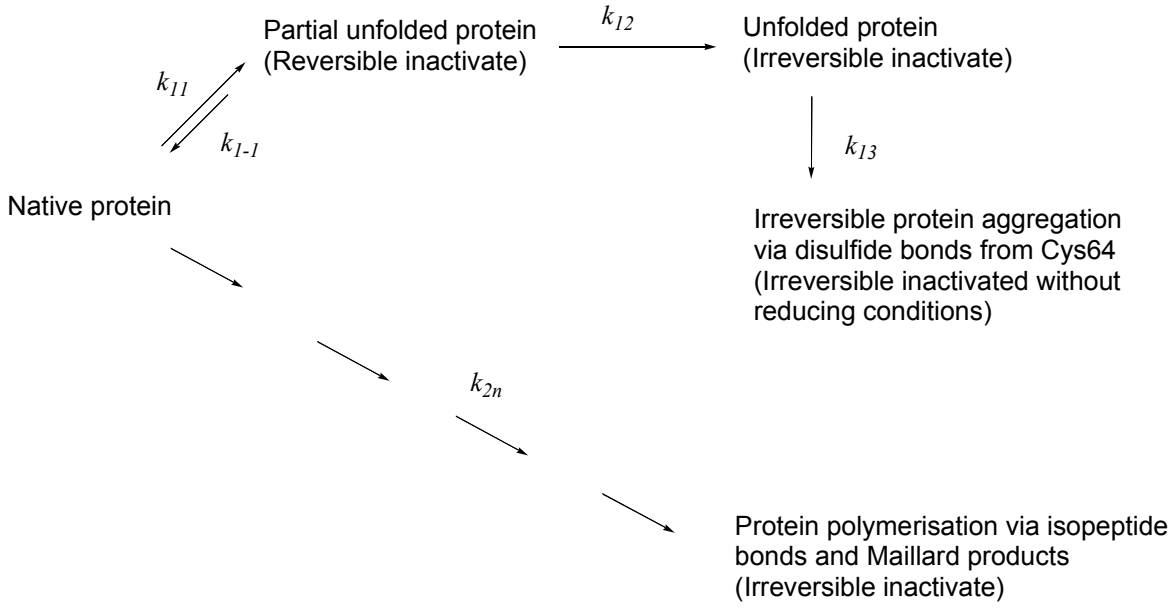

Figure 4.1-14 Summary scheme to represent the inactivation mechanism of microbial transglutaminase (Activa $_{TM}$ MP; Ajinomoto) under different temperature and pressure conditions.

The importance of maintaining the active thiol group of a MTG active site was investigated by Noguchi *et al*. (2001), who reported that, when Cys272 or Cys314 within the active sites of fish TG or human factor XIII, respectively, form hydrogen bridges with tyrosine residues (515 for fish TG and 560 human factor XIII) or disulfide bridges with cysteine residues (333 for fish TG and 374 for human factor XIII), the enzyme activity is suppressed immediately.

For this reason, in order to avoid disulfide formation at Cys64 and maintain the active thiol group of MTG under high pressure treatment, reduced glutathione was added to the MTG samples. Enzyme activities of native, non-reduced and reduced MTG samples were measured before and after treatment at 400 MPa at 40°C for 60 min. The residual activity of native MTG was considered 100%. A residual activity of 40% of non-reduced MTG samples was obtained after high pressure treatment, whereas the activity of reduced MTG samples was not significantly affected. These results can be interpreted that the activity of MTG is conserved with the protection of Cys64 (Jaenicke, 1983), by reduced glutathione, maintaining the thiol group in the active site free to react with the substrate and form the covalent intermediate between the thiol residue of Cys64 in the active site and glutamine residue (figure 2.1-1) in the first protein substrate reaction (Folk and Cole, 1966; Leblanc *et al*., 2001, Griffin *et al*., 2002, Chica *et al*., 2004).

Because the protein concentration in the sample is very low, it was not possible to distinguish quantitatively between the amount of enzyme inactivated due to a loss in conformation

(which could be a reversible activation), the amount of enzyme inactivated due disulphide bonds (irreversible inactivation in absence of a reducing agent) and the amount of enzyme inactivated due to Maillard product formation (irreversible inactivation).

Due to the complexity of the system, the kinetic analysis of MTG inactivation in this work was performed based on the transition state theory from the first fast irreversible inactivation step (eq. 4.1-3). It was considered that the reaction from the active to the inactive form proceeds via an active complex I*, which is found in equilibrium with the active form of the enzyme (Rademacher, 2000; Hinrichs, 2000).

$$N \underset{k_{-1}}{\overset{k_1}{\rightleftharpoons}} I^* \xrightarrow{k_2} I \qquad \text{(eq. 4.1-3)}$$

In the equation 4.1-3, N is the native and active MTG, I* is the transition state, I is the inactive and denatured state. k_1 and k_{-1} are rate constants for the reversible reaction and k_2 is the rate constant to achieve the irreversible inactivate state.

4.1.5 Pressure/temperature inactivation kinetic

For the kinetics analysis, it was established that after all the cases combination of temperature/pressure temperature, the enzyme must achieve 50% residual activity. Thereby, long times of incubations were needed, depending of the conditions. At 0.1 MPa and 50°C, MTG required 6 h to achieve 50% residual activity, whereas at 0.1 MPa and 10°C required until 144 h.

The inactivation constants (k_1) of the first fast step and (k_2) the inactivation constants of the second slow step, showed in table (4.1-3), were obtained using logarithmic data transformation of the residual activity: $\ln[A_p / A_{(0,t)}] = -k_1(t - t_0)$ as is illustrated in chapter 4.1.2. The response value $[\ln A/A_0]$ as a function of inactivation time for each constant temperature and pressure revealed that MTG inactivation fit well to a first-order model for the regarded first fast step, where the 50% of residual activity fell in this first fast step.

In the next section are presented the effect of pressure and temperature on the rate constants in the first fast step of the MTG inactivation.

Table 4.1-3 Estimated inactivation rate constants from de first and second (k_1 and k_2, respectively) isobaric/isothermal inactivation of MTG

	k (h^{-1})							
	10°C		30°C		40°C		50°	
(MPa)	k_1	k_2	k_1	k_2	k_1	k_2	k_1	k_2
0.1	0.0042	0.0027	0.364	0.0076	0.1733	0.0442	6.7070	0.1210
100	n.d	n.d	n.d	n.d	n.d	n.d	6.9768	0.1450
200	0.0106	0.0076[a,b]	0.1438	0.1108	0.2591	0.0564	6.1655	0.3352
300	n.d	n.d	n.d	n.d	n.d	n.d	4.7746	0.4420
400	0.0387	0.0328	0.4457	0.1154	0.8392	0.0875	9.7196	0.5779
500	n.d	n.d	n.d	n.d	n.d	n.d	10.9150	2.0521
600	0.2643	0.456	0.9421	0.1897	2.0545	4.342	18.1890	2.2551

Values given are the mean of two measurements with the associated 95% confidence interval.
[a] mean of two measurements with the associated 90% confidence interval.
[b] Activation tendency
n.d Not determined

Temperature and the rate constant

The pressure dependence of the rate constant *(k_1)* in a range from 0.1 to 600 MPa at different constant temperatures (10, 30, 40, 50°C) was calculated from the Eyring relation $\ln[k_1 / k_{1(0,t)}] = -\frac{\Delta V^*}{RT}(P - P_0)$ (from equation 2.4-33).

The temperature dependence of the MTG inactivation rate constants (k_1) in a range from 10 to 50°C at different constant pressures (0.1, 200, 400 and 600 MPa) was expressed as the activation energy, E_a, that can be estimated form Arrhenius relation $\ln[k_1 / k_{1(0,t)}] = -\frac{E_a}{R(T - T_0)}$ (from equation 2.4-32).

In the Arrhenius relation, $k_{1(0)}$ is the rate constant at temperature T_0, T is the value of the applied temperature and E_a is the activation energy at constant pressure. For the Eyring relation $k_{1(0)}$, is the rate constant at pressure P_0, P is the value of applied pressure, ΔV^* is the activation volume at a certain temperature and T is the absolute temperature. The R symbol represents the universal gas constant.

To analyse the effect of temperature on MTG inactivation based in the transition state theory, the relation *($\ln k_1/T$)* for each pressure were plotted as function of the inverse temperature *(1/T)* as is represented in figure 4.1-15.

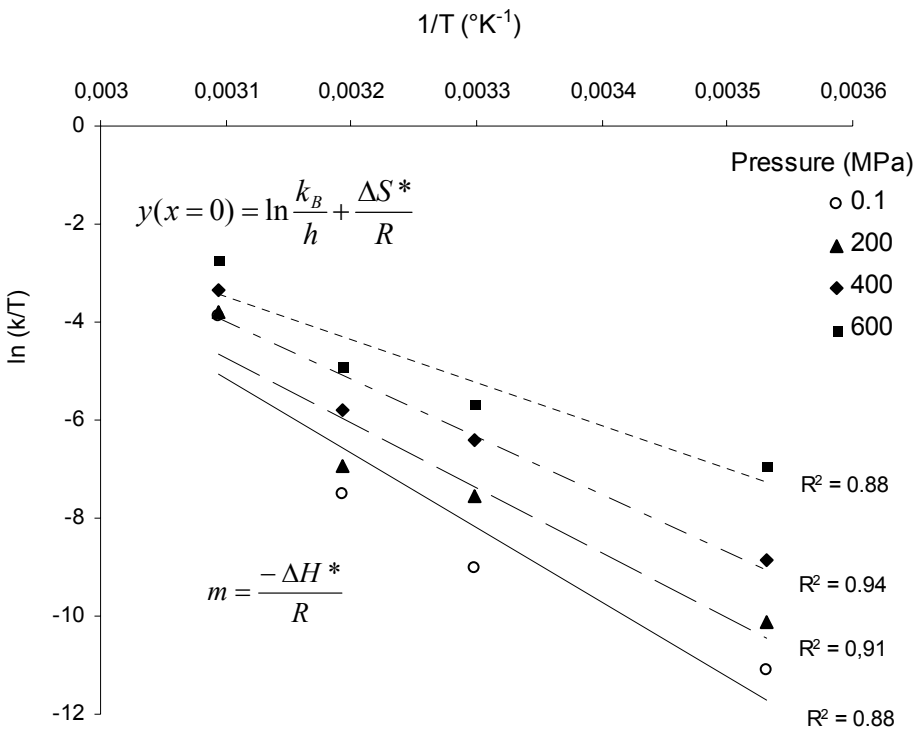

Figure 4.1-15 plot of $\ln (k_1/T)$ versus $1/T$ to access to Eyring equation

The plot produces a straight line with form $y = -mx + b$ and can be related with the Eyring equation obtaining:

$$\ln\frac{k_1}{T}=\frac{\Delta H^*}{R}\cdot\frac{1}{T}+\ln\frac{k_B}{h}+\frac{\Delta S^*}{R} \qquad \text{(eq. 4.1-4)}$$

k_B and h are Boltzmann and Plank constants, respectively.

Table 4.1-4 Activation energies, enthalpy and entropy values of MTG thermal inactivation from the first fast step.

Pressure (MPa)	E_a (kJ/mol)	ΔH* (kJ/mol)	ΔS* (J/mol)
0.1	129.4±0.6	126.90±0.5	154.19±1.7
200	110.5±4.5	107.98±4.5	104.94±17.1
400	97.72±0.6	95.18±0.6	71.38±0.9
600	73.66±1.2	71.12±1.2	1.17±0.4

The estimated values reported in table 4.1-4 shows that increasing pressures causes decreasing activation energies. Hence, the rate constants for enzyme inactivation are less temperature sensitive at 600 MPa than at atmospheric pressure. Low enthalpy and entropy

values at 600 MPa demonstrated that the enzyme inactivation is less temperature dependent at high pressure.

Pressure and the rate constants

To analyse the effect of pressure on MTG inactivation, rate constants ($\ln k_1$) of the inactivation at constant temperature were plotted as a function of pressure (figure 4.1-16). A synergistic effect of pressure and temperature was observed. For example, at 10, 30 and 40°C, an increase of the pressure results in an increase of the rate constants. However, at higher temperature a different behaviour is observed. At 50°C there is no increase of the rate constant within a pressure range from 0.1 to 300 MPa and only above 300 MPa the rate constants increase.

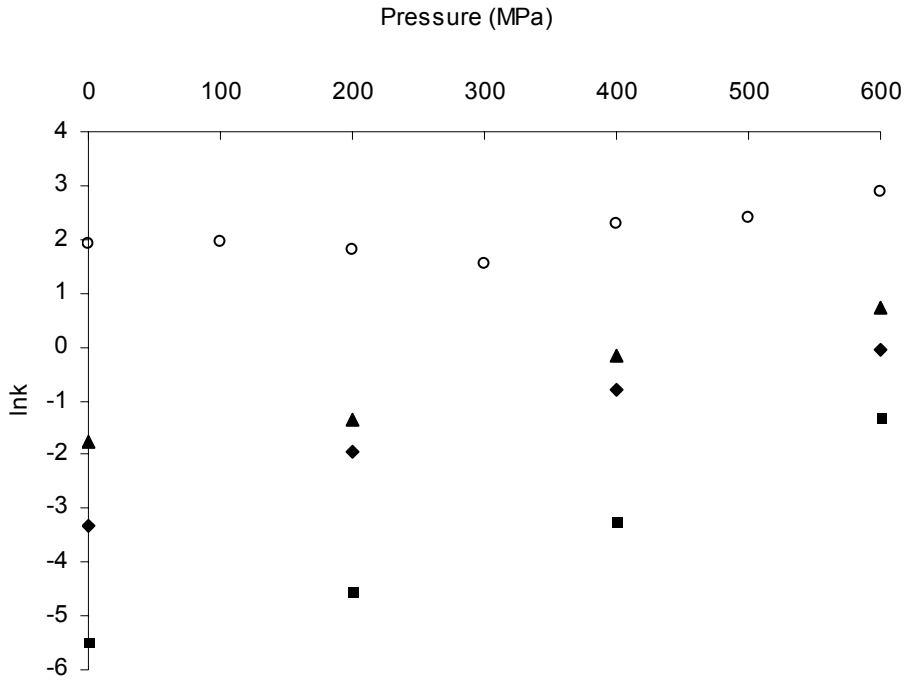

Figure 4.1-16 Inactivation of MTG by high-pressure treatment from 0.1 to 600 MPa and 10°C (■), 30°C (◆), 40°C (▲), 50°C (○)

Calculation of activation volumes from the Eyring relation was made to analyse the pressure effect on enzyme inactivation (figure 4.1-17). At low and medium temperatures, negative activation volumes of –16.2±0.5, -13.6±0.1, -11.20±0.3 cm^3/mol for 10, 30 and 40°C are obtained. However, at 50°C, two clear tendencies were observed. To analyse this phenomenon, the Eyring relation was applied separately on the pressure ranges 0.1-300 MPa and 300-600 MPa. Then a positive inactivation volume of about +3.02±2.0 cm^3/mol at

50°C in a pressure range from 0.1 to 300 MPa and a negative inactivation volume of -11.02±0.4 cm^3/mol at 50°C in a pressure range from 300 to 600 MPa, was calculated. When the pressure dependence of the inactivation rate constants k_1 for this temperature was analysed by a polynomial function $\ln k_1 = a + bP + cP^2$, the activation volume for each pressure can be calculated (table 4.1-4).

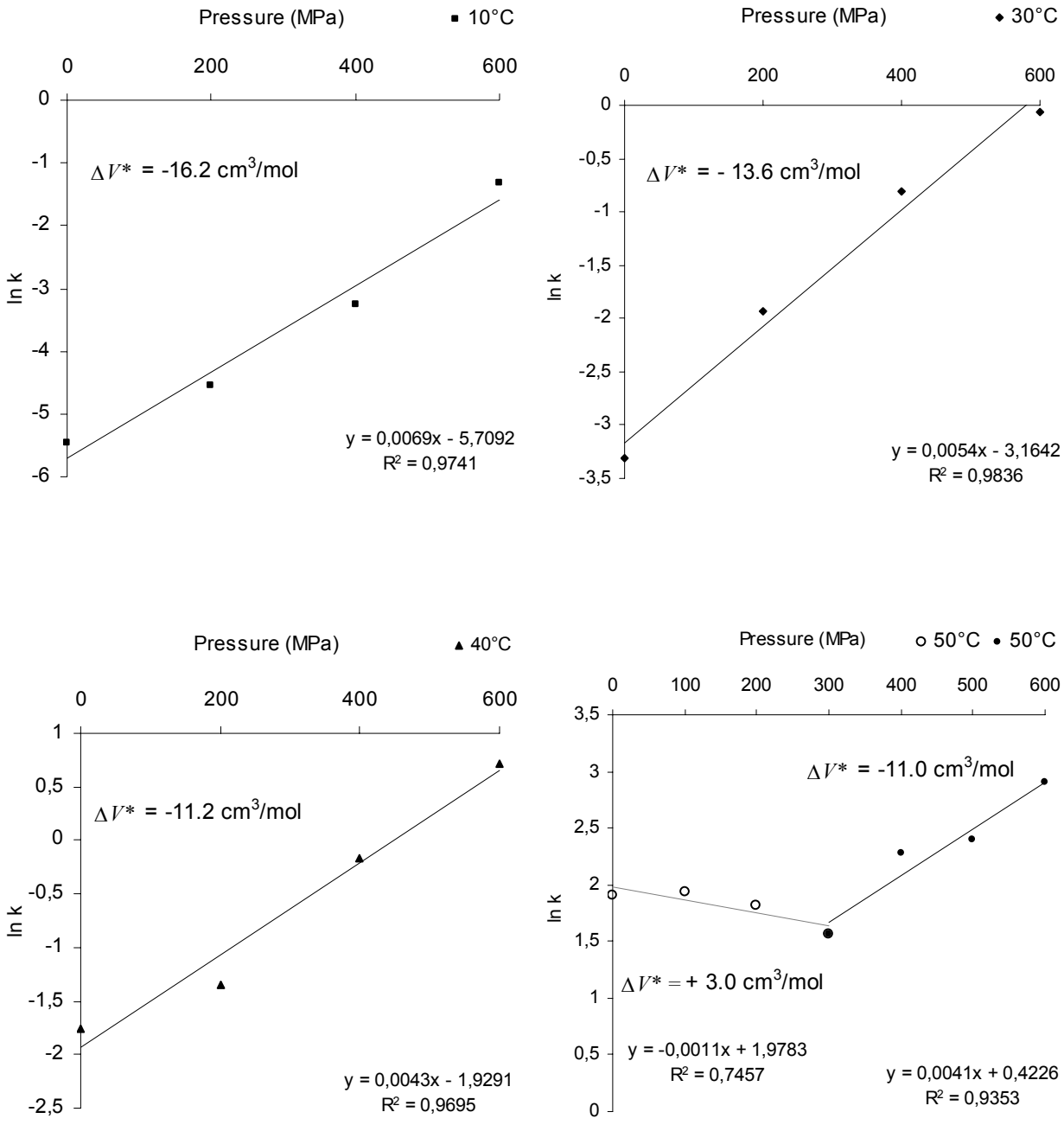

Figure 4.1-17 Inactivation of MTG by high-pressure treatment at 0.1, 200, 400 and 600 MPa and 10°C (■), 30°C (◆), 40°C (▲), 50°C (○,●)

The change of the algebraic sign of the activation volume occurred at a temperature around 50°C in a range from 170 to 300 MPa. That is in agreement with Hawley (1971), Weemaes *et al*. (1998) and Urzica (2004), who stated that although at medium temperature (45 to 60°C) and low pressure (200 to 350 MPa) it is very difficult to distinguish the irreversibility of biological reactions, the changes of the kinetic parameters are clearly observed.

The negative activation volumes of MTG show that in a temperature range from 10 to 40°C, high pressure could cause enzyme inactivation and protein unfolding, because there is a decrease in the volume of the protein-solvent system. Generally, negative values of the inactivation volume $(\Delta V^{*}<0)$ indicate that pressure induces protein unfolding. The charged and polar groups become exposed to the solvent leading to a hydration or solvation of amino acid residues. Elimination of packing defects in the molecule occurs. There is a volume effect of transfer of hydrophobic groups from the protein to solvent (Jaenicke, 1983; Frye and Royer, 1998). The hydration of non-polar groups increase with protein unfolding (Kitchen *et al*., 1992). In addition, activation volumes about -10 cm^3/mol could indicate covalent bond formation (Mozhaev *et al*., 1996). That can suggest that a part of the first inactivation step of MTG under high pressure could be also induced due to the formation of disulfide bonds at Cys64 of MTG.

Table 4.1-5 Activation volumes derived of the polynomial function of inactivation rate constants k_1 at 50°C. The figure at the right represents the detail of ln k_1 *vs* pressure at 50°C expressed as a polynomial function.

Pressure (MPa)	ΔV^{*} (cm^3/mol)
0.1	6.4
100	2.7
~172	~ 0.0
200	-1.1
300	-4.8
400	-8.6
500	-12.4
600	-16.1

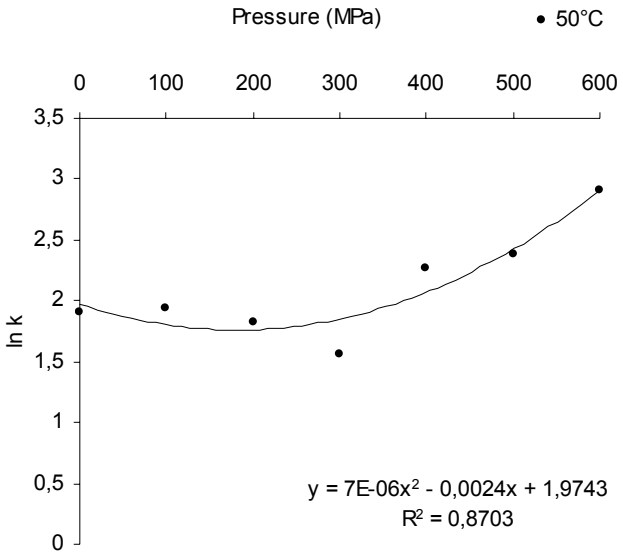

The positive activation volume of MTG at high temperature (50°C) at about 0.1 to 300 MPa, shows that pressure induces enzyme stabilization against heat denaturation and is in

agreement with other enzyme studies (Hamon *et al*., 1996; Mozhaev *et al*., 1996; Crelier *et al*., 2001). For example, the heat-labile pectin methylesterase from tomato was stabilised in a pressure range from 500 to 600 MPa (Crelier *et al*., 2001). The question whether pressure induces inactivation or stabilization on MTG can be answered by a stability phase diagram over the pressure/temperature plane. It is stated that “Enzymes in an ongoing process of denaturation are by definition not at thermodynamic equilibrium” (Jaenicke, 1983; Crelier *et al*., 2001). However, several authors have obtained “kinetic phase diagrams” from the inactivation rate constants over a pressure temperature plane (Weemaes *et al*., 1998; Van Loey *et al.*, 1998; Indrawati *et al.,* 2000; Crelier *et al*., 2001).

4.1.6 Pressure/temperature contour plot of active and inactivated MTG

In order to access the MTG stability under simultaneous application of pressure and temperature, a contour plot of the inactivation behaviour of the enzyme in a range from 10 to 50°C and 0.1 to 600 MPa was performed (figure 4.1-18). The pressure/temperature plane from the first fast step inactivation kinetic resulted by plotting residual activity obtained from each pressure and temperature combination of a time of 0.5, 0.75 and 1 h.

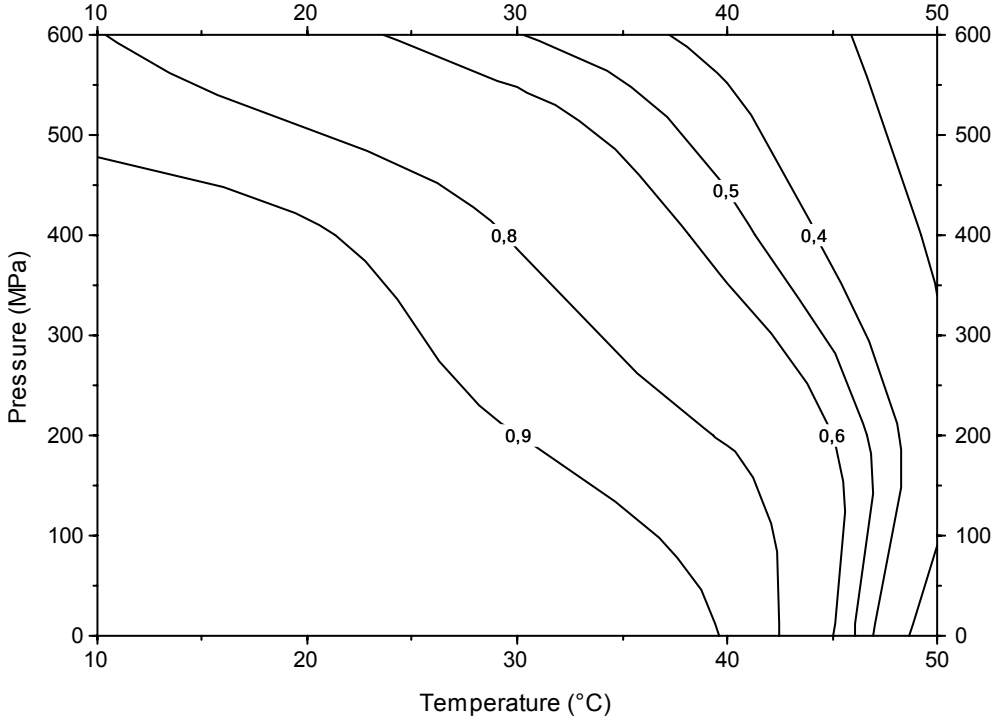

Figure 4.1-18 Pressure/temperature plane of active and inactive fractions of MTG in a 0.2 mol/L TRIS acetate buffer at pH 6 system after treatment time 0.75 h. Values from 0,9 to 0,4 indicate residual enzyme activity from 90 to 40%.

The different grade of enzyme activity showed that MTG is very stabile under high pressure. For example, a 90% enzyme activity remains after treatment at atmospheric pressure (0.1

MPa) and temperature lower than 40°C. In the same way, this 90% was maintained at pressure above 400 MPa at low temperature (10°C). A 50% activity remained at a maximal pressure of 450 MPa and a maximal temperature around 40°C.

These results show that MTG undergoes the same activation/inactivation behaviour as other enzymes (Weemaes *et al*., 1998; Indrawati *et al.*, 2000, Ly-Nguyen *et al*, 2003). An antagonist effect of pressure and temperature occurs when low pressure (below 300 MPa) is combined with high temperature (above 50°C). Microbial transglutaminase retains a high residual activity after 0.75 h at pressure/temperature treatment and confirm its high stability under high pressure in comparison to other enzymes. For example, the pressure/temperature plane of active and inactive fractions of lipoxygenase (LOX) from crude bean extract (Indrawati *et. al*., 2000) shows, that at temperature up to 60°C, pressure does not stabilised the enzyme against thermal inactivation, although low pressures give a slightly thermo stabilizing effect. Nevertheless, inactivation of LOX was faster than MTG. The inactivation constant values to perform the pressure/temperature diagram were ranged from 0.02 to 0.04 min^{-1}, whereas those for MTG were from 0.001 to 0.1 min^{-1}.

4.1.7 Hypothetical pressure/temperature MTG plane from the first and the second rate constants

Protein stability under the simultaneous effect of pressure and temperature can be analysed assuming a transition state between folded (native) and unfolded (denaturated) protein. The thermodynamic relation of Clausius-Clapeyron is applied on the equilibrium of these both states, i.e. when the free energy is zero. However, as is already mentioned, because prediction of the equilibrium state of biochemistry reactions is the central problem of its thermodynamics analysis (Alberty, 2005), calculation of equilibrium from experimental data was not possible due to the interference of side reactions. Thereby, in order to calculate an apparent equilibrium constant, Rugerio (2005) and Videa (2005) proposed a mathematic model equation of inactivation $f(A/A_0)$ as function of the time:

$$f = \frac{1}{\lambda_1 - \lambda_2}(k_1 - \lambda_2)\exp(-\lambda_1 t) - (k_1 - \lambda_1)\exp(-\lambda_2 t) \qquad \text{(eq. 4.1-5)}$$

Where: λ_1, λ_2, are obtained for the following equations

$$\lambda_1 = \frac{-\alpha + \sqrt{\alpha^2 - 4\beta}}{2}, \quad \lambda_2 = \frac{-\alpha - \sqrt{\alpha^2 - 4\beta}}{2}, \quad \alpha = k_1 + k_{-1} + k_2 \quad \text{and} \quad \beta = k_1 k_2$$

Based on the mathematical adjustment, they stated also, that, the commercial MTG undergoes its inactivation due to a complex system and a phase diagram with a definite line

that divides the native and denature state could be not performed. For this reason, it is only presented a hypothetical activation/inactivation plane that represents the stability behaviour of MTG under different pressures and temperature combinations. The continue line was performed from the kinetic of the first step and dashed line from the kinetic of the second slow step, which was calculated using the same mathematical methodology of the fist step (chapter 4.1-5). The apparent equilibrium line could be found between the both steps (figure 4.1-19).

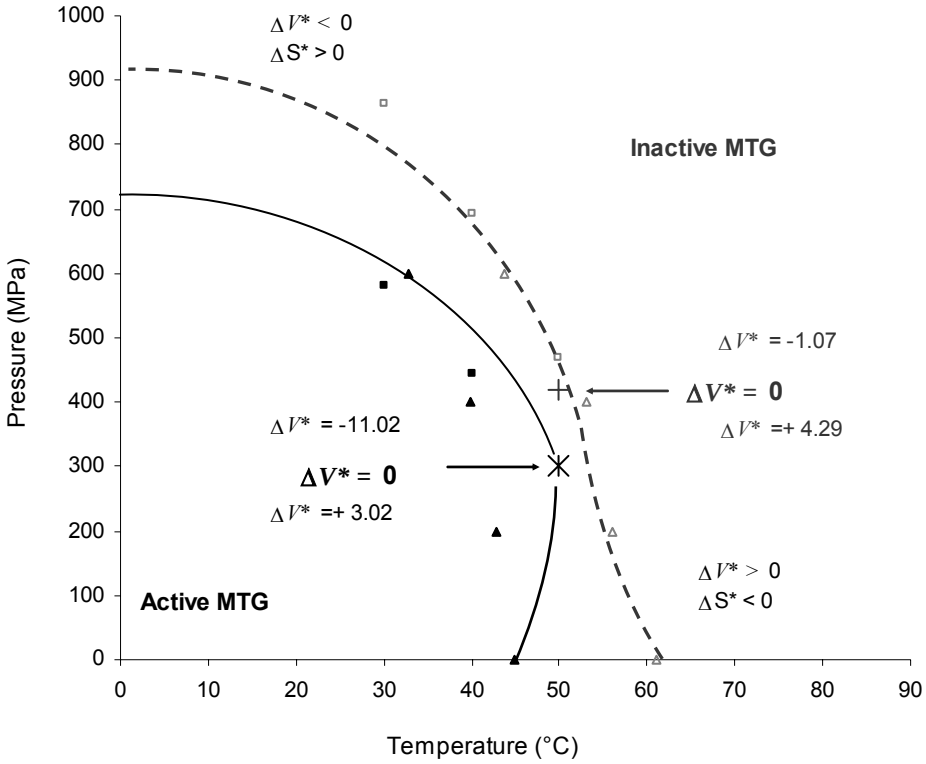

Figure 4.1-19 Hypothetical representation of the pressure/temperature plane of microbial transglutaminase in a 0.2 mol/L TRIS acetate buffer at pH 6 considering the first and second step inactivation kinetics. The continue line represent 50% enzyme activity within the first step inactivation. The dashed line represents the second step kinetic. The apparent equilibrium and the transition state could be located between the both lines.

The hypothetical pressure/temperature diagram and MTG stability is explained based exclusively on the transition state theory of the first step kinetic:

1.- Along pressure and temperature axis, as long as the free Gibbs transition energy difference is positive *($\Delta G^* > 0$),* the enzyme occurs in the active state and when the free Gibbs energy difference for the transition is negative *($\Delta G^* < 0$)*, the enzyme occurs in the inactivated state (Hawley, 1971, Zipp and Kauzmann, 1973). Protein stability principally depends on the combined effects of the exposure of the interior polar and non-polar groups and their interaction with water together with the consequential changes in the water-water

interactions. The enthalpy of transfer of polar groups from the protein interior into water is negative at higher temperatures, in contrast to the non-polar groups, which is positive (Privalov and Makhatadze, 1992). Then, the positive free Gibbs transition energy could be related to MTG stability and its activity based on hydrophobic interactions of its active site, which play an important role in the ordered state of the native soluble protein (chapter 4.1.3.1). The transfer of the hydrophobic groups of the active site (Phe254, Phe251; Tyr278, Tyr62, Tyr65 and Trp69) to the solvent required a substantial amount of work; thereby Gibbs free energy is positive.

2.- Along the atmospheric pressure axis (0.1 MPa), the stability of the enzyme decreases with increasing temperature, indicating a positive entropy activation $(\Delta S^*>0)$ contribution associated with the transition (Hawley, 1971). At 0.1 MPa, the MTG inactivation was induced at temperatures above 50°C. The enhancing entropy activation with increasing temperature can be related to the entropy of hydration of non-polar groups (Phe254, Phe251; Tyr278,Tyr Tyr62, Tyr65 and Trp69), which increases with temperature, indicating that they are less able to order the water of buffer at higher temperatures and contribute to the system's disorder by interfering with the extent of the hydrogen-bond network. In addition, there is an entropy gain from higher degree of freedom of the non-polar groups when the protein is unfolded (Privalov and Makhatadze, 1992).

3.- Pressure increase from 0.1 to 600 MPa in a range from 10 to 40°C leads to a negative activation volume and positive entropy $(\Delta V^*<0,\ \Delta S^*>0)$ suggesting that MTG inactivation as well as stabilisation processes are initiated by temperature and pressure (Hawley, 1979, Urzica, 2004).

4.- Increasing pressure from 0.1 to about 300 MPa at about 50°C, leads to a positive value of the activation volume $(\Delta V^* > 0)$, indicating that under this conditions pressure induces enzyme stabilisation (Hawley, 1971; Jaenicke, 1983; Urzica, 2004).

5.- A negative activation volume along with a negative entropy $(\Delta V^*<0,\ \Delta S^*<0)$ was not obtained, which indicates that cold denaturation of MTG at 10°C in a pressure range from 0.1 to 600 MPa did not occur (Doster and Gebhardt, 2003). Despite long time incubation at 200 MPa and 10°C for 144 h, MTG did not show constant inactivation behaviour. In the figure 4.1-19 can be observed that at low temperature (around 10°C) and high pressure (around 600 MPa), the difference between the first and second inactivation kinetic step is greater than at medium temperature (30 to 40°C). Then, it is proposed that around 10°C and high

pressure, the reversibility of enzyme inactivation is very high. Based on simulation models of peptides proposed by Nguyen and Hall (2004), who found that low temperature leads to increase the α-helixes content in molecule, it can be suggested that the α-helixes that surround MTG molecule were not destroyed at 10°C and 200 MPa and remained more stable, protecting the active site of the enzyme.

The hypothetical diagram for MTG in a 0.2 mol/L TRIS acetate buffer at pH 6 in absence of a reducing agent shows an antagonistic effect between pressure and temperature on the enzyme stability. An increase of pressure at constant temperature results in higher MTG stability. That could be explained by the principle of microscopic ordering, which states that increasing pressure leads to higher order of the molecules or a decrease in the entropy of a system (Mozhaev *et al*., 1996).

The pressure/temperature plane of active and inactivate fraction of MTG can be a tool for technical process. In this diagram, it is easy to locate the residual activity in different pressure and temperature combination. Then, based on this kinetic study, it was stated that MTG at 400 MPa and 40°C for 0.5 h remain high enzyme activity. Under this criterion, incubations of MTG with individual casein under atmospheric and high pressure conditions (0.1 and 400 MPa at 40°C) were performed to induce irreversible protein cross-linking. The affinities of MTG to individual caseins are presented in the following section.

4.2 Affinity of microbial transglutaminase to acid casein, α_{s1}- and β-casein under atmospheric and high pressure conditions

Several studies have demonstrated that caseins are good substrates for MTG (Traoré and Meunier, 1991; Oh *et al*., 1993; Rodriguez-Nogales 2005) because they contain numerous glutamine and lysine residues. However, MTG shows certain specificity, so not all glutamines of the individual casein are reactive (Oh *et al*., 1993). Caseins represent about 80% of the total protein in milk, containing mainly of α_{s1}-casein (38%), α_{s2}-casein (10%), ß-casein (36%) and κ-casein (13%). Each casein have a distinct primary structure (Dalgleish, 1997) and although there are similarities among them, there is already debate about, how these primary sequences determine their conformational structure and individual physical properties (Alais, 1997; Wong *et al*., 1996), which play a significant role for the affinity of MTG to casein (Christensen *et al*., 1996; Richter, 2004). In order to investigate wheatear MTG show different affinity to the different caseins as specific substrates under atmospheric and high pressure treatment, acid casein, ß- and α_{s1}-casein from bovine milk were isolated and

characterised. After caseins isolation, irreversible cross-linking from the individual caseins treated with MTG at 0.1 and 400 MPa at 40°C for 15 min was analysed using gel permeation chromatography.

4.2.1 Isolation and identification of the casein fractions

a) Purity control of isolated casein by electrophoresis using urea

Native polyacrylamide electrophoresis, using urea in the gels to dissociate the casein complex, was performed to control the purity of whole casein from isoelectric precipitation and ß-casein isolated by urea fractionation method (figure 4.2-1).

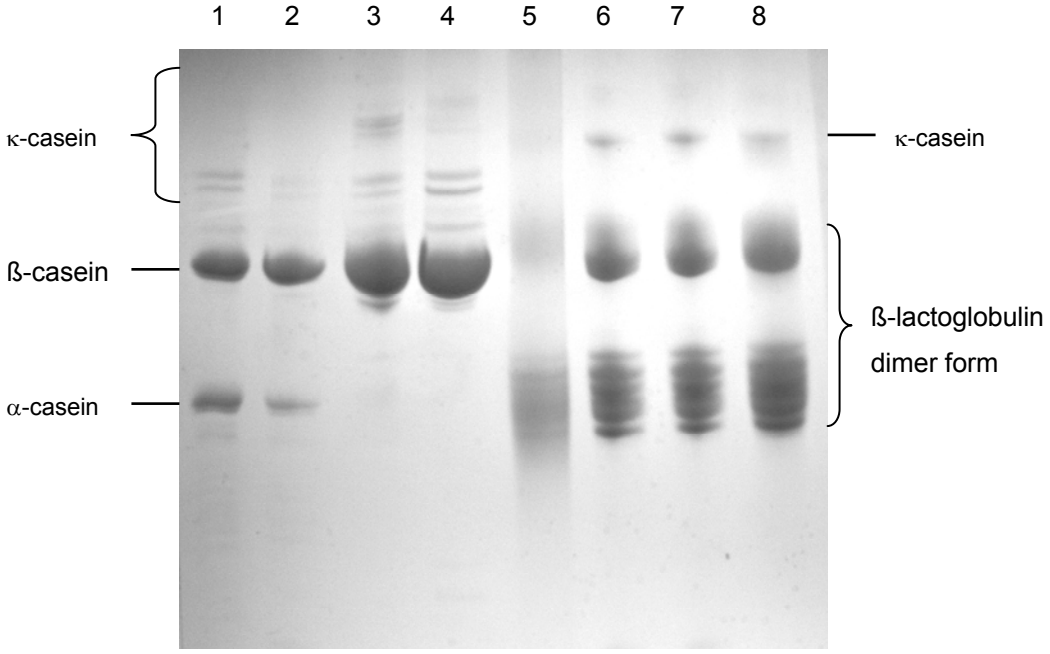

Figure 4.2-1 Native polyacrylamide electrophoresis of milk proteins 1) Acid casein. 2) Acid casein from isoelectric precipitation. 3) ß-casein standard. 4) ß-casein isolate. 5) ß-lactoglobulin purchased by Konrad and Lieske (1997). 6, 7) ß-Lactoglobulin isolate. 8) ß-Lactoglobulin standard.

In this procedure, the pH of the buffer was adjusted so that the milk proteins had the same negative charge, but different charge densities. Following the application of an electric field on the electrophoresis unit system, the milk proteins migrated towards the positively charged electrode and were separated in order of their charge density. Isolated whole casein (lane 2) was free of whey protein and showed only the characteristic bands of the different caseins. ß-casein (lane 4) contained residual amounts of κ-casein whereas ß-lactoglobulin (lane 6 and 7) showed the characteristic dimer bands. Isolation of acid casein by isoelectric precipitation and ß-lactoglobulin by salt precipitation were considered efficient separation

methods. ß-casein appears to be tenaciously associated with κ-casein, so a complete separation of both proteins was not possible with this method. For this reason, an ion-exchange chromatography had to be used to obtain isolates with higher purity.

b) Fractionation of acid casein by ion-exchange chromatography

Due to differences in their isoelectric points and net charge, the different proteins of acid casein can be fractioned by ion-exchange chromatography (Swaisgood, 1992). The individual caseins were isolated using ion-exchange chromatography in imidazole buffer with added urea; TCEP and a NaCl gradient. According to the isoelectric points of the proteins, the order of elution from ion-exchange chromatography was γ-casein, κ-casein, ß-casein, α_{s2}-casein and finally the α_{s1}-casein (figure 4.2-2). The results shows that a better dissociation of casein micelles is achieved using the combination of urea and TCEP in elution puffer.

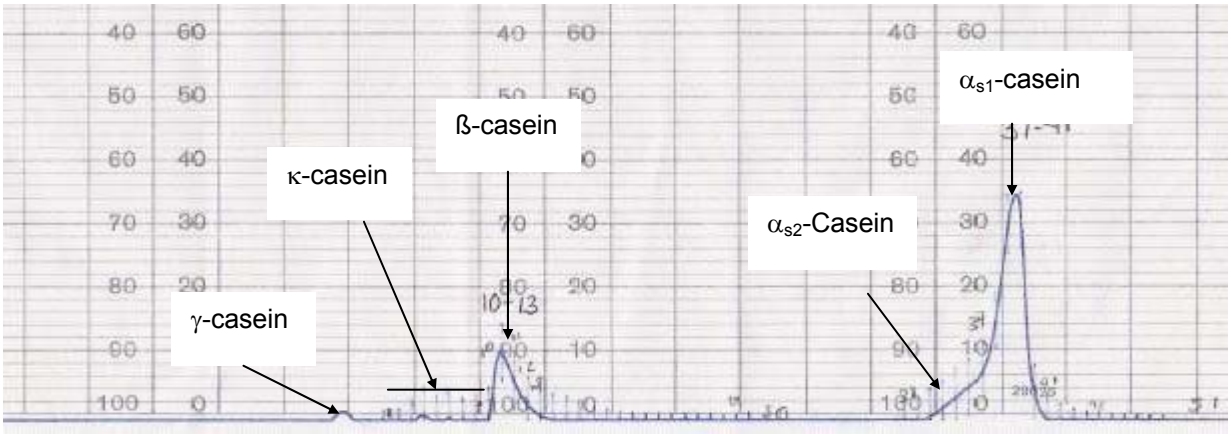

Figure 4.2-2 Ion exchange chromatography. Isolation of ß-casein and α_{s1}-casein from acid casein from isoelectric precipitation

4.2.2 Purity control of isolated caseins by electrophoresis

Polyacrylamide electrophoresis with urea in the gels was used to confirm the purity of isolated caseins after ion-exchange chromatography (figure 4.2-3). Isolated acid casein (lane 2 and 3) showed also the characteristic band of the different caseins. ß-casein isolated by differential solubility (lane 5) showed residual amounts of κ-casein, whereas the ß-casein and α_{s1}-casein isolated by ion-exchange chromatography showed a high purity (lane 9-11).

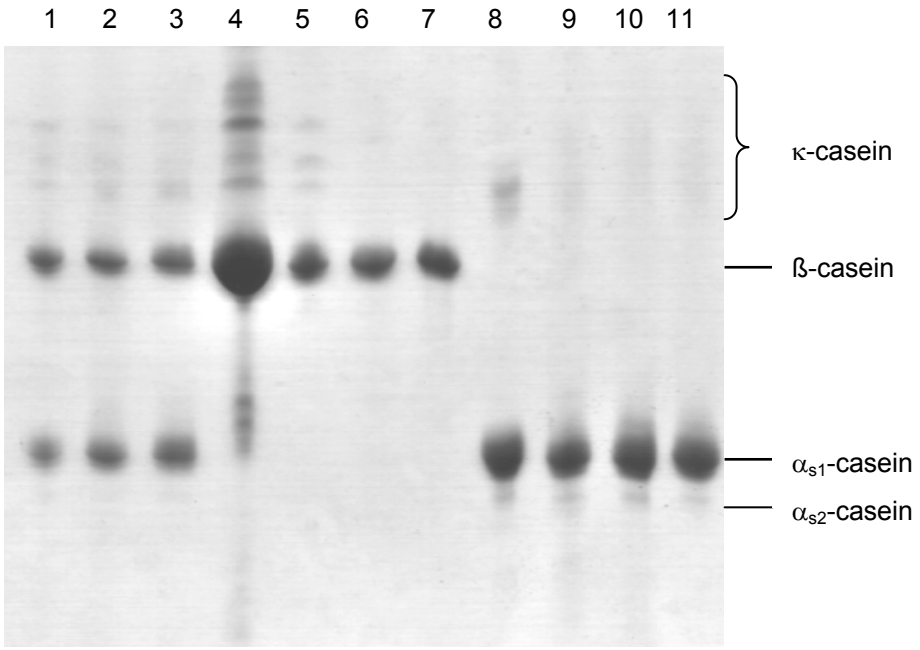

Figure 4.2-3 Native polyacrylamide electrophoresis of caseins. 1) Acid casein standard. 2, 3) Acid casein from isoelectric precipitation. 4) ß-casein standard isolated by differential solubility. 5) ß-casein isolated by differential solubility. 6, 7) ß-casein isolated by ion exchange chromatography. 8) α_{s1}-Casein standard (Merck). 9, 10, 11) α_{s1}-casein isolated by ion exchange chromatography.

a) Characterisation of isolated proteins by SDS-PAGE electrophoresis

After several fractionation runs using ion-exchange chromatography, sufficient amounts of the individual proteins were isolated and the fractions could be characterised by SDS-PAGE electrophoresis using a 12, 8 and 5% discontinuous concentration acrylamide gel (figure 4.2-4). After solubilisation of the samples in an anionic detergent (SDS), the charge of the proteins is masked with a negative net charge that is proportional to the molecule size (Westermeier, 1997). In addition, differences in the molecule form are compensated by the loss of the tertiary and secondary structures. Disulfide bonds formed between cysteine residues were reduced by DTT and the SH groups were protected by subsequent alkylation with iodo acetamide. Thus prepared, the electrophoretical mobility of milk proteins in a gel with sieving properties depends exclusively on molecular size.

Molecular weight values the individual casein fractions were estimated with a calibration curve using a Protein Test Mixture 6 (Serva, Heidelberg, Germany), which contained molecular weight markers in a range from 6.5 to 97.4 kDa. ß-Lactoglobulin showed a molecular weight of 18.4 kDa, a value close to that cited in literature (Cheftel *et al.* 1992, Alais 1997). However, ß-casein and α_{s1}-casein gave calculated molecular weights of 27.6 and 31.4 kDa, which are higher than the molecular weights reported by Cheftel *et al.* (1992).

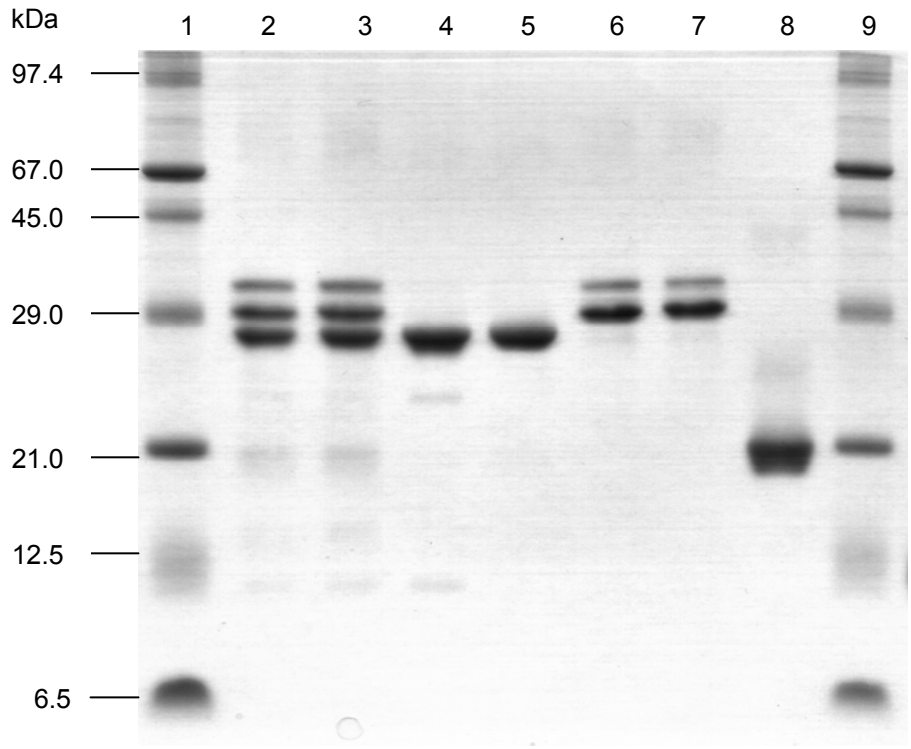

Figure 4.2-4 SDS-PAGE of milk proteins. 1) Molecular mass standard. 2) Non-reduced acid casein. 3) Reduced acid casein. 4) Non-reduced ß-casein. 5) Reduced ß-casein. 6) Non-reduced α_{s1}-casein. 7) Reduced α_{s1}-casein 8) Reduced ß-lactoglobulin 9) Molecular mass standard.

In order to study why the molecular weight of ß-casein and α_{s1}-casein differed from literature values, further electrophoresis experiments involving isolated milk proteins as well as independent standard proteins, Phosphorylase B (Serva, Heidelberg, Germany), bovine serum albumin (Sigma-Aldrich, Steinheim, Germany), egg albumin (Sigma-Aldrich, Steinheim, Germany), carbonic anhydrase (Serva, Heidelberg) and cytochromo C (Merck, Darmstand, Germany), were performed under the same conditions. Molecular weight of milk proteins and different protein standards were calculated using a calibration curve from the Protein Test Mixture 6 (Serva, Heidelberg, Germany).

Table 4.2-1 Calculated molecular weight of isolated milk proteins

Protein	Molecular weight (kDa)	
	Calculated	Literature (Cheftel *et al*., 1992; Wong *et al.*, 1996)
ß-lactoglobulin	18.4	18.2
ß-casein	27.6	23.9
α_{s1}-casein	35.8	23.6

Calculated weight of isolated ß-lactoglubulin was close to the data from literature (table 4.2-1). However, the values of ß-casein remain near the reported, but the value of α_s-casein remained 12 kDa higher (Cheftel *et al.,* 1992, Alais 1997). This experiment demonstrated that electrophoresis procedure was efficient for determining the molecular weight of globular milk protein but not for the isolated ß- and α_s-caseins. The determination of the exact molecular weight of α_{s1}-casein from acid casein obtained using SDS-electrophoresis following the procedure of Jovin *et al*. (1970) and Lane (1978) modified by Böhm (2002) was not possible owing to casein interaction with itself, with ions present in the buffer and the temperature conditions in the electrophoresis system. Ammonium sulphate fractionation and centrifugation in the presence of calcium (II) could be suggested as a more suitable method to avoid alterations of components, especially oxidation of SH groups during whole casein isolation (McKenzie, 1970).

Isolated acid-, ß- and α_{s1}-casein were used as substrate for the kinetic reaction with MTG under atmospheric and high pressure conditions. Because calculated molecular weight value of α_{s1}-casein is different to the date from literature, molecular weight 23 980 g/mol for ß-casein, 23 610 g/mol for α_{s1}-casein and 22 000 g/mol as is reported by Cheftel and Wong (Cheftel *et al.,* 1992, Wong *et al.*, 1996), were using to perform the kinetic study discussed in the next section.

4.2.3 Reaction kinetic studies

Enzymatic reaction of protein substrates

Kinetic analysis of the enzyme reaction with protein substrates is more complex than the reaction with peptide substrates containing only a single functionality that the enzyme recognizes. The protein could have multiple sites as substrates, and furthermore the enzyme can catalyse a processive chemical reaction with the formed products (Case and Stein, 2003).

Christensen *et al.* (1996) reported that there are a limited number of glutamine residues in bovine casein that are attacked by TG from pig liver. For α_{s1}-casein only 4 of 15 and for ß-casein only 5 of 21 glutamine residues were found to be catalytically competent for an acyl-transfer reaction catalysed by TG. If it is considered that these 4 and 5 glutamine residues of α_{s1}-casein or ß-casein act as substrates in a non-processive enzymatic reaction, this would result in several microscopic kinetic parameters. MTG would bind to each glutamine residue

of monomeric casein in n different ways, to produce n catalytic complexes to produce a unique final product that all pathways have in common (figure 4.2-5). When a progressive reaction is considered, the glutamine residues of the dimer and trimer (new oligomerisation products) act also as substrate. Then the n different ways increases considerably. That means that reaction of MTG with casein reflects a complex mechanism in which the reaction of each of the glutamine residues is governed by individual constants $(k_{cat}/K_m)_{n.}$

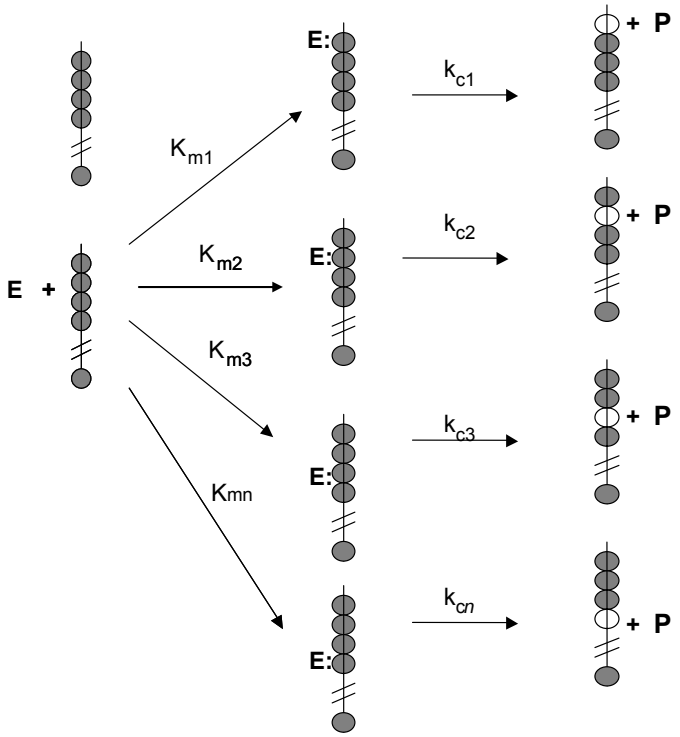

Figure 4.2-5 Minimal simulation mechanism of a non-processive reaction of MTG with α_{s1}-casein as poly-functional substrate (Modified from Case and Stein, 2003)

In the present work, the following conditions were established to analyse the kinetic parameters of MTG using protein substrates: 1) Initial velocity kinetics of non-processive enzymatic reaction of polymeric substrate. 2) The substrate concentration exceeded MTG concentration. Due to the complex kinetics, it was attempted to interpret the results of the experiments from the reaction of MTG with the individual caseins at the stage of a single MTG-monomeric casein complex formation.

4.2.4 Kinetic reaction model propose for the reaction of microbial transglutaminase with monomer of acid, $\alpha_{s1,}$- and ß-casein

The enzyme kinetics study was performed considering that the enzyme-catalysed reaction involves the conversion of a single substrate into a product. Where M is the monomer of

individual caseins with n number of glutamine residues, E is the enzyme MTG and P is the polymerisation product.

$$M + E \underset{k\text{-}_1}{\overset{k_1}{\rightleftharpoons}} M{:}E \xrightarrow{kcat} P$$

The time-dependent variation of the individual reactants was expressed in the following differential equations:

$$v = \frac{d[P]}{dt} = \frac{d[M]}{dt} = k_{cat}[EM] \qquad \text{(eq. 4.2-1)}$$

Considering that, when the reaction velocity remains constant with *[EM]* being formed and consumed at the same time; the maximum velocity V_{max} occurs when the enzyme E is saturated. At high concentrations of substrate, the reaction velocity reaches its maximum value and can be considered:

$$V_{max} = k_{cat}\,[E_T] \qquad \text{(eq. 4.2-2)}$$

After algebraic substitution, a final equation expression described by Henri-Michaelis-Menten is obtained (Copeland, 1996; Bisswanger, 2002).

$$v = \frac{V_{\max}[M]}{K_m + [M]} \qquad \text{(eq. 4.2-3)}$$

Measurement of V_{max} and K_m

The kinetic parameters V_{max} and K_m, k_{cat}**,** which define the behaviour of the enzyme MTG as a function of casein concentration as substrate, were determined graphically from untransformed data and by a mathematical model from adjusted data using DynaFit software (BioKing, Ltd, USA) and Sigma software (Systat GmbH) based on the following considerations:

K_m represents the substrate concentration *[M]* that leads to half-maximal velocity. Setting $[M]=K_m$, turns the equation 4.2-3 into expression:

$$v = \frac{1}{2}V_{\max} \qquad \text{(eq. 4.2-4)}$$

In the model of this work, it is considered that K_m and k_{cat} represents the sum of $\sum_{i=1}^{j=n} K_m$ and $\sum_{i=1}^{j=n} k_{cat}$ of the all kinetics from the n numbers of glutamine residues in the monomeric casein. In the same way, the $\sum_{i=1}^{j=n} \frac{k_{cat}}{K_m}$ ratio gives weight to turnover of the Henri-Michaelis-Menten complex between MTG and monomeric casein.

4.2.5 Monitoring of reaction

The decrease of the monomeric casein concentration $[M]$ from the reaction of whole, ß- and α-casein in a concentration range from 0.125 to 3.000 mg/mL incubated with 0.010 U/mL MTG in a 0.2 mol/L TRIS-acetate buffer pH 6.0 at 0.1 and 400 MPa at 40°C from 0 to 15 min was monitored by gel permeation chromatography under reducing and denaturing conditions using Superdex 200 HR 10/30, which showed good resolution of proteins in the molecular weight range from 10 000 to 600 000. Calibration curves were recorded with monomer of the different caseins in a range from 0.125 to 3.000 mg/mL, incubated with thermal inactivated MTG (0.010 U/mL) under the same conditions as the samples mentioned above. The concentration units expressed originally in mg/mL, were converted to mmol/mL considering the molecular weight of 23 980 g/mol for ß-casein, 23 610 g/mol for α_{s1}-casein and 22 000 g/mol as an average of the molecular weight of the major proteins contained in whole casein (Cheftel *et al.,* 1992, Wong *et al*, 1996).

When MTG (0.010 U/mL) was incubated with ß-casein (0.75 mg/mL) at 0.1 and 400 MPa at 40°C for 0, 5, 10 and 15 min, it was possible to monitor the reaction by measuring the decreased of monomeric casein to form irreversible covalent cross-linking with increasing time. A higher decline in the concentration of monomeric casein was observed during treatment at atmospheric pressure compared to high pressure (figure 4.2-7). Comparing the oligomer patterns of the different sample revealed a more pronounced formation of higher oligomer at atmospheric pressure than at 400 MPa. A qualitative similar monomer decrease was observed for 0.75 mg/mL α_{s1}-casein after treatment with 0.010 U/mL MTG in the same system and conditions. However, the reaction between MTG and α_{s1}-casein as substrate mainly led to formation of dimer. A higher decline in the concentration of monomeric casein was again observed after treatment at atmospheric pressure compared to high pressure (figure 4.2-8).

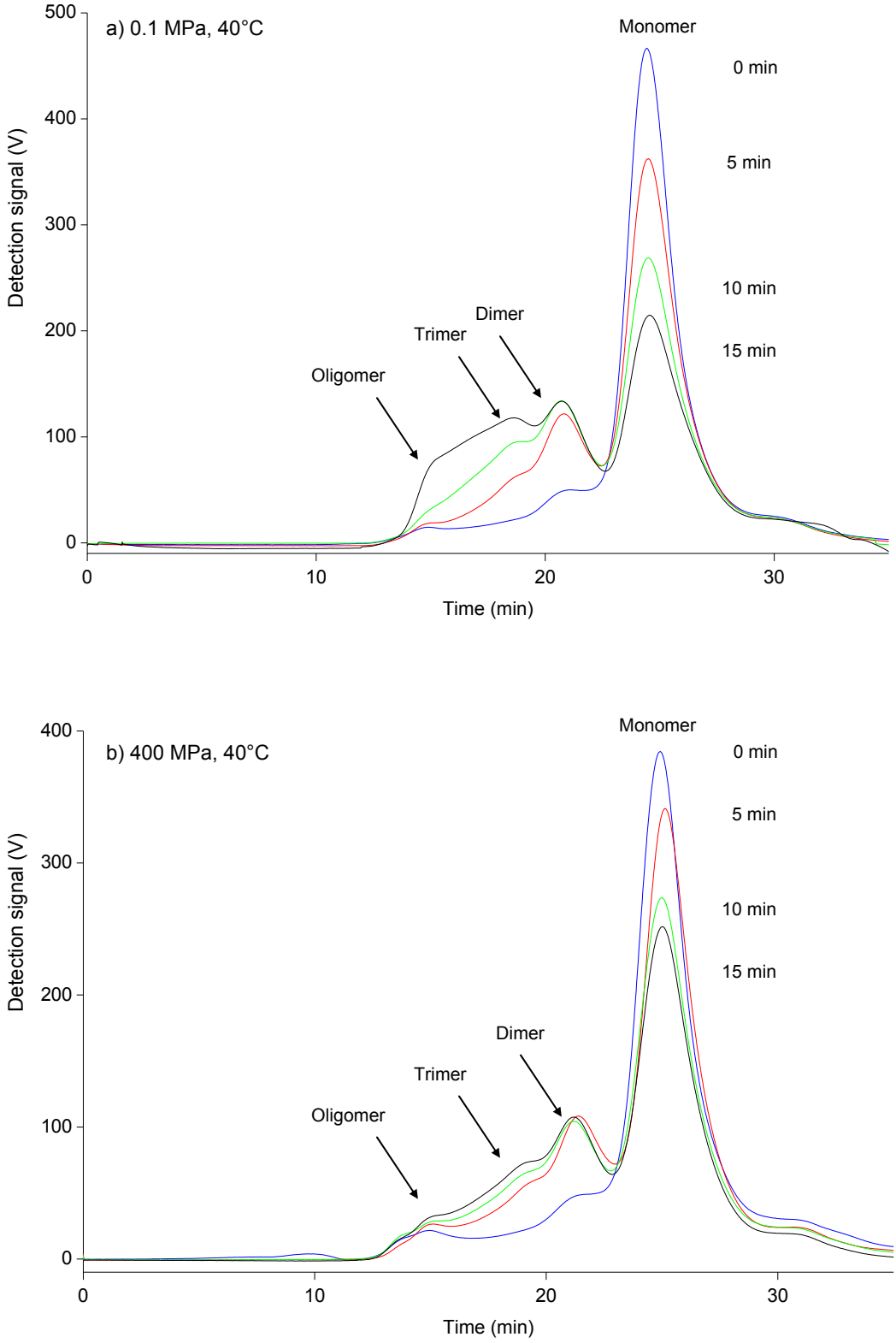

Figure 4.2-7 Gel permeation chromatograms of ß-casein samples (0.75 mg/mL) incubated with MTG (0.010 U/mL) in a 0.2 mol/L TRIS-acetate buffer pH 6.0 at 40°C for 0 to 15 min. (a) Reaction at 0.1 MPa. (b) Reaction at 400 MPa. UV-Detection: λ = 280 nm.

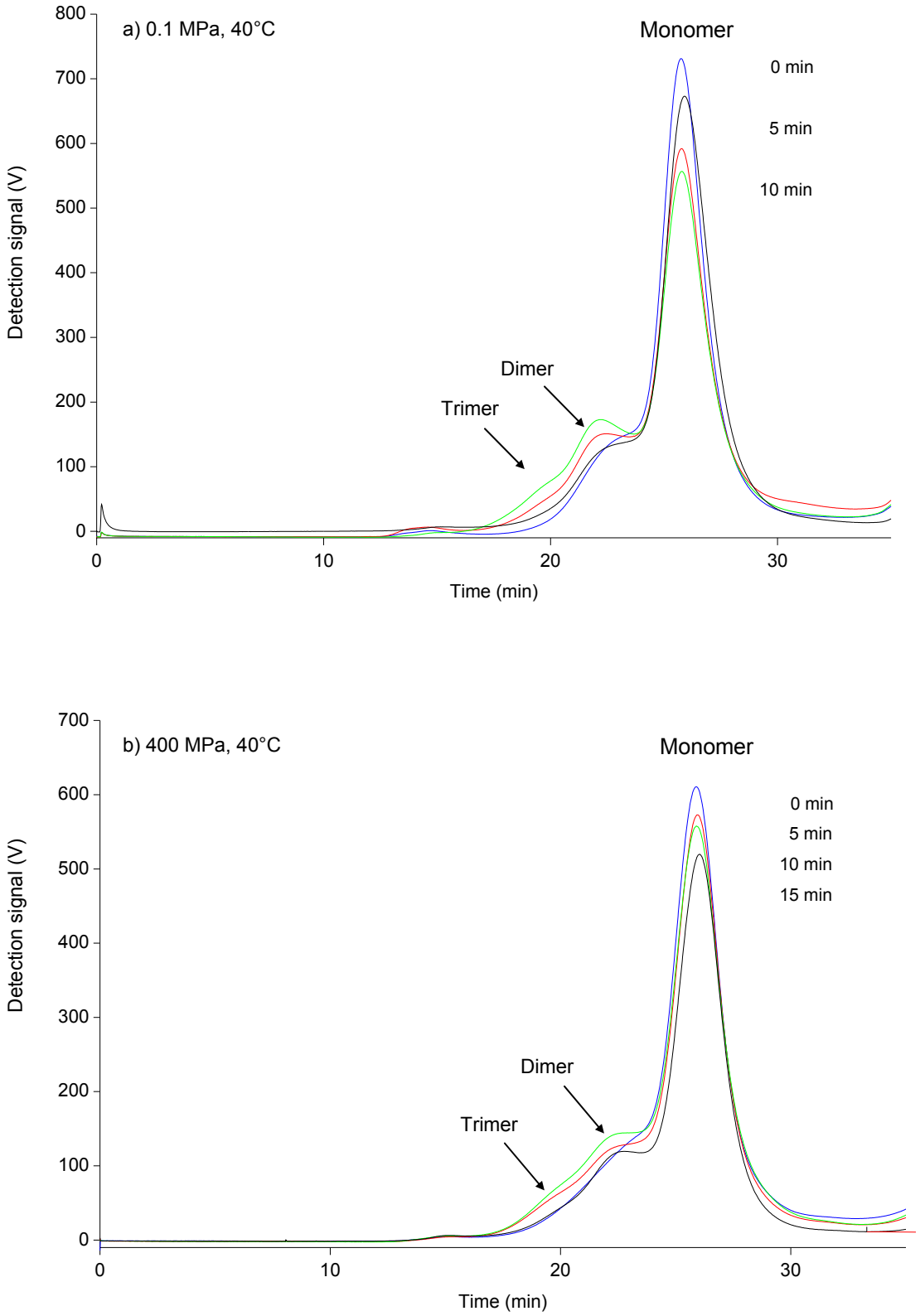

Figure 4.2-8 Gel permeation chromatograms of α_{s1}-casein samples (0.75 mg/mL) incubated with MTG (0.010 U/mL) in a 0.2 mol/L TRIS-acetate buffer pH 6.0 at 40°C for 0 to 15 min. (a) Reaction at 0.1 MPa. (b) Reaction at 400 MPa. UV-Detection: λ = 280 nm.

Reaction progress curves of α_{s1}-, ß- and acid casein were plotted from the remaining monomeric casein *[M] verus* time. The starting concentration ranged from 0.125 to 3 mg/mL (5 x 10^{-3} to 125 x 10^{-3}mmol/L) and reaction times were 0, 5, 10 and 15 min. The initial velocity (v_o) for each starting concentration was calculated as the slope of these linear plots. The reaction velocity was measured during the early phase of the reaction, for this reason $v = v_0$ was considered to be valid (figure 4.2-9).

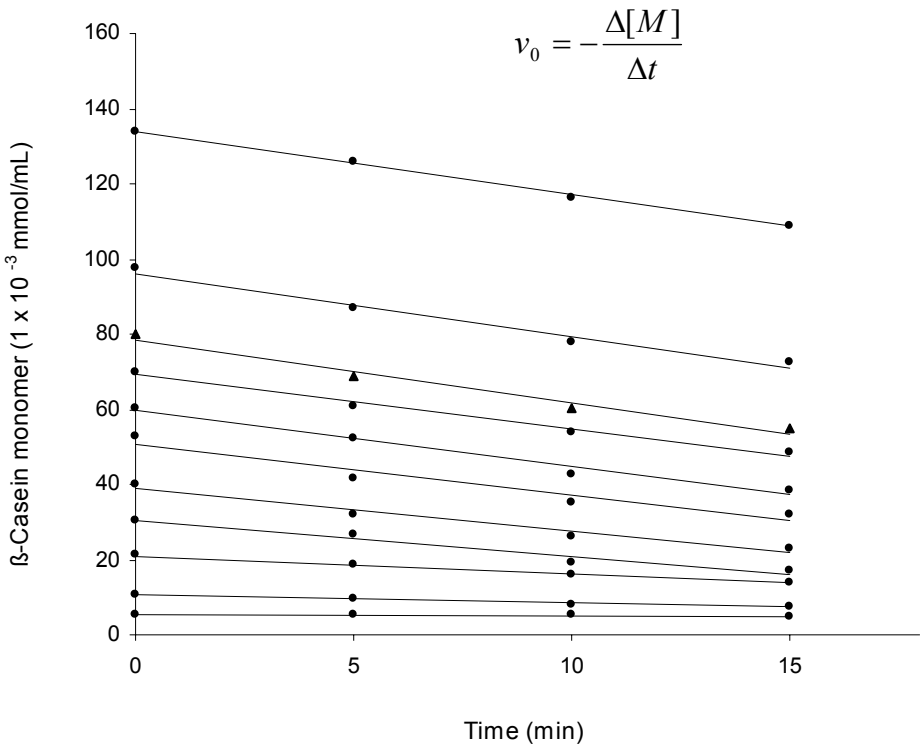

Figure 4.2-9 Reaction progress curves $-\Delta[M]/\Delta t$ for the loss of monomer as substrate during the reaction of different concentrations of ß-casein solutions with 0.010 U/mL MTG in 0.2 mol/L TRIS-acetate pH 6.0 buffer at 0.1 MPa pressure and 40°C.

The effect of individual casein concentrations on the reaction velocities was analysed by plotting reaction velocities $-\Delta[M]/\Delta t$ from ß- and α_{s1}- and acid casein, as a function of substrate concentrations (figure 4.2-10). Reaction velocities at 0.1 MPa and 40°C for ß-, α_{s1}- and acid caseins at low substrate concentrations displayed first-order behaviour and at high substrate concentration, the velocity switches to zero-order behaviour, implying no dependence on substrate concentration. The obtained models resemble a hyperbolic behaviour, which could be interpreted according to the Henrich-Michaelis-Menten (eq.4.2-3) (Copeland, 1996). In contrast, a hyperbolic model was not achieved for reaction of α_{s1}-casein under 400 MPa and 40°C.

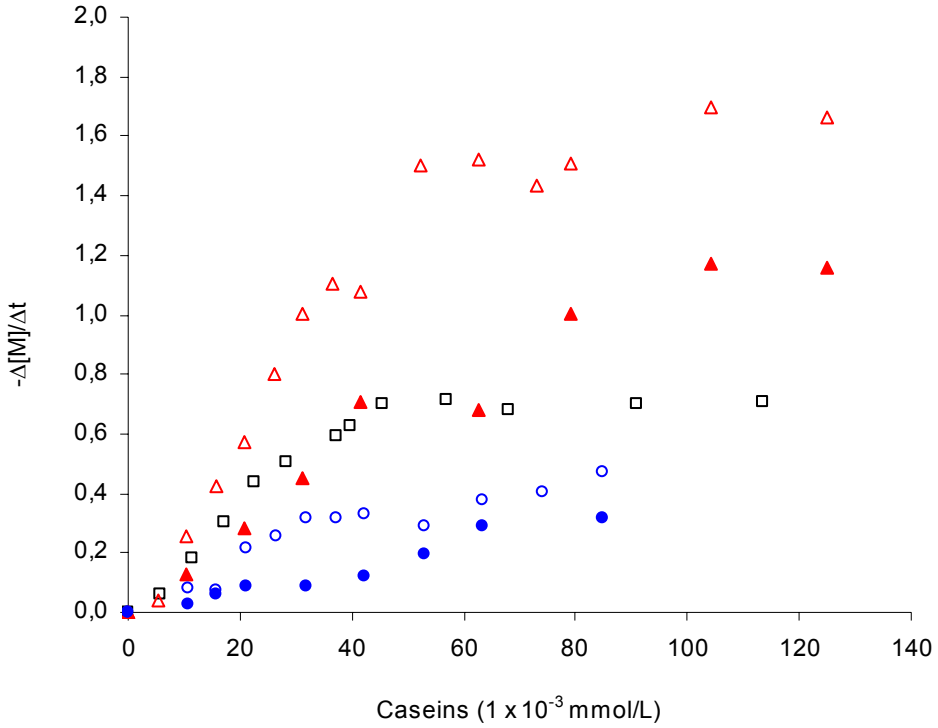

Figure 4.2-10 Plots of reaction velocities from ß- und α_{s1}-casein, measured as the slopes $-\Delta[M]/\Delta t$ shown in figure 4.2-9. Reaction of ß-casein with MTG at 40° C at 0.1 MPa (△) and 400 MPa (▲). Reaction of α_{s1}-casein with MTG at 40°C at 0.1 MPa (○) and 400 MPa (●). Reaction of acid casein with MTG at 40°C at 0.1 MPa (□).

The experimental kinetic values of V_{max} and K_m reported in table 4.2-2 were determined by interpolation of the plots of the initial velocity experimental measurements obtained at varying individual casein concentrations (figure 4.2-10).

Table 4.2-2. Graphical determination from untransformed data

	ß-Casein	α_{s1}-casein	Whole casein
V_{max} (1 x 10 $^{-3}$ mmol/L·min)			
0.1 MPa, 40°C	1.68	0.44	0.70
400 MPa, 40°C	1.16	0.30	n.d
K_m (1 x 10 $^{-3}$ mmol/L)			
0.1 MPa, 40°C	29.03	33.52	19.40
400 MPa, 40°C	39.22	45.31	n.d

n.d Not determined

The mathematical adjustment of the plots of reaction velocities as a function of casein concentration, as well as the values of V_{max} and K_m were performed by a nonlinear regression from experimental data with the equation 4.2-5 using Sigma plot software (Systat GmbH, Germany) and DynaFit software (BioKing, Ltd, USA) .

$$v = \frac{a \cdot x}{b + x} \qquad \text{(eq. 4.2-5)}$$

Where $x = [M]$, $a = V_{max}$ and $b = K_m$

4.2.6 Evaluation of reactions kinetic at atmospheric pressure

The adjusted hyperbolic behaviour of MTG reactions with individual caseins under atmospheric conditions is showed in figures 4.2-11 and the resulting kinetic parameters are exposed in table 4.2-3. The statistical evaluation of the values reported in the table 4.2-3 shows that the mathematical model fit were significant ($p < 0.05$) for ß-, α_{s1}-, and whole-casein kinetics carried out at 0.1 MPa and 40°C. This indicates that the adjusted values of V_{max} and K_m are acceptable. Maximal velocities of 2.66 x 10^{-3}, 0.79 x 10^{-3} and 1.32 x 10^{-3} mmol/L·min were obtained from ß-, α_{s1}-, and acid-casein, respectively. The V_{max} indicated the maximal reaction rate and described the steady-state equilibrium of the reaction catalysed by MTG.

Table 4.2-3. Kinetic values for reaction of MTG from adjusted dates using DynaFit software

	ß-Casein		α_{s1}-Casein		Acid casein	
	Coefficient	P>F	Coefficient	P>F	Coefficient	P>F
V_{max} (1 x 10^{-3} mmol/L·min)						
0.1 MPa, 40°C	2.7	0.0001	0.8	0.0011	1.3	0.0003
400 MPa, 40°C	2.6	0.0048	6717.09	0.9900	n.d	
K_m (1 x 10^{-3} mmol/L)						
0.1 MPa, 40°C	58.9	0.0006	64.4	0.04	49.9	0.0117
400 MPa, 40°C 0.1	144.1	0.0367	∞	-	n.d	-

Coefficients significant at 95 % confidence level. Values of "Prob>F" less than 0.05 indicate model terms are significant. Values greater than 0.10 indicate the model terms are not significant.

n.d Not determined

In the Henri-Michaelis-Menten kinetic reaction, the first reaction describes the binding of the substrate to the enzyme and constant K_m corresponds to the dissociation constant of the equilibrium under conditions, where the product formation is very slow compared to the dissociation process of the substrate (Copeland, 1996). Thereby, K_m for the complex reaction is a good approximation of the dissociation equilibrium of all substrates bounds of the enzyme and could describe the affinity of MTG to the monomeric casein.

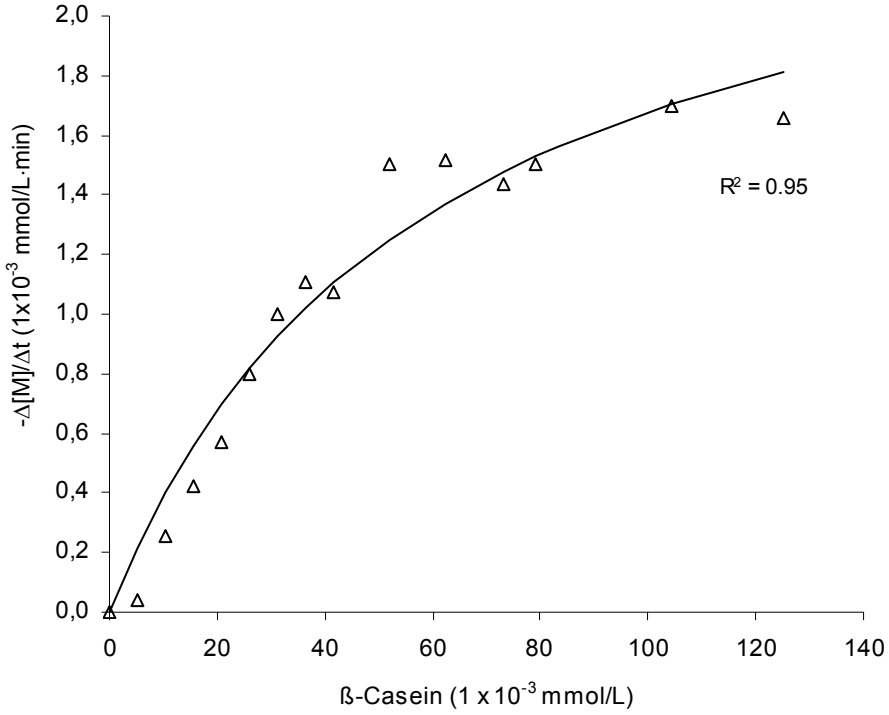

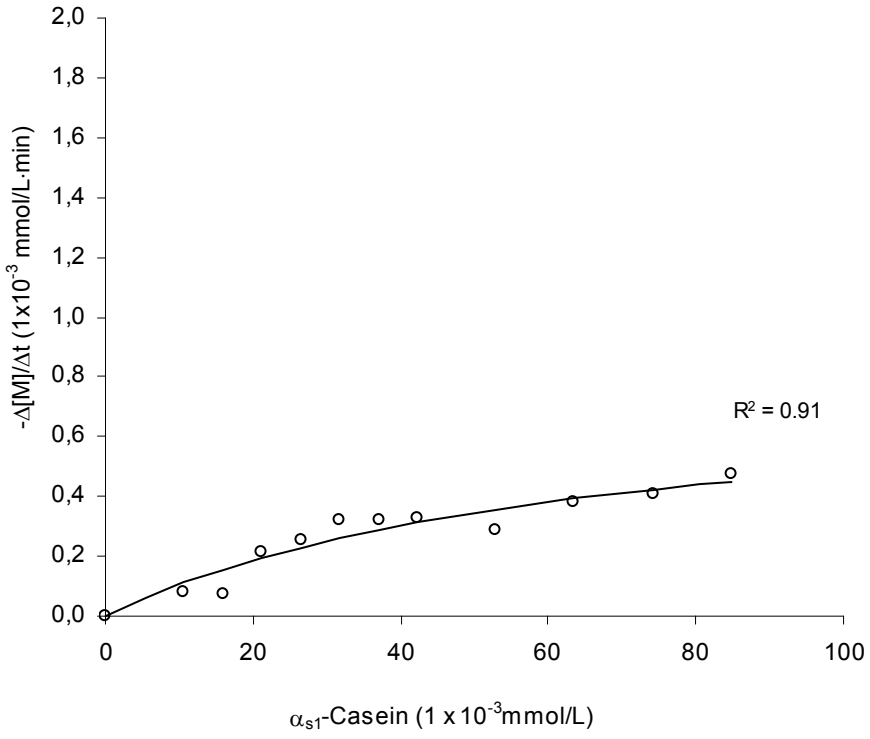

Figure 4.2-11 Plots of reaction velocities from ß-casein, measured as the slopes -Δ[M]/Δt shown in figure 4.2-9. (△) Experimental data from reaction of ß-casein with MTG at 0.1 MPa and 40°C. The continue line represent the adjusted data by the equation 4.2-5. (○) Experimental data from reaction of α_{s1}-casein with MTG at 0.1 MPa and 40°C. The continuous line represent the adjusted data by the equation 4.2-5

The K_m values of 59 x 10^{-3} for ß-casein, 64x 10^{-3} for α_{s1}-casein and 50 x 10^{-3} mmol/L for acid-casein suggested that although MTG achieved maximal velocity with ß-casein, it had the best affinity to acid casein followed by ß-casein and finally α_{s1}-casein. The later exhibited only 45% affinity of MTG compared to acid casein. The high MTG affinity to acid casein could be explained by the contribution of the potential reactive glutamine residues of κ-casein (Christensen *et al*., 1996). The Gln114 and Gln113 are located in the high soluble regions of κ-caseins, which are exposed to solvent. These regions surround the casein micelles with regard to this the affinity of MTG toward individual caseins at 0.1 MPa at 40°C followed the order: acid casein > ß-casein > α_{s1}-casein.

The second reaction step describes the catalytic rate or the rate of product formation and referred to as the turnover number k_{cat}, which is defined as the maximal number of product per active site per unit time. The k_{cat} was calculated from $V_{max} = k_{cat}\ [E_T]$ (eq. 4.2-2) and considering that Activa$_{TM}$ MP contain 7 mg protein per 1g powder (Bradford method) and 93 U per 1 g powder, the enzyme concentration of 0.01 U/mL using in the kinetic reaction is 1.98 x 10^{-5} mmoL/L. The obtained k_{cat} values were 136 min^{-1} for ß-casein at 0.1 MPa, 131 min^{-1} for ß-casein at 400 MPa; 40 min^{-1} for α_{s1}-casein at 0.1 MPa and 66 min^{-1} for acid casein at 0.1 MPa.

The value of the ratio k_{cat}/K_m is generally considered to be parameters of the catalytic efficiency of an enzyme (Copeland, 1996), thereby, the obtained k_{cat}/K_m values of 2 315 for ß-casein, 627 for α_{s1}-casein and 1 316 L/mmol·min for acid casein, indicate that at 0.1 MPa and 40°C, MTG in a 0.2 mol/L TRIS-acetate buffer pH 6 is more efficient to modify ß-casein followed by acid- and α_{s1}-casein. The tendencies of K_m and k_{cat} values, as well as k_{cat}/K_m ratio agree with reports by Traoré and Meunier (1992), who analysed the transfer reaction of Ca^{2+} activated TG from human placental factor $XIII_a$ with individual caseins at 37°C by the formation of ammonia. The kinetic reactions of individual caseins followed the Michaelis-Menten´s law. The K_m values of 100 x 10^{-3}, 34 x 10^{-3}, 50 x 10^{-3}, 130 x 10^{-3} mmol/L, as well as k_{cat} values of 97, 364 and 150 min^{-1} for α_s-, ß-, κ- and whole casein respectively were reported. Thus demonstrated that ß- and κ- casein are more susceptible for cross-linking by factor $XIII_a$ than α_{s1}-casein. The tendency of substrate specificity is also similar, k_{cat}/K_m ratios of 966 L/mmol·min for α_s-casein, 10 694 L/mmol·min for ß-casein, 4 800 L/mmol·min for κ-casein and 2 308 L/mmol·min for whole casein were reported. However, although the K_m of both works are similar, k_{cat} and k_{cat}/K_m radios could be not exactly comparable. That could be explained because both experiments were performed under very different conditions. Traoré

and Meunier (1992) analysed the transfer activity by the formation of ammonia, a secondary product obtained after the formation of the acyl enzyme intermediate from all potential glutamine residues in the system. In addition, the measurement was carried out by coupling the Ca^{2+} activated animal transglutaminase reaction to the reaction catalysed by glutamate dehydrogenase; whereas in our work, the kinetic behaviour was analysed by monitoring the decreased of monomeric casein, trying to anticipate that only the glutamine residues of monomeric casein react with MTG to form single enzyme-substrate complex.

The different affinities of MTG to individual caseins can be discussed by several theories:

1) Type of transglutaminase

The affinity of the enzyme to casein depends also on the type of transglutaminase. Studies by Gorman and Folk (1980) reported that distinct transglutaminases may recognize the same protein as substrate, but often with different affinity or with specificity for different glutamine residues.

2) Amino acid sequence of caseins.

Several authors explain that the amino acid sequence of proteins determines the reactivity of the glutamine residue, but there are yet no rules given to decide when a glutamine is potentially reactive. Coussons *et al.* (1992) proposed that the presence of positively charged lysine and arginine in a window of five residues C-terminal to a glutamine residue lowers the ability of the glutamine to be modified by guinea pig liver TG. However, several TG-reactive glutamines do not follow this charge rule. Aeschlimann *et al.* (1992) and Hohenadl *et al.* (1995) reported reactivity of two adjacent glutamines (Gln-Gln or Gln-X-Gln), where in κ-casein, only the second of two consecutive glutamines, Gln45, is recognized as an acyl donor. In the α_{s1}-casein, the first glutamine, Gln130, acts as the acyl donor. The situation, Gln-X-Gln, in which both residues act as acyl donors is found in ß-casein (Gln185-Thr-Gln187).

3) Localization of potential glutamine residues on the casein molecule.

The primary structure of the casein as well as its conformational structure determines whether a glutamine residue can be reactive. The localization of potential transglutaminase cross-linking sites in bovine caseins have been studied by labelling bovine casein with radioactive specific site probes in reactions catalysed by guinea pig TG and MTG. Christensen *et al*. (1996) reported individual caseins labelled with [^{14}C]-putrescine by guinea pig liver TG at Gln13, Gln108, Gln130 and Gln140 for α_{s1}-casein; Gln179, Gln169, Gln185

and Gln187 for α_{s2}-casein; Gln54, Gln56, Gln72, Gln79 and Gln182 for ß-casein; Gln29, Gln45, Gln114 and Gln163 for κ- casein. In our laboratory (chapter 2.5.3), Richter (2004), used ß-casein and labelled it with triglycine revealing four reactive glutamine residues, when the reaction is carried out with 4 U MTG/g protein: Gln (72 or 79 or 89), Gln (117 or 123 or 141 or 146 or160 or 167), Gln182, and Gln (188 or 194 or 195). When the reaction is catalysed by 20 U MTG/g protein, seven potential MTG-reactive glutamine residues were accessible, the four as mentioned above and additionally Gln54, Gln56, Gln184.

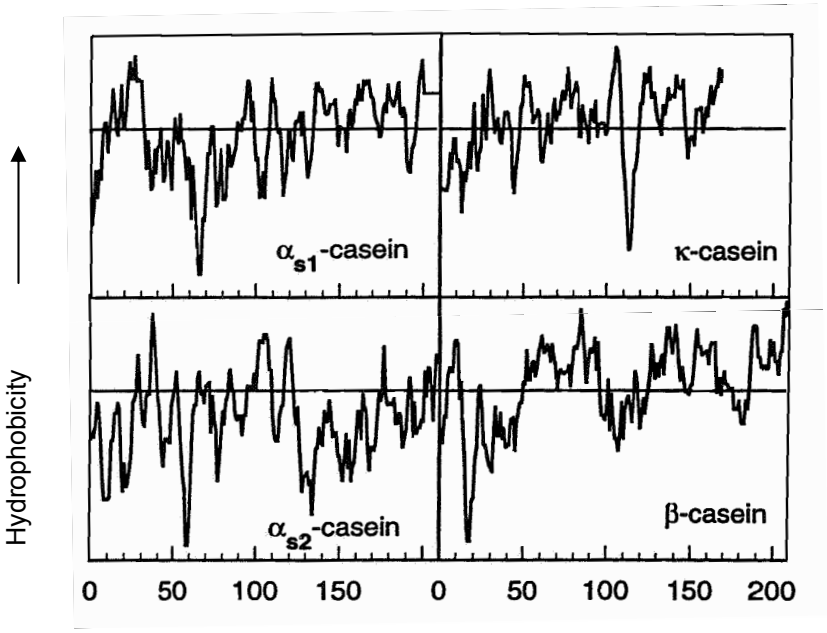

Figure 4.2-12 Hydrophobicity of the caseins along their peptide chains (Adopted from Dalgleish, 1997)

Most of the potential glutamine residues of ß-casein proposed by Christensen (1996) and Richter (2004) are located in hydrophobic regions (figure 4.2-12 and 4.2-13), which contradicts the theory of Aeschlimann (1992), who stated that the reactive glutamines are located in surface regions exposed to the solvent or flexible extension of the proteins, as patches of hydrophilic residues are often found in their vicinity. Richter (2004) suggests that MTG has preference to react with residues located in ordered domains of ß-casein. Although the high concentration of proline in caseins should lead to little order in the protein, a molecular modelling reported by Cheftel *et al*. (1992), estimates a contend of 10% α-helix (97 to 103 and 138 to 146), 13% ß-sheet (52 to 60, 77 to 87 and 187 to 195) and 77% of random coil. Based on this, the Gln141 or Gln146 are located in a α-helix region and Gln54 or Gln56, Gln79, Gln88, Gln94 or Gln95 are located in a ß-sheet region, while Gln72 and Gln89 can react because they are situated at the end of a ß-sheet or in a flexible region.

The lower affinity of MTG to the monomer of α_{s1}-casein compared to ß-casein may be due the fact that the former contains fewer reactive glutamine residues and furthermore, that the hydrophobic and charged residues are not uniformly distributed, therefore glutamine residues are masked when the protein tends to self-associate e.g. in 0.2 mol/L TRIS-acetate buffer pH 6.0. The potential reactive glutamines of α_{s1}-casein proposed by Christensen *et al*. (1996), Gln13 are located in the hydrophilic region (figure 4.2-13), but Gln108, Gln130 and Gln140 are located among the residues 100 to 199, which have a high degree hydrophobicity (Richardson *et al*. 1992) and are probably responsible, in part, for the pronounced self-association of the α_{s1}-monomers association in aqueous solutions.

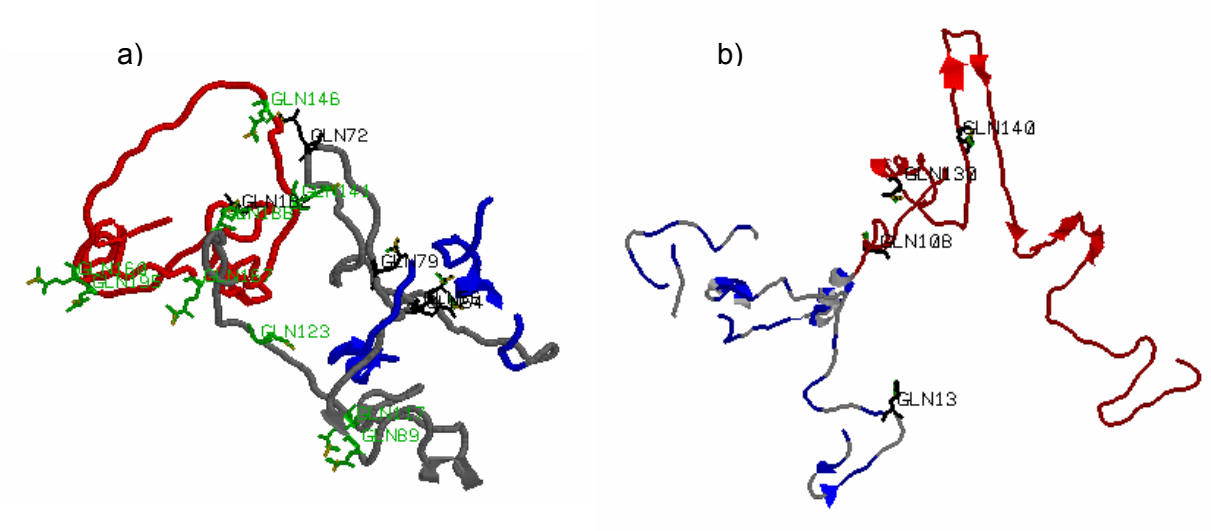

Figure 4.2-13 a) Three dimensional modeling of bovine ß-casein (Adopted from Kumosinski *et al*., 1993): Color blue represent the N-terminal portion (residues 1 to 40). Color red represents the C-terminal portion with many apolar residues resulting in its high hydrophilicity. Color black are the potential glutamine residues proposed by Christen *et al*. (1996) and color green the potential glutamine residues proposed by Richter (2004). b) Three dimensional modeling of bovine α_{s1}-casein (Adopted from Kumosinski *et al*., 1991): Color red represents the C-terminal half of the molecule (residues 100 to 1999), resulting in its very high hydrophobicity and self association. Color black are the potential glutamine residues proposed by Christen *et al*. (1996).

4) Glutamine/Lysine ratio

The Gln/Lys ratio of α_s-casein (0.8) is lower than the Gln/Lys radio of ß-casein (2.1). Traoré and Meunier (1991) report that the relation of glutamine/lysine residue of individual caseins also correlates with casein reactivity.

4.2.7 Evaluation of reactions kinetic at high pressure

The adjustment of the kinetical data of MTG reactions with individual caseins under high pressure conditions (400 MPa and 40°C) is shows in figure 4.2-13 and the resulting parameters V_{max} *and* K_m are summarised in table 4.2-3. The maximal velocity from

experimental data decreased to 1.16 mmol/L·min for ß-casein and to 0.30 mmol/L·min for α_{s1}-casein, which are approximately a 69 % of maximal velocity of α_{s1}- and ß-caseins from the reaction at 0.1 MPa at 40°C. However, the kinetical adjusted values (table 4.2-3) pointed on different reaction orders at 0.1 MPa at 40°C. The residual value of regression analysis between experimental and adjusted data of individual caseins were acceptable ($R^2 > 0.85$), the coefficient of the estimate hyperbole was significant ($p < 0.5$) for ß-casein, but not significant ($p > 0.05$) for α_{s1}-casein, which indicates that the calculated values of V_{max} and K_m are not acceptable for α_{s1}-casein. The adjustment data appeared follow a first-order kinetic with infinite values of V_{max} and K_m and demonstrated that reaction of MTG with α_{s1}-casein under high pressure had not a Henri-Michaelis-Menten behaviour.

The non-Michelian kinetic reaction behaviour of α_{s1}-casein under high pressure could be explained by:

1) Low solubility of α_{s1}-casein: Copeland (1996) reported that limitations of the substrate solubility could cause errors in calculating kinetic parameters due to low solubility of α_{s1}-casein in 0.2 mol/L TRIS-acetate buffers pH 6. The experiments ere limited to 1.9 mg α_{s1}-casein/mL with possible affects on the estimation of V_{max} and K_m.

2) Self association of α_{s1}-casein. Thermal and high pressure treatment at 400 MPa and 40°C could cause a drastic self association of α_{s1}-casein leading to a low affinity to MTG and non Henri-Michaelis-Menten kinetic.

The self association of caseins has been discussed by different authors (Rollema, 1992; Mora-Gutierrez *et al*. 1993, Stevenson *et al*. 1996, Roos-Murphy, 2000). There are several factors that induce this effect, for example, in all the genetic variants of α_{s1}-casein, the particle weight increases by increasing ionic strength in the solution (Rollema, 1992). However, variant C showed strongest association, possibly due to the reduction in charge, which does not favour the salvation of the protein. Increase of protein concentration, as well as temperature or pressure also cause self association and increase of the particle weight (Thomson, 1970). For example, a study about the influence of high pressure treatments on casein micellar structure is reported by Law *et. al*. (1998), who analysed structural changes in casein micelles from caprine milk under high pressure treatment. At room temperature (20°C) and high pressure (500 MPa), the micelles are destroyed into small soluble particles. Increasing temperature to 45°C at 500 MPa, causes higher particle solubility. However, at a temperature of 45°C in a pressure range from 300 to 400 MPa, no soluble casein aggregates are formed.

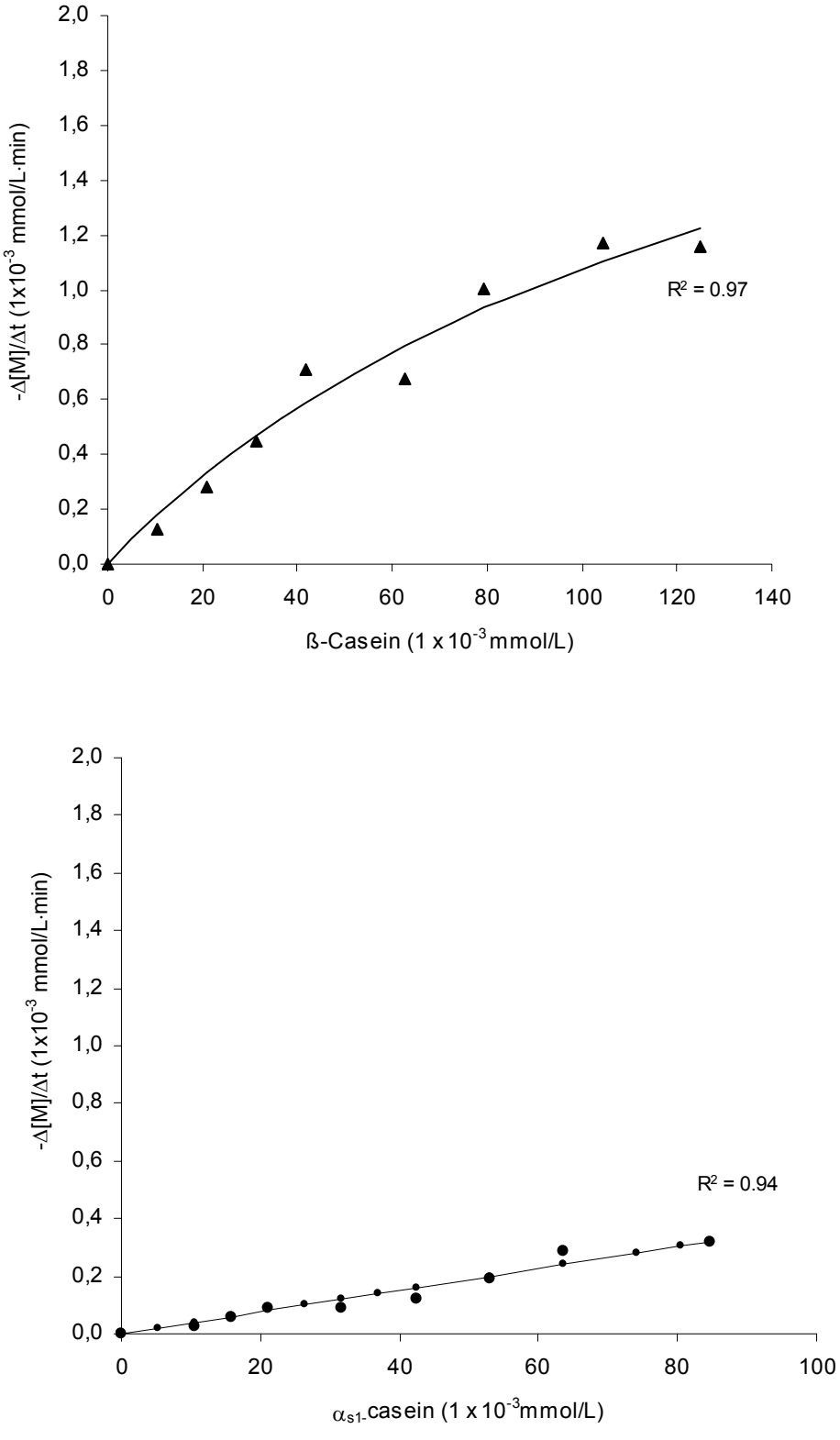

Figure 4.2-13 Plots of reaction velocities from α_{s1}-caseins, measured as the slopes $-\Delta[M]/\Delta t$ shown in figure 4.2-9. (▲) Experimental data from reaction of ß-casein with MTG at 400 MPa and 40°C. The continue line represent the adjusted data by the equation 4.2-5. (●)Experimental data from reaction of α_{s1}-casein with MTG at 400 MPa and 40°C. The continue line represent the adjusted data by the equation 4.2-5.

A study about the influence of temperature is reported by Datta *et al.* (1999), who found that casein treated at temperature-dependent conditions undergoes reversible protein reassociation. To study the self association behaviours of α_{s1}-casein, dynamic light scattering experiments were performed (Sood and Slaterry 1997). In solutions of α_{s1}-casein in a concentration of 3 mg/mL in a 0.2 mol/L TRIS-acetate buffer, pH 6.0, at 0.1 MPa and 40°C, the molecule occur as a monomer with a size of 10 nm radius and also as associates with radius from 36 to 119 nm. Increasing the α_{s1}-casein concentration to 4 and 5 mg/mL caused increasing agglomerate sizes from 22 to 168 nm and from 23 to 215 nm, respectively. A solution of α_{s1}-casein in a concentration of 3 mg/mL in the same buffer treated at 400 MPa and 40°C for 15 min also shows higher agglomerate size (about 22 to 650 nm radius) compared to 0.1 MPa and 40°C samples. Increasing amount of associated α_{s1}-casein was obtained by increasing protein concentration in a system of 0.2 mol/L TRIS-acetate buffer pH 6.0 under thermal and high pressure treatment. Under these conditions, Gln108, Gln130 and Gln140 of α_{s1}-casein could be hidden in the associated hydrophobic region and were not accessible to MTG.

The analysed kinetic parameters showed that the affinity of MTG to ß- and α_{s1}-casein was higher at atmospheric pressure than at high pressure. The k_{cat} values of ß-casein at 0.1 MPa (136 min^{-1}) and at 400 MPa (131 min^{-1}) are very similar and could be suggest that there are the same number of ε-(γ-glutamyl) lysine isopeptide per active site per min in the reaction of MTG with ß-casein at atmospheric and high pressure. That is in agree with Partschefeld, who observed the same numbers of reactive glutamine residues of ß-casein in the samples treated at these same conditions. However, the k_{cat}/K_m ratio of the reaction of MTG with ß-casein carried out at 0.1 MPa and 40°C was 2 315 L/mmol·min, whereas the k_{cat}/K_m value decrease to 1 316 L/mmol·min when the same reaction was performed at 400 MPa and 40°C. This behaviour showed that the reaction efficiency of MTG with ß-casein falls drastically under high pressure treatment. Furthermore, k_{cat}/K_m ratio of the reaction from α_{s1}-casein with MTG performed at 400 MPa and 40°C cannot be calculated because this reaction shows a non-Michelian kinetic behaviour.

Affinity of MTG to individual casein under atmospheric and high pressure treatment is different to the affinity of MTG to other substrate. For example, Lee and Park (2002) reported a kinetic study from the reaction of MTG with (CBZ)-L-glutamylglycine at 25°C in a pressure range from 0.1 to 600 MPa (figure 2.1-7). A K_m value around 25 mM and a V_{max} of 928 U of the reaction at 0.1 MPa and 25°C were reported. Increasing pressure gave similar K_m values of 29 and 27 and 30 mM and maximal velocities of 1 042, 858, and 756 Units for 400, 500

and 600 MPa, respectively. The kinetic reactions of this system indicated that the affinities of the MTG to (CBZ)-L-glutamylglycine remain similar and only the V_{max} of pressurised MTG were changed. Opposite behaviour is observed for MTG-ß-casein system, where the obtained V_{max} remain from 2.7 x 10^{-3} to 2.3 x 10^{-3} mmol/L·min after treatment at 40°C 0.1 and 400 MPa, respectively, whereas the K_m increased to 59 x 10^{-3} to 144 x 10^{-3} mmol/L.

The phenomenon could be suggested, that (CBZ)-L-glutamylglycine, a small molecule (337 g/gmol) did not drastically affect at 400 MPa and 25 °C conditions. The single active glutamine residue of the peptide remains free to react with MTG and for this reason the affinity of this enzyme-substrate is similar under atmospheric and high pressure conditions. In contrast, caseins are more complex systems because they are polymeric molecules with a great molecular weight (~22 000 to ~24 000 g/gmol). In addition, their hydrophilic and hydrophobic regions can be affected by ion strength, high pressure and thermal conditions. Then, the loss of affinity in the MTG-casein complex and its enzyme efficiency can be explained by the following reasons:

1) Inactivation of the enzyme at high pressure:
The inactivation kinetic and the influence of high hydrostatic pressure on microbial transglutaminase discussed in chapter 4.1 demonstrate that the enzyme activity of MTG decreased to 74% after treatment at 400 MPa and 40°C for 15 min.

2) Constance of potential reactive glutamine under different pressure.
Partschefeld *et al.* (2005) found that in solutions of ß-casein treated with MTG (20 U/g protein), the 15% polymerisation degree of the native sample increased to 70% after treatment at 0.1 MPa at 40°C for 1 h, whereas in treatment at 400 MPa at 40°C for 1 h, only a polymerisation degree of 33% was observed. Moreover, analysis of peptide fragments demonstrated that the numbers of reactive glutamine residues of ß-casein in samples treated at atmospheric and high pressure were the same.

3) Conformational changes of casein structures under thermal and high pressure treatment.
Based on the published protein structures of α_{s1}- and ß-casein (Kumosinski, 1991; Richardson *et al*., 1992; Cheftel *et al*., 1992; Kumosinski *et al*., 1993; Christen *et al.*, 1996), it can be proposed that the conformation of individual caseins in a 0.2 mol/L TRIS-acetate buffer pH 6.00 at 400 MPa and 40°C are modified leading to casein association. Kumosinski *et al*. (1993) stated, that, because ß-casein, is a protein with little order and charged groups preferably located in certain region (figure 4.2.12 and 4.2-13), it is possible the formation of

tetramer structures with a centrally located hydrophobic region and hydrophobic groups at each end (Kumosinski, 1993). The resulting structure contents intermolecular cavities to easy accessibility to enzymes. Berry and Creamer (1975) reported that residues 189 to 190 and the C-terminal valine, where there are non-potential glutamine residues, remain exposed on the aggregated structure. For this reason, it could be suggested that after treatment at 400 MPa and 40°C, the potential glutamine residues proposed by Christen *et al.* (1996), Gln54, Gln56, Gln72, Gln79, Gln182, remain located in cavities of the ß-casein agglomerates (figure 4.3.14) and could be accessible to react with MTG.

For α_{s1}-casein, the high degree hydrophobicity exhibited by the carboxyl of molecule (residues 100 to 199) is probably responsible of the high self-association of this molecule. Kumosinski (1991) questioned a specific aggregation site, which could be related either to local secondary structure or to clustering of aromatic residues. The molecular modelling of this author suggested that the hydrophobic portion of residues 136 to 159 involved sheet-sheet interactions to form α_{s1}-casein dimmers. Then, the potential glutamine residues suggested by Christen et al. (1996), Gln108, Gln130, Gln140, remain hidden on the associated structure (figure 4.2-13 and 4.2-14). The association models suggested by Horne (1998), described a train-loop-train and a trail-train structure for α_{s1}- and ß- casein, respectively. Both models can be polymerised or self-associated by hydrophobic interactions, for the reason it would be possible that, after high pressure treatment, agglomerates with cavities for ß-casein and crystalline agglomerates for α_{s1}-casein were formed (figure 4.2-14).

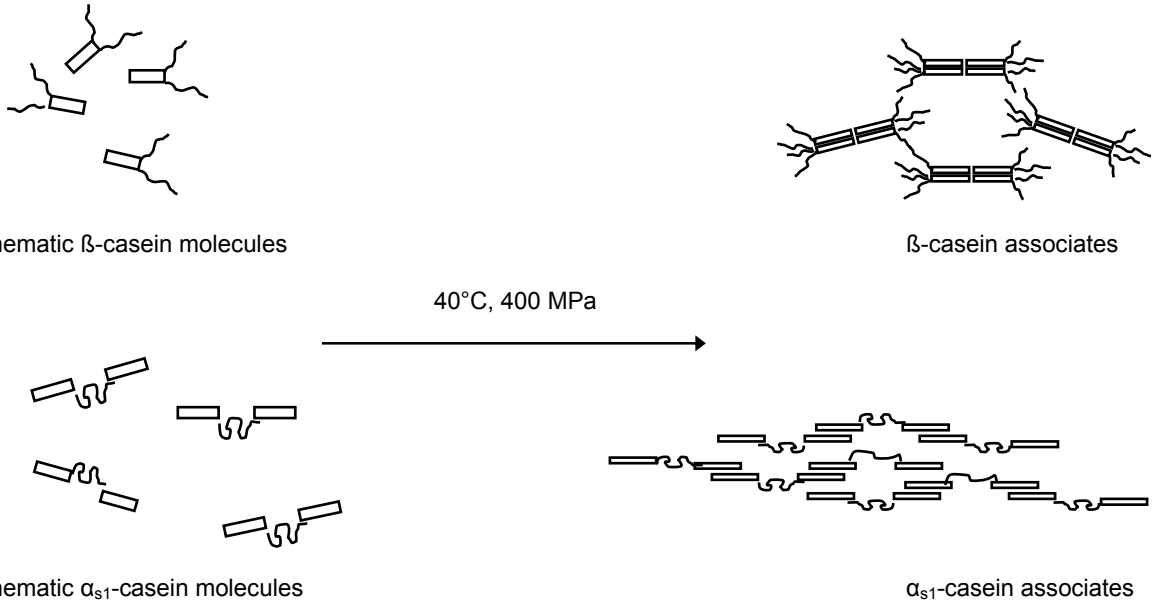

Figure 4.2.14 Hypothetic representation of α_{s1}- and ß-casein association in a 0.2 mol/L TRIS-acetate buffer pH 6.00 at 400 MPa and 40°C

The reaction between MTG with α_{s1}- or ß-casein at atmospheric pressure (0.1 MPa) and 40°C for 15 min induced casein polymerisation, demonstrated that enzyme accept both casein as substrate with a better affinity to ß-casein than α_{s1}-casein. The simultaneous reaction of MTG with both caseins at 400 MPa and 40°C for 15 min did not increase the polymerisation grade. No more glutamine residues were expose to solvent and only inactivation of the enzyme was achieved. Furthermore, temperature and high pressure treatment could cause an aggregation of α_{s1}-casein, thus covering potential reactive glutamine residues in the interior of the agglomerate.

Resuming, the kinetic values stated that MTG showed a good affinity and catalytic efficiency to acid and ß-casein. However, the affinity of MTG to individual caseins under atmospheric pressure is higher than the affinity of MTG to individual caseins under high pressure. Thereby, for a technical application, a mathematic model was suggested in order to know the optimal conditions of MTG activity and glucono-δ-lactone concentration in the preparation of acid gels at atmospheric pressure and a constant temperature.

4.3 Influence of covalent cross-linking on storage modulus of acid gels obtained by transglutaminase and glucono-δ-lactone

The rheological properties of food have considerable importance and the appearance of milk gels plays an important role in consumer's acceptance. The addition of MTG causes the formation of gels with covalent bonds as additional stabilizing elements, which, depending on parameters like pH and temperature, affect gel rheology and stabilize colloidal properties. In order to investigate the influence of MTG action on the viscoelastic properties of Gdl-induced casein gels under condition that are relevant for milk products, rheological properties, namely the gel strength and gelation time, were measured.

4.3.1 Preliminary rheological study of casein gelation

Acid gels were obtained from casein solutions induced by acidification at a pH value around 4.6. The gelation occur when the casein molecules reach their isoelectric point causing partial molecular unfolding and exposure of hidden reactive groups. These groups react intermolecular to form a network (Walstra *et al.*, 1999). Incorporation of the inorganic acid HCl rapidly shifted to low pH value, leading to a fast precipitation of the casein to form a nonhomogenous gel. In contrast, the gradual hydrolysis of glucono-δ-lactone (Gdl) to

gluconic acid in casein solution slowly shifts the pH to values below 4.6 (Berlitz *et al*., 1992), thus loading to continuous network.

Different concentrations of Gdl with and without MTG (6 U/g protein) were added to casein solutions (5% w/v) and then incubated at 40°C. Slow reduction of the pH from 6.8 to 4.6 was achieved in approximately 50 min in samples that contained concentrations of 0.334 g Gdl/g casein and the incorporation of enzyme did not influence the pH change caused by Gdl (figure 4.3-1).

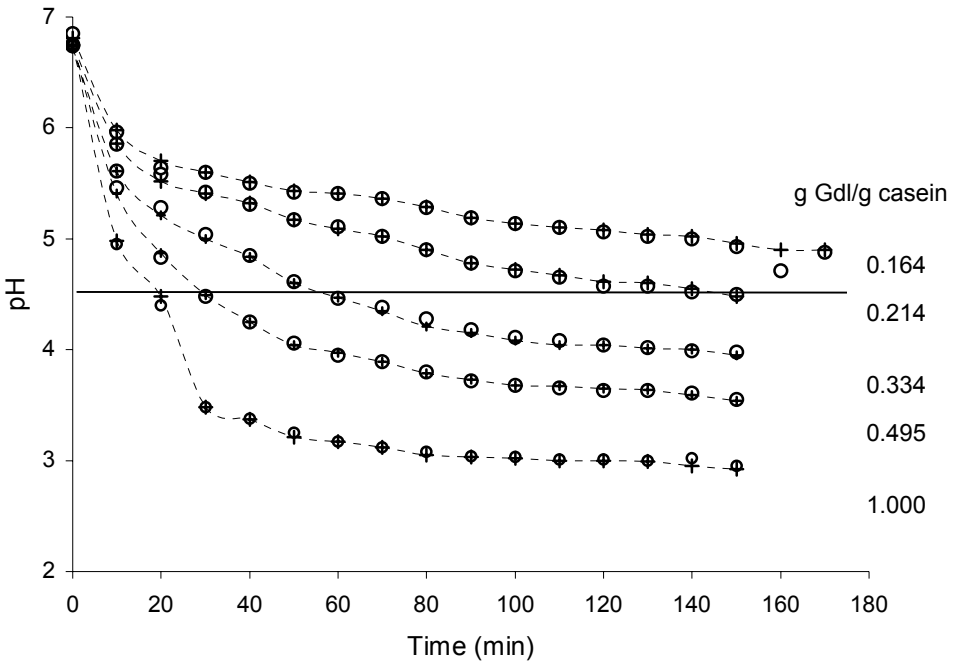

Figure 4.3-1 Change of pH during slow acidification of casein solution (5% w/v) at 40°C. Addition of Gdl in absence (○) and presence (- + -) of 6 U MTG.

The influence of the simultaneous application of Gdl and MTG on rheological properties of gels was analysed by the storages modulus (G´) as an indicator of firmness, loss modulus (G´´) displaying fluidity and the radio G´´/G´ (loss factor; tan δ) indicating the sol (tan δ>1) - gel (tan<1) transition (Ross-Murphy *et al*., 1994). The viscoelastic properties of gels were characterised by means of oscillation tests, where samples are subjected to a harmonically shear deformation (Suck T, 1992; Mezger and Neuber, 1992).

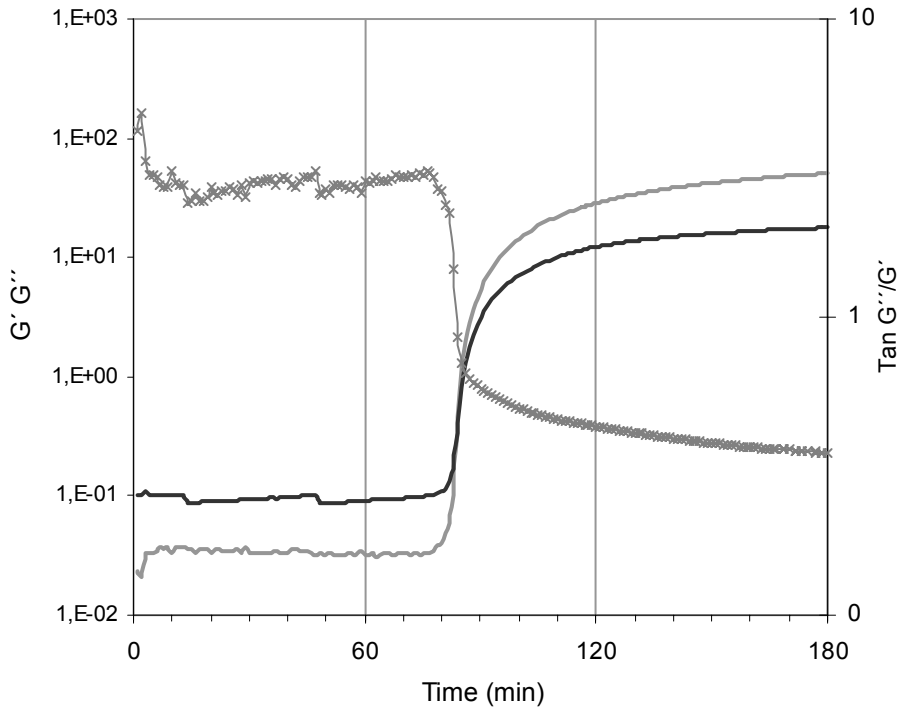

Figure 4.3-2 Gelation curve of 5 %w/v casein solution in the presence of 0.214 g Gdl/g protein at 40°C, amplitude gamma 10% and frequency 1Hz. (**—**) Storage modulus G`(Pa). (—) Loss modulus G´´ (Pa). (-x-) Loss factor, Tan G´´/G´.

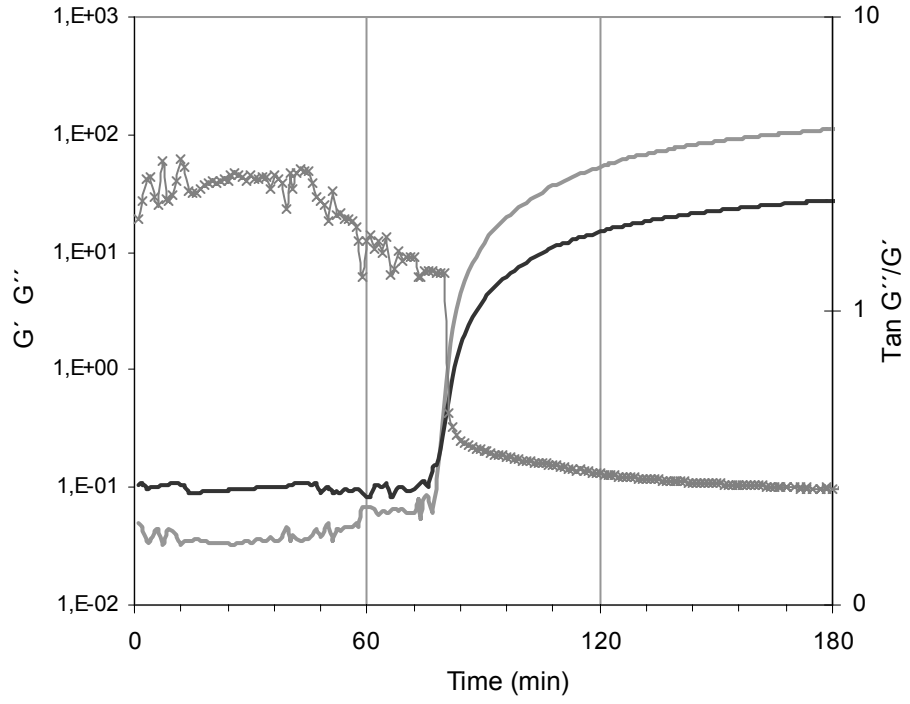

Figure 4.3-3 Gelation curve of 5 %w/v casein solution in the presence of 0.214 g Gdl/g protein and 6 U MTG/g protein at 40°C, amplitude gamma 10% and frequency 1Hz. (**—**) Storage modulus G`(Pa). (—) Loss modulus G´´ (Pa). (-x-) Loss factor, Tan G´´/G´.

Exemplarily, the addition of 0.214 g Gdl/g protein at 40°C slowly reduced the pH from 6.8 to 5.0 within 70 min. During that period, tan δ was above 1, meaning that the product was in a predominantly liquid state. The initial tan δ value of 4.21 decreased to 2.64 within the first 10 min and kept at that level up to 70 min (figure 4.3-2). Between 70 and 80 min, tan δ diminished drastically, indicating the onset of gel formation. G´ exceeded G´´ after 84 min, and tan δ declined to 0.861, corresponding to the formation of a viscoelastic solid. Within the time range up to 180 min, G´ reached a maximum of 50.7 Pa. Similar solutions (0.214 g Gdl/g protein) containing 6 U MTG/g protein also required 70 min to reach pH 5.0 (tan δ = 1.53). The gelation time was 81 min and after 180 min the storage modulus G´ was 110 Pa. As compared to the control experiment, the gelation time was slightly reduced, and it was observed a more than two fold increase in G´ (figure 4.3-3).

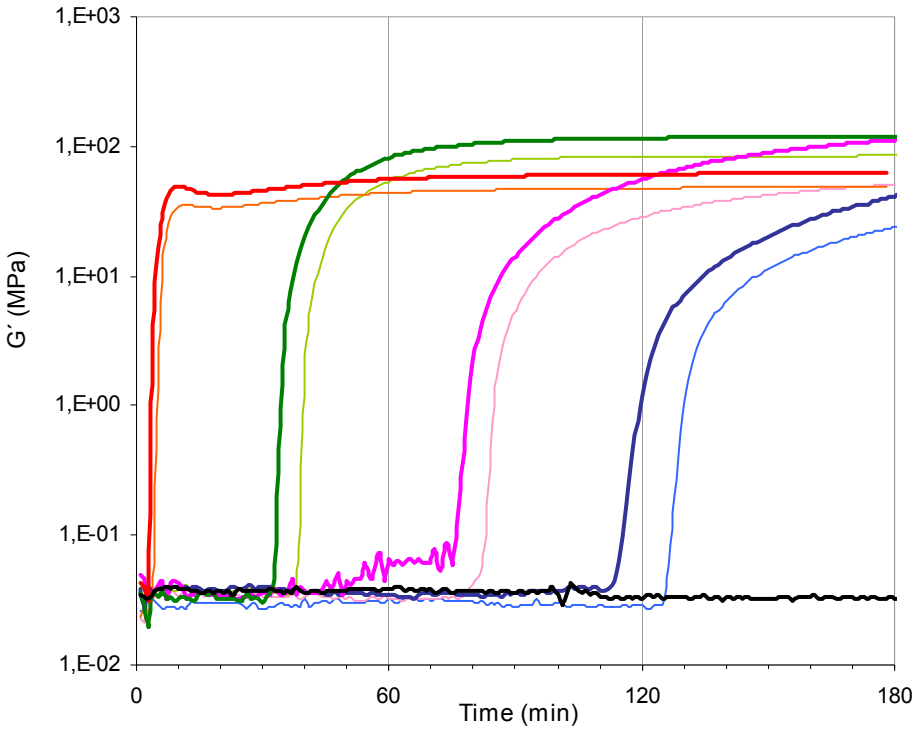

Figure 4.3-4 Gelation curve of a casein solution 5 % in the presence different Gdl concentration and 6 U MTG/g protein at 40°C, amplitude gamma 10% and frequency 1Hz. (—)1 g Gdl/g protein with 6 U MTG/g protein, (—) 1 g Gdl/g protein without MTG. (—) 0.334 g Gdl/g protein with 6 U MTG/g protein, (—) 0.334 g Gdl/g protein without MTG. (—) 0.214 g Gdl/g protein with 6 U MTG/g protein, (—) 0.214 g Gdl/g protein without MTG. (—) 0.164 g Gdl/g protein with 6 U MTG/g protein, (—) 0.164 g Gdl/g protein without MTG. (—) 6 U MTG/g protein without Gdl.

Generally, the gelation time decreased with an increasing amount of Gdl added to the system, however higher concentrations of Gdl caused the formation of weaker gels (figure 4.3-4). Addition of 1 g Gdl/g protein caused gelation within 5 min and a storage module value G´ of 48.9 Pa after 180 min. With the simultaneous addition of 1 g Gdl/g protein and 6 U

MTG/ g protein the gelation time was 4 min and the storage modulus 63.7 Pa. Gels from samples containing 1 g Gdl/g protein and MTG were weaker than gels from samples containing 0.214 g Gdl/g protein and MTG (G´=111.0 Pa). This could be caused by the rapid drop of pH to below 5 along with inactivation of the enzyme, which is stabile in the range from 5 to 9. However, addition of very low Gdl concentrations was not optimal, resulting in very weak gels and drastically increased gelation time. For example in samples with the addition of 0.164 g Gdl/g, the gelation was achieved in 168 min without enzyme and 117 min with enzyme. The G´ values after 180 min were 23.7 and 40.9 Pa in sample with and without enzyme, respectively.

Casein solutions without Gdl did not form gels at all. The gels obtained from samples with only addition of Gdl showed G´ values in a range from 23.7 to 84.8 Pa, these gels were formed because the hydrophobic interactions, electrostatic bridges and hydrogen bonds reacted as intermolecular forces that stabilize acid gels (Oakenfull *et al*., 1997). However the gels formed from samples with the simultaneous addition of Gdl and MTG were stabilized with the combination of covalent and non-covalent bonds and obtained G´ values range from 40.9 to 118 Pa (table 4.3-1), which demonstrates that the combination of both protein cross-linking forces results in a higher firmness of the gel.

Table 4.3-1 Effect of MTG and Gdl concentration on storage modulus G´ (Pa) of acid gels

g Gdl/g casein	G´(Pa)	
	0 U MTG/g protein	6 U MTG/g protein
0.000	0.01^{d}	0.03^{c}
0.164	23.7^{c}	40.9^{b}
0.214	50.7^{b}	111.0^{a}
0.334	84.0^{a}	118.0^{a}
1.000	48.0^{b}	63.3^{b}

Mean values with different letters within columns are significantly different ($p<0.05$). Gels were prepared with MTG and Gdl added to 5 % w/v casein. The samples were oscillated at an amplitude gamma of 10%, 1 Hz at 40°C. G´ was measured after 180 min.

4.3.2 Central composite rotatable design to study the behaviour of casein gelation with the simultaneous application of glucono-δ-lactone and microbial transglutaminase

Based on the preliminary study, a central composite rotatable design (CCRD) with two factors and two levels was used to estimate the influence of MTG and Gdl concentration on the gelation time and elastic properties. Dimensional independent variables were MTG

concentration with a range from 0.98 to 5.82 U MTG/g protein and the Gdl concentration with a range from 0.214 to 0.334 g Gdl/g protein. For statistical purposes, dimensionless variables were coded as:

x_1 = (MTG concentration – 3.41)/2.42 (eq. 4.3-1)

and

x_2 = (Gdl concentration – 0.274)/0.06 (eq. 4.3-2)

Table 4.3-2 Arrangement and responses of central composite rotatable design (CCRD)

Experiment No.	Independent variables				Dependent variables	
	Uncoded		Coded			
	UTG/g casein	g GdL/g Casein			G´ (Pa)	Time of gelation (min)
	x_1	x_2	x_1	x_2	y_1	y_2
1	5.80	0.334	1	1	120.0	32.0
2	5.8	0.214	1	-1	165.0	58.0
3	0.98	0.334	-1	1	76.4	34.0
4	0.98	0.214	-1	-1	77.6	66.0
5	3.41	0.358	0	1.414	82.0	30.0
6	3.41	0.189	0	-1.414	79.0	97.0
7	6.83	0.274	-1.414	0	122.0	48.0
8	0.00	0.274	1.414	0	92.0	41.0
9	3.41	0.274	0	0	116.0	47.0
10	3.41	0.274	0	0	112.0	49.0
11	3.41	0.274	0	0	116.0	47.0
12	3.41	0.274	0	0	112.0	49.0
13	4.41	0.274	0	0	112.0	49.0

Gels were prepared with MTG and Gdl added to 5 % w/v solutions of commercial casein. Rheological oscillation measurement was performed at an amplitude gamma of 10%, 1 Hz at 40°C. G´ was measured after 180 min.

To evaluate the influence of the MTG as well as Gdl concentration on the gel firmness expressed as G´, a statistical model was used. The resulting surface plot is visualizing the mathematical model fit to the experimental data.

a) Effect of simultaneous application of microbial transglutaminase and glucono-δ-lactone on storage modulus

A quadratic model was suggested as best fit for a sequential model by sum of square and lack of fit tests for the surface response G´. Table 4.3-3, displaying individual terms analysed by ANOVA, shows that the significant terms were x_1 (MTG) and x_{22} (Gdl) (p<0.05), hence the possible mathematic model to predict G´ under untested conditions was:

$$y_1 = 124 + 24.29\, x_1 - 13.70\, x_{22} \qquad \text{(eq. 4.3-3)}$$

Table 4.3-3 Analysis of individual model coefficients.

	y_1 Storage Modulus G´(Pa)		y_2 Gelation time (min)	
	Coefficient	Prob>F	Coefficient	Prob>F
Constant	114.00	0.0081	49.39	0.0002
x_1	24.29	0.0012	-2.87	0.4118
x_2	-5.24	0.2952	-19.09	0.0001
x_1x_1	3.35	0.5221	-	-
x_2x_2	-13.70	0.0280	-	-
x_1x_2	-10.95	0.1388	-	-

Coefficients significant at 95 % confidence level. Values of “Prob>F” less than 0.05 indicate model terms are significant. Values above 0.10 indicate the model terms are not significant.

The interpretation of this model is, that the MTG concentration has a significant influence on G´ (p<0.5) and that the firmness of the gels increases in linear proportion with the MTG activity at each Gdl concentration (p<0.05). Maximal firmness in the experiments (134.3 Pa) was obtained at an activity of 5.62 U MTG/g protein between a range from 0.242 to 0.374 g Gdl/g protein (figure 4.3-5).

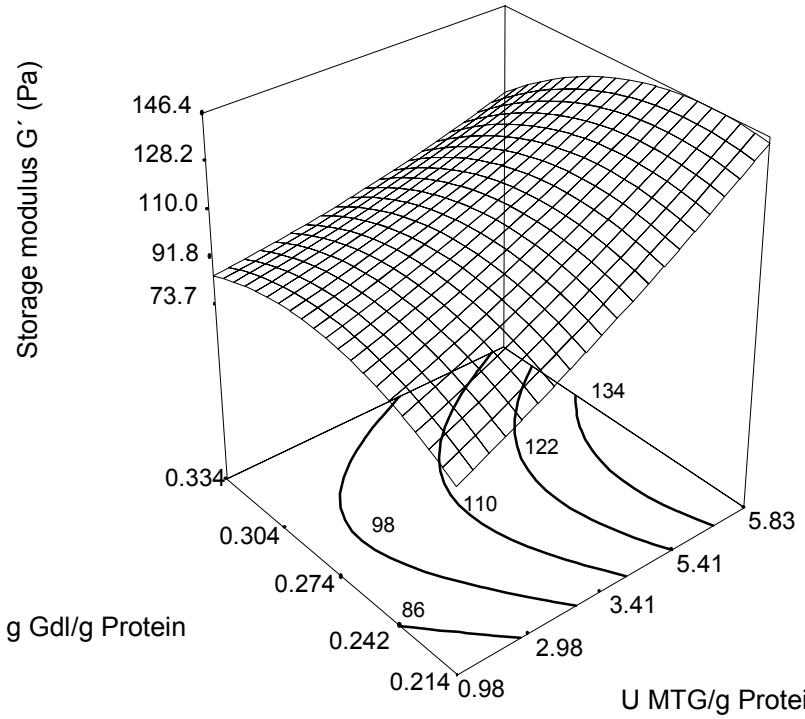

Figure 4.3-5 Surface plot of storage modulus G´ (Pa) with MTG activity from 0 to 6.83 U MTG/g protein and Gdl concentration from 0.189 to 0.358 g/g protein.

In contrast, the influence of the Gdl concentration is governed by a quadratic term, showing that there is an optimum of carrying out the reaction.

b) Effect of simultaneous application of microbial transglutaminase and glucono-δ-lactone on gelation time

Subsequent analysis of the analytical data concerning the gelation time showed the best fit for a linear model. The individual term x_2 (MTG) was significant ($p<0.05$) and x_1 (MTG) was not significant ($p>0.05$) on the gelation time as dependent variable (table 4.3-3). The gelation time could be predicted by:

$$y_1 = 49.39 - 19.09\, x_2 \qquad \text{(eq. 4.3-4)}$$

The interpretation of this model is, that the Gdl concentration has significant influence on the gelation time ($p<0.05$), while it is independent of the MTG activity ($p>0.05$). At 0.242-0.274 g Gdl/g protein and 5.83 U MTG/g protein the maximal firmness (136 $\pm$ 2 Pa) was reached in a time between 49 to 59 min respectively (figures 4.3-5, 4.3-6).

The results confirmed that all variables like enzyme activity, Gdl concentration, pH and temperature affected the gel rheology and colloidal properties (Schorsch *et al*., 2000a; Schorsch *et al*., 2000b), which in food production could be controlled, depending food characteristics of the market. For example, gelation of acid meat protein suspension at low temperatures (4°C) is used to produce restructured meat products (Ngapo *et al.,* 1996). In contrast, as Gdl hydrolysis to gluconic acid depends on temperature, higher temperatures produce stronger gels (Totosaus *et al.,* 2000). In the resent years, MTG is also used in yogurt production (Ajinomoto, 2002). Traditionally, milk is incubated with MTG followed by heat treatment to enzyme inactivation before addition of starter culture, but this step causes increasing time process. For this reason, knowing that simultaneous application of MTG and Gdl induce increase on storages modulus on acid gels, it can be suggested that MTG can be added to the milk at the same time of the starter culture and the enzyme reaction can be proceed during the fermentation. Obviously, milk is a complex system that needs a detail study as is confirmed by Lorenzen *et al.* (2002).

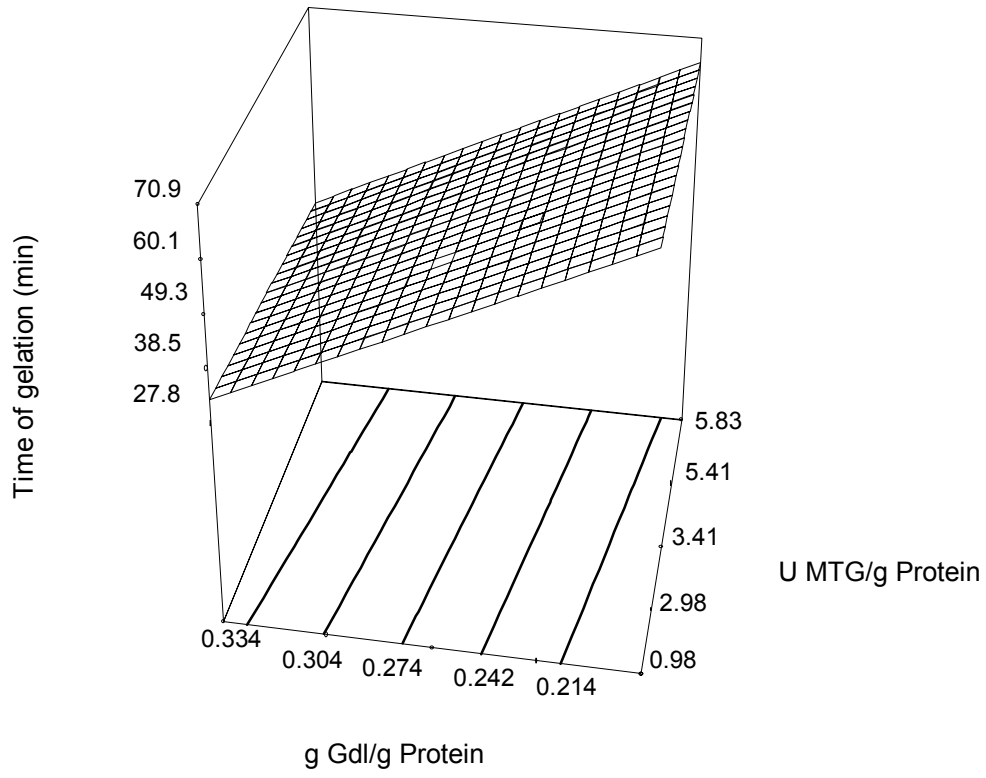

Figure 4.3-6 Surface plot of gelation time (min) with MTG activity from 0 to 6.83 U MTG/g casein and Gdl concentration from 0.189 to 0.358 g/g casein

Gels induce by acidification are mainly stabilised by non-covalent interactions. As the addition of MTG causes the formation of gels with covalent bonds as additional stabilising element, the protein in such sample should be oligomerised. To monitor nature and extend of this protein cross-linking, gel permeation chromatography was performed.

4.3.3 Effect of oligomerisation degree on gel firmness

Oakenfull *et al.* (1997) mentioned that acid treated caseins form non-covalent bonds like electrostatic interactions and hydrogen bonds while temperature- and high pressure treatment additionally leads to covalent bonds through disulfide linkages, building up a three-dimensional network. As the pre-treatment of the protein samples in these experiments included the application of both acid and heat, DTT was added in order to reduce disulfide bonds and the chromatography was performed in buffered urea to break non-covalent interactions.

The comparison of reduced an non-reduced samples (without DTT) from gels obtained with addition of 1 g Gdl/g protein showed, that peaks for dimeric, trimeric and oligomeric protein molecules disappear completely (figure 4.3-7), meaning that acid gels are formed by reversible cross-linking. On the other hand, casein treated exclusively by MTG (6 U/g protein) showed a high degree of oligomerisation that was not reducible compared to the initial casein (figure 4.3-8). Despite the effective way MTG acts on caseins, it is not possible to create a gel only by the introduction of isopeptides.

As already mentioned, simultaneous action of MTG and Gdl lead to gel stiffening. For example, gel from a 5 % w/v casein solution with addition of 5.8 U MTG + 0.214 g Gdl/g protein and 6.8 U MTG + 0.274 g Gdl/g protein after 180 min at 40 °C reached a G´= 165 Pa and G´= 122 Pa, respectively. The degree oligomerisation of these samples (figure 4.3-9) showed that the gels with a G´ value of 165 Pa exhibited less dimers and trimers but more oligomers than gels with a G´ value of 122 Pa.

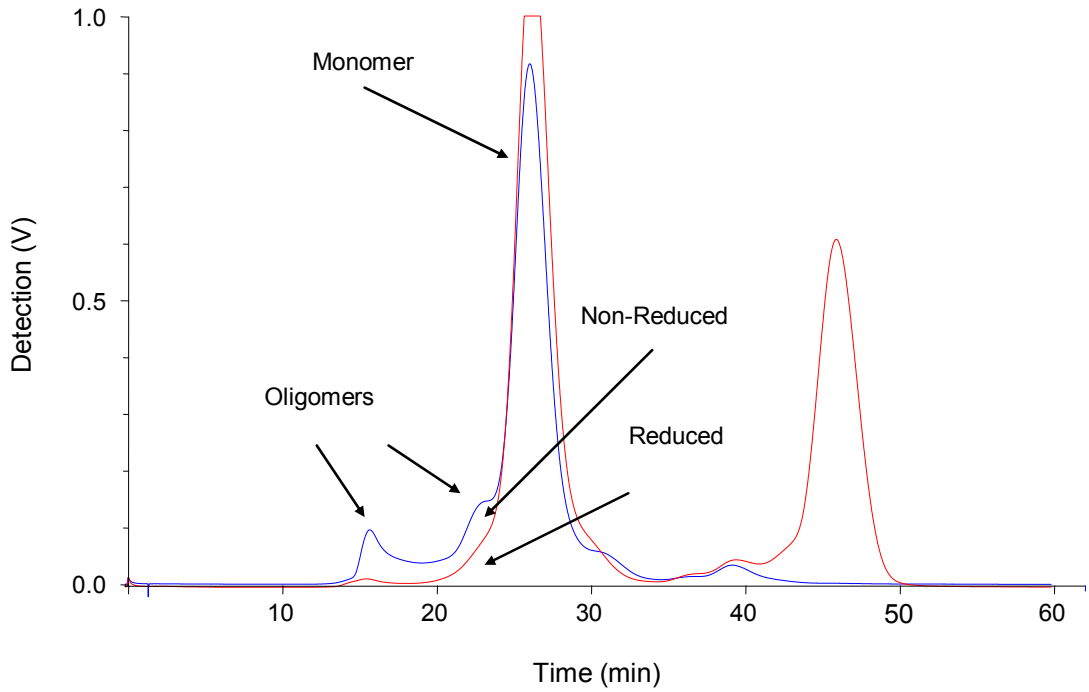

Figure 4.3-7. Gel permeation chromatography of acid gel from 5% w/v casein solutions incubated with and 1 g Gdl/g protein for 1h at 40 °C.

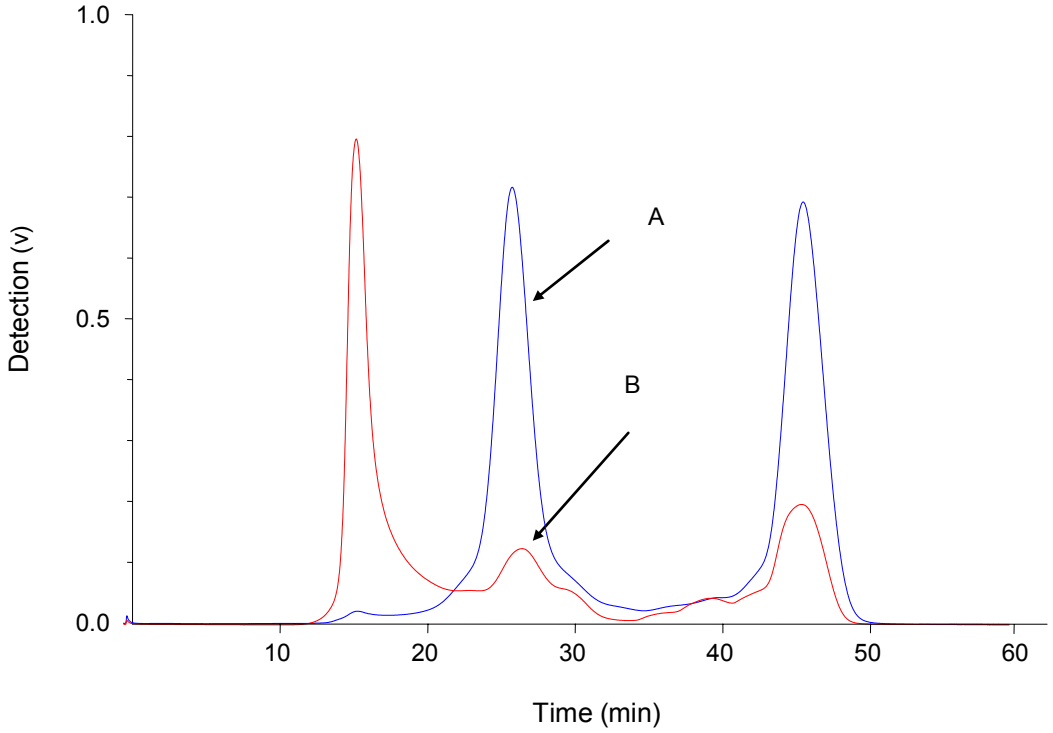

Figure 4.3-8 Gel permeation chromatography under reducing conditions (DTT) of samples from 5 % w/v casein solutions incubated for 3h at 40°C. (A) Without MTG. (B) With 6 U MTG/g protein.

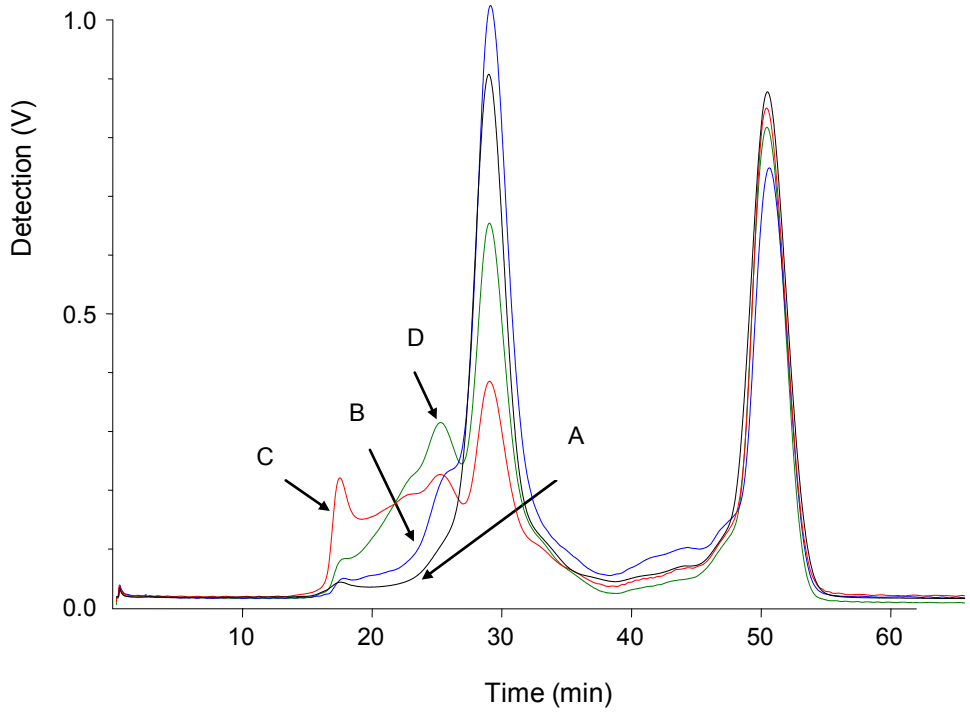

Figure 4.3-9 Gel permeation chromatography of gel from 5% w/v casein solutions incubated with different Gdl and MTG concentrations for 3 h at 40 °C. (A) Casein without treatment, (B) casein with 0.98 U MTG/g protein and 0.334 g Gdl/g protein, (C) casein with 5.8 U MTG/g protein and 0.214 g Gdl/g protein, (D) casein with 6.8 U MTG/g protein and 0.274 g Gdl/g protein.

The gels obtained with 0.98 U MTG and 0.334 g Gdl/g casein had G´ value of 76.4 Pa and the lowest contents of oligomers. The comparison between rheological and chromatographical studies demonstrated that the firmness in the gels is related with oligomerisation grade. That can be explained because there are relation between the degree of polymerisation and isopeptide N^{ε}-(γ-glutamyl)- lysine formation (Lauber *et al.*, 2000). Then, this work confirmed the studies of Lauber *et al.* (2000) and suggested that isopeptide formed via MTG are additional stabilizing elements in casein gel network. Moreover, application of MTG by an optimal Gdl concentration is also important to achieve a stable network.

5 Proposes for further studies

After to know the affinity to monomeric casein, a polymeric enzymatic study could be interesting to investigate the affinity of MTG with dimers and trimers into the polymerisation reaction at atmospheric conditions.

Kinetic reaction from MTG with acid-, ß- and α_{s1}-casein showed that affinity did not increase under high pressure. However, because ß-lactoglobulin during high pressure treatment achieved news potential glutamine residues (Richter, 2004) it can investigate, whether the reaction kinetics of MTG with this protein as substrate has a Michaelis-Menten-Henri behaviour and whether its affinity increase during high pressure conditions.

Formation of Maillard product were found in a system of MTG:lactosa:maltodextrin. Nevertheless, Maillard reaction is a cascade of consecutive and parallel reactions and its reaction grade depend of the chemical composition of the reactants, as well as, conditions of the system. For this reason, experimental models with different type and radio of the reactants at different temperature, pressure and controlled pH are important to plan, in order to investigate the effect of pressure on mechanisms reaction of Maillard product.

6 Summary

Kinetic inactivation of factor $XIII_a$ and MTG were performed in a pressure range from 0.1 to 400 MPa at 40°C within a time from 0 to 60 min in a TRIS-acetate buffer at pH 6.0. The inactivation of both enzymes at these conditions followed a first order reaction model. The high inactivation rate constant of 26.6 $x10^{-3}$ min^{-1} for factor $XIII_a$ at low pressure (50 MP) indicated that this enzyme is much easier to inactivate than MTG, which achieved an inactivation rate constant value of 9.7 $x10^{-3}$ min^{-1} at higher pressure (200 MPa). An inactivation volume of -10.17 ± 0.5 cm^3/mol confirmed that MTG is very stable under high pressure.

The stability of MTG under high pressure and thermal treatment was related to its conformational changes. Enzyme inactivation was accompanied by secondary and tertiary structure changes until an irreversible protein precipitation is achieved. The tertiary structure, represented by circular dichroism spectra in the aromatic region showed differences among native and MTG samples treated under high pressure, as well as at elevated temperature. Tyrosine bands, indicating protein unfolding, increased proportionally with increasing pressure treatment above 400 MPa. Nevertheless, compared to pressure, a maximal enhancement could be observed after thermal treatment at 0.1 MPa at 80°C. That demonstrated the exposure of hydrophobic groups to the protein surface with a concomitant protein unfolding. The spectra in the far ultraviolet region showed that increasing high pressure and high temperature lead to alterations in the secondary structure. The mathematical algorithms CONTIN used to calculate secondary structures stated that the 24.5% of α-helix of native MTG decreased to 17.2% after a treatment at 400 MPa at 40°C for 60 min and to 6.5% after a treatment at 0.1 MPa at 80°C for 2 min. However, ß-strand structures remained relatively stable after these several treatments. MTG is arranged in a way that the active site is located between β-strand domains that are surrounded by α-helices, the results of this investigation suggested that MTG activity is related with the relative stability of α-helix and the outstanding stability of the central β-strand structure.

The irreversible precipitated protein observed at 600 MPa at 40°C for 60 min and 0.1 MPa at 80°C for 2 min was caused principally by the formation of disulfides bonds, because high pressure and high thermal treatment lead to the exposition of the Cys64 residue towards the solvent with the subsequent ability to react with neighbouring cysteine residues. Furthermore, the reaction between protein and reducing sugars resulted in the formation of Maillard products. Furosine, as an indicator of the early stages of Maillard reaction was

measured. Concentration values of 261.0 μg/g protein from samples treated at 600 MPa and 40°C and 238.5 μg/g protein from samples treated at and 0.1 MPa and 80°C for 2 min were obtained. Pentosidine a subsequent product observed in the advanced Maillard reaction was also present. Concentrations of 13.7 and 6.7 μg/g protein were obtained in the samples treated at 600 MPa and 40°C for 60 min and 0.1 MPa and 80°C for 2 min, respectively.

Kinetic inactivation studies of MTG in a pressure range from 0.1 to 600 MPa at 10, 30, 40, and 50°C within a long time range from 0 to 140 h were performed in order to study MTG stability under the simultaneous effect of pressure and temperature. The inactivation kinetic showed a first and very fast step and a second very slow step suggesting irreversible inactivation behaviour. Activation energy and entropy difference decreased with increasing pressure. Thereby, the inactivation rate constants of enzyme were less temperature dependent at high pressure. The effect of pressure and temperature on MTG inactivation had a synergistic behaviour. At temperatures of 10, 30, and 40°C, increasing pressure leads to increasing inactivation rate constants. However at 50°C a tendency change occurred. Negative activation volumes of –16.2±0.5, -13.6±0.1, -11.2±0.3 cm^3/mol were obtained for 10, 30 and 40°C respectively and for treatment at 50°C a positive value of about +3.0±2.0 cm^3/mol in a pressure range from 0.1 to 300 and a negative volume of –11.0±0.4 cm^3/mol MPa from 300 to 600 MPa were calculated.

A pressure/temperature diagram from inactivation rate constants was performed to represent MTG stability. The diagram shows that in a pressure and temperature range from 0.1 to 550 MPa and 10 to 40°C, pressure induces MTG stabilization against heat denaturation. At 50°C in range from 0.1 to 300 MPa, pressure induces also enzyme stabilization again heat denaturation, but at the same temperature and above 300 MPa the enzyme was inactivated.

After MTG stability analysis, reaction kinetics from MTG with individual caseins in a TRIS-acetate buffer pH 6.0 were performed under atmospheric pressure (0.1 MPa) and high pressure (400 MPa) at 40°C. The reaction was monitored by gel permeation chromatography under in three assumptions: 1) The initial velocity kinetics was obtained from a non-progressive enzymatic reactions with the products. 2) The substrate concentration exceeded enzyme concentration. 3) The sum of the individual catalytic constants of the reactive glutamine residues inside caseins are represented by a single MTG-monomeric casein complex.

Enzyme reaction kinetics of MTG with the individual caseins carried out at 0.1 MPa at 40°C showed Michaelis-Menten-Henri behaviour with maximal velocities of 2.7 x 10^{-3}, 0.8 x 10^{-3}, and 1.3 x 10^{-3} mmol/L·min and K_m values of 59 x 10^{-3}, 64 x 10^{-3} and 50 x 10^{-3} mmol/L of ß-, α_{s1}-, and acid-casein, respectively. This suggested that MTG achieved a maximal velocity with ß-casein, but had the best affinity with acid casein followed by ß- casein and finally α_{s1}-casein.

Enzyme reaction kinetics of ß-casein carried out at 400 MPa and 40°C also showed a Michaelis-Menten-Henri behaviour with a similar maximal velocity of 2.6 x 10^{-3} mmol/L·min, but the K_m value of 144 x 10^{-3} mmol/L showing kinetical similarity to a non-competitive inhibition. The reaction of MTG with α_{s1}-casein under high pressure did not fit in to Henri-Michaelis-Menten kinetics.

Kinetic parameters showed that the affinity of MTG to ß- and α_{s1}-casein under atmospheric pressure is higher than the affinity of MTG to these caseins under high pressure. This loss of affinity can be explained by a constant number of reactive glutamine residues of casein, although the protein is unfolding at high pressure, a decrease of enzyme activity of MTG to 74% after treatment at 400 MPa at 40°C for 15 min and self association of casein under thermal and high pressure treatment.

Fur technological application, the formation of acid milk gels was studied under the influence of MTG within its range of pH stability. Simultaneous addition of MTG and different concentrations of glucono-δ-lactone (Gdl) to casein solutions (5% w/v) at 40°C was analysed. Gels firmness was accessed by oscillation rheometry and gel permeation chromatography. Oscillation rheometry data showed that the time of gelation decreased with an increasing Gdl concentration added to the system, however higher concentrations of Gdl caused the formation of weaker gels. Addition of 1 g Gdl/g protein without MTG caused gelation within 5 min and a storage module value G´ of 48.9 Pa. With the simultaneous addition of 1 g Gdl/g protein and 6 U MTG/ g protein the gelation time was 4 min and the reached storage modulus was 63.7 Pa. However, the addition of 0.21 g Gdl/g protein and 6 U/g protein MTG increase the gelation time to about 69 min, but, a higher module value G´ of 111.0 Pa was achieved. Addition of high Gdl concentration caused a rapid drop of pH below 5 leading to a fast enzyme inactivation. However addition of very low Gdl concentrations was also not optimal.

The simultaneous influence of MTG and Gdl concentration on the gelation time and elastic properties was evaluated by a central composite rotatable design (CCRD). The resulting quadratic storage modulus model showed that, MTG concentration had a significant influence on storage modulus G´ and, that the firmness of the gels increase in direct proportion with MTG activity with the existence of a optimum Gdl concentration, whereas the resulting linear model of the gelation time stated that Gdl concentration has a significant influence on the gelation time, while it is independent of the MTG activity. A maximal firmness of 136 $\pm$ 2 Pa was reached between a range of 0.24 - 0.27 g Gdl/g protein and 5.8 U MTG/g within a time from 49 to 59 min. Gel permeation chromatography analysis demonstrated that acid gels induced by Gdl were formed by reversible cross-linking like electrostatic interactions and hydrogen bonds as well as disulfide bonds caused by temperature treatment. Whereas, the addition of MTG proved the formation of non-reversible cross-linking like oligomers based on N^{ε}-(γ-glutamyl)- lysine, which gave more firmness and stabilization on the casein gel network.

7 References

Abbasi S, Dickinson E (2002) High pressure-induced rheological changes of low-methoxyl pectin plus micellar casein mixtures. J Agric Food Chem 50:3359-3565

Aberer W, Hahn M, Klade M, Seebacher U, Spök A, Wallner K, Witzani H (2002) Collection of information of enzymes. European Communities, Luxembourg, Belgian

Alberty R (2005) A short history of the thermodynamics of enzyme-catalyzed reactions. J Biol Chem 279:27831-27836

Aeschlimann D, Paulsson M, Mann K (1992) Identification of Gln^{726} in nidogen as the amine acceptor in transglutaminase-catalyzed cross-linking of laminin-nidogen complexes. J Biol Chem 267:11316-11321

Ajinomoto (2002) Product Information Activa ® MP. Ajinomoto Foods Deutschland GMBH, Hamburg

Alais C (1997) Ciencia de la leche (10 ed) Compañía Editorial Continental, México D.F.

Ando H, Adachi M, Umeda K, Matsura A, Nonaka M, Uchio R Tanaka H , Motoki M (1989) Purification and characteristics of novel transglutaminase derived from microorganisms. Agric Biol Chem 53:2613-2617

Aschaffenburg R (1963) Preparation of ß-casein by a modified urea fractionation method. J Dairy Res 30:259-260

Atkins P (2000) Physical Chemistry. Oxford University Press (6 ed) New York

Barciszewski J, Jurczack J, Porowski S, Specht T, Erdmann A (1999) The role of water structure in conformational changes of nucleic acids in ambient and high pressure conditions. Eur J Biochem 260: 293 – 307

Berg H (1993) Reaction of lactose during heat treatment of milk: A quantitative study. Ph.D. Thesis, Agricultural University, Wageningen, Holand

Berlitz, H., Grosch, W., (1992) Lehrbuch der Lebensmittelchemie, 4. Aufgabe, Srpinger-Verlag, Berlin, Heidelberg

Berry G, Creamer L (1975) The association of bovine ß-casein. The importance of the C-terminal region. Biochem 14:3542-3545

Beychok S (1965) Side-chain optical activity in cystine-containing proteins: Circular dichroism studies. Biochem 53: 999-1005

Bisswanger H (2002) Enzyme Kinetics. WILEY-VCH, Inc. Weinheim

Böhm A (2003) Untersuchungen zur Proteolyse von Para-κ-Casein: Von Modell zum Käse. Dissertation, Technische Universität Dresden, Germany

Brandt A, Erbersdobler, H (1972) Zur Bestimmung von Furosin in Nahrungs- und Futtermitteln. Landwirtschaftliche Forschung, Sonderheft, 28/II: 115-119 cited by Krause R

(2005) Untersuchungen zur Bildung von Furosin und N-terminalen 2(1H)-Pyrazinonen. Dissertation, Technische Universität Dresden, Germany
Case A, Stein R (2003) Kinetic analysis of the action of tissue transglutaminase on peptide and protein substrate. Biochemistry 42:9466-9481

Cheftel J, Cuq J, Lorieut D (1992). Lebensmittelproteine: Biochemie – Funktionelle Eigenschaften – Ernährungsphysiologie – Chemische Modifizierung. B. Behr´s Verlag, Hamburg, pp 193-229

Chen S, Wu J, Wu C (1987) The preparation of concentrated passion fruit juice by the methods of flavour recovery and enzyme treatment. J Chinese Agric Chem Soc 25: 177-187

Chen, Yang J, Chau K (1974) Determination of the helix and ß form of proteins in aqueous solution by circular dichroism. Biochemistry 13: 3350-3359

Chica R, Gagnon P, Keillor J, Pelletier J (2003) Tissue transglutaminase acylation: Proposed role of conserved active site Tyr and Trp residues revealed by molecular modelling of peptide substrate binding. Protein Sci 13: 979-991

Christensen B, Sørensen E, Højrup P, Petersen T, Rasmussen, L (1996) Localization of potential transglutaminase cross-linking sites in bovine caseins. J Agric Food Chem 44: 1943-1947.

Chung S, Shrager R, Folk J (1970) Mechanism of action of guinea pig liver transglutaminase. VII Chemical and stereochemical aspects of substrate binding and catalysis. J Biol Chem 245:6424-6435

Copeland R (1996) Enzymes. Wiley-VCH, Inc. New York

Corredig M, Kerr W, Wicker L (2001) Particle size distribution of orange juice cloud after addition of sensitized pectin. J Agric Food Chem 49: 2523-2526

Coussons P, Price N, Kelly S, Smith B, Sawyer L (1992) Factors that govern the specificity of transglutaminase catalysed modification of proteins and peptides. Biochem J 282:929-930

Crelier S, Robert M , Claude J, Juillerat M (2001) Tomato (*Lycopersicon esculentum*) pectin methylesterase and polygalacturonase behaviors regarding heat- and pressure-induced inactivation. J Agric Food Chem 49: 5566-5575

Dalgleish D (1997) Structure-function relationships of caseins. In: Srinivasan Damodaran, Alain Paraf (eds) Food protein and their applications. Marcel Dekker, New York, pp 199-223

Datta N, Deeth H (1999) High pressure processing of milk and dairy products. Aust J Dairy Technol 54: 41-48

Della Mea M, Caparrós-Ruiz D, Claparols I, Serafini-Fracassini D, Rigau J (2004) AtPng1p. The first plant transglutaminase. Plant Physiol 135: 2046-2054

Del Duca S, Dondini L, Della Mea M, Munoz de Rueda P, Serafini Fracassi D (2000) Factors affection transglutaminase activity catalysing polyamine conjugation to endogenous substrates in the entire chloroplast. Plant Phys Biochem 38:429-439

Doster W, Gebhardt (2003) High pressure – unfolding of myoglobin studied by dynamic neutron scattering. Chem Phys 292:383-387

Dubey V, Jagannadham M (2003) Differences in the unfolding of procerain induced by pH, guanidine hydrochloride urea and temperature. Biochemistry 42:12287-12297

Earnshaw R (1996) High pressure food processing. Nutri Food Sci 2: 8 –11

Farnsworth G, Hendricks G, Gotcheva V, Akuzawa R, Guo M (2002) Effects of enzymatic cross-linking on the consistency and structure of probiotic goat milk yoghurt. J Dairy Sci 85 (Suppl. 1.):120

FDA (2002) GRAS Notice No. GRN 000095. Office of Food Additive Safety, Center for Food Safety and Applied Nutrition

Fink M, Chung S, Folk J (1980) Gamma-Glutamylamine cyclotransferase: Specifity toward ε-(L-γ -glutamyl)-L-Lysine and related compounds. Proc Natl Acad Sci USA 77:4564-4568

Folk J, Cole P (1965) Structural requirements of specific substrates for guinea pig liver transglutaminase. J Biol Chem 240:2951-2959

Folk J, Cole P (1966) Mechanism of action of guinea pig liver transglutaminase. I Purification and properties of the enzyme: Identification of a functional cysteine essential for activity. J Biol Chem 241:5518-5525

Folk J (1969) Mechanism of action of guinea pig liver transglutaminase. VI Order of substrate addition. J Biol Chem 244:3707-3713

Frye K, Royer C (1998) Probing the contribution of internal cavities to the volume change of protein unfolding under high pressure. Protein Sci 7: 2217-2222

Ghoshal A, Swaminathan C, Thomas C, Surolia A, Varadarajan R (1999) Thermodynamic and kinetic analysis of the *Escherichia coli* thioredoxin-C´ fragment complementation system. Biochem J 339: 721-727

Gorovits B, Raman C, Horowitz P (1994) High hydrostatic pressure induces the dissociation of cpn60 tetradecamers and revels a plasticity of the monomers. J Biol Chem 270: 2061-2066

Gorman J, Folk J (1980) Structural features of glutamine substrates for human plasma factor XIIIa (Activated blood coagulation factor XIII). J Biol Chem 255:419-424

Grandhee S, Monnier V (1991) Mechanism of formation or the Maillard protein cross-link pentosidine. Glucose, fructose, and ascorbate as pentosidine precursors. J Biol Chem 266:11649-11653

Gratzer W, Holzwarth G, Doty P (1961) Polarization of the ultraviolet absorption bands in α-helical polypeptides. Proc Natl Acad Sci USA 47: 1785-1791

Greenfield N, Fasman G (1969) Computed circular dichroism spectra for the evaluation of protein conformation. Biochemistry 8:4108-4116

Griffin M, Casadio R, Bergamini C (2002) Transglutaminase, Nature´s biological glues. Biochem J 368:377-396

Hamon V, Dallet S, Legoy M (1996) The pressure dependence of two ß-glucosidases with respect to their thermostability. Biochim Biophys Acta 1294:195-203

Harte F, Leudecke B, Swanson B, Barbosa-Cánovas G (2003) Low-fat set yoghurt made from milk subjected to combination of high hydrostatic pressure and thermal processing. J Dairy Sci 86:1074-1082

Hernández A, Cano M (1998) High-pressure and temperature effects on enzyme inactivation in tomato puree. J Agric Food Chem. 46:266-270

Hazová B, Jančovičová J, Dodok L, Buchtová V, Staruch L (2002) Use of transglutaminase for improvement of pastry produced by frozen-dough technology. Czech J Food Sci 20:215-222

Hawley S (1971) Reversible pressure-temperature denaturation of chymotrypsinogen. Biochemistry 10:2436-2442

Henle T, Walter I, Krause H, Klostermeyer H (1991) Efficient determination of individual Maillard compounds in heat-treated milk products by amino acid analysis. Int Dairy J 1:125-135

Henle T, Schwarzenbolz U, Klostermeyer H (1997) Detection and quantification of pentosidine in foods. Z Lebensm Unters Forsch 204:95-98

Hernández A, Cano M (1998) High pressure and temperature effects on enzymes inactivation in tomato puree. J Agric Food Chem 46:266-270

Hill V, Ledward D, Ames J (1996) Influence of high hydrostatic pressure and pH on the rate of Maillard browning in a glucose-lysine System. J Agric Food Chem 44: 594-598

Hinrichs, J (2000) Ultrahochdruckbehandlung von Lebensmitteln mit Schwerpunkt Milch und Milchprodukte- Phänomene, Kinetik und Methodik. VDI Berlag, Düsseldorf

Hodge J (1953) Dehydrated Foods. Chemistry reactions in model systems. J Agric Food Chem 1:928-943

Hohendadl C, Mann K, Mayer U, Timpl R, Paulson M, Aeschlimann D (1995) Two adjacent N-terminal glutamines of BM-40 (osteonectin, SPARC) act as amine acceptor sides in transglutaminase$_c$-catalyzed modification. J Biol Chem. 270: 23415-23420

Hultsch C, Bergmann R, Pawelke B, Pietzsch J, Wuest F, Johannsen B, Henle T (2004) Biodistribution and catabolism of 18F-labelled isopeptide N^{ε}-(γ-glutamyl)-L-lysine. Amino Acids 29:405-413

Horne D (1998) Casein interactions: casting light on black boxed, The structure in dairy products. Int Dairy J 8:171-177

Iametti S, Donnizzelli E, Vecchio G, Rovere P, Gola S, Bonomi F (1998) Macroscopic and structural consequences of high pressure treatment of ovalbumin solutions. J Agric Food Chem 46:3521-3527

Indrawati, Van Loey A, Ludikhuyze L, Hendrickx M (2000) Kinetics of pressure inactivation at subzero and elevated temperature of lipoxygenase in crude green (*Phaseolus vulgaris* L) extract. Biotechnol Prog 16:109-115

Ikeuchi Y, Nakagawa N, Endo T, Suzuki A, Hayashi T, Ito T (2001) Pressure induced denaturation of monomer ß-lactoglobulin is partially irreversible: comparison of monomer form (high acid pH) with dimmer form (neutral pH). J Agric Food Chem. 49: 4052-4059

Isaacs N, Coulson M (1996) Effect of pressure on processed modelling the Maillard reaction. J Phys Org Chem 9:639-644

Jaenicke, R (1983) Biochemical Process under high hydrostatic pressure. Naturwissenschaften 70:332-341

Johnson W (1999) Analyzing protein circular dichroism spectra for accurate secondary structures. Proteins Struct Funct Genet 35:307-312

Jovin T, Dante M, Chrambach A (1970) Multiphasic buffer system output. Natl Techn Inf Serv. Sprinfield VA USA PB 196 085-196 091 cited by Westermeir R, Fichmann J, Gronua S, Schikle H, Theßeling G, Weisner P (1997) Electrophoresis in practice (2 ed) VCH GmbH, Weinheim

Kalamaki M, Harpster M, Palys J, Labavitch J, Reid D, Brummell D (2003) Simultaneous transgenic suppression of LePG and LeExp1 Influences rheological properties of juice and concentrates from a processing tomato variety. J Agric Food Chem 51:7456-7464

Kalchayanand N, Sikes A, Dunne C, Ray B (1998) Factors influencing death and injury of food-borne pathogens by hydrostatic pressure-pasteurization. Food Microbiol 15:207-214

Kanaji T, Ozaki H, Takao T, Kawajiri H, Ide H, Motoki M, Shimonishi Y (1993) Primary structure of microbial transglutaminase from *Streptoverticillium* sp. Strain s-8112. J Biol Chem 668:11565–11572

Kashiwagi T, Yokoyama K, Ishikawa K, Ono K, Ejima, D, Matsui H, Suzuki E (2002) Crystal structure of microbial transglutaminase from *Streptoverticillium mobaraense*. J Biol Chem 277:44252-44260

Kato M, Sato Y, Shirai K, Hayashi R, Balny C, Lange R (2003) The propeptide in the precursor form of carboxypeptidase Y ensures cooperative unfolding and the carbohydrate moiety exerts a protective effect against heat and pressure. Eur J Biochem 270: 4587 – 4593

Kauzmann W, Bodanszky A, Rasper J (1961) Volume changes in protein reactions II. Comparison of ionisation reactions in proteins and small molecules. J Am Chem Soc 84: 1777-1788

Keenan R, Young D, Tier C, Jones A, Underdown J (2001) Mechanism of pressure-induced gelation of milk. J Agric Food Chem 49:3394-3402

Kitchen D, Reed L, Levy R (1992) Molecular dynamics simulation of solvated protein at high pressure. Biochemistry 31:10083-10093

Klotz I (1986) Introduction to Biomolecular Energetics. Academic Press, London

Konrad G, Lieske B (1997) Neues Verfahren zur technischen Isolierung von nativen ß-lactoglobulin aus Molke durch enzymattische Hydrolyse und Ultrafiltration Dtsch Milchwirtsch 48:13: 479-482

Krause R (2005) Untersuchungen zur Bildung von Furosin und N-terminalen 2(1H)-Pyrazinonen. Dissertation, Technische Universität Dresden, Germany

Krzikalla K, Pfister M, Dehne L, Heinz V, Knorr D, Mörsel J-T, Reupert D (2005) A new application of high pressure processing for preservation of fresh salami-style sausage. Euro

Food Chem XIII and Deutscher Lebensmitteltag 19 - 21 September 2005, Hamburg, Germany

Kumosinski T, Brown E, Farrell H (1993) Three-dimensional Molecular modeling of bovine caseins: An energy-minimized ß-casein structure. J Dairy Sci 76:931-945

Kumosinski T, Brown E, Farrell H (1991) Three-dimensional Molecular modeling of bovine caseins: α_{s1}-casein. J Dairy Sci 74:2889-2895

Lane L (1978) A simple method for stabilizing protein–sulfhydryl groups during SDS-gel electrophoresis. Anal Biochem 86**:**655-664

Lauber S, Henle T, Klostermeyer, H. (2000) Relationship between the crosslinking of caseins by transglutaminase and the gel strength of yogurt. Eur Food Res Technol 210:305-309.

Lauber S, Noack I, Klostermeyer H, Henle T (2001) Stability of microbial transglutaminase to high pressure treatment. Eur Food Res Technol 213:273-276

Lauber S, Krause I, Klostermeyer H, Henle T (2002) Microbial transglutaminase crosslinks ß-casein and ß-lactoglobulin to heterologous oligomers under high pressure. Eur Food Res Technol 216: 15-17

Law A, Leaver J, Felipe X, Ferragut V, Reyes P, Guamis B (1998) Comparison of the effects of high pressure and thermal treatments on the casein micelles in goat´s milk. J Agric Food Chem 46: 2523-2530.

Lee E, Park J (2002) Pressure inactivation kinetics of microbial transglutaminase form Streptoverticillium mobaraense. J Food Sc 67:103-107

Leblanc A, Gravel C, Labelle J, Keillor J (2001) Kinetic studies of guinea pig liver transglutaminase reveal a general-base-catalyzed deacylation mechanism. Biochemistry 40:8335-8342

Li T, Hook J, Drickamer H, Weber G () Plurality of Pressure-Denatured Forms in Chymotrypsinog and Lysozyme. Biochemistry 15:5571-5580

Lorenzen P, Neve H, Mautner A Schlimme E (2002) Effect of enzymatic cross-linking of milk proteins on functional properties of set-style yogurt International. Int J Dairy Technol

Ludescher R, (1996). Physical and chemical properties of amino acids and proteins. In: Shuryo Nakai, H Wayner Modler (eds) Food proteins: Properties and characterization. Wiley-VCH Publisher, New York, pp 23-70

Ly-Nguyen B, Van Loey A, Fachin D, Verlent I, Duvetter T, Son T, Smout C, Hendrickx M (2002a) Strawberry pectin methylesterase (PME): Purification, characterization, thermal and high pressure inactivation. Biotechnol Prog 18:1447-1450

Ly-Nguyen B, Van Loey A, Fachin D, Verlent I, Indrawati, Hendrickx M (2002b) Partial purification, and high pressure inactivation of pectin methylesterase from carrots (*Daucus carrota* L.). J Agric Chem 50:5437-5444.

Ly-Nguyen B, Van Loey A, Smout C, Verlent I, Duvetter T, Hendrickx M (2003) Effect on mild-heat and high pressure processing on banana pectin methylesterase: a kinetic study. J Agric Food Chem 51:7954-7979

Manavalan P, Johnson W (1987) Variable selection method improves the prediction of protein secondary structure from circular dichroism spectra. Anal Biochem 167: 76-85

McKenzie H (1970) Whole casein: Isolation, properties, and zone electrophoresis. In: Hugh A McKenzie (ed) Milk proteins, Academic Press, New York, pp 87-116

Mezger T, Neuber S (1992) Untersuchung des Fleiß- und Deformationsverhaltens an Lebensmitteln. ZFL 43:170-177

Mora-Gutierrez A, Farrell H, Kumosinski H (1993) Comparison of calcium-induced associations of bovine and caprine caseins and the relationship of α_{s1}-casein content to colloid stabilisation: A thermodynamic linkage analysis. J Dairy Sci 76:3690-3697

Moffitt W (1956) The optical rotatory disperion of simple polypeptides II. Proc Natl Acad Sci USA 42:736-746.

Moreno F, Molina E, Olano A, López-Fandiño R (2003) High-pressure effects on Maillard reaction between glucose and lysine. J Agric Food Chem 51:394-400

Motoki M, Okiyama A, Nonoka M, Tanaka H, Uchi R, Mastura A, anodo H, Umeda K (1989) Manufacture of molded meat using transglutaminase. Jap Kokai Tokkyo Doho JP 0279956 cited by Zhu Y, Rinzema A, Tramper J, Bol J (1995) Microbial transglutaminase-a review of its production and application in food processing 44:277-282

Mozhaev V, Heremans K, Frank J, Masson P. Balny C (1996) High pressure effects on protein structure and function. Proteins Struct Funct Genet 24:81-91

Møller R, Stapelfeldt H, Skibsted L (1998) Thiol reactivity in pressure-unfolded ß-lactoglobulin. Antioxidative properties and thermal refolding. J Agric Food Chem 46: 425-430

Mulkerrin M (1996) Protein structure analysis using circular dichroism. In: Henry A Havel (ed) Spectroscopic Methods for Determining Protein Structure in Solution. VCH Publishers, New York, pp 5–27

Ngapo T, Wilkinson B, Chong R (1996) 1,5-Glucono-δ-lactone-induced gelation of myofibrillar protein at chilled temperatures. Meat Sci 42:3-13

Nanoka M, Ito R, Motoki M, Nio N (1997) Modification of several proteins by using Ca^{2+}-independent microbial transglutaminase with high pressure treatment. Food Hydrocolloid 11:351-353

Neuman T., Kauzmann W., Zipp A (1973) Pressure dependence of weak acid ionisation in aqueous buffers. J Phys Chem 77: 2687-2691

Nguyen H, Hall C (2004) Phase diagrams describing fibrillization by polyalanine peptides. Biophys J 87:4122-4134

Noguchi K, Ishikawa K, Yokoyama K, Ohtsuka T, Nio N, Suzuki E (2001) Crystal structure of red sea bream transglutaminase. J Biol Chem 276:12055-12059

Nosoh Y, Sekiguchi T (1991) Protein stability and stabilization through Protein Engineering. Ellis Harwood, New York

Oakenfull D, Pearce J, Burley R (1997) Protein gelation. In: Srinivasan Damodaran, Alain Paraf (eds). Food Proteins and their Applications, Marcel Dekker, New York, pp 111-142

Oh S, Catignani G, Swaisgood H (1993) Characteristics of an immobilized form of transglutaminase: A possible increase in substrate specificity by selective interaction with a protein spacer. J Agric Food Chem 41:1337-1342

Olivares S (1990) Paquetes de diseños experimentales FAUANL Versión 2. Facultad de Agronomía, Universidad Autónoma de Nuevo León, Mexico

Paladini A, Weber G (1981) Pressure-induced reversible dissociation of enolase. Biochemistry 20:2587-2592

Patel A, Chaffotte A, Goubard F, Pauthe E (2004) Urea-induced sequential unfolding of fibronectin: a fluorescence spectroscopy and circular dichroism study. Biochem 43: 1724-1735

Partschefeld C (2004) Untersuchungen zu Reaktionsorten enzymatischer Quervernetzung unter hohem hydrostatischen Druck. Thesis, Lebensmittelchemie, Technische Universität Dresden, Germany

Partschefeld (2005) Personal communication. Lebensmittelchemie, Technische Universität Dresden, Germany

Partschefeld C, Döhler A (2005) Personal communication. Lebensmittelchemie, Technische Universität Dresden, Germany

Pauling L, Corey R (1951) The pleated sheet, a new layer configuration of polypeptide chains. Proc Natl Acad Sci USA 37: 251-256

Privalov P, Makhatadze G (1992) Contribution of hydration and noncovalent interactions to the heat capacity effect on protein unfolding. J Mol Biol 224:715-723

Provencher S, Gloeckner J (1981) Estimation of globular protein secondary structure from circular dichroism. Biochemistry 20: 33-37

Quadrifoglio F, Urry D (1968) Ultraviolet rotatory properties of polypeptides in solution. II. Poly-L-serine. J Am Chem Soc 90:2760-2765

Raczyński G, Snochowski M, Buraczewski S (1976) Metabolism of ε-(γ-L-glutamyl)-L-lysine in the rat. Br J Nutr 34:291-296

Ramírez J, Santos I, Morales O, Morrissey M, Vázquez M (2000) Application of microbial transglutaminase to improve mechanical properties of surimi from Silver carp. Cienc y Tecnol Aliment 3:21-28

Rasper J, Kauzmann W (1961) Volume changes in protein reactions I. Ionization reaction of proteins. J Am Chem Soc 84: 1771-1777

Redemacher B (1999) Hochdruckbehandlung von Milch. Untersuchung zur Inaktivierung von Mikroorganismen und Enzymen und deren kinetische Beschreibung, Technische Universität München, Germany

Richardson T, Sangsuk O, Jimenez-Flores R (1992) Molecular modelling and genetic engineering of milk proteins. In: P F Fox (ed) Advanced dairy chemistry-1: Proteins. Elsevier Applied Science, London, pp 545-577

Richter S (2004) Reaktionsorte enzymatischer Protienquervernetzung unter Normal- und Hochdruck. Thesis, Lebensmittelchemie, Technische Universität Dresden, Germany

Rodriguez-Nogales J (2005) Enzymatic cross-linking of ewe's milk proteins by transglutaminase. Eur Food Res Technol 00:1-8

Rollema H (1992) Casein association and micelle formation. In: P F Fox (ed). Advanced Dairy chemistry-1: Proteins. Elsevier Applied Science, London, pp 111-135

Rosenheck K, Doty P (1961) The far ultraviolet absorption spectra of polypeptide and protein solutions and their dependence on conformation. Proc Natl Acad Sci USA 47: 1775-1785

Ross-Murphy S (1994) Rheological methods. In: Simon B. Ross-Murphy (ed). Physical techniques for the study of food biopolymers. Blackie Academic and Professional, London, pp 343-392

Rugerio M (2005) Thermodynamic and kinetic investigations on the inactivation of microbial transglutaminase by temperature and pressure. Effect and preliminary studies of its inhibitors. Thesis, División de Ingeniería y Arquitectura, Instituto Tecnológico y de Estudios Superiores de Monterrey, Mexico.

Samarasinghe S, Campbell D, Jonas A, Jonas J (1992) High-resolution NMR study of the pressure-induced unfolding of lysozyme. Biochem 31: 7773-7778

Sakamoto H, Motoki M, Soeda T, Anodo H, Umeda K, Matsura A (1992) Stabilizer composition for transglutaminase. Jpn Kokai Kokkyo Koho JP 0427194 cited by Zhu Y, Rinzema A, Tramper J, Bol J (1995) Microbial transglutaminase-a review of its production and application in food processing. Appl Microbiol Biotechnol 44:277-282

Sarkar P, Doty P (1966) The optical rotatory properties of the ß-configuration in polypeptides and proteins. Proc Natl Acad Sci USA 55: 981-989

Schlimme E, Buchheim W (1995) Milch und ihre Inhaltsstoffe. Institut für Chemie und Physik. Verlag Th Mann, Gelsenkirchen

Schorsch C, Carie H, Clark A, Norton I. (2000a) Cross-linking casein micelles by microbial transglutaminase conditions for formation of transglutaminase-induced gels. Int Dairy J 10:519-528

Schorsch C, Carie H, Clark A, Norton I. (2000b) Cross-linking casein micelles by microbial transglutaminase: influence of cross-links in acid induced gelation. Int Dairy J 10:529-539

Schulz G, Schirmer R (1979) Principles of protein structure. Springer-Verlag, New York

Schwarzenbolz U (2000) Untersuchungen zu nichtenzymatischen Glydosylierungs- und Quervernetzungsreaktionen von Milchproteinen. Dissertation, Technische Universität München, Germany

Schwarzenbolz U, Klostermeyer H, Henle T (2002) Maillard reaction under high hydrostatic pressure: studies on the formation of protein-bound amino acid derivatives. In: Horiuchi S, Taniguchi N, Hayase F, Kurata T, Osawa T (eds) The Maillard reaction in food chemistry and medical science: Update for the postgenomic era, 7th International Symposium on the Maillard Reaction. Elsevier Science ,Amsterdam, 1245:223-227.

Seguro k; Kumazawa Y, Kuraishi C, Sakamoto H, Motoki M (1996) The ε-(-γ-glutamyl) lysine moiety in crosslinked casein in an avaible source of lysine for rats. J Nutr 126:2557-2562

Sell D, Monnier V (1989) Structure elucidation of a senescence cross-link from human extracellular matrix. J Biol Chem 264:21597-21602

Shouqin Z, Jun S, Changzheng W (2005) High hydrostatic pressure extraction of flavonoids from propolis. J Chem Technol Biotechnol 80:50-54

Silva J, Miles E, Weber G (1986) Pressure dissociation and conformational drift of the beta dimmer of tryptophan syntase. Biochemistry 25:5780-5786

Sood S, Slatterry C (1997) Monomer characterization and studies of self-association of the major ß-casein of human milk. J Dairy Sci 80:1554-1560

Smith J, Van Ness H, Abboh M (1997) Introducción a la termodinámica en ingeniería química. (5 ed) McGraw-Hill, México D.F.

Springer K (2004) Nichtenzymatische Quervernetzung von Milchproteinen unter Hochdruck. Thesis, Lebensmittelchemie, Technische Universität Dresden, Germany

Sreerama N, Woody R (1993) A self-consistent method for the analysis of protein secondary structure from circular dichroism. Anal Biochem 209: 32-44

Sreerama N, Woody R (1994) Protein secondary structure from circular dichroism spectroscopy. Combining variable selection principle and cluster analysis with neutral network, ridge regression and self-consistent methods. J Mol Biol 242:497-507

Sreerama N, Woody R (2000) Estimation of protein secondary structure from circular dichroism spectra: Comparison of CONTIN, SELCON, and CDSSTR methods with an expanded reference set. Anal Biochem 287:252-260.

Stevenson E, Law A, Leaver J (1996) Heat-induced aggregation of whey proteins is enhanced by addition of thiolated ß-casein. J Agric Food Chem 44: 2825-2828

Stippl V, Delgado A, Becker T (2005) Ionization equilibria at high pressure. Eur Food Res Technol 221:151-156

Suck T (1992) The significance of viscoelasticity in foodstuff rheology. Rheology 92: 182-186

Sun D, Grant T, Dure L, Wicker L (1998) Secondary structure and stability of marsh grapefruit thermolabile pectinesterase. J Agric Food Chem 46: 3480-3483

Suzuki A (2003) Current development of high pressure processed foods in Japan. Institute of Food Technologist. Annual Meeting, 12 -16July 2003, Chicago, USA

Swaisgood H (1992) Chemistry of caseins. In: P F Fox (ed) Advanced Dairy Chemistry-1: Proteins. Elsevier Applied Science, London, pp 63-107

Tanaka N, Mitani D, Kunigi S (2001) Pressure-induced perturbation on the active site of ß-amylase monitored from the sulfhydryl reaction. Biochemistry 40: 5914-5920

Tamaoka T, Itoh N, Hayashi R (1991) Agric Biol Chem 55:2071-2074 cited in Moreno F, Molina E, Olano A, López-Fandiño R (2003) High-pressure effects on Maillard reaction between glucose and lysine. J Agric Food Chem 51:394-400

Tate S, Meister A (1985) γ-glutamyl transpeptidase from kidney. Methods Enzymol 113:400-419

Tauscher B (1995) Review: Pasteurization of food by hydrostatic high pressure: chemical aspects. Z Lebensm Unters Forsch 200:3-13

Téllez-Luis, González-Cabriales, Ranírez J, Vázquez M (2004) Production of transglutaminase by *Streptoverticillium ladakanum* NRRL-3191 grown on media made from hydrolysates of sorghum straw. Food Technol Biotechnol 42: 1-4

Tewari, G., Jayas, D, Holley R (1999) High pressure processing of foods: an overview. Sci Aliment 19: 619-661

Thompson M (1970) α_s- and ß-caseins. In: Hugh A McKenzie (ed) Milk proteins, Academic Press, New York pp 117-169

Totosaus A, Gault N, Guerrero I (2000) Dynamic rheological behaviour of meat proteins during acid induced gelation. Int J food Sci Tech 3:465-472

Touch V, Hayakawa S, Fukada K, Aratani Y, Sun Y (2003) Preparation of Antimicrobial Reduced Lysozyme Compatible in Food Applications. J. Agric. Food Chem 51: 5154-5161

Traoré F, Meunier J (1991) Cross-linking of caseins by human placental factor XIIIa. J Agric Food Chem 39:1892-1896

Uresti R, Velazquez G, Ramírez J, Vázquez M, Torres J (2005) Effect of combining microbial transglutaminase treatments and high pressure processing on the mechanical properties of restructured products from arrowtooth flounder. Institute of Food Technologist. Annual Meeting, 15 - 20 July 2005, New Orleans, USA

Urzica A (2004) High hydrostatic pressure inactivation of Bacillus *subtilis var. niger.* spores: the influence of the pressure build-up rate on the inactivation. Dissertation. Ruprecht-Karls-Universität, Heidelberg, Germany

Van den Broeck I, Ludikhyze L, Weemaes C, Van Loey A, Hendrickx M (1999) Thermal inactivation kinetics of pectinesterase extracted from oranges. J Food Proc Press. 23: 391-406

Van Loey A, Ooms V, Weemaes C, Van den Broeck I, Indrawati S, Hendrickx M (1998) Thermal and pressure-temperature degradation of chlorophyll in broccoli (*Brassica oleracea* L. *italica*) juice: A kinetic study. J Agric Food Chem 46:5289-5294

Venere A, Rossi A, Matteis F, Rosato N, Agrò A, Mei G (2000) Opposite effects of Ca^{2+} and GTP binding on tissue transglutaminase tertiary structure. J Biol Chem 275:3915-3921

Videa M (2005) Personal communication. División de Ingeniería y Arquitectura, Insituto Tecnológico y de Estudios Superiores de Monterrey, Mexico.

Walstra P, Geurts T, Noomen A, Jellema A, Van Boekel M (1999) Dairy Technology: Principles of Milk Properties and Process, Marcel Dekker, New York

Weemaes C, Ludikhuyze L, Van den Broeck I, Hendrickx M (1998) High pressure inactivation of polyphenoloxidases. J Food Sci 63: 873-877

Weber Gregorio (1993) Thermodynamics of the association and the pressure dissociation of oligomeric proteins. J Phys Chem 97:7108-7115

Westermeier R (1997) Electrophoresis in practice (2 ed) Wiley-VCH, Weinheim

Wong D, Camirand W, Pavlath A (1996) Structure and functionalities of milk proteins. Food Sci Nutr 36: 807-844

Zhou J, Zhu L, Balny C (2000) Inactivation of creatine kinase by high pressure may precede dimmer dissociation. Eur J Biochem 267:1247-1253

Zhu Y, Rinzema A, Tramper J, Bol J (1995) Microbial transglutaminase - A review of its production and application in food processing. Appl Microbiol Biotechnol 44:277-282

Zipp A, Kauzmann W (1973) Pressure denaturation of metmyoglobin. Biochemistry 12: 4217 – 4228

Appendix

Data of the chapter 4.1

Figure 8.1-1 Calibration curve of enzyme activity method (Folk and Cole, 1969)

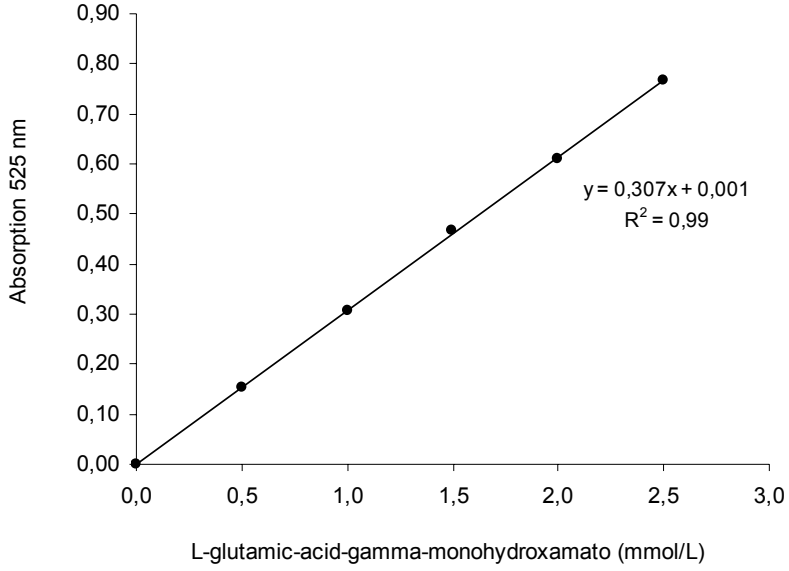

Table 8.1-1 Residual activity of MTG after treatments at different pressure and 40°C

Time (h)	Pressure (MPa)			
	0.1	200	400	600
0.00	1.00	1.00	1.00	1.00
0.25	0.98	0.92	0.91	0.40
0.50	0.89	0.82	0.59	0.34
0.75	0.89	0.76	0,52	0.25
1.00	0.84	0.63	0.45	0.25
1.50	0.70	0.60		
2.00	0.67		0.40	0.12
3.00	0.54	0.41	0.25	0.10
4.50	0.52	0.37		
7.00	0.38			
8.00	0.38	0.41	0.23	
9.00	0.39			
10.00	0.41			
11.00	0.39			
12.00	0.27	0.25		
18.80	0.26			
23.37	0.21			

Values given are the mean of two measurements with the associated 95% confidence interval

Table 8.1-2 Residual activity of MTG after treatments at different pressure and 10°C

Time (h)	Pressure (MPa)			
	0.1	200	400	600
0	1.00	1.00[a]	1.00	1.00
1		0.96[a]		0.93
2				0.54
3	0.98		0.79	0.40
4		1.06[a]		0.38
5			0.67	
12	0.93	1.00[a]	0.61	
16			0.56	
18		0.87[a]		
24	0.89	0,44[a]	0.41	
36		0.54[a]		
40		0.66[a]		
48	0.77	0.54[a]		
54				
72	0.70			
91	0.65			
144	0.58			

Values given are the mean of two measurements with the associated 95% confidence interval
[a] 90% confidence interval.

Figure 8.1-2 Residual activity of MTG after treatments at different pressure and 10°C

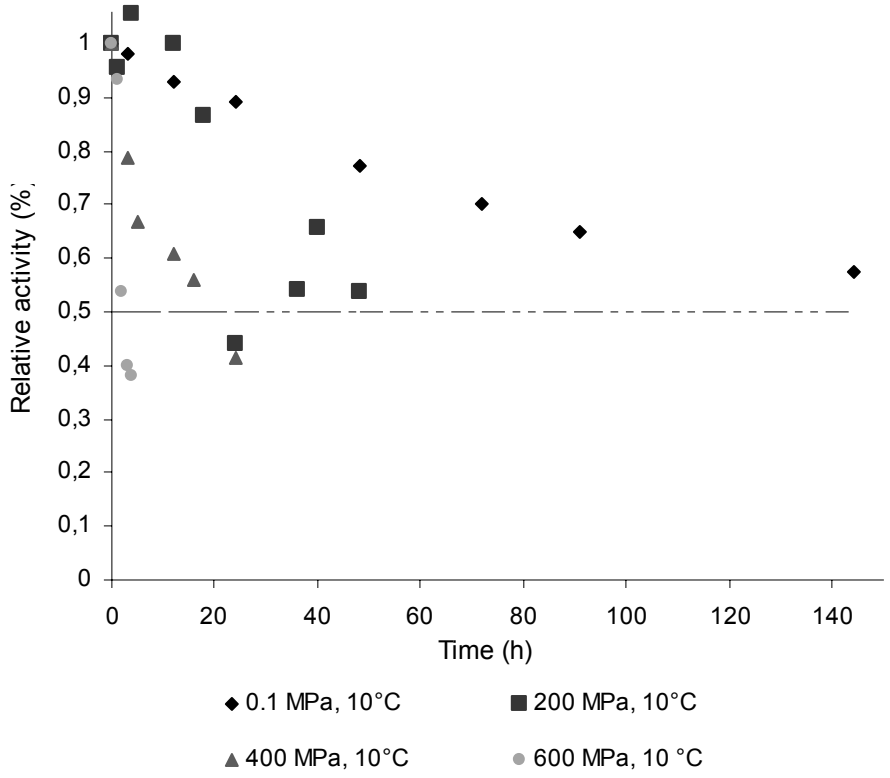

Table 8.1-3 Residual activity of MTG after treatments at different pressure and 30°C

Time (h)	Pressure (MPa)			
	0.1	200	400	600
0.00	1.00	1.00	1.00	1.00
0.17	0.99			
0.25		0.83	0.84	0.82
0.33	0.93			
0.50		0.93	0.82	0.58
0.75	0.90	0.88	0.73	0.51
1.00	0.89	0.83	0.60	0.39
1.50		0.70	0.54	
2.00	0.85	0.69		0.34
3.00			0.47	0.27
4.00	0.81	0.69		
5.00	0.68			
6.00	0.72	0.52		
7.00	0.71			
8.00		0.35		
12.00	0.62			
18.00	0.56			
20.00	0.49			
23.00	0.47			
43.58	0.40			

Values given are the mean of two measurements with the associated 95% confidence interval

Figure 8.1-3 Residual activity of MTG after treatments at different pressure and 30°C

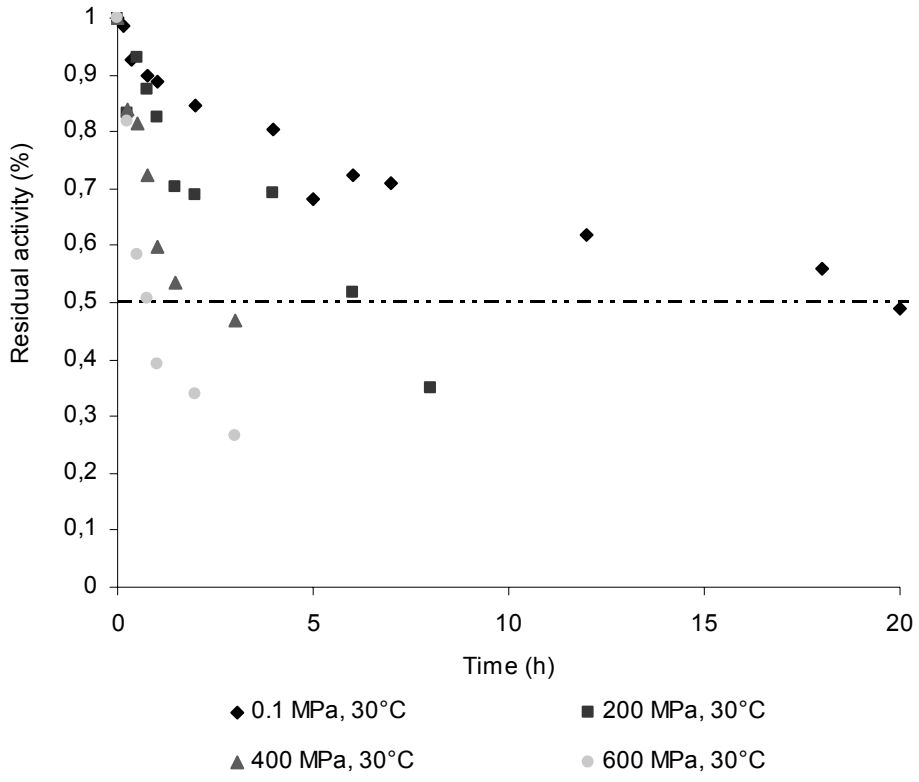

Table 8.1-4 Residual activity of MTG after treatments at different pressure and 50°C

Time (h)	Pressure (MPa)						
	0.1	100	200	300	400	500	600
0.00	1.00	1.00	1.00	1.00	1.00	1.00	1.00
0.05	0.71	0.52	0.59	0.60	0.40	0.37	0.28
0.08	0.57	0.43	0.50	0.58	0.28	0.23	0.23
0.13	0.36	0.33	0.37	0.62	0.24	0.22	0.22
0.15	0.32	0.30	0.36	0.42	0.17	0.13	0.21
0.17	0.36	0.40	0.53		0.43		
0.25	0.28						
0.33	0.27	0.30	0.49	0.33	0.40	0.18	0.15
0.50	0.24	0.27	0.38	0.49	0.31	0.18	0.15
0.75	0.22	0.25	0.28	0.16	0.23	0.05	0.13
1.00	0.22	0.24	0.34	0.15	0.24	0.05	0.16
1.50	0.19	0.22	0.22	0.17	0.19		0.14
2.00	0.19						0.13
3.00	0.18	0.20	0.16	0.10	0.17		
4.00	0.15						
5.00	0.15						
6.00	0.13						

Values given are the mean of two measurements with the associated 95% confidence interval

Figure 8.1-4 Residual activity of MTG after treatments at different pressure and 50°C

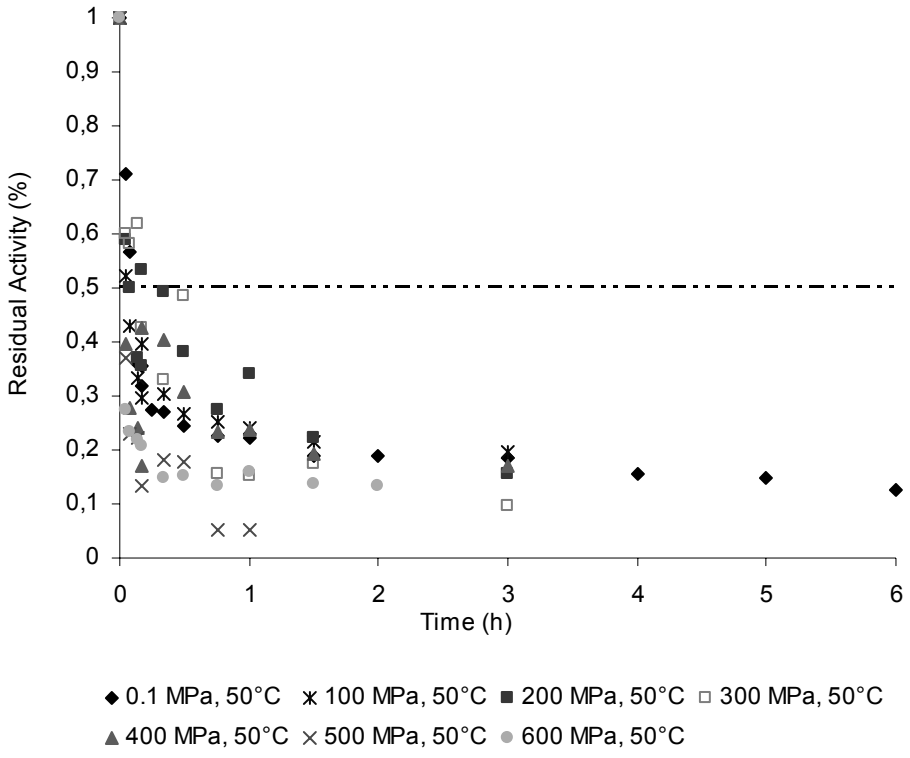

Figure 8.1-5 Kinetic pressure/temperature diagram of MTG

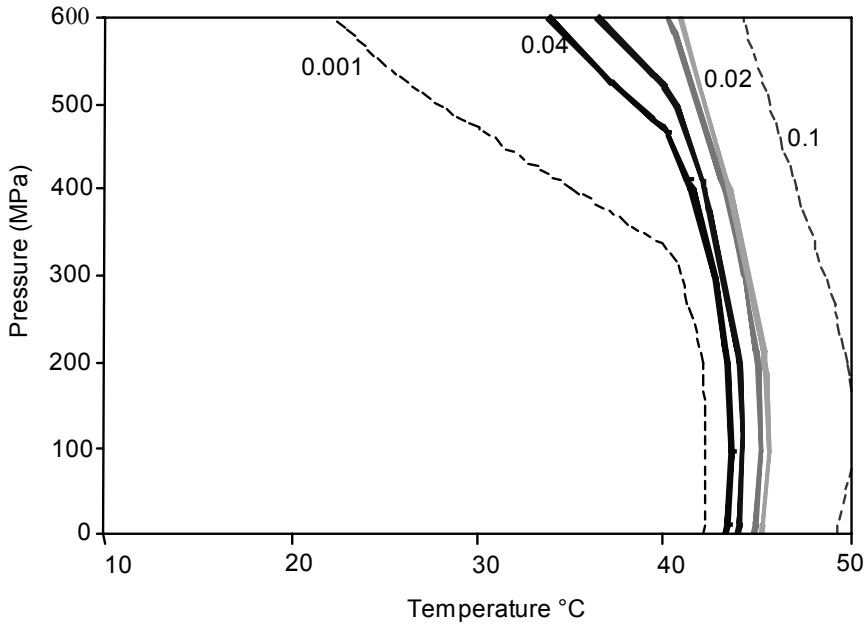

The k_1 values are in the range from 0.001 to 0.1 min^{-1}

Figure 8.1 6 Calculation of apparent temperatures at different pressure, when apparent Gibbs energy is zero at first fast step (a) and second slow step (b).

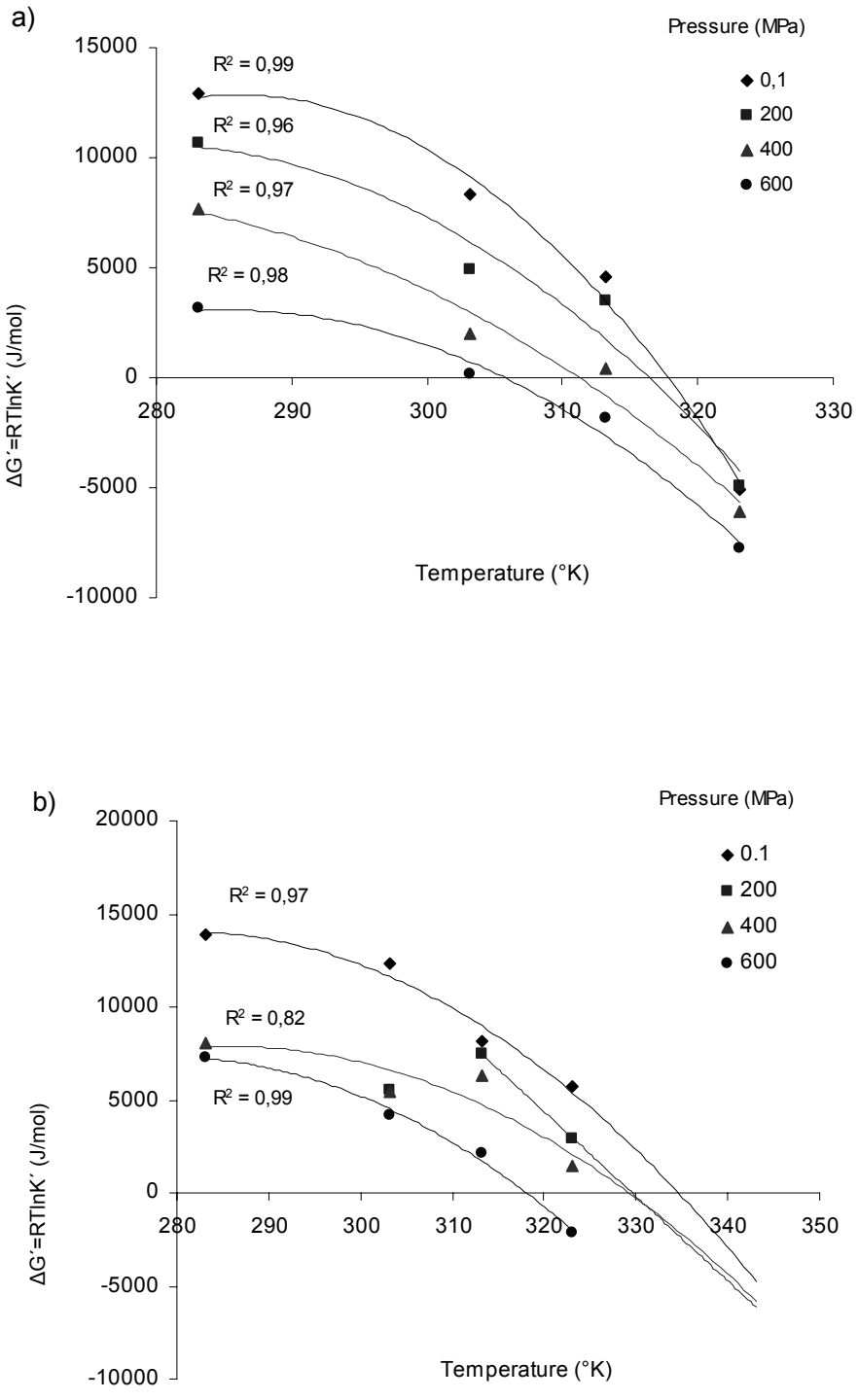

K´ is the apparent equilibrium constant

Data of the chapter 4.2

Figure 8.2-1 Calibration curve of acid casein

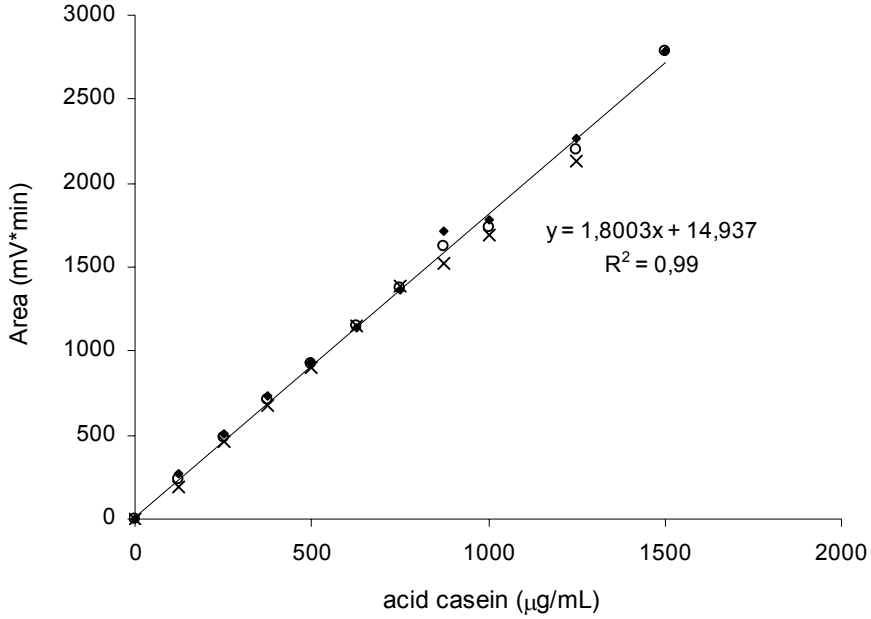

Figure 8.2-2 Calibration curve of ß-casein

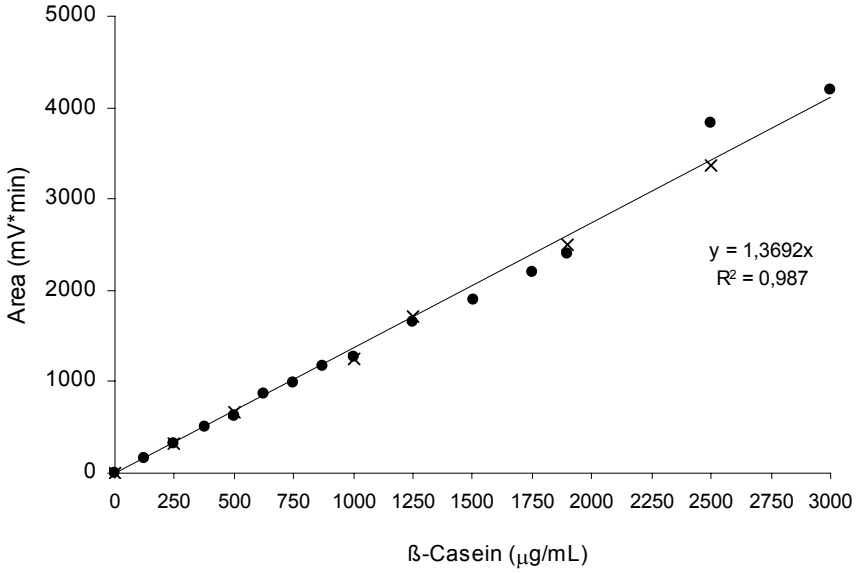

Figure 8.2-3 Calibration curve of α_{s1}-casein

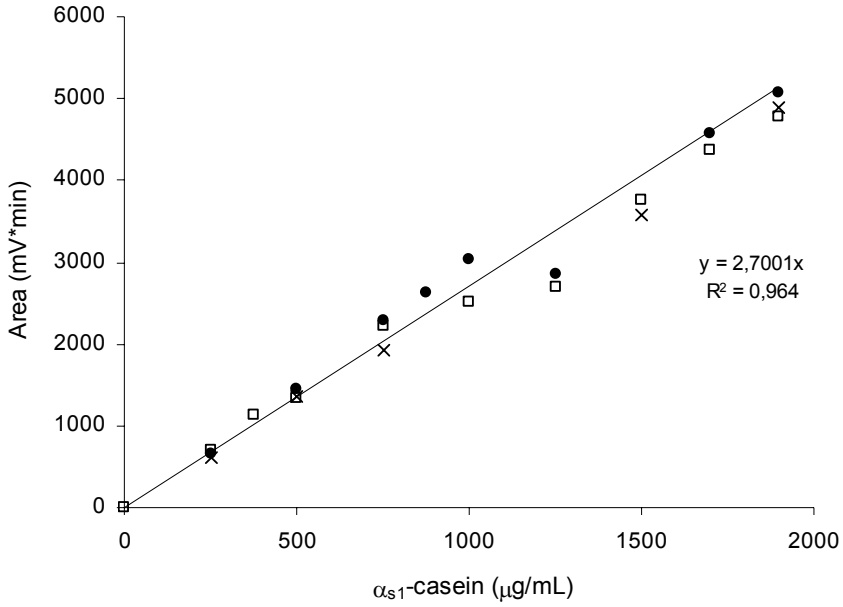

Figure 8.3-4 Hanes Diagram of enzyme kinetic reaction of MTG with ß-casein at 40°C at 0.1 MPa (△) and 400 MPa (▲).

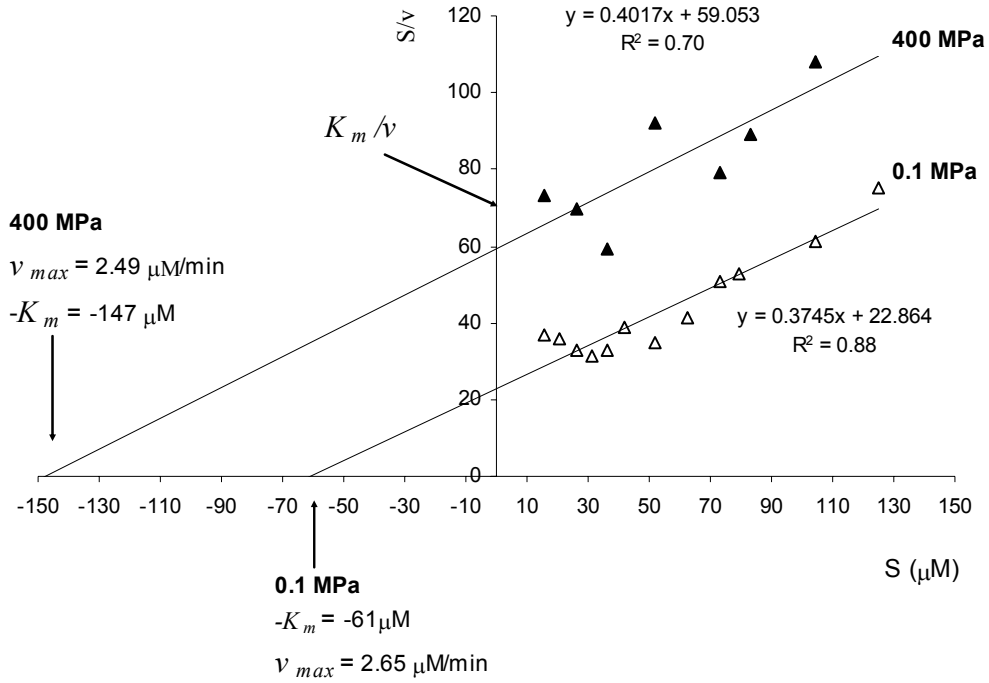

Figure 8.3-5 Hanes Diagram of enzyme kinetic reaction of MTG with α_{s1}-casein at 40°C at 0.1 MPa (○) and 400 MPa (●).

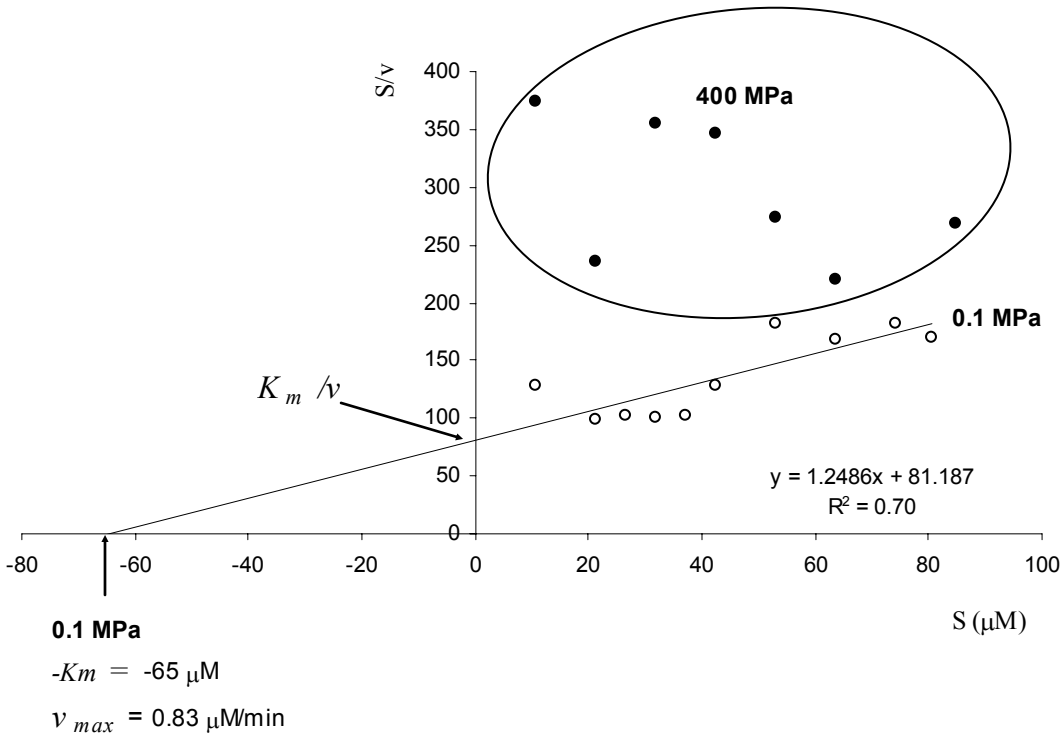

Publications

Papers

Menéndez O., Schwarzenbolz U., Rohm H., Henle T. (2004) Casein gelation under simultaneous action of transglutaminase and glucono-δ-lactone. Nahrung Food 48: 165 – 168

Menéndez O., Rawel H., Schwarzenbolz U., Henle T. (2004) Effect of high hydrostatic pressure on the secondary structure of microbial transglutaminase. Czech. J. Food Sci. 22: 295 - 298

Menéndez O., Rawel H., Schwarzenbolz U., Henle T. (2006) Stability of microbial transglutaminase structure under high pressure treatment. J Agric Food Chem 54:1716-1721

Conference

Menéndez O., Rawel H., Schwarzenbolz U., Henle T. (2005) Strukturelle Veränderung von mikrobieller Transglutaminase unter Hochdruck. 15. Arbeitstagung Regionalverband Süd-Ost Sachsen, Sachen-Anhalt, Thüringen, 17 – 18 März 2005. Jena, Germany

Posters

O. Menéndez, U. Schwarzenbolz, D. Ziems, T. Henle (2003). Casein gelation under simultaneous action of transglutaminase and gluco-δ-lactone. Deutsche Gesellschaft für Milchwissenschaft, 18 – 19 September 2003 Osnabrück, Germany

Menéndez O., Schwarzenbolz U., Ziems A., Henle T. (2003). Influence of covalent cross-linking on storage modulus of acid casein gels obtained by transglutaminase and gluco-δ-lactone. Deutscher Lebensmittelchemikertag, 6 – 11 Oktober 2003 München, Germany

Menéndez O., Rawel H., Schwarzenbolz U., Henle T. (2004) Relation between the enzyme activity and the conformational structure of microbial transglutaminase after high pressure treatment. 33 Deutscher Lebensmittelchemikertag, 13 – 15 September 2004 Bonn, Germany

Menéndez O., Rawel H., Schwarzenbolz U., Henle T. (2004) Effect of high hydrostatic pressure on the secondary structure of microbial transglutaminase. Chemical Reaction in Food V, 29 September – 1o. Oktober 2004 Praga, Czech Republic

Declaration

Erklärung

Hiermit versichere ich, dass ich die vorliegende Arbeit ohne unzulässige Hilfe Dritter und ohne Benutzung anderer als der angegebenen Hilfsmittel angefertigt habe; die aus fremden Quellen direkt oder indirekt übernommenen Gedanken sind als solche kenntlich gemacht. Die Arbeit wurde bisher weder im Inland noch im Ausland in gleicher oder ähnlicher Form einer anderen Prüfungsbehörde vorgelegt.

Die Dissertation wurde an der Technischen Universität Dresden unter der wissenschaftlichen Betreuung von Herrn Prof. Dr. rer. nat. Dr.-Ing. habil. Thomas Henle, Professur für Lebensmittelchemie, angefertigt.

Erfolglose Promotionsverfahren haben durch mich bis jetzt nicht stattgefunden.

Die Promotionsordnung der Fakultät Mathematik und Naturwissenschaften der Technischen Universität Dresden in der aktuell gültigen Fassung vom 16.04.2003 erkenne ich in allen Teilen an.

Orquídea de María Pastora Menéndez Aguirre